PNL-8500 Pt. 2
UC-407

Pacific Northwest Laboratory Annual Report for 1992 to the DOE Office of Energy Research

Part 2: Environmental Sciences

Staff Members
of Pacific Northwest Laboratory

March 1993

Prepared for
the U.S. Department of Energy
under Contract DE-AC06-76RLO 1830

Pacific Northwest Laboratory
Richland, Washington 99352

Preface

This 1992 Annual Report from Pacific Northwest Laboratory (PNL) to the U.S. Department of Energy (DOE) describes research in environment and health conducted during fiscal year 1992. This year the report consists of four parts, each in a separate volume.

The four parts of the report are oriented to particular segments of the PNL program, describing research performed for the DOE Office of Health and Environmental Research in the Office of Energy Research. In some instances, the volumes report on research funded by other DOE components or by other governmental entities under interagency agreements. Each part consists of project reports authored by scientists from several PNL research departments, reflecting the multidisciplinary nature of the research effort.

The parts of the 1992 Annual Report are

Part 1:	Biomedical Sciences		
	Program Manager:	J. F. Park	J. F. Park, Report Coordinator S. A. Kreml, Editor
Part 2:	Environmental Sciences		
	Program Manager:	R. E. Wildung	L. K. Grove, Editor
Part 3:	Atmospheric Sciences		
	Program Manager:	W. R. Barchet	R. E. Schrempf, Editor
Part 4:	Physical Sciences		
	Program Manager:	L. H. Toburen	L. H. Toburen, Report Coordinator W. C. Cosby, Editor

Activities of the scientists whose work is described in this annual report are broader in scope than the articles indicate. PNL staff have responded to numerous requests from DOE during the year for planning, for service on various task groups, and for special assistance.

Credit for this annual report goes to the many scientists who performed the research and wrote the individual project reports, to the program managers who directed the research and coordinated the technical progress reports, to the editors who edited the individual project reports and assembled the four parts, and to Ray Baalman, editor in chief, who directed the total effort.

T. S. Tenforde
Health and Environmental Research Program

Previous reports in this series:

Annual Report for

1951	HW-25021, HW-25709
1952	HW-27814, HW-28636
1953	HW-30437, HW-30464
1954	HW-30306, HW-33128, HW-35905, HW-35917
1955	HW-39558, HW-41315, HW-41500
1956	HW-47500
1957	HW-53500
1958	HW-59500
1959	HW-63824, HW-65500
1960	HW-69500, HW-70050
1961	HW-72500, HW-73337
1962	HW-76000, HW-77609
1963	HW-80500, HW-81746
1964	BNWL-122
1965	BNWL-280, BNWL-235, Vol. 1-4; BNWL-361
1966	BNWL-480, Vol. 1; BNWL-481, Vol. 2, Pt. 1-4
1967	BNWL-714, Vol. 1; BNWL-715, Vol. 2, Pt. 1-4
1968	BNWL-1050, Vol. 1, Pt. 1-2; BNWL-1051, Vol. 2, Pt. 1-3
1969	BNWL-1306, Vol. 1, Pt. 1-2; BNWL-1307, Vol. 2, Pt. 1-3
1970	BNWL-1550, Vol. 1, Pt. 1-2; BNWL-1551, Vol. 2, Pt. 1-2
1971	BNWL-1650, Vol. 1, Pt. 1-2; BNWL-1651, Vol. 2, Pt. 1-2
1972	BNWL-1750, Vol. 1, Pt. 1-2; BNWL-1751, Vol. 2, Pt. 1-2
1973	BNWL-1850, Pt. 1-4
1974	BNWL-1950, Pt. 1-4
1975	BNWL-2000, Pt. 1-4
1976	BNWL-2100, Pt. 1-5
1977	PNL-2500, Pt. 1-5
1978	PNL-2850, Pt. 1-5
1979	PNL-3300, Pt. 1-5
1980	PNL-3700, Pt. 1-5
1981	PNL-4100, Pt. 1-5
1982	PNL-4600, Pt. 1-5
1983	PNL-5000, Pt. 1-5
1984	PNL-5500, Pt. 1-5
1985	PNL-5750, Pt. 1-5
1986	PNL-6100, Pt. 1-5
1987	PNL-6500, Pt. 1-5
1988	PNL-6800, Pt. 1-5
1989	PNL-7200, Pt. 1-5
1990	PNL-7600, Pt. 1-5
1991	PNL-8000, Pt. 1-5

Foreword

This report summarizes progress in environmental sciences research conducted in FY 1992 by Pacific Northwest Laboratory (PNL) for the U.S. Department of Energy's (DOE's) Office of Health and Environmental Research. The research is directed toward developing a fundamental understanding of subsurface and terrestrial systems as a basis for both managing these critical resources and addressing such formidable environmental problems as environmental restoration and global change. These studies are making outstanding contributions in a number of scientific disciplines and in the interdisciplinary research so critical to obtaining a system-level perspective. The Technology Transfer section of this report describes a number of examples in which fundamental research is laying the groundwork for the technology needed to resolve important environmental problems. The Interactions with Educational Institutions section of the report illustrates the results of a long-term, proactive program to make PNL facilities available for university and preuniversity education and to involve educational institutions in research programs. Other sections of the report summarize Laboratory-Directed Research and Development projects intended to nurture new cutting-edge scientific capabilities, identify PNL-university collaborations, and summarize publications and presentations, which provide an important measure of the success of these efforts.

Each project in the PNL research program is also a component of an integrated approach conducted at the laboratory, intermediate, and field scales, and designed to examine multiple phenomena at increasing levels of complexity. This approach is being implemented with a strong emphasis on multidisciplinary teaming. The complex areas under investigation include the effect of fundamental geochemical and physical phenomena on the diversity and function of microorganisms in deep subsurface environments, new ways to address subsurface heterogeneity, and new ways to determine the key biochemical and physiological pathways (and corresponding DNA markers) that control nutrient, water, and energy dynamics in arid ecosystems and, consequently, the response of these systems to disturbance and climatic change. University liaisons continue to expand, so that more than 30 universities nationwide are now included. These relationships both strengthen the research and help train the scientists who will address long-term environmental problems in the future.

The Environmental Science Research Center has enabled PNL to enlarge on fundamental knowledge of subsurface science to develop new concepts and tools for understanding natural systems, and also to reach out to the universities and transfer this knowledge for use by government and industry. New PNL investments have been made to develop advanced concepts for addressing chemical desorption kinetics, redesigning enzymes, scaling subsurface properties to account for heterogeneity in natural systems, and using tools from molecular biology to help understand fundamental ecological processes. This report reflects the results of past investments and the growth of PNL's technical strengths, strong multidisciplinary interactions, and rapidly developing facilities for simulating and quantifying environmental phenomena.

Raymond E. Wildung
Program Manager
Environmental Sciences

Contents

Subsurface
Science

Subsurface Science

The contamination of the subsurface environment by mixed radioactive and hazardous waste is a major concern for DOE lands and for many other waste sites across the nation. To estimate health risks and assist in cleanup activities, the scientific community is now being asked to 1) predict the rates at which these contaminants migrate through subsurface environments and 2) develop more effective techniques for degrading, mobilizing, or immobilizing contaminants *in situ*. It is especially difficult to predict transport and the results of efforts at contaminant remediation on DOE lands, where the codisposal of radionuclides, metal ions, salts, organic solutes, and organic liquids into the ground has created unique environmental situations.

The basic scientific studies described in this report address the fundamental chemical, microbiological, and hydrologic processes that control the behavior of contaminants in subsurface environments. The focus is on DOE-specific contaminants, but the broader scientific benefits being realized include better predictions of the subsurface behavior of organic/inorganic mixtures and organic liquids generally, under a variety of geochemical and hydrogeologic conditions. Subsurface chemistry studies are investigating multisolute sorption, the effects and complexation of cosolvents, and the relationship between surface sorption and microbial degradation on subsoil and aquifer materials. Microbiological investigations concern the nature of microorganisms in different deep hydrogeologic environments; the physical, geochemical, and hydrologic factors that govern the distribution and function of these microorganisms; and the ability of these microorganisms to alter radionuclide chemistry and degrade complexing ligands. Hydrologic research is defining the flow physics of multiphase mixtures of organic liquids and water in saturated and unsaturated porous media, and systematically examining how subsurface heterogeneities affect transport.

Multidisciplinary studies of chemical transport are being performed both in laboratory columns and in a unique Subsurface Environmental Research Facility, where the combined effects of microbiology, chemistry, and hydrology can be assessed at a scale that is intermediate between those of the laboratory and the field. In field research, the final phase of the Hanford deep microbiological exploration effort has begun. This effort is addressing the roles of electron acceptors and donors in governing the presence and function of microorganisms in deep saturated zones. Overall, this research is playing an important role in improving contaminant migration models and developing effective strategies to reduce contaminant migration rates and remove contaminants from groundwater.

Subsurface Chemistry of Organic Ligand-Radionuclide Mixtures

J. M. Zachara, J. P. McKinley, J. E. Szecsody, C. C. Ainsworth, and J. C. Westall

Organic substances impact the geochemical behavior of metal ions and radionuclides in groundwater systems, affecting their speciation and aqueous concentrations, long-term mineralogic associations, and transport velocities. Both natural and anthropogenic organic ligands react with metal cations, forming complex ions that have different charge, size, and reactivity from the parent ions. Aqueous complexation may induce valence changes to the metal cation and alter its surface coordination reactions with mineral solids. Together, these effects tend to increase the subsurface mobility of the metal cation or radionuclide. However, in other situations, humic substances may bind to subsurface mineral solids, thereby increasing the coordinative affinity of these surfaces for metal or radionuclide cations and reducing radionuclide mobility.

Despite the ubiquity of natural organic ligands (i.e., low-molecular-weight organic acids and higher-molecular-weight humic substances) in subsurface waters and the frequent codisposal of organic ligands with radionuclides on DOE sites,

scientific knowledge remains insufficient to predict the complex geochemical behavior of organically bound radionuclides in vadose zones and groundwater. However, the simple (and common) assumption that organically bound metals or radionuclides are nonreactive in groundwater is incorrect, and making the assumption will lead to erroneous predictions of subsurface behavior.

This project is investigating the thermodynamics and kinetics of geochemical reactions that occur between organic substances and radionuclides/metal cations on mineral surfaces. We are 1) evaluating chemical, mineralogic, and microbiologic factors that control these reactions in subsurface sediments and 2) determining the overall impacts of organic ligand-metal interactions on radionuclide transport through mineralogically heterogeneous porous media. A particular emphasis of our research is the interfacial geochemistry of natural mineral surfaces, which can exhibit nonideal behavior as a result of the presence of organic and inorganic coatings, strongly sorbed ions, and minor surface-structural impurities. To evaluate basic scientific hypotheses regarding co-contaminant surface chemistry, the research uses chemical mixtures (involving cobalt, uranium, humic substances, aminocarboxylic acid chelating agents, and organic acids) that have been selected for multi-investigator experiments within the Co-Contaminant Chemistry Subprogram of DOE's Subsurface Science Program. Laboratory experimentation involves the interaction of these contaminant mixtures with model/reference sorbents and subsurface materials whose properties were carefully selected to allow us to isolate and investigate such reactions as surface coordination, ion exchange, mineral dissolution, and electron transfer and their effects on aqueous concentrations and transport velocities of radionuclide cations.

FY 1992 Research Highlights

Research in three major areas is being pursued:

- Influence of mineral-bound humic substances and dissolved organic ligands [ethylenediamine tetraacetic acid (EDTA), citrate, and oxalate] on the sorption of cobalt and uranium by subsurface materials containing iron oxides and smectite

- Influence of adsorption reactions on the microbiological degradation rates of organic acid-radionuclide aqueous complexes

- Reactive transport of cobalt-EDTA and uranium-organic acid complexes through mineralogically heterogeneous porous media in an intermediate-scale flow cell.

Surface-chemical and geochemical models are used extensively in the research as a basis for 1) identifying dominant surface reactions and complexes; 2) incorporating the complex effects of pH, ionic strength, and competing ions; and 3) predicting the contributions made by adsorption reactions in multiprocess experiments involving microbiology and water flow.

In FY 1992, resources were directed toward activities in each of these research areas. The research is summarized in the three subsections that follow.

Influence of Mineral-Bound Humic Substances and Dissolved Organic Ligands. During FY 1992, we continued to investigate the influence of mineral-bound humic substances on the sorption of radionuclide cations by subsurface materials. The research is determining whether coatings of organic material on aquifer particles can influence the retardation of radionuclide cations in groundwater. Such coatings develop in natural systems over long periods, as groundwaters with low concentrations of humic substances and other surface-active natural organic compounds circulate past sorbing aquifer surfaces, such as iron and aluminum oxides and layer silicates. The general hypothesis that the reactivity of aquifer materials to radionuclide cations is governed by these organic coatings (rather than by the underlying mineral matrix) is so far unresolved.

We hypothesize that, at the low metal concentrations representative of radionuclide contamination at DOE sites, humic coatings augment rather than mask the sorption characteristics of the mineral material. We have further speculated

that the humic substance, when sorbed to the surface of aquifer material, would enhance metal binding in an linear, additive fashion. We therefore refer to this as the "additivity hypothesis."

These hypotheses have been evaluated using reference humic substances from the International Humic Substances Society, a subsurface mineral isolate containing kaolinite and iron/aluminum oxides, and single-phase mineral components representative of the natural material (kaolinite, goethite, and gibbsite). Testing these hypotheses has required that we first measure the metal-binding properties of the humic substance and the mineral phase separately, as discrete components, and then evaluate the sorption behavior of the combined system in which the organic material exists as a coating on the mineral surface. Experiments to characterize and model the acid-base chemistry of the humic substance and its binding reactions with cobalt have been performed at Oregon State University (OSU). PNL staff have investigated the sorption of cobalt to both the subsurface mineral materials and the humic-coated sorbents. Research during FY 1992 focused on integrating the experimental results from PNL and OSU by means of computer modeling of the metal-binding reactions to the humic substances and to the humic-coated mineral sorbents.

To describe the acid-base chemistry of one of the humic substances [leonardite humic acid (LHA)] and its complexation reactions with cobalt(II), a four-site complexation model (L_1, L_2, L_3, L_4) within the computer code FITEQL was developed at OSU. The model explicitly accounts for the effects of ionic strength on cobalt(II) complexation through competitive mass action of the electrolyte cations on ionized sites (L_1^-, L_2^-, L_3^-, L_4^-). The model provides good simulations of metal ion binding over ranges of pH, ionic strength (Figure 1), and metal ion concentration. Although the complexation model was developed to resolve the additivity hypothesis, it has also provided new insights into the proton balance of

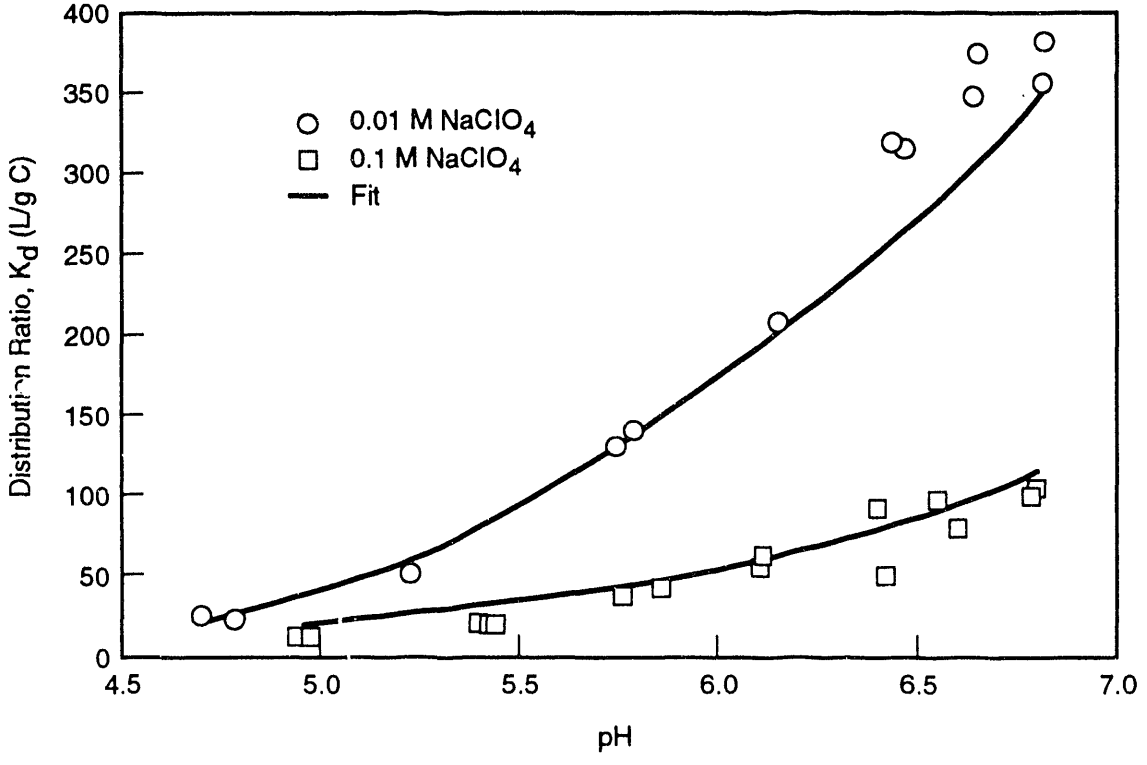

FIGURE 1. Cobalt(II) Complexation (10^{-6} mol/L) to Leonardite Humic Acid (10 mg/L) at Different pH Values and Ionic Strengths. Solid lines represent calculations made with the four-site model. The magnitude of complexation is presented as the K_d (i.e., concentration bound/concentration free).

humic substances and the importance of electrolyte/humate complexation reactions. In FY 1993, the humate complexation model will be linked with a multiple-site adsorption model to more rigorously evaluate hypotheses relating to the humate-coated mineral sorbent.

In FY 1991, we demonstrated that mineral-bound humic substances can significantly enhance cobalt(II) adsorption by mineral materials, especially over the pH range from 4.5 to 7.0 (data shown in Figure 2). These results implied that organic coatings must be considered to allow accurate forecasting of subsurface migration velocities of metal cations, such as cobalt. In FY 1992, we initiated simple calculations to test whether this sorption enhancement could be described by an additive model, i.e., whether the sorption of the coated material equals the sum of what would be expected from the separate sorbing phases. The calculations were performed using a composite distribution coefficient (K_d) approach, in which the K_d values (which vary with pH for both the organic and mineral phases) were calculated from individual humate and mineral complexation models. The calculations showed that the behavior of the humate-coated subsurface mineral mixture did indeed conform to the additive model (Figure 2) over much of the experimental pH range. This result suggests that the sorption behavior of subsurface materials with organic coatings can be predicted if the complexation behaviors of the individual organic and mineral phases are understood.

Uranium, in its metallic, pentavalent, and hexavalent states, is a common subsurface contaminant at many DOE sites. Under ambient, oxygen-rich conditions, metallic and pentavalent uranium are oxidized to hexavalent uranium, which exists as uranyl ion (UO_2^{2+}) in solution. Hexavalent uranium is more soluble and more mobile than uranium in other valence states. In addition, uranyl forms a strong complex with carbonate ion, which limits its interaction with solid surfaces at alkaline pH values and further enhances its mobility. Surface interactions of uranyl may also be strongly influenced by ionic

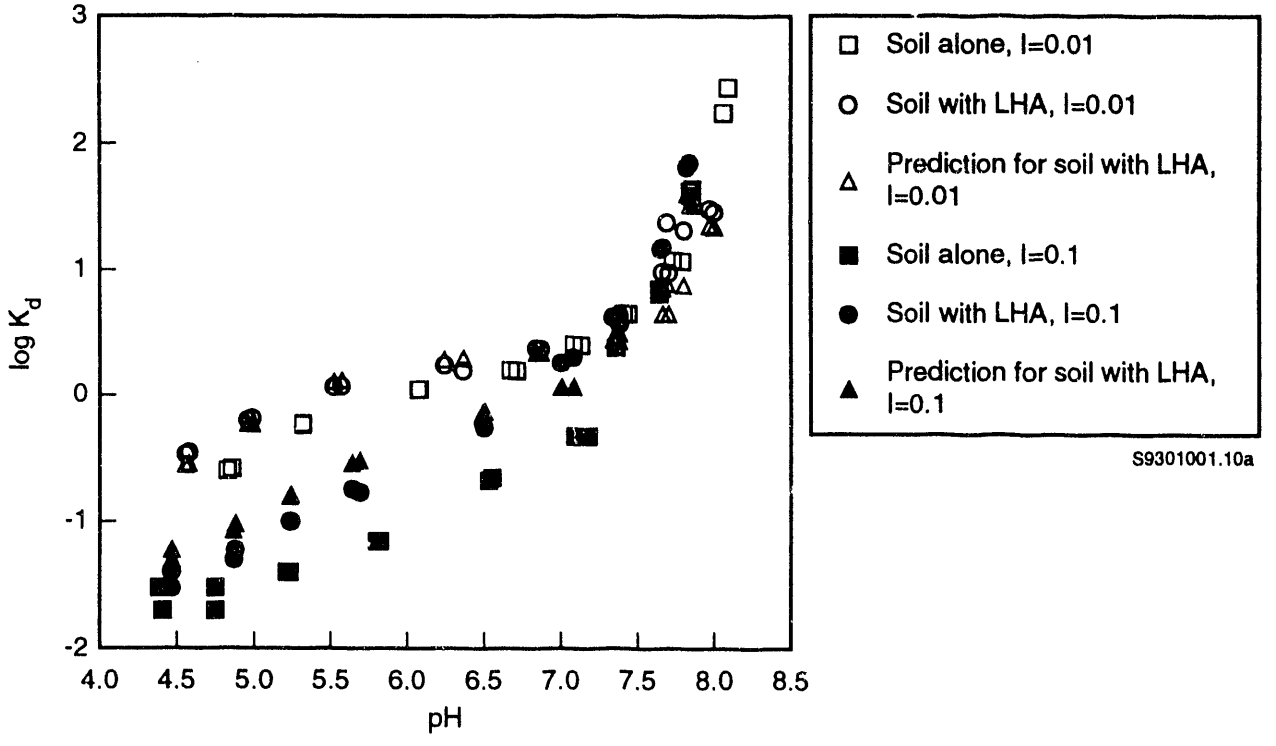

FIGURE 2. Influence of Mineral-Bound Humic Substances (in this case, LHA) on the Adsorption of Cobalt(II) by Soils Containing Kaolinite, Goethite, and Hematite. Ionic strengths were 0.01 and 0.1 (measured as $NaClO_4$).

speciation, as a result of the formation of uranyl hydroxide complexes with differing uranyl stoichiometry and charge at different solution pH values. The surface chemical interaction of uranium with solid mineral surfaces is thus a complex function of oxidation-reduction (redox) state, ionic speciation, and surface chemistry.

Given the complexity of uranium geochemistry, it is initially necessary to develop an understanding of the systematic controls on uranium mobility through the investigation of monomineralic subsystems. With the exception of adsorption to iron oxides (Hsi and Langmuir 1985), little detailed research has been published on the interaction of uranyl ion with subsurface minerals, particularly with respect to the aluminosilicate clay minerals. These minerals are abundant components of subsurface sediments, influencing both the mobility of uranium in groundwaters and the remediation of uranium-contaminated sites on DOE lands. Therefore we are focusing on experimentation with subsurface smectite clays, initially in the absence of organic complexants. When this chemical system is understood and successfully modelled numerically, organic complexants (such as citrate) will be investigated. Organic complexants were common cleaning agents in uranium-related manufacturing activities and were disposed of with uranium waste.

Research in FY 1992 was conducted with smectites that were extracted from the Kenoma soil and from the Ringold and Cape Fear formations. In addition, we used a Clay Minerals Society reference smectite, Wyoming montmorillonite (SWy-1), because it is a widely recognized mineral whose properties have been the subject of many experimental studies. The smectites were prepared by gravimetric separation, followed by dithionite citrate buffer extraction of iron oxides, ammonium oxalate extraction to remove amorphous alumina, and peroxidation to remove organic matter. Suspensions were sodium saturated and dialyzed in deionized water, then freeze-dried to provide a stock of uniform material. Adsorption experiments were performed using smectite suspensions containing 1 meq/L of charge as measured by cation exchange capacity, in the presence of 2 mg/L uranyl, at ionic strengths of 0.1, 0.01, and 0.001, in an inert-atmosphere glovebox.

Uranium adsorption on SWy-1 in sodium electrolyte showed significant variation with ionic strength (Figure 3a). Uranyl adsorption on SWy-1 contrasted with that observed for the subsurface smectites (Figure 3b) as a result of their different particle morphologies. Based on these findings, a conceptual model was developed to allow adsorption modeling of the experimental data. In the model, aqueous uranyl speciation is hypothesized to influence the speciation of surface-bound uranyl. Uranyl and certain of its hydrolysis products compete with other dissolved cations for fixed-charge basal plane sites (X^-). Amphoteric oxide-like sites on clay particle edges (SOH) complex uranyl species as a function of pH. The proportionation of edge and basal plane sites controls the pH at which adsorption to X^- or adsorption to SOH predominates.

Aqueous uranyl speciation was computed using the best estimates of formation constants that could be derived from a thorough review of published data (Grenthe 1992). Over the pH range of interest, the aqueous species of uranyl and its hydroxide complexes include UO_2^{2+}, UO_2OH^+, $UO_2(OH)_2^0$, $(UO_2)_2(OH)_2^{2+}$, $(UO_2)_3(OH)_5^+$, and $UO_2(OH)_3^-$. However, the neutral complex $[UO_2(OH)_2^0]$ was not included in the adsorption modeling because its existence has never been spectroscopically confirmed and because reported values for its log K vary significantly (-22 to -29).

The chemical modeling program FITEQL was used to model adsorption data within the limits of the conceptual model. Results of modeling for SWy-1 at two ionic strengths (0.1 and 0.001) are presented in Figure 4 along with experimental results. At low ionic strength, data were well reproduced by a combination of ion exchange on fixed-charge sites (X^-) at low pH and edge-site complexation (SOH) at higher pH; the model fit includes a pattern of decreasing uptake as pH rises, then a slight increase in total uptake as edge-site complexation becomes effective as pH approaches 8. Decreasing sorption with increasing pH is the result of the speciation of uranyl

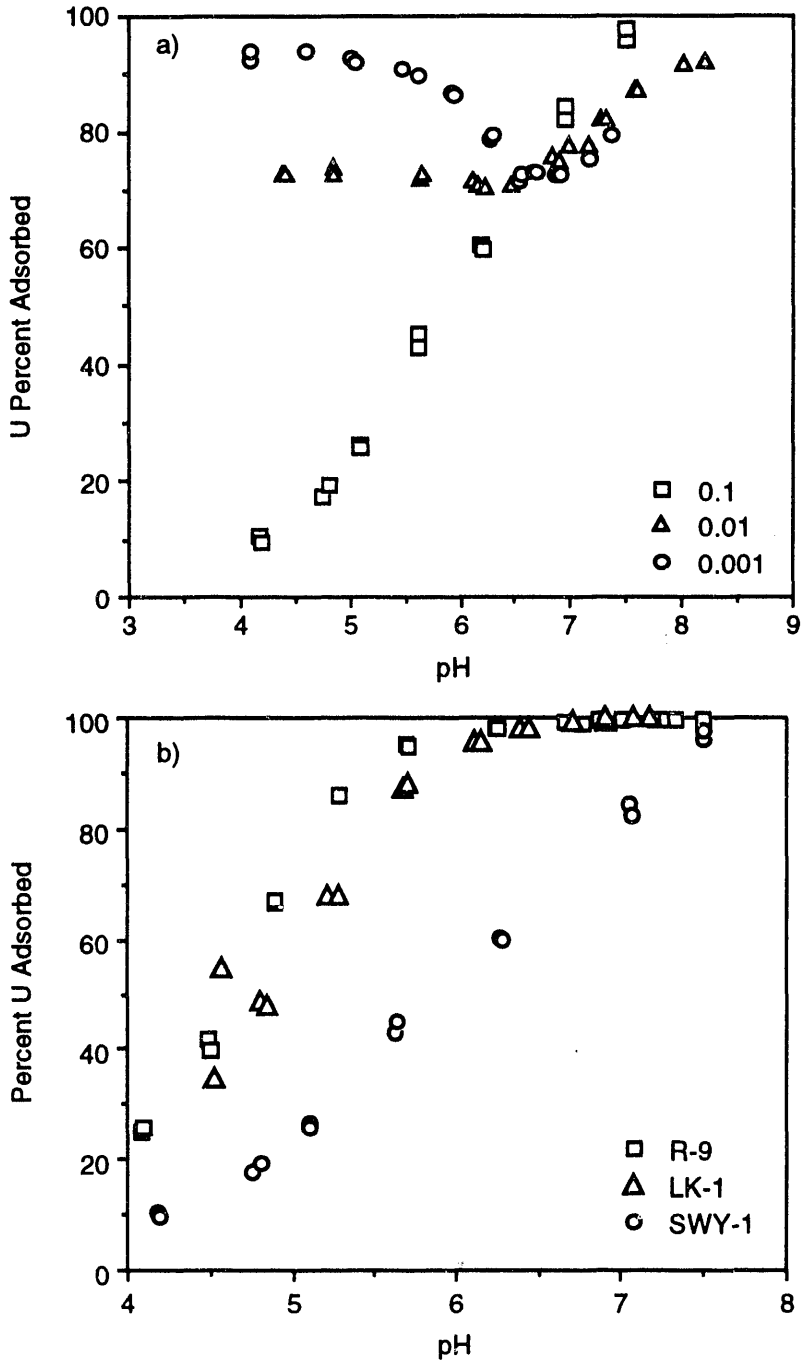

FIGURE 3. Uranyl (UO_2^{2+}) Adsorption to a) SWy-1 at Varying Ionic Strengths and b) SWy-1 and Two Subsurface Smectites at I = 0.1

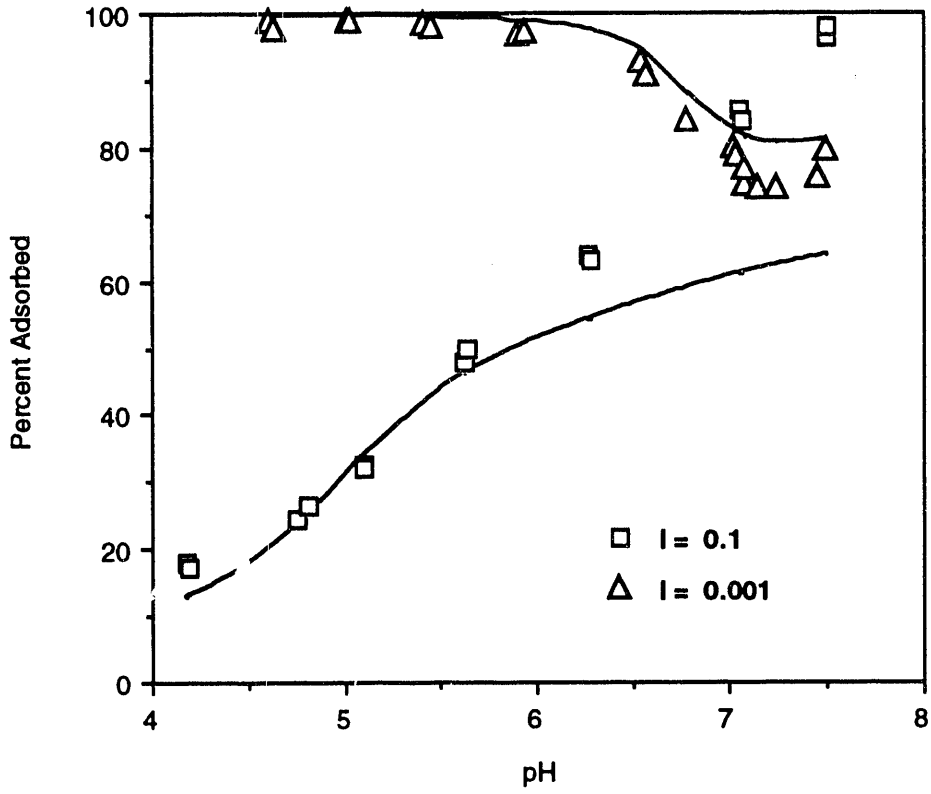

FIGURE 4. Comparison of Observed (symbols) and Computed (solid lines) Adsorption on SWy-1 at Two Ionic Strengths

changing from a divalent to a monovalent species. At higher ionic strengths, model computations again agree with experimental data for low pH. Higher concentrations of sodium are computed to suppress ion exchange of uranyl by mass action, consistent with the experimental data. The lack of agreement between the model and the experimental data for I = 0.1 above pH 6 suggests that the edge complexation of $(UO_2)_3(OH)_5^+$ must be considered explicitly.

The surface speciation scheme developed through adsorption modeling requires direct confirmation to validate it as a chemical model of the system. To meet that purpose, a set of collaborative experiments was initiated with researchers at Los Alamos National Laboratory (LANL). Smectite slurries were equilibrated with 20 mg/L uranyl at low, intermediate, and high pH, then centrifuged to concentrate the smectite with adsorbed uranyl. The resultant paste was loaded into vials in an inert atmosphere, sealed, and sent to LANL for surface spectroscopic examination by laser-induced fluorescence spectroscopy and Raman spectroscopy to determine the chemical identity of adsorbed species. These experiments are still under way.

Influence of Adsorption Reactions on Microbiological Processes. Sorption influences both the transport of organic contaminants through subsurface materials and the persistence of biodegradable organic contaminants. For instance, sorption may limit microbial degradation rates if organic compounds that are present in the sorbed state are consequently unavailable as a carbon source. As a result, degradation measurements made in the absence of subsurface materials may overestimate the extent of degradation that occurs in the vadose and saturated zones.

Research in FY 1991 showed that 1) the microbial degradation of aromatic organic acids

(catechol, salicylate, and phthalate) that were sorbed to γ-Al_2O_3 was slower than the degradation of the corresponding aqueous compounds and 2) desorption from the solid phase was the rate-limiting reaction. In FY 1992, we developed additional information on the kinetics of adsorption/desorption for three aliphatic acids that sorb to goethite (α-FeOOH) to improve our understanding of desorption limitations on microbial degradation. The sorbates were citric acid (pK_{a1} = 3.13, pK_{a2} = 4.76, pK_{a3} = 6.40), oxalic acid (pK_{a1} = 1.23, pK_{a2} = 4.19), and propionic acid (pK_a = 4.87). Experiments were conducted to evaluate the sorption of the organic acids as a function of pH, ionic strength, and concentration of the organic acid. A relaxation kinetic technique (the pressure-jump technique) was applied to evaluate the mechanism of organic acid adsorption to and desorption from the surface of goethite, as a basis for understanding the factors governing the desorption rate and, hence, the rate of microbial degradation of sorbed organic ligands.

Propionic, oxalic, and citric acids adsorbed to goethite via a surface complexation reaction that is affected by the pH, surface charge, aqueous speciation of the sorbates, and other aqueous and solid phase phenomena. Adsorption increases with decreasing pH, as surface charge becomes more positive (Figure 5). The adsorption of all three organic acids also decreases as ionic strength increases, suggesting that the sorption process was dominated by an outer-sphere complexation reaction. This conclusion contrasts with the findings of Parfitt et al. (1977), who employed infrared (IR) spectroscopy to show that the oxalate anion forms a binuclear, inner-sphere complex at the goethite surface.

The pressure-jump technique was used to investigate the adsorption/desorption mechanism and its dependence on ionic strength. Three distinct relaxations were observed for both citrate and oxalate over a 13-sec time frame; these are possibly indicative of individual surface reactions. The three reciprocal relaxation times (τ^{-1}) varied

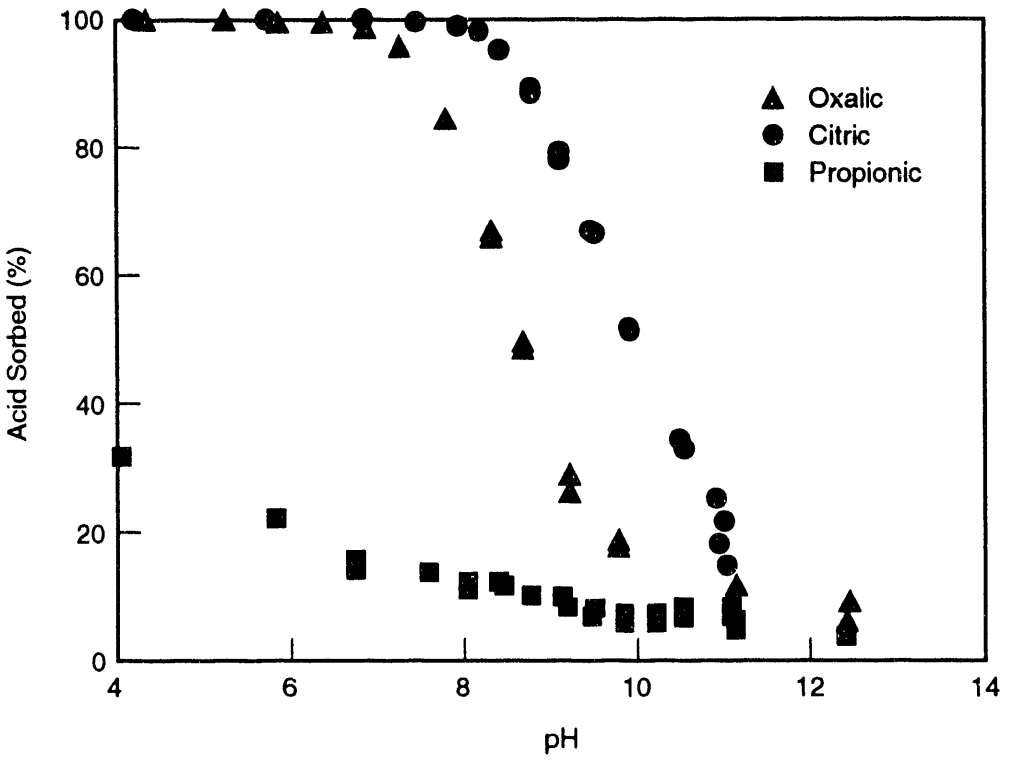

FIGURE 5. Fractional Adsorption of Three Organic Acids (10^{-4} mol/L) to Goethite (20 g/L; I=0.01) as a Function of pH

as a function of pH (and hence surface loading), but at constant pH they did not shift as ionic strength was varied. Although more data are needed to identify the specific reactions responsible for this kinetic behavior, we have hypothesized a reaction scheme that is consistent both with the pressure-jump and batch adsorption data and with the previously published IR spectra (Figure 6). The reaction sequence involves 1) the formation of an outer-sphere complex, followed by 2) the formation of a monodentate inner-sphere complex, and 3) the subsequent formation of a binuclear surface complex. We believe that the three species coexist on surfaces. This reaction sequence would account for the three relaxation times and the observed shift in pH adsorption edge with ionic strength. Further technical developments are needed in understanding the factors that govern the kinetics of organic acid desorption from mineral sorbents, as a basis in turn for understanding degradation rates in the presence of metabolizing microorganisms.

Transport Experiments with Cobalt-EDTA. The migration of ^{60}Co as complexes with strong organic ligands such as EDTA is a significant subsurface transport vector in the mobilization of radioactive materials from DOE sites. We hypothesize that movement of organically complexed cobalt in groundwaters is controlled by time-variant reactions with iron and aluminum oxides, and that accurate knowledge of the extent and rates of these reactions is necessary to predict cobalt movement in the subsurface. We have also speculated that the spatial distribution of iron and aluminum oxides in subsurface sediments controls the overall subsurface migration velocity of organically bound cobalt. We hypothesize that there is a fundamental relationship between the relative size and distribution of lenses of iron/aluminum oxides compared to the size of the flow system and the chemical distribution that is observed.

To address these hypotheses, a multiyear series of studies has been planned that will culminate

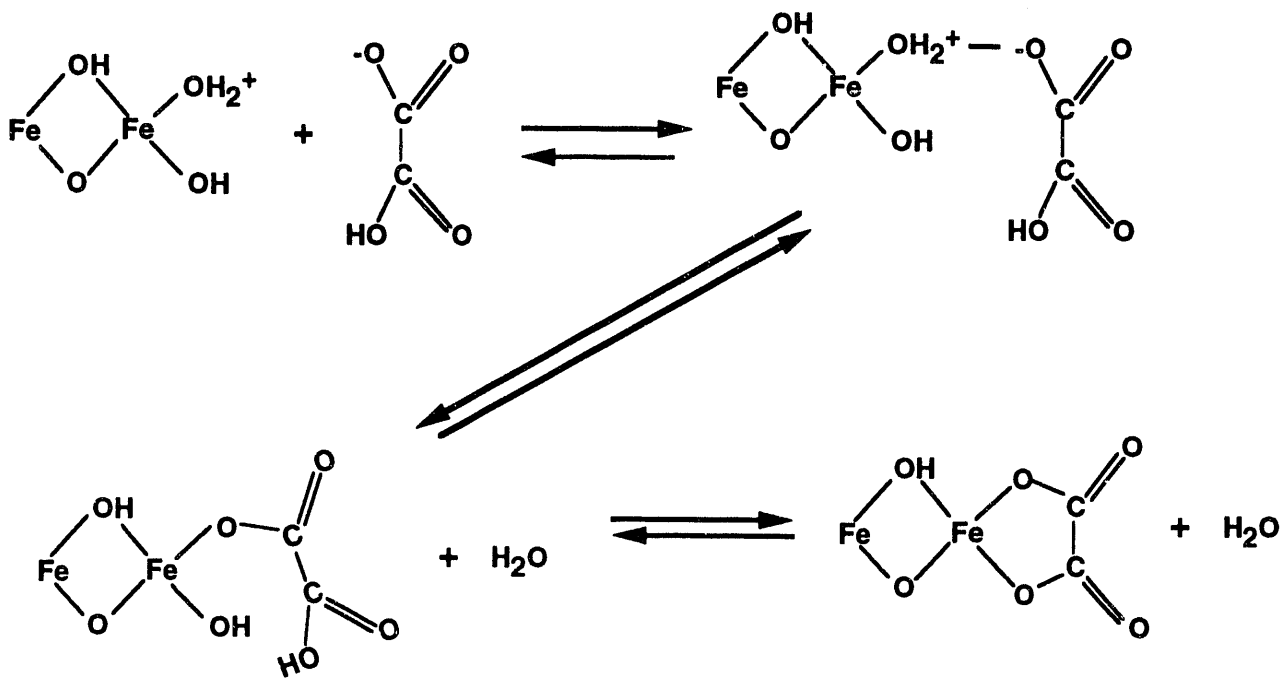

FIGURE 6. Hypothesized Reaction Mechanism for Adsorption/Desorption of Oxalate on Goethite

in reactive transport experiments with cobalt-EDTA in intermediate-scale flow cells containing both idealized and natural mineralogic heterogeneities. Research in this experimental series was initiated in FY 1992, beginning with batch and column studies of cobalt(II)-EDTA interactions with a laboratory-synthesized iron oxide-coated sand. These experiments will provide background data and models for further intermediate-scale transport experiments in which the migration of cobalt(II)-EDTA through sandy material containing lenses or stringers of iron, aluminum, and manganese oxides will be studied.

Batch studies with the iron-coated sand showed that cobalt(II) undergoes typical cation adsorption (i.e., fractional adsorption increasing with increasing pH), in contrast to EDTA complexes [calcium-EDTA, iron(III)-EDTA, cobalt(II)-EDTA], which adsorb as anions. Cobalt and calcium-EDTA, however, are unstable on the iron oxide surface and exchange with the solid phase, producing iron(III)-EDTA and the free metal [e.g., cobalt(II)]. The surface-exchange reaction is suggested by the data shown in Figure 7, where the solution concentrations of EDTA and iron increase with time after the initial adsorption of cobalt(II)-EDTA by iron-coated sand. The surface-induced breakup of the cobalt(II)-EDTA complex is also confirmed by the disparate concentrations of aqueous cobalt(II) and EDTA as determined by counting (^{60}Co, ^{14}C). Time studies at other pH values show more significant differences between EDTA and free cobalt(II) as they reequilibrate with the solid phase. At low pH, more free cobalt(II) desorbs into solution after the breakup of the cobalt(II)-EDTA complex.

The goal of our research with cobalt(II)-EDTA is to evaluate its complex time-variant reactions (adsorption, dissolution) with subsurface solid phases, as a basis for understanding the migration of cobalt(II)-organic complexes in the field. We believe that the rate of cobalt(II)-EDTA dissociation during transport will be strongly

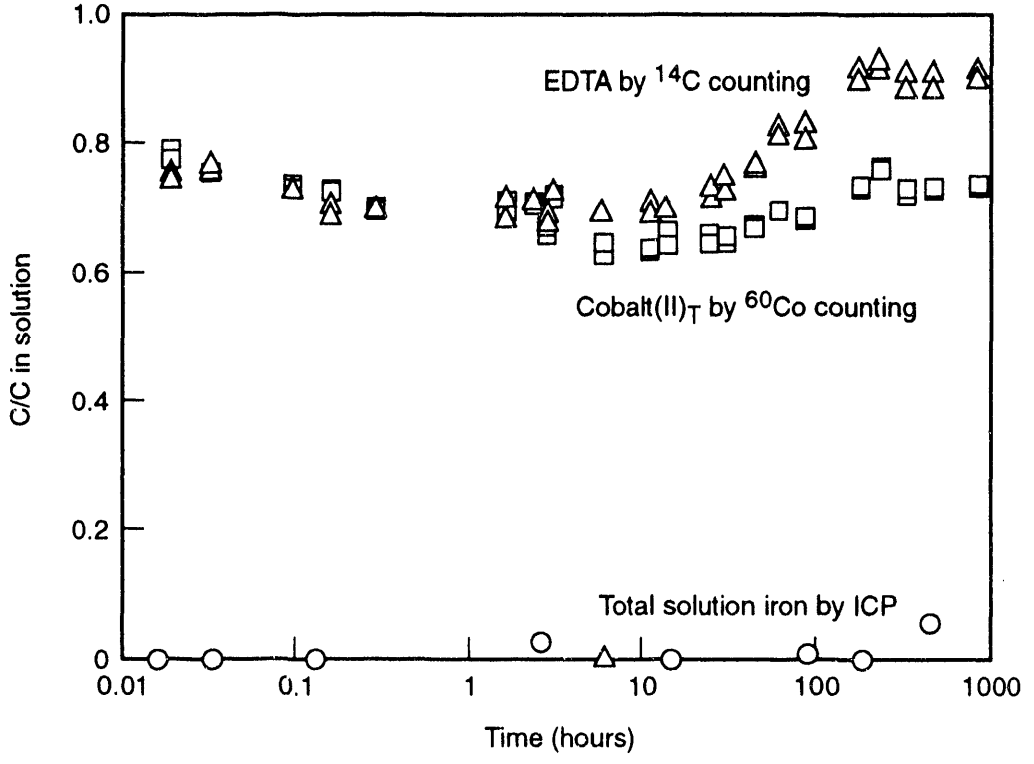

FIGURE 7. Sorption of Cobalt(II)-EDTA on Sand Coated with 0.3% (by mass) Ferrihydrite. The experiment was performed with dual labels (^{60}Co and ^{14}C-EDTA) whose energies allow species-specific counting.

dependent on flow velocity, as a result of multi-ion and mass-transfer effects. To address the effect of the rate of water flow on cobalt(II)-EDTA stability, two column experiments were conducted at pH 6.5. These experiments demonstrated the significant finding that cobalt mobility changes over time as a result of kinetically controlled reactions with the iron oxide surface (Figure 8). Initially, the intact complex is eluted from the column although its velocity is retarded by adsorption. The subsequent breakthrough of cobalt(II) is slower than that of EDTA, as a result of surface exchange with iron(III), producing iron(III)-EDTA and free cobalt(II). Cobalt(II) breakthrough occurs after that of EDTA (meaning that cobalt does not reach as high a concentration in the same length of time) because free cobalt(II) adsorbs more strongly than does iron(III)-EDTA at pH 6.5. Retardation factors estimated from the batch adsorption experiments [cobalt(II)-$EDTA^{2-}$, R_f = 3; iron(III)-$EDTA^{-}$, R_f = 2.6; and cobalt(II), R_f = 20] indicate that EDTA breakthrough will change little over time. In contrast, the cobalt R_f increases from 3 to 20 over time as the complex is destabilized. Such time-dependent retardation behavior will have major effects on the field-scale behavior of organically complexed ^{60}Co.

To date, laboratory experiments and simulations have shown that the subsurface mobility of organically complexed cobalt can be influenced

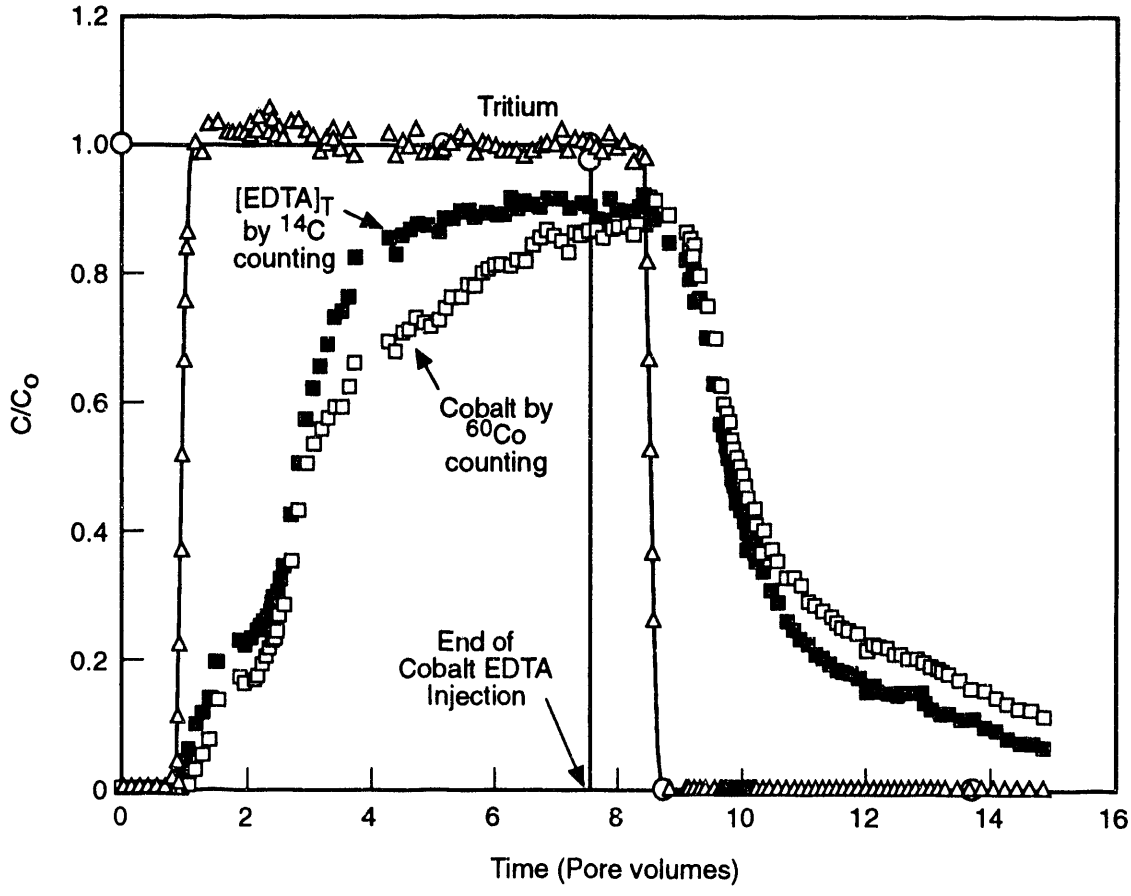

FIGURE 8. Transport of Tritium and Cobalt(II)-EDTA Through a Column with Iron Oxide-Coated Sand [0.6% (by mass) Ferrihydrite]. Electrolyte was 10^{-3} mol/L $Ca(ClO_4)_2$ maintained at pH 6.5 with piperazine-N N'bis[2-ethanesulfonic acid] (PIPES) buffer. Initial breakthrough of tritium at 1.0 pore volume (10 h) is unretarded. Both cobalt(II) and EDTA injected as cobalt(II)-EDTA initially exhibit retarded but simultaneous breakthrough. The subsequent slower movement of cobalt(II) is caused by a slow surface exchange reaction that produces iron(III)-EDTA and free cobalt(II).

by adsorption and dissolution reactions with iron oxide surfaces. Aluminum and manganese oxide surfaces will also influence cobalt mobility, and their effects will be studied in the future in collaboration with other projects in the Co-Contaminant Chemistry Subprogram. To evaluate the effect of oxide lenses on cobalt mobility in the field, we will study the influence of the spatial distribution of these lenses in a series of meter-scale laboratory experiments. Future research will also include collaborative experiments with microbiologists to examine the coupled effects of geochemical and microbial reactions on the mobility of organic complexes.

Future Research

Priority will be given in FY 1993 to the completion of research with cobalt-EDTA. An experiment on cobalt(II)-EDTA reaction and transport in an intermediate-scale flow cell with stringers of laboratory-synthesized iron and manganese oxide-coated sand will be completed, in collaboration with other Co-Contaminant Chemistry Subprogram investigators. The experiment will test hypotheses about the kinetics of cobalt(II)-EDTA oxidation to cobalt(III)-EDTA and the competitive effects arising from the cobalt(II)-EDTA-induced dissolution of iron oxide [resulting in cobalt(II) and iron(III)-EDTA] in mineralogically heterogeneous porous media. The transport experiment will be followed by a batch experimental study of cobalt(II)-EDTA interactions with a number of natural iron oxide sands in which the iron oxide crystal form, surface area, and morphology vary, in order to document the general applicability of results from the flow-cell experiment to diverse subsurface environments.

Laboratory experiments will also be initiated to investigate the effects of citrate and oxalate on the chemistry of uranium(VI) sorption by subsurface smectites of differing particle morphology. Hypotheses on the importance of aqueous speciation, surface complexation to clay mineral edges, and organic-ligand-promoted mineral dissolution will be tested. These experiments will be followed late in FY 1993 by research to assess whether adsorption of uranium complexes (e.g., uranium-oxalate, uranium-citrate) controls the rates of microbial degradation of the organic ligand (e.g., oxalate, citrate) in smectite suspensions inoculated with specific subsurface microflora. This experimental series, while evaluating important scientific hypotheses regarding subsurface biogeochemistry, will provide necessary background information for uranium-ligand microaquifer experiments planned for FY 1994. These experiments will involve uranium-ligand transport through sand-filled flow cells with smectite lenses and a subsurface microbial inoculum.

In FY 1993, we will continue to evaluate how adsorption and desorption control the bioavailability of organic acids both as free ligands and when complexed to uranium and cobalt. The investigations will include static batch studies with and without known microflora, as well as continued use of the pressure-jump technique.

References

Grenthe, I., ed. 1992. *Chemical Thermodynamics. Volume 1. Chemical Thermodynamics of Uranium*. Nuclear Energy Agency Organization for Economic Co-operation and Development, North-Holland Elsevier Science Publishers, Amsterdam, The Netherlands.

Hsi, C-K. D, and D. Langmuir. 1985. "Adsorption of Uranyl onto Ferric Oxyhydroxides: Application of the Surface Complexation Site-Binding Model." *Geochimica et Cosmochimica Acta* 49:1931-1941.

Parfitt, R. L., V. C. Farmer, and J. D. Russell. 1977. "Adsorption on Hydrous Oxides I. Oxalate and Benzoate on Goethite." *Journal of Soil Science* 28:29-39.

Chemistry/Microbiology Controlling Chelated Radionuclide Transport

D. C. Girvin and H. Bolton, Jr.

Synthetic chelating agents, such as ethylenediaminetetraacetic acid (EDTA), nitrilotriacetic acid (NTA), and diethylenetriaminepentaacetic acid (DTPA), form strong water-soluble complexes with a wide range of radionuclide and metal ions. These synthetic chelating agents have therefore been used to decontaminate nuclear reactors and for other nuclear waste processing. The codisposal of these synthetic chelating agents with radionuclides has resulted in an increase in radionuclide transport in the subsurface environment. At specific DOE sites, enhanced ^{60}Co migration in soil and subsoil pore waters has been reported. (The dissolved ^{60}Co in these pore waters exists predominantly as anionic species, with up to 90% of the cobalt associated with EDTA.) The enhanced radionuclide transport at these mixed-waste disposal sites is presumably caused by the reduced adsorption of the chelated radionuclide by subsurface materials relative to the adsorption of the unchelated radionuclide. Under these conditions, a decrease in chelate concentration via biodegradation would be beneficial, resulting in a decrease in radionuclide migration. However, other subsurface conditions can exist in which the chelation of radionuclides would have increased radionuclide adsorption and led to a decrease in radionuclide mobility. Under such conditions, biodegradation of the chelate would be undesirable.

Because current scientific understanding of both adsorption and biodegradation of chelated radionuclides and the physicochemical and microbiological parameters that influence these processes is limited, it is impossible to assess their role in controlling chelated radionuclide transport at DOE mixed-waste sites. This lack of knowledge also precludes our manipulating geochemical and microbiological conditions in the subsurface environment to limit radionuclide migration when synthetic chelating agents are present.

Synthetic chelates can be used as models of native organic compounds that also complex radionuclides and metals. Understanding the interactions of adsorption and biodegradation of synthetic chelates (for which thermodynamic data are readily available for modelling purposes) can aid in interpreting data for native organic complexants, for which only limited thermodynamic data are available. This project focuses on 1) the adsorption of synthetic chelates and chelated radionuclides, 2) the subsurface physicochemical conditions that influence microbial biodegradation and transformations of synthetic chelates, and 3) the synergy between adsorption and microbial processes. The modeling of the aqueous speciation is integral to all aspects of this project.

FY 1992 Research Highlights

Chelated Radionuclide Adsorption. The goal of this segment of the research is to mechanistically describe adsorption of chelated radionuclides for a range of subsurface materials and conditions present at DOE waste sites. The current focus of this research is the adsorption of cobalt(II)-EDTA, cobalt(III)-EDTA, and cobalt(II)-NTA by aluminum oxides, specifically δ-Al_2O_3 and gibbsite [α-$Al(OH)_3$], and iron oxides, specifically goethite (α-FeOOH) and ferrihydrite ($Fe_5HO_8 \cdot H_2O$), in the absence of microbiological activity. Cobalt and EDTA were selected for study because of their known co-migration in pore waters at some DOE sites. Iron and aluminum oxides have been chosen because they are important sorbents in many subsoils and subsurface materials and may exert a significant influence on radionuclide attenuation and mobility. Investigation of the cobalt-EDTA iron oxide system began in FY 1992 in support of the intermediate-scale experiments with cobalt-EDTA that were being conducted within the Co-Contaminant Chemistry Subprogram of DOE's Subsurface Science Program. Selected results describing cobalt(II)-EDTA adsorption behavior on α-FeOOH are presented in a later section. The cobalt-NTA-gibbsite system is being utilized in interactive studies of chelated radionuclide adsorption-biodegradation, also discussed in a later section. In this section, selected results for the NTA- and cobalt-NTA-gibbsite system will be presented and the success of the mechanistic modeling approach for quantitatively describing cobalt(II)-EDTA adsorption by δ-Al_2O_3 will be discussed.

Batch experiments were conducted with NTA or equal-molar cobalt and NTA concentrations of 1 μM, gibbsite concentrations of 7.5 g/L in all suspensions, and background electrolyte concentrations varying from 0.01 to 1 M $NaClO_4$. Adsorption edges were measured as a function of pH (5 <pH <10) under a N_2 atmosphere to minimize dissolved carbon dioxide in solution. Adsorption equilibrium was reached in less than 6 h; however, all experiments were conducted for 24 h. Adsorption of cobalt and NTA was quantified by dual-labeled scintillation counting of ^{60}Co and ^{14}C-labeled NTA tracers; γ-counting of ^{60}Co served as an independent measure of cobalt adsorption. Dissolved aluminum in solution was measured by inductively coupled plasma mass spectrometry (ICP-MS). Aqueous speciation and solubility calculations for measured cobalt, NTA, and dissolved aluminum concentrations were performed using the MINTEQ code (Felmy et al. 1984). These calculations excluded possible surface complexation (adsorption) reactions.

Adsorption edges for cobalt without NTA (referred to as cobalt-only) and for NTA without cobalt (NTA-only) show typical cation-like and ligand-like adsorption behavior, respectively (Figure 1a). Evidence in the literature strongly suggests that divalent cations form inner-sphere surface complexes with iron oxides and δ-Al_2O_3 (Hayes 1987; Brown 1990). By analogy, for cobalt-only adsorption on gibbsite (Figure 1a), we expect formation of inner-sphere complexes with the singly coordinated aluminol edge sites (≡AlOH) [i.e., ≡AlOCo and ≡AlOCo(OH)]. For the NTA-only adsorption edge (Figure 1a), we hypothesize that the dominant adsorbed species forming are ≡AlNTA and ≡AlHNTA$^-$. This is based on aqueous speciation of NTA in the presence of dissolved aluminum (Figure 1b).

Adsorption of cobalt, introduced into the gibbsite suspension as an equimolar cobalt-NTA chelate and referred to hereafter as Co w/NTA (Figure 1a), is essentially cation-like, with a suppression of adsorption between pH 7 and 10, relative to cobalt-only adsorption. Aqueous speciation indicates that Co^{2+} is the dominant cobalt species below pH 7, because dissolved aluminum outcompetes cobalt for NTA. Thus, for pH <7, cation-like cobalt adsorption would be expected. Aqueous speciation calculations suggest that for pH >7, cobalt-NTA$^-$ is a major species. This would suggest anion-like adsorption of Co w/NTA; however, this behavior is not observed. As noted above, all aqueous speciation calculations presented here neglect the competitive effects of adsorption on the multiple aqueous equilibria. The similarity of the Co w/NTA adsorption edge to that of the cobalt-only adsorption edge for pH >7 suggests that the ≡AlOH sites of the gibbsite outcompete the NTA for cobalt. That is, the formation of the ≡AlOCo surface complex is thermodynamically favored over that of the aqueous cobalt-NTA complex. This is consistent with the modest strength of the equilibrium constant for the aqueous cobalt-NTA complex (log K = 12) relative to that of cobalt-EDTA (log K = 18) for which ligand-like adsorption of Co w/EDTA is observed for 5 <pH <10. However, suppression of the Co w/NTA edge and enhancement of the NTA w/Co edge for 7.5 < pH <10 indicates that some of the cobalt-NTA complex persists in this pH region. The enhancement of NTA adsorption for pH >8 in the presence of cobalt (Figure 1a) suggests that a surface bridging complex forms, in which cobalt is coordinated directly to a surface aluminol group, while maintaining at least one carboxylate bond to NTA (e.g., ≡AlOCo-NTA, where the single "-" indicates the carboxylate bond). Thus, in this pH region the data suggest that both cobalt and cobalt-NTA adsorption occur. Adsorption of NTA in the presence of equimolar cobalt below pH 7.5 is identical to NTA-only adsorption (compare the NTA w/Co and NTA-only edges in Figure 1a). Our aqueous speciation calculation for cobalt-NTA suggests that the dominant adsorbed species are ≡AlNTA and ≡AlHNTA, similar to the case for NTA-only adsorption.

To investigate the nature of the electrostatic interactions between NTA, cobalt, and cobalt-NTA and the surface aluminol groups, adsorption edges were measured as a function of the ionic strength of the background electrolyte in gibbsite suspensions. The influence of electrostatics provides evidence to support the molecular nature of surface interactions to be used in the mechanistic modeling of cobalt-NTA adsorption. With respect to the 0.01 M adsorption edge, the NTA-only adsorption edge is displaced to lower

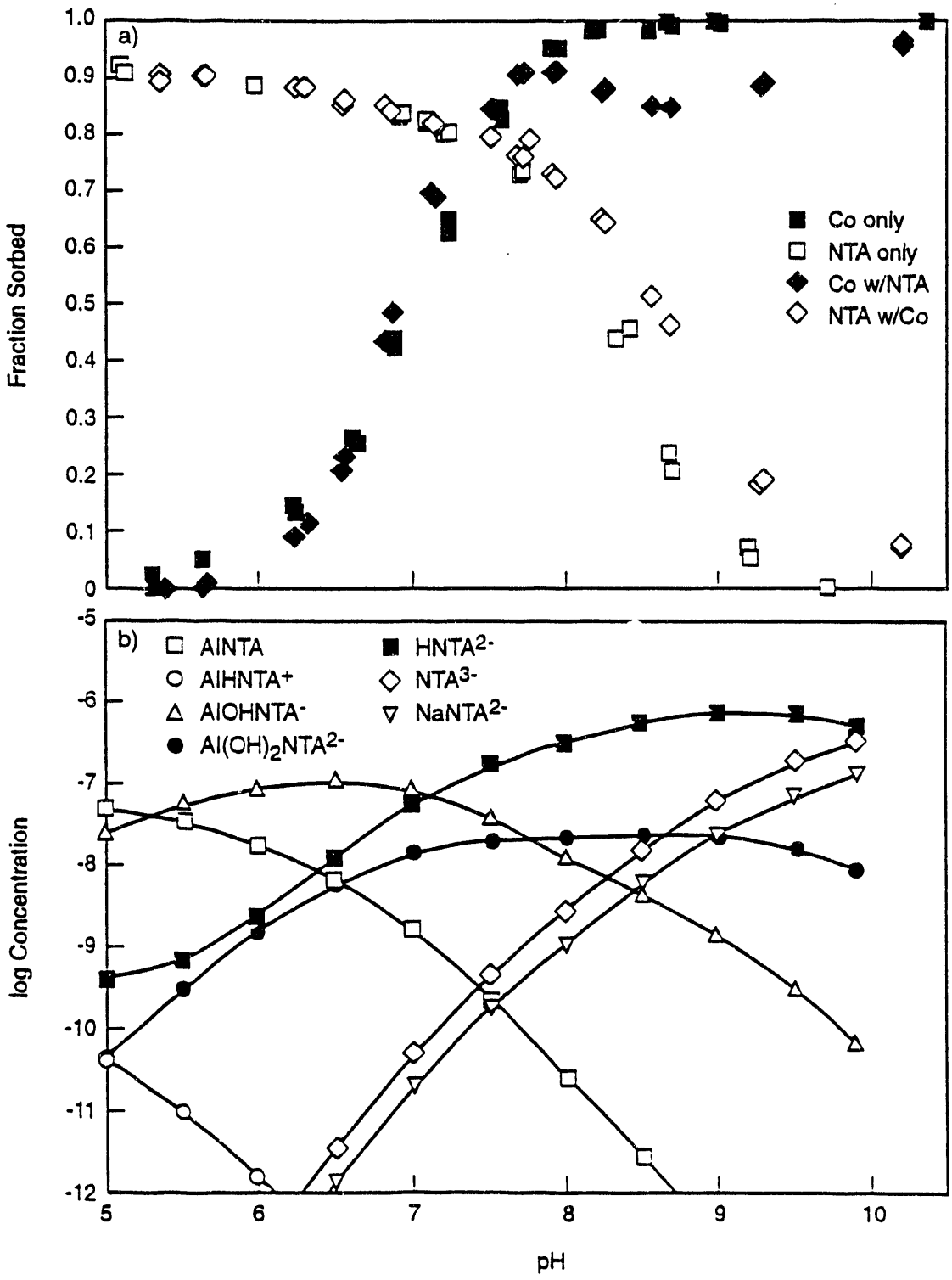

FIGURE 1. Graphs of a) Adsorption of 1 μM Cobalt-Only, NTA-Only, and Cobalt-NTA by Gibbsite (7.5 g/L) in 0.01 M $NaClO_4$ and b) Aqueous Speciation for 1 μM NTA-Only Adsorption in 0.01 M $NaClO_4$ (Figure 1a) Using Measured NTA and Aluminum Solution Concentrations

pH levels by a relatively minor amount as ionic strength increases (Figure 2a). As the ionic strength increases from 0.01 to 1 M, the decrease in the pH at which 50% adsorption occurs (ΔpH50) is 0.25 pH units (Figure 2a). However, for pH >8.5, the 1 M edge no longer parallels the 0.01 M edge but rather levels off and increases slightly with increasing pH. This difference is attributed to adsorption of $NaNTA^{2-}$. For pH >8.5, the dominant aqueous species is $NaNTA^{2-}$ in the 1 M system (Figure 2b), although it is only a minor species in the 0.01 M system (Figure 1b). The adsorption of $NaNTA^{2-}$ should be relatively weak (e.g., electrostatically bound), because it adsorbs only when it becomes the dominant solution species. For pH <8.5, the aqueous aluminum-NTA species distribution is similar at both ionic strengths (Figures 1b and 2b), indicating that $\equiv$AlNTA and $\equiv$AlHNTA$^-$ may be the dominant adsorbed species. The ΔpH50 observed here (0.25) for NTA is similar to that observed by Hayes (1987) for inner-sphere complexation of selenite by goethite, for the same change in ionic strength. The ΔpH50 shift indicates that the NTA surface complexes are relatively insensitive to electrostatic effects associated with changes in ionic strength. By analogy with the observations of Hayes (1987), NTA may form inner-sphere surface complexes with the aluminol edge sites of gibbsite; however, this hypothesis must be verified by direct surface spectroscopic measurements. Based on this inner-sphere hypothesis, we propose the following NTA adsorption reactions for describing NTA adsorption in the NTA-gibbsite system:

$$\equiv AlOH + NTA^{3-} = \equiv AlNTA^{\circ} + OH^-$$

$$\equiv AlOH + NTA^{3-} + H^+ = \equiv AlHNTA^+ + OH^-$$

In addition, we propose the formation of an outer-sphere $NaNTA^{2-}$ surface complex, given by the reaction

$$\equiv AlOH + NTA^{3-} + Na^+ =$$

$$\equiv AlO^- \text{---} NaNTA^{2-} + H^+$$

where the symbol "---" is used to indicate that $NaNTA^{2-}$ is an outer-sphere complex. These reactions, in addition to the formation of the surface bridging complex, should completely describe NTA adsorption in the cobalt-NTA system. We are continuing to examine the ability of these and possibly other reactions to mechanistically describe the observed NTA adsorption behavior.

The adsorption of EDTA-only by δ-Al_2O_3 (Figure 3) and cobalt in the presence of equal-molar EDTA (Figure 4) was discussed qualitatively in last year's annual report and by Girvin et al. (in press). In FY 1992 we described this adsorption quantitatively using the triple-layer adsorption model (TLM) and derived thermodynamic adsorption constants for individual adsorption reactions using the model. The EDTA-only adsorption data (Figure 3) can be described by two outer-sphere surface coordination (adsorption) reactions:

$$\equiv AlOH + Al^{3+} + EDTA^{4-} + H^+ = \equiv AlOH_2^+ \text{---} AlEDTA^- \quad :\log K = 5.6 \qquad (1)$$

$$\equiv AlOH + Al^{3-} + EDTA^{4-} = \equiv AlOH_2^+ \text{---} AlOHEDTA^{2-} \quad :\log K = 4.0 \qquad (2)$$

The TLM couples these two reactions with 1) reactions describing the protonation of the δ-Al_2O_3 surface, 2) reactions between the surface and electrolyte ions, 3) electrostatic interactions within the double layer, 4) all relevant aqueous speciation reactions, 5) the analytical totals and/or activities of constituents in the system, and 6) mass-balance equations that equate the concentrations of all computed species to the analytical totals. The thermodynamic equilibrium constants for reactions (1) and (2) were derived from the measured adsorption data at 0.01 M $NaClO_4$ using the nonlinear least-squares fitting code FITEQL. The FITEQL code incorporates all TLM reactions and iterates on the value of the equilibrium adsorption constants until the best fit to the adsorption data is obtained, one that simultaneously satisfies all equilibrium and mass-balance constraints. The

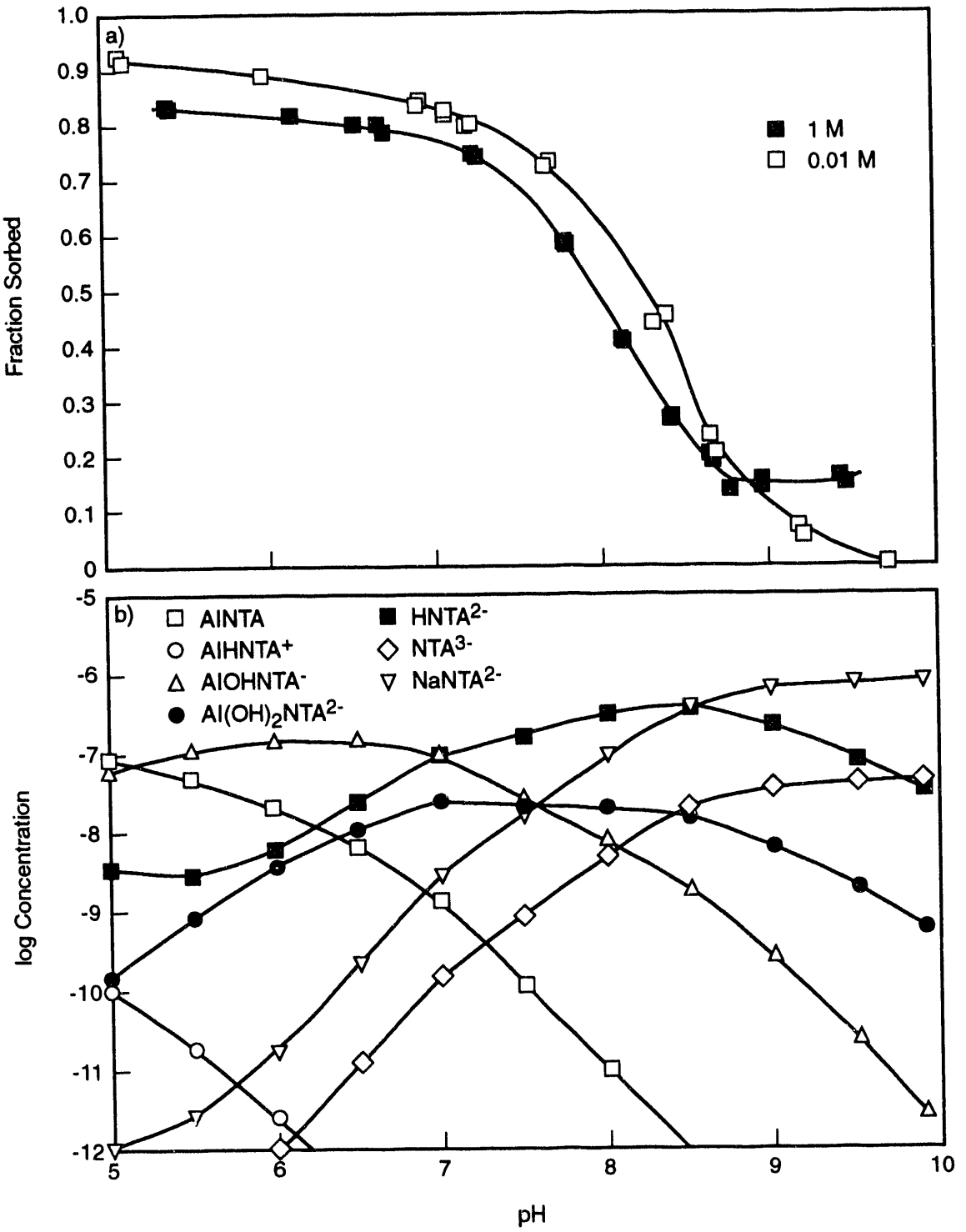

FIGURE 2. Graphs of a) Adsorption of 1 μM NTA-Only by Gibbsite (7.5 g/L) in 0.01 and 1.0 M $NaClO_4$ and b) Aqueous Speciation for 1 μM NTA-Only Adsorption in 1.0 M $NaClO_4$ Using Measured NTA and Aluminum Solution Concentrations

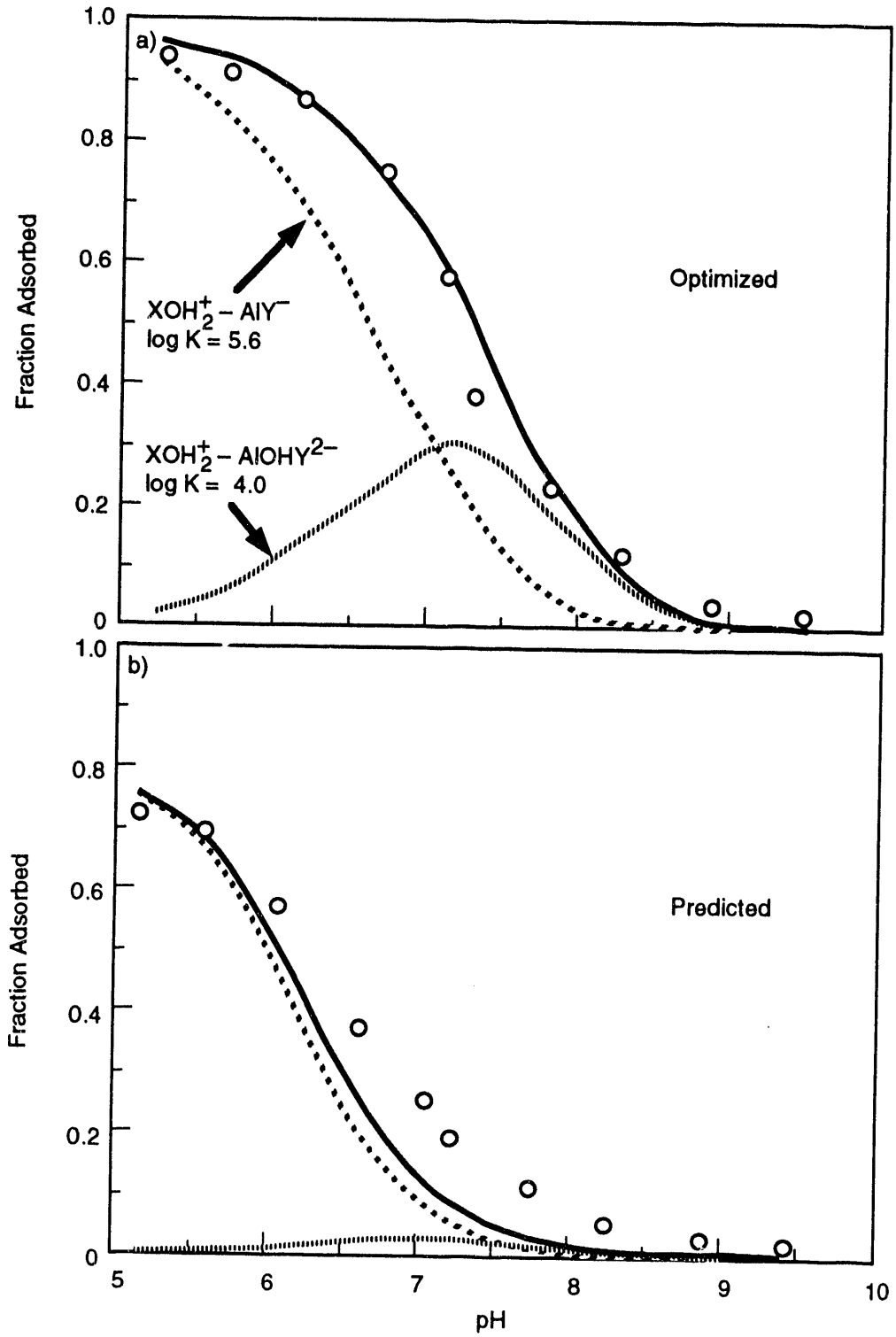

FIGURE 3. Simulation (solid curve) of 0.5 μM EDTA Adsorption by δ-Al_2O_3 (1 g/L) in a) 0.01 M $NaClO_4$ (data points) Using FITEQL to Derive Adsorption Constants for Individual Surface Species and b) 0.1 M $NaClO_4$ (data points) Using Adsorption Constants Derived from 0.01 M $NaClO_4$ Data. Dashed curves indicate contribution of individual surface species.

best fit of the data for reactions (1) and (2) and the constants derived are shown by the solid line through the data points in Figure 3a. The two sets of dashed lines (Figure 3a) represent the contribution of each adsorbed EDTA species to the total EDTA adsorbed. Using these reactions and the values for K derived from the 0.01 M $NaClO_4$ adsorption data, a shift in EDTA-only adsorption edge was predicted for a 0.1 M $NaClO_4$ suspension (solid line, Figure 3b). This prediction agrees quite well with the significant shift observed in EDTA-only adsorption edge at this ionic strength (data points, Figure 3b). Many other individual reactions and combinations of reactions were examined; however, none of these could provide an acceptable description of the observed data for both ionic strengths shown in Figure 3. Reactions for inner-sphere surface complexes predicted no shift in the adsorption edge with ionic strength and were thus inconsistent with the data, at least in the context of the TLM.

The adsorption of cobalt by δ-Al_2O_3 in the presence of equal-molar EDTA is ligand-like over the range of conditions studied (Figure 4). This behavior is due primarily to the large stability constant for the formation of the anionic $CoEDTA^{2-}$ complex (log K = 18) and is in sharp contrast to cobalt adsorption by gibbsite in the presence of equal-molar NTA (discussed above). The adsorption of cobalt in the presence of equal-molar EDTA (referred to as Co w/EDTA) is described in the context of the TLM by the following outer-sphere reactions:

$$\equiv AlOH + Co^{2+} + EDTA^{4-} + H^{+} = \equiv AlOH_2^{+} \text{---} CoEDTA^{2-} \quad :\log K = 9.3 \tag{3}$$

$$\equiv AlOH + Co^{2+} + EDTA^{4-} + 2H^{+} = \equiv AlOH_2^{+} \text{---} CoHEDTA^{2-} \quad :\log K = 4.5 \tag{4}$$

The agreement between the simulation (solid curve, Figure 4a) of Co w/EDTA adsorption at 0.01 M $NaClO_4$ (data points, Figure 4a) and reactions (3) and (4) is excellent. This simulation included EDTA adsorption reactions (1) and (2) because the dissolved aluminum competes with cobalt for the EDTA and the EDTA adsorbs to form aluminum-EDTA complexes. It is clear from the relative values of the adsorption constants for reactions (1) through (4) that cobalt-HEDTA is the most strongly bound surface complex. Using reactions (3) and (4) and the values for K derived from the adsorption data for 0.01 M $NaClO_4$ Co w/EDTA, a shift in EDTA adsorption edge was predicted for a 0.1 M $NaClO_4$ suspension (solid line, Figure 4b), which is in excellent agreement with the observed adsorption edge for Co w/EDTA at this ionic strength (data points, Figure 4b).

The modeling results shown here indicate that this mechanistic approach for modeling adsorption and its mathematical representation in terms of the TLM can be used to quantitatively describe EDTA and cobalt-EDTA adsorption by δ-Al_2O_3. The applicability of this modeling approach to quantitatively describing adsorption in the cobalt-NTA-gibbsite and cobalt-EDTA-iron oxide systems is currently being investigated. The incorporation of this mechanistic description of adsorption into solute transport codes should enhance the accuracy of predictions of radionuclide transport for intermediate-scale experiments and at DOE field sites.

Chelate Biodegradation. This research is quantifying chelate persistence in the subsurface environment and determining biological and geochemical limitations on the degradation of synthetic chelates. The research has used subsurface sediment samples from the Deep Microbiology Subprogram of DOE's Subsurface Science Program to obtain initial estimates of chelate persistence (Bolton et al., in press). Previously isolated microorganisms that degrade synthetic chelates are being used to provide information on the optimal environmental conditions for chelate biodegradation and also to provide basic information on chelate degradation metabolites and how geochemical conditions influence the persistence of chelates and the fate of chelated metals and radionuclides. These isolates or consortia are also being used in studies of chelated radionuclide adsorption and biodegradation from which combined adsorption-biodegradation models will be developed.

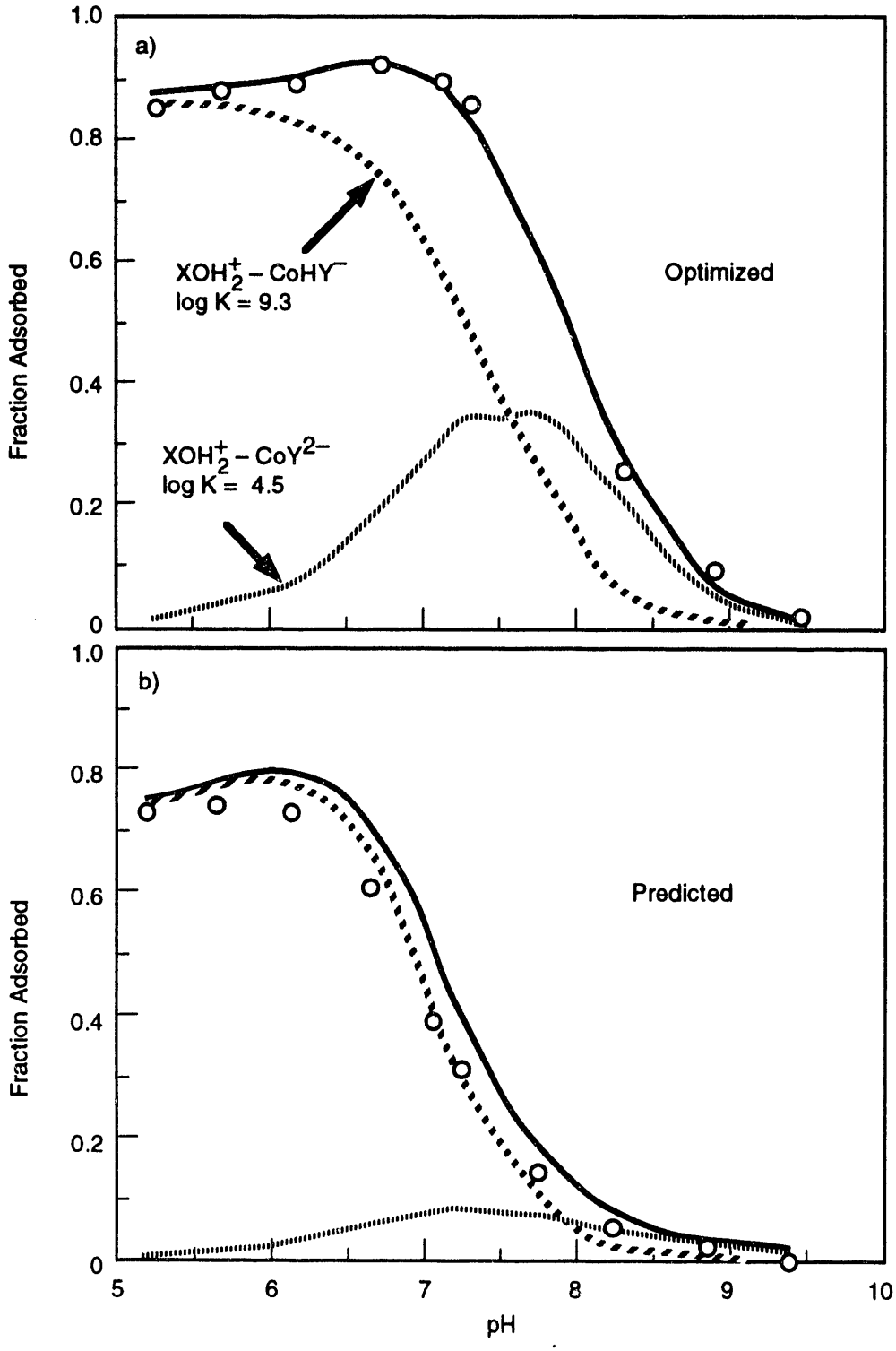

FIGURE 4. Simulation (solid curve) of 0.5 μM Cobalt-EDTA Adsorption by δ-Al_2O_3 (1 g/L) in a) 0.01 M $NaClO_4$ (data points) Using FITEQL to Derive Adsorption Constants for Individual Surface Species (dashed curves) and b) 0.1 M $NaCl_2O_3$ (1 g/L) in 0.1 M $NaClO_4$ (data points) Using Adsorption Constants Derived from 0.01 M $NaClO_4$ Data. Dashed curves indicate contribution of individual surface species.

Transport in groundwater of some radionuclides that are complexed with synthetic chelates may decrease if the synthetic chelate is degraded. The synthetic chelate NTA can be degraded in waters, aquatic and subsurface sediments, soils, and sewage; bacterial strains able to degrade NTA have also been isolated from these sources. However, because the aqueous speciation of the NTA was not specified or controlled in many past studies, it is not known what form of the NTA was degraded, and the form may have changed during the experiments. As a result, it is not possible to identify the metal-NTA complexes that were degraded based on results of past studies. In addition, metal toxicity may have influenced chelate degradation.

Thus even though there have been many studies of NTA degradation, there is currently only limited understanding of how the aqueous speciation of the NTA will influence its degradation. The aqueous speciation of synthetic chelates such as NTA varies depending on pH and on the concentrations and types of metal ions present. At low pH, metals and protons compete for the NTA, but at higher pH hydroxyl and carbonate ions compete with the NTA for the metal ion. As a result, multiple equilibria dictate the form of the chelate available for degradation.

The objective of this study was to determine how the speciation of NTA influenced NTA mineralization to carbon dioxide and to examine the hypothesis that the thermodynamic stability constant of the metal-NTA complex dictates the rate of NTA degradation. This hypothesis states that NTA complexes with metals with larger thermodynamic stability constants will degrade more slowly than those with smaller stability constants. To investigate this hypothesis, a well-defined system was used: a single microorganism in a defined aqueous phase. The NTA-degrading *Pseudomonas* strain ATCC 29600 is well characterized and so was chosen for our studies. Our approach was as follows: First, identify the simplest defined liquid medium that would support NTA mineralization by strain 29600 so that the aqueous speciation of the NTA could be controlled and modeled. Second, determine whether NTA mineralization follows first-order kinetics and determine the optimal cell concentration for mineralization. Third, confirm that $^{14}CO_2$ evolution from the mineralization of ^{14}C-labeled NTA concurred with the loss of NTA from solution. Fourth, test the hypothesis by comparing the kinetic parameters of NTA mineralization for metal-NTA complexes whose thermodynamic stability constants varied over a wide range. Last, demonstrate that mineralization of the various metal-NTA complexes was not affected by metal toxicity.

Mineralization of ^{14}C-labeled NTA to $^{14}CO_2$ occurred in the various media including nutrient-containing solution (minimal medium), pH 7 buffers {piperazine-N, N'-bis[2-ethane-sulfonic acid] (PIPES) and N-[2-hydroxyethyl] piperazine-N'-[2-ethanesulfonic acid] (HEPES)}, and deionized water, all with a similar first-order rate constant (Table 1). The asymptote calculated for the mineralization of NTA in minimal medium was significantly greater than those for water or buffer; however, the percentage increase was relatively minor (Table 1). Water and HEPES and PIPES buffers had the same calculated asymptotes (Table 1). This agreement indicates that nutrients were not necessary for the mineralization of NTA by strain 29600. This lack of need for nutrients allowed us to use a very simple system to test our hypothesis and also greatly simplified the aqueous speciation modeling of our experiments. Solutions buffered for pH were used in all subsequent experiments, because pH influences the speciation of the NTA, the metal, and the metal-NTA complex. Therefore, PIPES buffer was used and was able to maintain solutions at pH 6 or 7 ± 0.05 throughout the experiments. The PIPES buffer also has a low complexing ability for a wide range of metals, so that it would not compete with the NTA for complexing the metals in solution.

At varying concentrations of NTA, NTA mineralization followed first-order kinetics, with mineralization being directly proportional to the NTA concentration, as demonstrated by the similar first-order rate constants for NTA concentrations ranging from 52.3 to 0.05 μM (Table 2). The calculated asymptote for 0.52 μM NTA was significantly greater than those for the other concentrations, but the percentage increase was actually relatively minor (Table 2). The ability of

TABLE 1. First-Order Rate Constants and Asymptotes for NTA Mineralization to CO_2 by Strain 29600 in Various Media. NTA was present at a concentration of 5.23 μM and strain 29600 was present at a cell density of 10^8 CFU/ml.

Medium	Rate Constant, per hour	Asymptote, %
Water	0.041a[(a)]	58a
HEPES (pH 7)	0.049a	56a
PIPES (pH 7)	0.043a	60a
Minimal Medium (pH 7)	0.044a	67b

(a) Numbers in the same column that are followed by the same letter are not significantly different (95% confidence interval).

TABLE 2. First-Order Rate Constants and Asymptotes for NTA Mineralization to CO_2 by Strain 29600 at Various NTA Concentrations. Strain 29600 was present at a cell density of 10^8 CFU/ml in 0.01 M PIPES (pH 7) buffer.

NTA Concentration, μM	Rate Constant, per hour	Asymptote, %
52.3	0.030a[(a)]	51a
5.23	0.034a	53a
0.52	0.036a	58b
0.05	0.031a	51a

(a) Numbers in the same column that are followed by the same letter are not significantly different (95% confidence interval).

strain 29600 to mineralize low NTA concentrations (i.e., $\leq$5.23 μM) makes this model system comparable to groundwater containing synthetic chelates at the Oak Ridge and Maxey Flats nuclear waste sites. The cell density used in the studies described here was 10^8 colony-forming units (CFU) per milliliter. At this cell density, there was no lag period for NTA mineralization when NTA-induced cells were used, and viable cell numbers remained constant throughout the experiment. As cell density decreased to $\leq$6.7 log CFU/ml, a lag in the mineralization of NTA was seen, although cell numbers remained approximately the same throughout the experiment. We wanted no growth of strain 29600 during our experiments, to ensure similar cell densities in the various metal-NTA experiments and allow for first-order kinetic modeling of NTA mineralization. The lack of measurable growth of strain 29600 resulted from the absence of growth nutrients during the mineralization experiments, the low concentration of organic compound (5.23 μM), and the high starting cell density.

Measuring the evolution of $^{14}CO_2$ from ^{14}C-labeled NTA provided a good indicator of the removal of NTA from solution. There was an inverse relationship between the amount of $^{14}CO_2$ evolved and the disappearance of NTA from solution (Figure 5a). A substantial amount of $^{14}CO_2$ was initially dissolved in the aqueous phase, particularly during the early phases of NTA mineralization, and was released into the head space on acidification (Figure 5b). The initial rapid rate of $^{14}CO_2$ production by strain 29600 in the aqueous phase apparently exceeded the rate of $^{14}CO_2$ exchange at the liquid-air interface; as a result there was an initial increase in the aqueous concentration of dissolved $^{14}CO_2$. This behavior will result in underestimation of the extent of mineralization of NTA at any given time. Subsequent measurements of NTA mineralization involved acidification at each sampling time to determine total $^{14}CO_2$ produced. Our trapping efficiency for $^{14}CO_2$ was 100%; all of the ^{14}C was accounted for by either $^{14}CO_2$ or ^{14}C remaining in solution.

The hypothesis tested with our simple aqueous system was that the stability of the metal-NTA complex dictates the rate of NTA degradation. Specifically, the NTA degradation rate for various metal-NTA complexes would decrease as the thermodynamic stability constants for the metal-NTA complex increase. To ensure that cobalt, copper, and nickel would be predominantly free metal ions for our metal treatments without NTA, we chose to use PIPES buffer at pH 6 rather than pH 7. This adjustment ensured that, for cobalt, copper, and nickel, the free metal ion was the dominant metal species in solution at 5.23 μM, with minimal formation of metal hydroxides or carbonates, as calculated by the aqueous speciation model MINTEQ (Table 3). For example, at pH 6 copper is present predominantly as Cu^{2+} (Table 3), but at pH 7 more

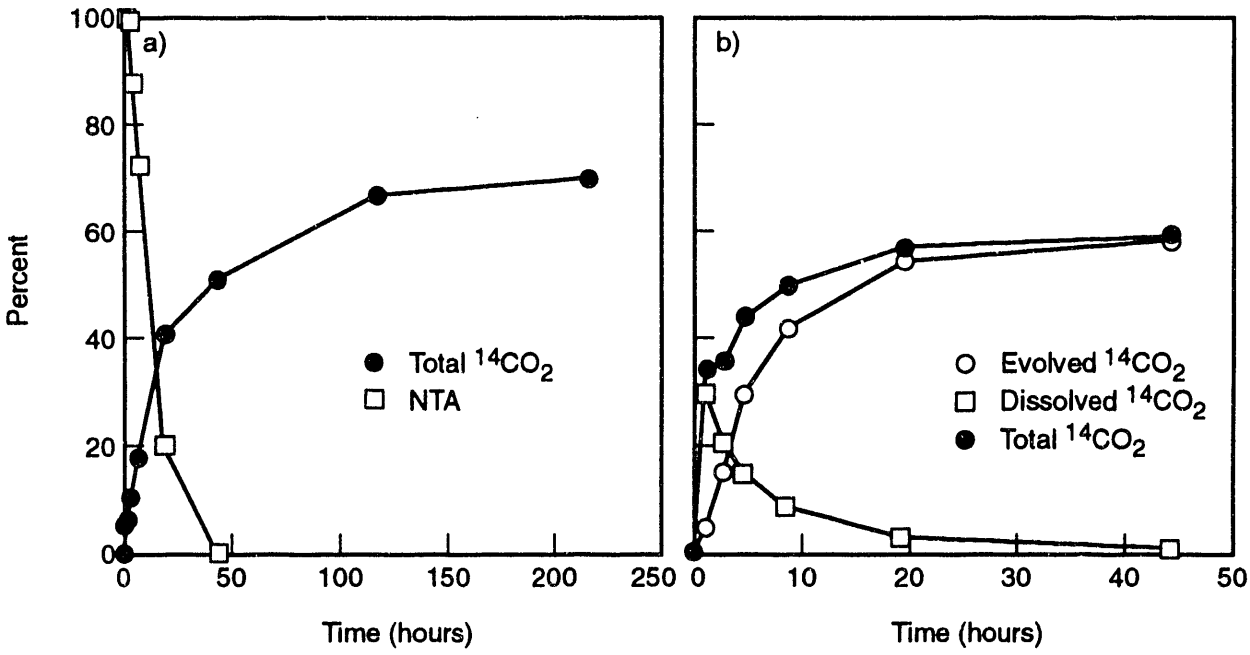

FIGURE 5. Mineralization of a) 523 and b) 5.23 μM NTA in 0.01 M PIPES pH 7 Buffer by Strain 29600 at 10^8 CFU/ml. a) Disappearance of 523 μM NTA and appearance of total $^{14}CO_2$ (evolved + dissolved). b) Appearance of evolved $^{14}CO_2$ and dissolved $^{14}CO_2$ and their sum (total $^{14}CO_2$) at an initial NTA concentration of 1 μM. Evolved $^{14}CO_2$ was assayed in the initial CO_2 trap. Dissolved $^{14}CO_2$ was assayed by placing a fresh CO_2 trap in the head space and acidifying the sample to drive off dissolved $^{14}CO_2$.

than 50% of the copper would be present as $Cu(OH)^{\circ}_2$ (data from MINTEQ). Iron and aluminum were present as hydroxide species in solution at pH 6 (Table 3). Aqueous speciation of NTA in the various metal-NTA solutions demonstrated that the metal-NTA complex was the dominant form of NTA in solution (Table 4). The various metal-NTA complexes were mineralized at different rates (Table 5), demonstrating a direct effect of the complexed metal on the mineralization of NTA. The metals were chosen to provide a range in their thermodynamic formation constant for the metal-NTA complexes (Table 5). No relationship was discernible between the thermodynamic stability constants for the various metal-NTA complexes and the first-order rate constants, the asymptotes, or the initial rates of NTA mineralization (Table 5). The mineralization of nickel-NTA, copper-NTA, and aluminum-NTA was less than that of the other metal-NTA complexes, as indicated by their smaller rate constants and asymptotes. These data disprove our stability constant hypothesis; neither the thermodynamic stability nor the formation constant of the metal-NTA complex correlated with the rate of NTA mineralization.

TABLE 3. Aqueous Speciation of the Metals in pH 6 Buffer (0.001 M PIPES, 0.01 M KNO_3) Containing 5.23 μM Metal

Metal	Aqueous Speciation of Metal[a]
Co	Co^{2+} (100%)
Fe	$FeOH_2^+$ (98.5%); $Fe(OH)_3$ (1.5%)
Al	$Al(OH)_3$ (46%); $Al(OH)_2^+$ (42%); $AlOH^{2+}$ (6%); $Al(OH)_4^-$ (5%); Al^{3+} (1%)
Cu	Cu^{2+} (95%); $CuNO_3^+$ (2.5); $CuOH^+$ (2.5); $Cu(OH)_2$ (1%)
Ni	Ni^{2+} (100%)

(a) Metal species (percent of the total metal present as listed species) calculated from MINTEQ (Felmy et al. 1984).

TABLE 4. Aqueous Speciation of the NTA in pH 6 Buffer (0.001 M PIPES, 0.01 M KNO_3) containing 5.23 μM metal and NTA

Metal-NTA Complex	Aqueous Speciation of NTA[a]
no metal	$HNTA^{2-}$ (100%)
Co	$CoNTA^-$ (88%); $HNTA^{2-}$ (12%)
Fe	$FeOHNTA^-$ (96%); FeNTA (2%); $HNTA^{2-}$ (2%)
Al	$AlOHNTA^-$ (78%); AlNTA (16%); $Al(OH)_2^+$ (2.5%); $Al(OH)_3$ (2.5%); $Al(OH)_2NTA^{2-}$ (1%)
Cu	$CuNTA^-$ (100%)
Ni	$NiNTA^-$ (97%); $HNTA^{2-}$ (3%)

(a) NTA species (percent of the total NTA present as listed species) calculated from MINTEQ (Felmy et al. 1984).

Some of the metals we used, such as nickel, copper, and aluminum, which gave the lowest rates of NTA mineralization (Table 5), can also be toxic to microorganisms. However, the mineralization of ^{14}C-labeled glucose was not inhibited by any of the metals at 5.23 μM (Figure 6a). Glucose is a non-complexing organic, which means that the metals would be predominantly present as either the free metal or the metal hydroxide ions in solution (Table 3). If these ions were being taken up by the cell, they were not inhibiting cellular respiration or the generation of $^{14}CO_2$ from ^{14}C-labeled glucose (Figure 6a). However, the amount of the metal ion in the cell or its location may differ when it is taken up as the free metal ion rather than the metal-NTA complex. To determine whether this was the case, the metals were also added as the metal-NTA complex to cells induced on NTA, and the incubations were analyzed for ^{14}C-labeled glucose mineralization. The mineralization of ^{14}C-labeled glucose was not inhibited by any of the metal-NTA complexes at 5.23 μM (Figure 6b). Because the cells were induced on NTA, both NiNTA and glucose could be taken up by the cell and mineralized. That both were indeed taken up was demonstrated by the mineralization of ^{14}C-labeled glucose when unlabeled NTA was present (Figure 6b) and by the mineralization of ^{14}C-labeled NTA when unlabeled glucose was present (data not shown). This indicated that the metal itself did not inhibit general cellular metabolism, but that rather the complexed metal was influencing only NTA mineralization.

TABLE 5. First-Order Rate Constants, Asymptotes, Initial Mineralization Rates, and Thermodynamic Stability or Formation Constants (log K_f) for Various Metal-NTA Complexes. Strain 29600 was present at a cell density of 10^8 CFU/ml in pH 6 buffer (0.001 M PIPES, 0.01 M KNO_3) containing equal-molar metal and NTA (5.23 μM).

Metal-NTA Complex	Rate Constant, per hour	Asymptote, %	Initial Mineralization Rate,[a] % per hour	log K_f[b]
no metal	0.672a[c]	59ab	40a	0
Co	0.260b	57b	15b	11.7
Fe	0.209b	65a	14b	17.8
Al	0.124c	60ab	7c	13.7
Cu	0.114cd	41c	4cd	14.2
Ni	0.063d	34d	2d	12.8

(a) Rate constant multiplied by the asymptote.
(b) Obtained from the aqueous speciation model MINTEQ for pH 6, 25°C, 0.01 M KNO_3 (Felmy et al. 1984).
(c) Numbers in the same column that are followed by the same letter are not significantly different (95% confidence interval).

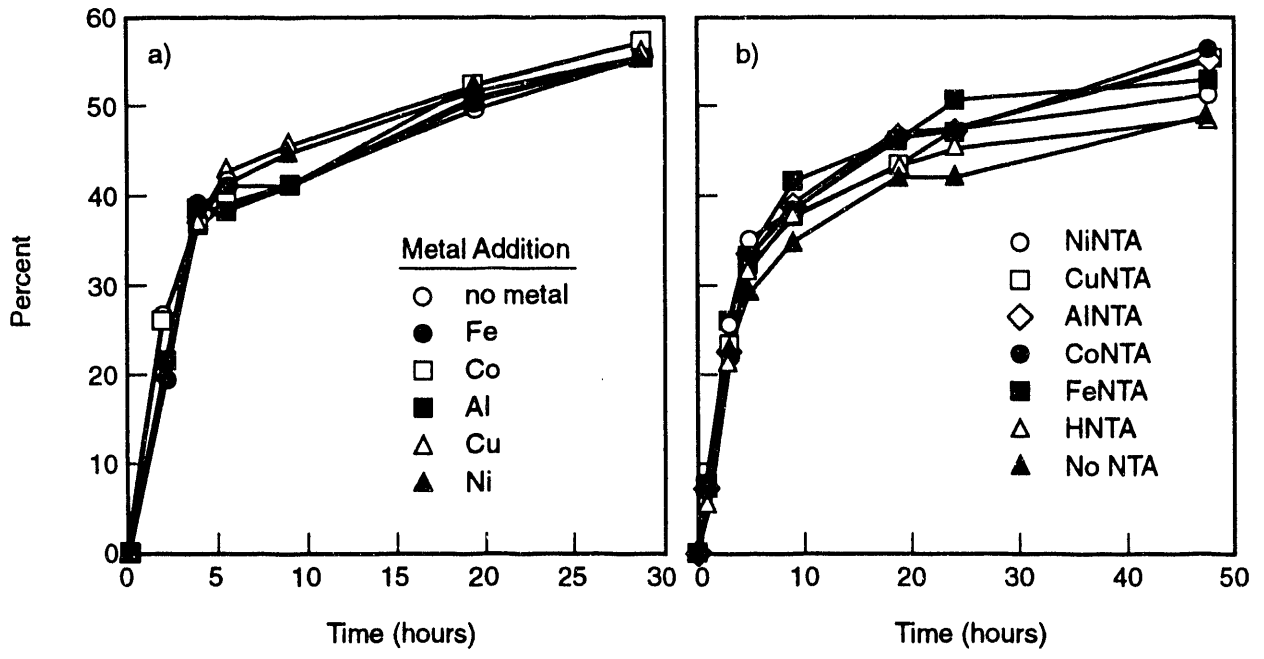

FIGURE 6. Mineralization of Glucose at 5.23 μM by Strain 29600 at 10^8 CFU/ml with a) Various Metals or b) Various Metal-NTA Complexes Separately Added at 5.23 μM in pH 6 Buffer (0.001 M PIPES, 0.01 M KNO_3)

The differences in mineralization of the various metal-NTA complexes may be due to differences in the lability of the various metal-NTA complexes. Lability is a kinetic property of a metal-chelate complex that represents the ability of the chelated metal to exchange for a free metal in solution. This exchange or dissociation is related to the ability and frequency of making and breaking the metal-carboxyl oxygen and the metal-nitrogen bonds of NTA. The lability of the metal-NTA complex also determines the rate at which NTA is redistributed among the thermodynamically favorable species in solution. If strain 29600 was able to take up or mineralize only the $HNTA^{2-}$ form of NTA, this limitation would account for the variations in NTA mineralization observed when different metals are complexed. When no metals are present, the free acid $HNTA^{2-}$ is the predominant form of NTA in solution from pH 5 to 8. For a metal-NTA complex, the exchange of the metal with a hydrogen ion to form $HNTA^{2-}$ will be much slower for a kinetically inert metal complex than for a more labile complex. Information on the lability of metal-NTA complexes is limited, but the lability of various metal-EDTA complexes is known to differ depending on the complexed metal. Among divalent transition metals, nickel-EDTA is relatively inert. Isotopic exchange measurements of the metal in cobalt-EDTA and nickel-EDTA show that cobalt-EDTA is more labile than nickel-EDTA by a factor of 25. Although no direct measurements of metal exchange rates have been published for cobalt-NTA and nickel-NTA, it is reasonable to conclude, given the similarity of the coordinating moieties, that the relative labilities of cobalt-NTA and nickel-NTA are similar to those observed for the corresponding metal-EDTA chelates. Thus, the presumed nonlability of nickel-NTA relative to cobalt-NTA is consistent with nickel-NTA having a lower rate of NTA mineralization.

In summary, NTA mineralization occurred in simple aqueous systems, with mineralization following first-order kinetics. Thermodynamic stability constants did not indicate the degradability of specific metal-NTA complexes when the metals were present at non-inhibitory concentrations. Our new hypothesis to explain the differences in NTA mineralization when NTA is complexing different metals is that the lability of the various metal-NTA complexes dictates the rate of NTA degradation. If this hypothesis

holds, a mechanistic understanding of metal-NTA degradation will require investigations of the lability of various metal-NTA complexes and of the way the metal-determined lability influences the mineralization of NTA.

Chelate Adsorption - Biodegradation Interactions. This research is investigating the mutual interactions of chelate adsorption and biodegradation and the influence of microbial activity on chelate and radionuclide adsorption. During FY 1992, these interaction studies focused on the limitation imposed on chelate degradation rates by chelate adsorption and desorption. The hypothesis being tested is that adsorbed chelates are unavailable for degradation. The chelate becomes available for degradation only through desorption of the chelate into the aqueous phase. Thus the rate of chelate desorption limits the degradation rate. To test this hypothesis, we selected a model system consisting of NTA or cobalt-NTA, the NTA-degrader *Pseudomonas* strain ATCC 29600, and the naturally occurring mineral gibbsite (as the adsorbent).

Background studies were conducted in FY 1991 to determine 1) the rates of degradation of NTA and metal-NTA chelates by strain 29600 in the absence of chelate adsorption and 2) the adsorption of NTA and cobalt-NTA by gibbsite in the absence of microbial activity. Integration of this information was essential for the design and interpretation of NTA-gibbsite-*Pseudomonas* sp. experiments to address our hypothesis. The integration of chemical and biological information and the design of interaction experiments for this system formed the basis of the interaction studies conducted in FY 1992. Briefly the design is as follows: A known quantity of ^{14}C-labeled NTA adsorbed to gibbsite particles is introduced into a suspension of *Pseudomonas* sp. At this point more than 99% of the NTA in the system is adsorbed to the gibbsite; that is, the solution concentration of NTA, which is readily available for degradation, is less than 1% of the total NTA in the system. The NTA begins to desorb immediately and thus, according to our hypothesis, becomes available for degradation. However, the form of the NTA in solution, and thus the degradation rate, depend on the pH of the solution. The speciation for NTA-only and cobalt-NTA systems and degradation rates for the individual aqueous species are summarized in Table 6. The pH of the suspension is buffered to minimize shifts in speciation during the course of the experiment. The rate of NTA mineralization as a function of time is measured as evolved $^{14}CO_2$ in the NTA-gibbsite-*Pseudomonas* sp. system and compared to a control having the same aqueous NTA species, solution pH, and total NTA. Experiments have so far been conducted at pH 6 and 8 for the NTA-only system, in which the dominant species are $HNTA^{2-}$ and $AlOHNTA^{-}$, respectively; further experiments will be conducted in FY 1993 for the cobalt-NTA system at pH 7, where the dominant species is $Co\text{-}NTA^{-}$. The total NTA or cobalt-NTA concentration in the systems is 1 μM and the solid-to-solution ratio is 7.5 g/L. These conditions are identical to those used in the abiotic NTA adsorption experiments described above in the section on chelated radionuclide adsorption.

TABLE 6. NTA and Cobalt-NTA Aqueous Speciation as a Function of pH in the Presence of Aluminum from the Dissolution of Gibbsite

Chelate	pH	Solution Species
NTA	6.0	AlOHNTA (85%), AlNTA (15%)
	7.0	AlOHNTA (45%), HNTA (45%)
	8.0	HNTA (90%)
Co-NTA	6.0	AlOHNTA (60%), CoNTA (20%), AlNTA (20%)
	7.0	CoNTA (85%), AlOHNTA (8%), HNTA (7%)
	8.0	CoNTA (35%), HNTA (65%)

Mineralization of NTA is significantly slower in systems where the NTA is initially adsorbed to the gibbsite. For example, NTA degradation at pH 8 in the absence of gibbsite (curve A, Figure 7) is very rapid, essentially complete within 1 h, but mineralization of the NTA that is initially adsorbed to the gibbsite is much slower, with the asymptote not yet being reached at 50 h (Curve B, Figure 7).

The NTA mineralization curves with and without the presence of gibbsite were analyzed using a first-order model of the two-step process,

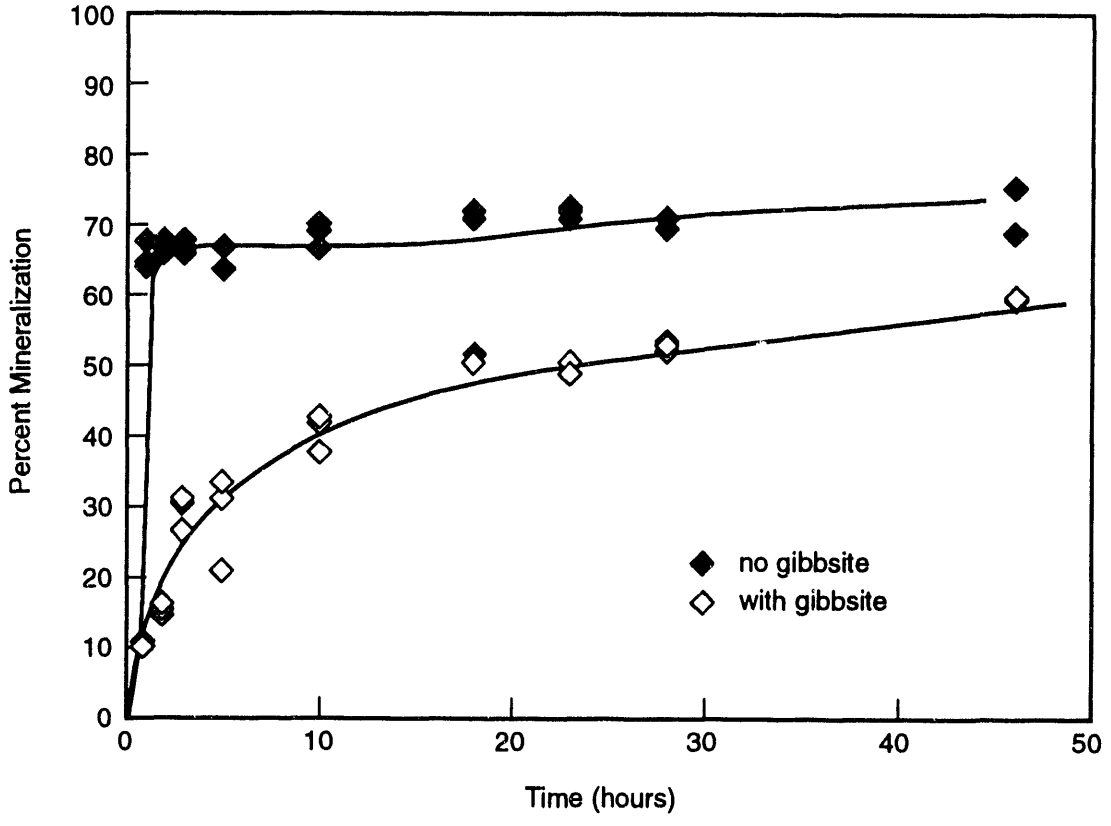

FIGURE 7. Mineralization of NTA at pH 8 of 1 μM Solution NTA without Gibbsite Present and 1 μM NTA Initially Adsorbed to Gibbsite

$$\underset{}{\textit{NTA adsorbed}} \xrightarrow[\textit{(desorption)}]{(k_d)} \qquad \textit{NTA aqueous} \xrightarrow[\textit{(mineralization)}]{(k_{HNTA})} CO_2 \qquad (5)$$

This analysis yields rates for solution mineralization of NTA, $k_{HNTA} = 3.0\ h^{-1}$, and desorption $k_d = 0.042\ h^{-1}$. Thus the net mineralization rate for NTA in the presence of gibbsite is less than that observed for NTA in solution by a factor of 70.

In FY 1993 we will conduct experiments at lower cell densities (similar to those used in the initial NTA mineralization studies) to obtain mineralization rates in the controls (no adsorption). The results will allow more accurate determination of first-order rate constants for NTA mineralization. The results to date demonstrate that NTA degradation is limited by adsorption (Figure 7) and that our simple model [(Equation (5)] must be modified to include a two-step desorption process. These limits will be investigated in more detail in FY 1993.

Collaborative Intermediate Scale Experiments. A collaborative intermediate-scale experiment, which is multidisciplinary in scope, was designed in FY 1992. This project supplied data and aided in the design of a collaborative experiment concerning cobalt(II) and cobalt(III)-EDTA transport at an intermediate scale. The experiment is a coupled geochemical-microbial experiment. Results from the project (Girvin et al., in press) suggest that subsurface microorganisms might be exposed to cobalt(III)-EDTA if cobalt(II) and EDTA were co-disposed. This information was then used in another project to investigate the enzymatic reduction of cobalt(III)-EDTA to cobalt(II)-EDTA by iron-reducing microorganisms. Iron-reducing microorganisms can reduce cobalt(III)-EDTA to cobalt(II)-EDTA, suggesting

that a geochemical-microbial intermediate-scale experiment investigating cobalt(II)-EDTA oxidation to cobalt(III)-EDTA by manganese oxides could be coupled to a microbial experiment investigating the microbial reduction of cobalt(III)-EDTA to cobalt(II)-EDTA by iron-reducers.

Investigation of cobalt-EDTA adsorption by several iron oxides that differ in their crystallinity and crystal structure began in FY 1992. Our objective is to determine the relative importance of the different iron oxides occurring at DOE sites as chelate sorbents; these experiments will also support the cobalt-EDTA-iron oxide intermediate-scale experiments being conducted within the Co-Contaminant Chemistry Subprogram of DOE's Subsurface Science Program. In general, the behavior of cobalt-EDTA adsorption by iron oxides is completely different from that observed for δ-Al_2O_3 under similar experimental conditions. For example, the Co w/EDTA adsorption edge for an equal-molar cobalt-EDTA, α-FeOOH system (Figure 8) is significantly different from that observed for a corresponding δ-Al_2O_3 system (Figure 4a). The behavior of the cobalt is intermediate between that observed for the cobalt-EDTA-δ-Al_2O_3 system and that of the cobalt-NTA-gibbsite system (Figure 1a). In the case of the cobalt-EDTA-α-FeOOH system (Figure 8), the shape of the Co w/EDTA adsorption edge can be understood in terms of the high stability constant for iron(III)-EDTA (log K = 25), the resultant solubilization of α-FeOOH by the EDTA, and the subsequent competition of Fe^{3+} with Co^{2+} for the EDTA. Our preliminary conclusion, based on equal-molar cobalt-EDTA adsorption on δ-Al_2O_3 (Figure 4a), gibbsite (data not shown), and α-FeOOH (Figure 8) is that each chelated radionuclide will exhibit different adsorption behavior, depending on the bulk solubility and surface properties of the metal-oxide adsorbent.

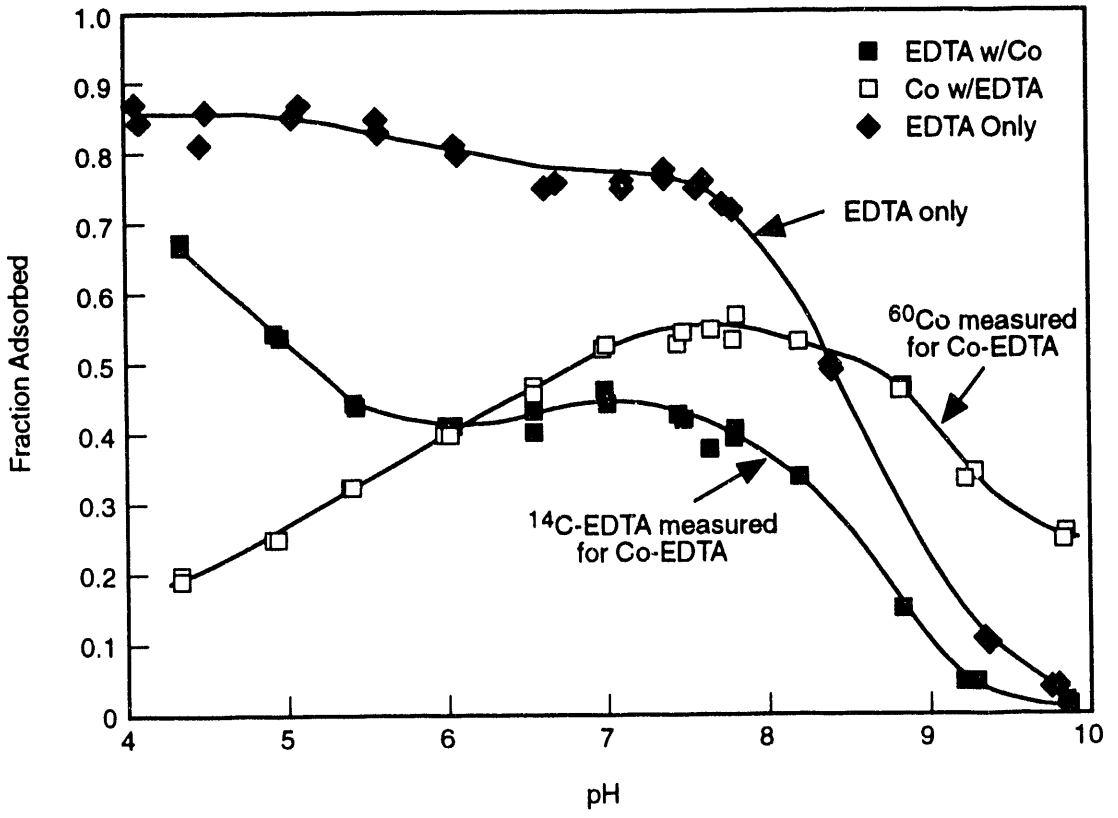

FIGURE 8. Adsorption of 1 μM EDTA and Cobalt-EDTA by Goethite (2 g/L) in 0.01 M $NaClO_4$

Future Research

The continued investigation of chelated radionuclide adsorption on oxides, smectitic clays, and subsoils dominated by oxides and/or clays, along with biodegradation studies of synthetic chelates and microbial-driven geochemical modifications of the subsurface environment, will extend the applicability of this research to several DOE sites. In addition, surface-catalyzed oxidation of cobalt(II)-EDTA to cobalt(III)-EDTA by iron and manganese oxides will be investigated to determine the mechanisms and conditions under which cobalt oxidation may be occurring at DOE field sites. Finally, adsorption-biodegradation interactive studies will be completed for the NTA, cobalt-NTA, *Pseudomonas* strain 29600, and gibbsite system, and new studies will be started for an analogous EDTA system, using an EDTA-degrading organism and/or consortium (Nortemann 1992) and either gibbsite or an iron oxide as the model subsurface sorbent. These combined chemical-microbiological studies on progressively more complex systems have two objectives. The first is to quantify the effects of each process on the other, and the second is to provide the critical background and process information in support of intermediate-scale experiments that are using these chelates, organisms, and model subsurface sorbents to determine the effect of flow on chemical-microbiological interactions. Mathematical representations of chemical, microbiological, and flow processes and their influences on one another will eventually be incorporated into transport codes to simulate and predict radionuclide and chelate mobility. The understanding developed within this project, combined with model development in other projects within the Subsurface Science Program, will aid in the evaluation of effective remediation strategies at DOE sites where chelates and radionuclides have been co-disposed.

References

Bolton, H., Jr., S. W. Li, D. J. Workman, and D. C. Girvin. "Biodegradation of Synthetic Chelates in Subsurface Sediments from the Southeast Coastal Plain." *Journal of Environmental Quality* (in press).

Brown, G. E. 1990. "Spectroscopic Studies of Chemisorption Reaction Mechanisms at Oxide-Water Interfaces." In *Reviews in Mineralogy, Vol. 23, Mineral-Water Interface Geochemistry*, ed. M. F. Hochella, Jr., and A. F. White, pp. 309-363. Mineralogical Society of America, Washington, D.C.

Felmy, A. R., D. C. Girvin, and E. A. Jenne. 1984. *MINTEQ - A Computer Program for Calculating Aqueous Geochemical Equilibria*. EPA 600/3-84-032, National Technical Information Service, Springfield, Virginia.

Girvin, D. C., P. L. Gassman, and H. Bolton, Jr. "Adsorption of Aqueous Cobalt Ethylenediaminetetraacetate by δ-Al_2O_3: Effects of Oxidation State, Ionic Strength, and Sorbent Concentration." *Soil Science Society of America Journal* (in press).

Hayes, K. F. 1987. *Equilibrium, Spectroscopic and Kinetic Studies of Ion Adsorption at the Oxide/Aqueous Interface*. Ph.D. Dissertation, Stanford University, Stanford, California.

Nortemann, B. 1992. "Total Degradation of EDTA by a Mixed Culture and a Bacterial Isolate." *Applied Environmental Microbiology* 58:671-676.

Chemical Desorption, Dissolution, and Partitioning

C. C. Ainsworth

A variety of solid and liquid waste materials were discharged to the ground at DOE production sites over a 40-year period. Unplanned releases and direct discharges have contaminated soils and groundwaters at many DOE sites. Remediation of groundwater plumes is often viable, but the treatments generally neglect the mass of material sorbed to the solid matrix, which can act as sources for future contaminant plumes and may involve a mass of contaminant significantly larger than that observed in a plume. However, the interactions and reactions that control the mobilization of solid phase contaminants are not

yet well understood. Reactions that control the release of sorbed contaminants from subsurface materials (e.g., desorption, dissolution) must be better understood to facilitate prediction of contaminant mobility and identification of rational geochemical strategies to enhance and hasten restoration of waste sites.

FY 1992 Research Highlights

This project was conducted under the auspices of PNL's Environmental Science Research Center, as part of its basic program to develop new scientific knowledge to use natural processes in subsurface environmental restoration. Research has focused on three areas: 1) collection and characterization of metal-contaminated materials from beneath a disposal pond (for use in studies of mobilization of metals from contaminated natural materials); 2) the effect of residence time and calcite recrystallization on the sorption/desorption of cadmium, cobalt, copper, manganese, nickel, and lead; and 3) the effect of recrystallization of iron oxides on the desorption of cadmium, cobalt, and lead as affected by residence time. In FY 1992, research focused specifically on the collection, characterization, and mobilization of uranium from sediments collected beneath the 300 Area process ponds at the Hanford Site and on the effect of residence time on metal/radionuclide sorption by calcite.

Uranium in the 300 Area Pond Sediments and Its Mobilization. The two 300 Area process ponds are unlined surface impoundments constructed in 1943 and 1948 that were used for disposal of radioactively (principally uranium) and chemically contaminated wastewaters from the 300 Area of the Hanford Site until they were retired in 1975. The geologic material underlying the 300 Area process ponds is part of the Hanford formation (consisting of coarse-grained deposits); the deposits are typically graded materials from boulders to sands, with thin layers of silts, clays, and caliche ($CaCO_3$); in addition, carbonate coatings on gravels occur sporadically throughout the pond profiles. More than 62,000 kg of uranium was disposed of to the two ponds; other radionuclides also disposed of to the ponds included small quantities of ^{60}Co, ^{234}Th, and ^{137}Cs. The contaminant inventory disposed of to both ponds is estimated as silver (1,900 kg), cadmium (140 kg), chromium (8,000 kg), copper (110,000 kg), mercury (100 kg), lead (8,000 kg), nickel (18,000 kg), and zinc (8,000 kg).

Seventeen samples were collected from beneath the 300 Area process ponds; the reactive mineral phases ($CaCO_3$, iron oxides, clays) observed in these samples are common to a number of other DOE locations. These samples represent a profile by 1-m intervals extending to about 8 m below the pond surface and about 2 m below the saturated zone. Extensive secondary $CaCO_3$ (caliche) layers about 1.5 m below the pond floor proved to contain metals in concentrations that are greater than in the other sampled layers by one to three orders of magnitude. Heavy metals in the $CaCO_3$ layer include copper, uranium, chromium, nickel, lead, zinc, and mercury (Table 1). Although the total concentration of cobalt is low in the sampled sediments, it is believed that the total γ-ray activity (approximately 2500 Bq/g) is due to ^{60}Co and ^{137}Cs.

During FY 1992, studies were initiated on those process pond caliche sediments that are highly contaminated with uranium and copper, to investigate the solubilization of these metals. In these studies, sediments were equilibrated with water and the resulting aqueous phase was sampled with time. The aqueous concentrations of calcium, copper, sodium, magnesium, uranium, chlorine, sulfate, and dissolved inorganic carbon reached their maximum levels within approximately 24 h and remained constant throughout the 96-day study. Data collected to date from solubilization studies suggest that the soluble uranium is present as the uranium(VI) hydroxide schoepite (UO_2OH_2). Aqueous copper concentrations observed in these studies were calculated to be in equilibrium with tenorite (CuO). The major uranium species were calculated to be the carbonato complexes $UO_2CO_3^{\circ}$ and $UO_2(CO_3)^{2-}$. Geochemical modeling suggests that if the partial pressure of carbon dioxide (pCO_2) is increased, a significant increase in the uranium(VI) aqueous concentration will result; for example, if the pCO_2 is increased by a factor of ten, the aqueous uranium(VI) concentration is calculated to increase by a factor of 6 to 8 (Figure 1).

TABLE 1. Solid Phase Concentrations ($\mu g/g$) of Selected Metals from Two Sediment Profiles in the 300 Area North Process Pond. NP-4 (0.9- and 1.2-m depths) represents a profile through a caliche layer, and NP-1 (1.4-, 1.8-, 4.9-, and 7.6-m depths) is a profile that did not have a caliche layer present.

	Depth, m					
Element	0.9	1.2	1.4	1.8	4.9	7.6
Cu	15000	4900	32400	5540	1740	353
U	3100	3510	1880	386	59	45
Cr	1417	1490	737	283	43	<32
Ni	530	600	623	230	43	34
Zn	187	200	166	115	112	108
Pb	119	127	98	24.7	9	10
Ag	320	373	116	17	4.2	<4

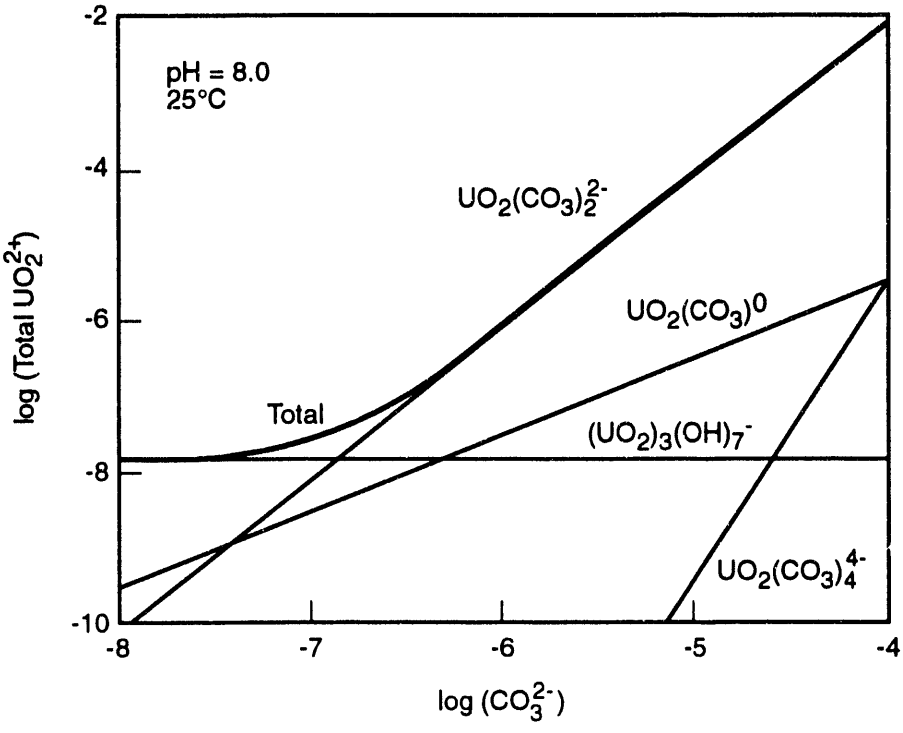

FIGURE 1. Calculated Total Aqueous Uranium (VI) Concentration and UO_2^{2+} Speciation in Equilibrium with Schoepite as a Function of CO_3^{2-} Concentration at pH 8.0 and 25°C

Effect of Calcite Recrystallization on the Sorption of Metals as a Function of Residence Time. In the environments surrounding DOE waste sites, and in particular at the Hanford Site, sorption of aqueous divalent metal contaminants by calcite ($CaCO_3$) presents a potentially significant mineral phase for scavenging contaminant metals in calcareous surface, subsurface, and groundwater environments. As noted above, a discontinuous caliche layer is present in the sediments below the 300 Area process ponds and appears to be a major sink for many contaminants of interest (Table 1).

Scavenging of divalent metal cations (Me^{2+}) by $CaCO_3$ is generally a surface-localized process. Sorption to the calcite surface typically occurs either by exchange with the surface calcium or by complexation to the carbonate groups bound in the hydrated layer. However, the sorption

process varies for different sorbate metals and is not necessarily straightforward. Zachara et al. (1991) found that 1) a series of divalent metals sorb to calcite in the order cadmium > zinc ≥ manganese > cobalt > nickel; 2) desorption is correlated to metal hydration energies, (the lower the hydration energy, the less can be desorbed); 3) cadmium and manganese behaved like a surface precipitate or solid solution; and 4) zinc, cobalt, and nickel appeared to remain on the calcite surface as a hydrated complex. That study did not follow the sorption process beyond 48 h; however, even in that length of time the magnitude of sorption for all of the metals studied was sufficiently large to suggest that calcite could act as an important sorbent. Although several other studies have addressed metal-calcite interactions over relatively short times, little is known about the sorption process beyond the initial rapid uptake of metals. The same long-term process is hypothesized to occur for many metals of interest and should be correlated with the recrystallization rate of the calcite itself.

Laboratory studies of metal adsorption were performed to quantify the influences of pH, metal ionic radii, and free energy of hydration (Δ^0G_{hyd}) on the long-term adsorption/desorption behavior of metals on calcite. The fractional sorption of divalent cadmium, cobalt, copper, manganese, and nickel to calcite increases as a function of pH. Examples of the pH edges for cadmium, nickel, and copper are shown in Figure 2. The pH adsorption edge for all the metals except copper increased with pH. That for copper increased with pH until about pH 8.0; the decreasing sorption beyond pH 8 that was observed for copper is believed to be the result of the increasing dominance of the aqueous $Cu(CO_3)_2^{2-}$ species. In all cases, however, the fractional increase parallels the decrease in the aqueous Ca concentration. Although the sorption behavior of the metals shown in Figure 1 could also be caused by precipitation of Me-carbonate, -hydroxide, or -hydroxycarbonate solid, the 24-h pH edge data for all metals are consistent with a surface exchange reaction

$$Ca_{(surface)} + Me^{2+}_{(aq)} = Me_{(surface)} + Ca_{(aq)} \quad (6)$$

in which only the uncomplexed divalent metal exchanges with surface calcium.

With time, the aqueous phase concentrations of all of the metals except copper tend to decrease, as a result of a slow sorption process that is believed to be related to the recrystallization of the calcite (Figure 2). The rate of metal fractional sorption beyond 24 h appears to be different for each of the metals and is a reflection of the surface Me^{2+} concentration, the recrystallization rate, and their dependence on pH. Even though the long-term sorption rate process is not considered first order, the disappearance of the metal from solution can be modeled as a pseudo-first-order reaction.

The first-order rate constant (k) for metal uptake after 24 h is not constant over the pH range of interest (Figure 3). The change in k that occurs with pH, however, reflects the variation in surface concentration of a given metal with pH, and hence the pseudo-first-order rate constant's dependence on the initial (24-h) surface loading.

These preliminary results suggest that the initial sorption of the Me^{2+} metals currently under study is 1) fast and related to the pH, 2) dependent on the aqueous metal speciation, and 3) dependent on the aqueous calcium concentration. After the initial sorption process has occurred, however, further uptake of cadmium, cobalt, manganese, and nickel is dependent on the surface concentration of the Me^{2+} species and the rate of calcite recrystallization, but independent of the metal itself. This independence may be a result of the fact that all of the metals examined to date have similar ionic radii and therefore would not be limited by size constraints. Copper incorporation into calcite, on the other hand, appears to be minimized by the severe distortion in the six-coordinate octahedron caused by the Jahn-Teller effect and by its large free energy of hydration (-498.7 kcal/mol).

Future Research

Uranium in the 300 Area Pond Sediments and Its Mobilization. The data collected to date suggest that formation of the uranium(VI) carbonato complexes will solubilize uranium present as schoepite, without any kinetic constraints related

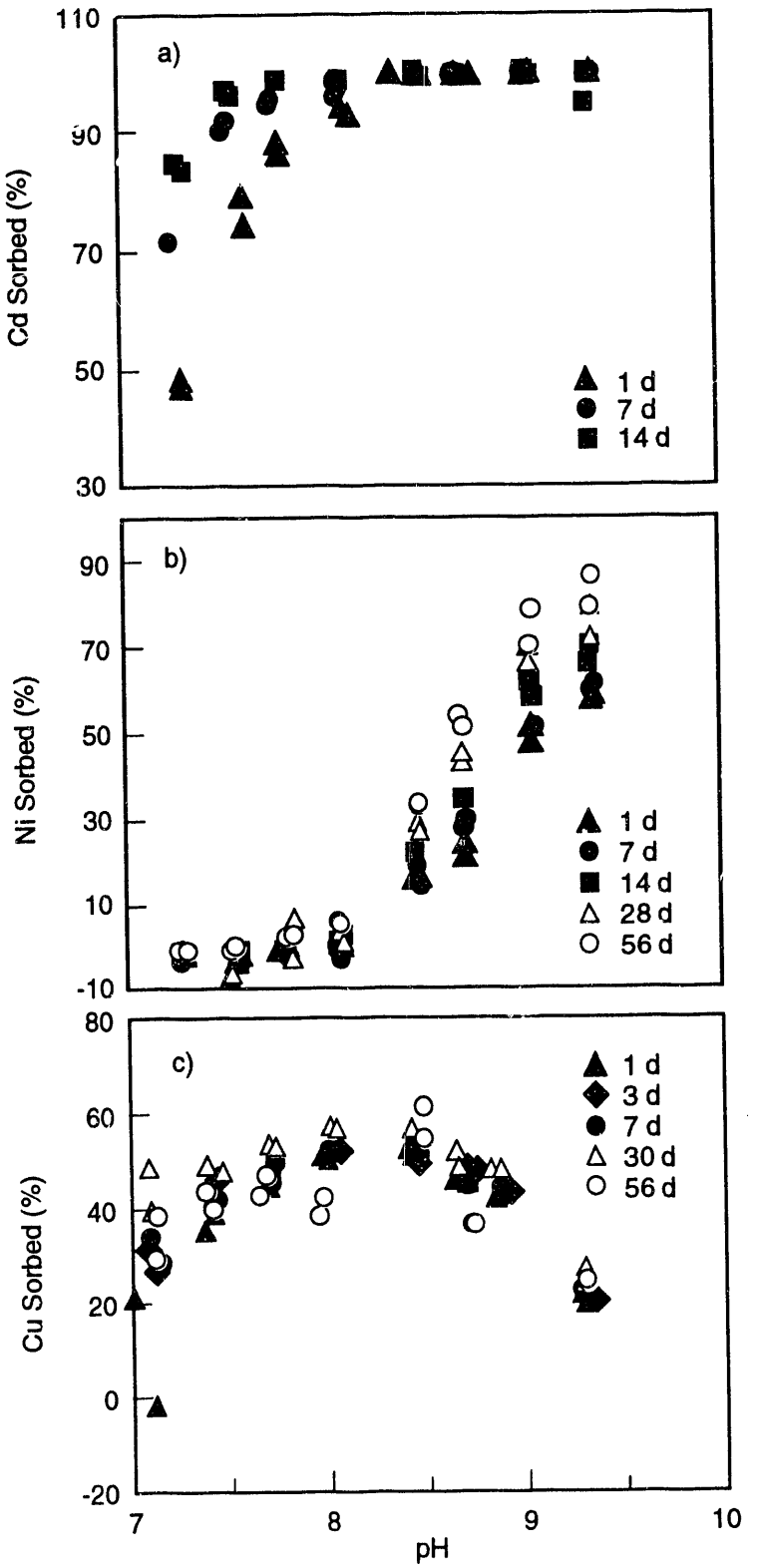

FIGURE 2. Fractional Adsorption of a) Cadmium, b) Nickel, and c) Copper to Calcite as a Function of pH and Residence Time

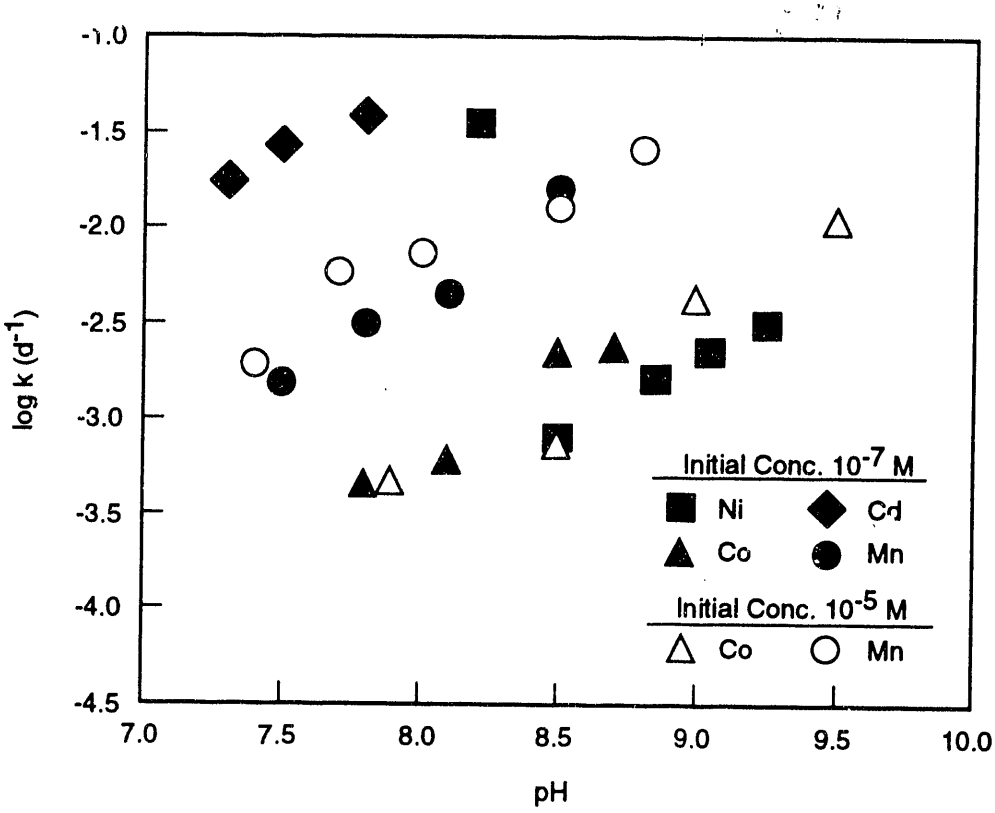

FIGURE 3. Pseudo-First-Order Rate Constants for the Disappearance of Aqueous Cadmium, Cobalt, Manganese, and Nickel from a Calcite Suspension (t > 24 h) as a Function of pH and of Initial Manganese and Cobalt Aqueous Concentrations

to schoepite dissolution. However, in nonarid environments, attenuation of uranium(VI) typically occurs through exchange with clay minerals and interaction with iron and aluminum oxide. Although cation exchange reactions are believed to be rapid and non-rate-limiting with respect to uranium(VI) mobilization, desorption from oxide surfaces is usually much slower, and therefore the solubilization of sorbed uranium may limit the desorption rate. Research in FY 1993 will continue to explore 1) the remobilization of uranium(VI) from collected sediments from the 300 Area ponds, 2) remobilization of uranium sorbed to clays by cation exchange, and 3) the release of uranium from iron and aluminum oxide-dominated subsurface materials. The research activities will focus on the kinetics of uranium release.

Effect of Calcite Recrystallization on the Sorption of Metals as a Function of Residence Time. The calcite recrystallization studies were completed in FY 1992, and no additional studies to investigate pure phase calcite recrystallization are being contemplated. Instead, research during FY 1993 will emphasize 1) investigations of real-world contaminated subsurface materials, 2) remobilization of copper and uranium from contaminated subsurface materials, and 3) manipulation of geochemical parameters to enhance remobilization.

References

Zachara, J. M., C. E. Cowan, and C. T. Resch. 1991. "Sorption of Divalent Metals on Calcite." *Geochimica et Cosmochimica Acta* 55:1549-1562.

Microbial Sequestration and Bioaccumulation of Radionuclides and Metals

H. Bolton, Jr.

Contributors

N. L. Valentine (EMCORE) and M. T. Kingsley (NORCUS)

In the past, many inorganic contaminants, including radionuclides and toxic metals, have been disposed of at DOE sites. In some instances, these inorganic contaminants have migrated into the subsurface environment, and they may migrate farther to contaminate domestic groundwater supplies. Currently, economical approaches to remediate or stabilize these deep contaminated zones are limited by a lack of understanding of the geochemical and biological factors that affect the wastes. Radionuclide and metal inorganic wastes must be either immobilized before further subsurface migration occurs or removed from the contaminated subsurface environment by pumping and surface treatment. Pump-and-treat technologies are costly and not feasible for deep, inaccessible sediments. However, one promising process for radionuclide and metal immobilization is bioimmobilization, or the bioaccumulation of radionuclides and metals by subsurface microorganisms. Bioaccumulation is a specific microbial sequestering mechanism in which mobile radionuclides and metals become associated with the microbial biomass with both intra- and extracellular sequestering ligands. Radionuclides and metals can accumulate either intracellularly or extracellularly, in association with various components of the cell wall or exopolymers (capsules or slime layers). Because most microorganisms in the subsurface environment are associated with stationary strata, bioaccumulation of mobile radionuclides and metals would initially decrease inorganic waste transport. However, information on this microbially mediated process is currently limited. How long the inorganic wastes would remain immobilized, the selectivity of the bioaccumulation process for specific inorganic wastes, the mechanisms involved, and how the geochemistry and growth conditions of the subsurface environment influence bioaccumulation are all currently unknown. With stimulation of the growth and activity of subsurface microorganisms, the transport of radionuclides and metals in subsurface environments may be effectively reduced by bioaccumulation. A question remains: Although subsurface microorganisms may be able to reduce radionuclide and metal transport, will contaminants subsequently be remobilized as the microorganisms are starved or degraded? Therefore, this research is being conducted to determine the selectivity of the bioaccumulation process for specific metals, the mechanisms and kinetics of bioaccumulation, and the extent of any remobilization of inorganic wastes during various stages of microbial growth.

FY 1992 Research Highlights

This project was conducted under the auspices of PNL's Environmental Science Research Center, as part of its basic program to develop new scientific knowledge and concepts for using natural processes in subsurface environmental restoration. Before initiation of this project, there was limited information on the ability of subsurface microorganisms to immobilize inorganic contaminants. The goal of our research in FY 1992 was threefold: First, to complete the survey (begun in FY 1991) of inorganic contaminant bioaccumulation by a wide variety of subsurface microbial isolates during the cellular resting stage. Second, to sample and characterize the microbial ecology of a site contaminated by radionuclides and metals. Third, to start in-depth mechanistic investigations of radioactive metal bioaccumulation by a single subsurface microorganism. Because work in this third research area did not start until near the end of FY 1992, it will not be discussed here, but will be referred to in the "Future Research" section.

Bioaccumulation of Heavy Metals by Subsurface Bacteria. The goal of this research was to determine the bioaccumulation of radioactive ^{109}Cd, ^{57}Co, ^{63}Ni, and $^{85,90}Sr$ by microorganisms isolated from three distinct subsurface environments. These metals have different specificities for ligand-binding sites, with strontium preferring nitrogen and oxygen, while cadmium prefers phosphorus and sulfur, and cobalt and nickel are less selective. The use of these metals with their different specificities for

ligand-binding sites was intended to provide an initial indication of the possible dominant ligands associated with subsurface microorganisms. Also, ^{60}Co and ^{90}Sr are radionuclides disposed of at DOE sites that are of concern because of their mobility in the subsurface environment. Our objective was to determine inorganic contaminant bioaccumulation during the resting stage of growth, using subsurface bacteria isolated from three distinct subsurface environments at DOE sites.

The first hypothesis we tested was that subsurface bacteria from different subsurface environments would have different abilities to bioaccumulate metals. Previous DOE microbiological research has shown that subsurface bacteria were very diverse at various locations, suggesting that microbial populations at various subsurface locations might be unique. The second hypothesis was that Gram-positive and Gram-negative subsurface bacteria would have different abilities to bioaccumulate inorganic contaminants. Eubacteria can be divided into two main cell wall types, distinguished by the Gram stain as either Gram-positive or Gram-negative. It is convenient to study these two cell wall types, because they have different mechanisms to biosorb radionuclides and metals. Gram-positive walls usually contain large amounts of peptidoglycan and anionic polymers, such as teichoic or teichuronic acid. The cell walls of Gram-negative bacteria are distinctly different, having an outer membrane of lipids, proteins, and polysaccharides outside the peptidoglycan layer. Our third hypothesis was that subsurface bacteria resistant to metals would bioaccumulate less metal than metal-sensitive strains, and our final hypothesis was that subsurface microorganisms have developed unique abilities to sequester and bioaccumulate radionuclides and metals. The subsurface environment can be low in nutrients (i.e., oligotrophic), and essential nutrients may be concentrated by subsurface microorganisms. Selected radionuclides and metals would presumably be analogs of these nutrient elements and would also be bioaccumulated. Also, subsurface microorganisms may have developed general, non-specific sequestering mechanisms, which would allow bioaccumulation of both nutrients and inorganic contaminants.

The microorganisms used in these studies were isolated from sediments obtained from boreholes drilled at the Hanford Site (59 strains), the Idaho National Engineering Laboratory (INEL) (30 strains), and the Savannah River Site (SRS) (47 strains). Microorganisms were also used that had been isolated from surface soil adjacent to the boreholes at Hanford (11 strains), INEL (6 strains), and SRS (6 strains). Microorganisms were all grown on the same solid medium [peptone-trypticase-yeast extract-glucose (PTYG)], rinsed off the plates, washed twice, and suspended in 0.001 M Piperazine-N, N'-bis[2-ethane-sulfonic acid] (PIPES) buffer at pH 6. The PIPES buffer is a pH buffer with very low metal-complexation capability. The cells were stored overnight in PIPES buffer with no carbon source, to ensure that resting and/or starved cells were used in our assays. Aqueous speciation modeling of our experimental system ensured that the metals used in these studies were present as the free metal ion with a valence of two. Because of the limits on metal solubility and possible toxic effects from the metals, our experiments were all conducted at 1 μM metal concentrations. All data are reported per gram dry weight of cells.

Subsurface bacteria from Hanford accumulated more metal than strains isolated from subsurface sediments from either SRS or INEL (Table 1). These data demonstrate that microorganisms from different subsurface systems have different abilities to bioaccumulate metals during resting or starvation stages of growth. All three sampling sites were located in uncontaminated subsurface systems, so that data presented here are for microorganisms cultured from a relatively contaminant-free environment. When the strains from all three locations were averaged together, the amount of metal bioaccumulated or removed from solution decreased in the order cadmium > nickel > cobalt > strontium (Table 1). This pattern of metal uptake demonstrates that subsurface bacteria do have a selectivity for metal uptake. The average values in Table 1 do not show the wide range with which subsurface bacteria removed metals from solution. The range for metal bioaccumulation after 1 h was 6.02-0.009, 3.00-0.001, 2.79-0.004, and 1.27-0.000 μmol metal/g dry weight for cadmium, cobalt, nickel, and strontium, respectively.

TABLE 1. Metal Bioaccumulation by and Metal Resistance of Subsurface Bacteria from the Hanford Site (Hanford), Idaho National Engineering Laboratory (INEL), and the Savannah River Site (SRS). The main effect means of location, metal, time, and Gram stain are presented.

Treatment	Bioaccumulation, μmol metal/g dry weight	Resistance, MIC, μg metal[a]
Location		
Hanford	0.70a[b]	47.2b
SRS	0.37b	69.7a
INEL	0.23c	91.1a
Metal		
cadmium	1.09a	34.1c
cobalt	0.28c	66.6b
nickel	0.40b	93.7a
strontium	0.16d	nd[c]
Time (hours)		
1	0.54a	na[d]
4	0.51ab	na
8	0.45bc	na
24	0.42c	na
Gram stain		
Positive	0.51a	54.6b
Negative	0.41a	82.3a

(a) MIC = minimum inhibitory concentration.
(b) Main effect means in the same column that are followed by the same letter are not significantly different ($p \leq 0.05$).
(c) nd = not determined.
(d) na = not applicable.

When the samplings at 1 and 24 h are compared (Table 1), there is a 22% decrease in the amount of metal bioaccumulated. The location and metal interaction was significant (Figure 1). Hanford isolates had significant differences in the uptake of all four metals, while INEL and SRS isolates had the highest amounts of cadmium bioaccumulated and the same amounts of nickel, cobalt, and strontium (Figure 1).

When all four metals were averaged, Gram-positive and Gram-negative bacteria both bioaccumulated the same amount of metal (Table 1). This disproved our hypothesis about a difference in the ability of Gram-positive and Gram-negative isolates to remove different amounts of metal from solution. Apparently the cell wall structure of subsurface microorganisms is not a major influence on metal uptake by resting cells.

Subsurface isolates were tested for their resistance to cadmium, cobalt, nickel, and strontium using metal-impregnated filter disks placed onto inoculated agar. The minimum inhibitory concentration (MIC) that produced a measurable inhibition of growth around the disk was measured. When the MICs of the four metals were averaged, the MIC for isolates from Hanford was significantly lower than those for SRS or INEL isolates (Table 1). The metals had differing MICs when all isolates were analyzed together, and decreased in the order nickel > cobalt > cadmium (Table 1). No data for strontium are presented in Table 1 because no isolate was sensitive to strontium at even the highest concentration (500 μg).

An inverse relationship between metal bioaccumulation and metal resistance was found (Table 1). Cadmium was bioaccumulated the

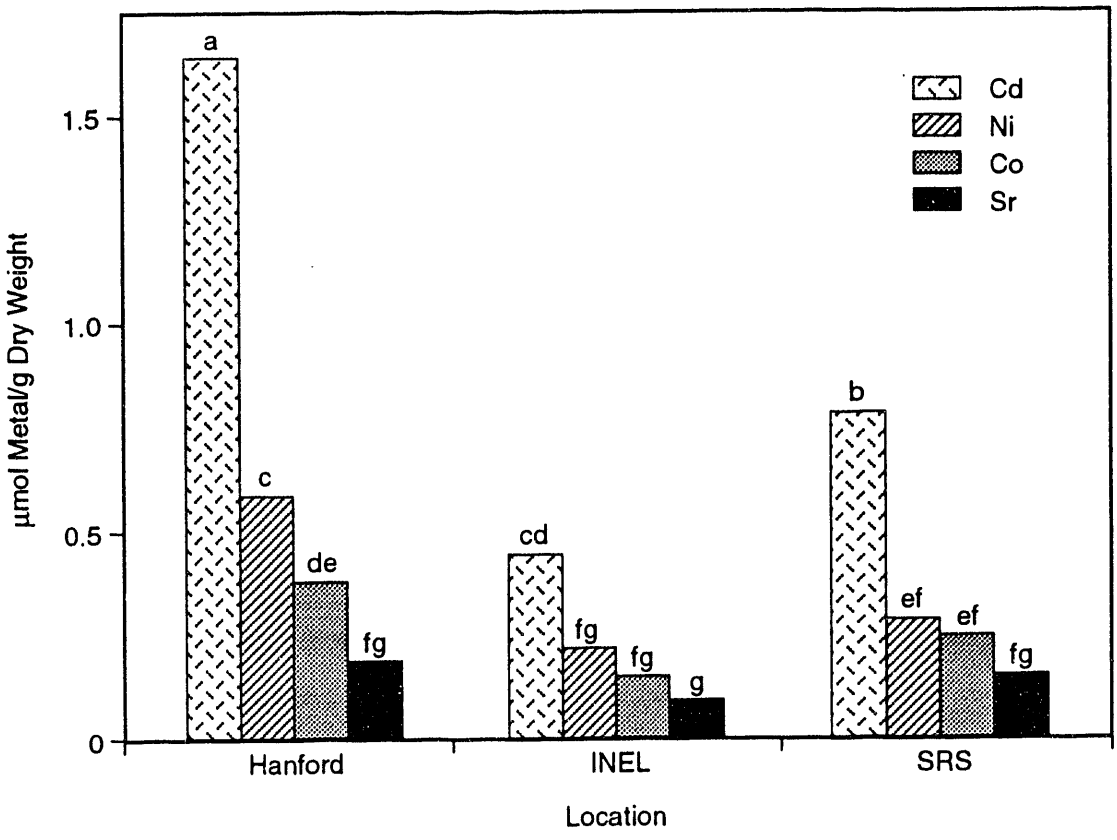

FIGURE 1. Bioaccumulation of Cadmium, Nickel, Cobalt, and Strontium by Subsurface Bacteria from the Hanford Site (Hanford), Idaho National Engineering Laboratory (INEL), and the Savannah River Site (SRS). Bars labeled with different letters are significantly different by Fischer's protected least significant different mean separation test ($p \leq 0.05$).

most and was the metal to which bacteria were most sensitive (i.e., smallest MIC). Also, Hanford isolates had the largest average amount of metal removed from solution and the lowest MIC values (Table 1). Thus there appears to be an inverse relationship between metal bioaccumulation and metal resistance. Gram-negative bacteria were more resistant than Gram-positive bacteria when all the metals were averaged together (Table 1).

Subsurface isolates were no better than surface isolates at bioaccumulating metals (Table 2). Subsurface and surface isolates from all three locations bioaccumulated the same amount of strontium (Table 2). The Hanford subsurface and surface isolates bioaccumulated the same amounts of cadmium, but the surface isolates bioaccumulated more cobalt and nickel. Surface isolates from INEL and SRS bioaccumulated more cadmium, cobalt, and nickel than subsurface isolates (Table 2). This disproves our hypothesis that subsurface bacteria have unique capabilities that allow them to remove more metals from solution than surface isolates. However, these studies were conducted on isolates cultured on the same medium and in the resting or starved physiological state. Inferences cannot be made to other stages of growth or long-term starvation.

Microbial Ecology of a Radionuclide- and Metal-Contaminated Waste Site. Microorganisms isolated from sediments from a site contaminated with metals and radionuclides may differ from isolates from more pristine environments in their ability to bioaccumulate metals. For this reason, a site at Hanford was selected for obtaining

TABLE 2. Metal Bioaccumulation by Surface and Subsurface Bacteria from the Hanford Site (Hanford), Idaho National Engineering Laboratory (INEL), and the Savannah River Site (SRS)

	Bioaccumulation, μmol metal/g dry weight			
Location	Cadmium	Cobalt	Nickel	Strontium
Hanford - surface	1.58b[a]	0.87e	1.14d	0.20ij
Hanford - subsurface	1.66b	0.38hi	0.59fg	0.19ij
SRS - surface	1.92a	1.23c	1.12d	0.20ij
SRS - subsurface	0.79ef	0.24ij	0.28hij	0.15j
INEL - surface	1.48b	0.82e	0.90e	0.22ij
INEL - subsurface	0.45gh	0.15j	0.21ij	0.09j

(a) Means in table that are followed by the same letter are not significantly different ($p \leq 0.05$).

near-surface sediments contaminated with varying concentrations of both radionuclides and metals from which we would isolate organisms for study. From 1948 to 1975, the 300 Area processing pond at the Hanford Site was used for the disposal of radioactive and metal-contaminated waste waters from laboratories and nuclear fuel fabrication facilities. After waste discharges to the pond ceased, the pond dried. This processing pond basin offered a unique opportunity to obtain near-surface sediments that had been contaminated with both radionuclides and metals for several decades. Our objectives were to determine the viable populations of microorganisms in the sediments and to test several hypotheses about how the addition of both radionuclides and metals influenced the microbial ecology of the sediments. Our first hypothesis was that viable populations of microorganisms would be lower in the more contaminated sediments. Second, we expected that long-term metal exposure would result in enhanced metal resistance. Finally, microorganisms from the most radioactive sediments should have enhanced radiation resistance.

Sediments were obtained from two locations within the dried pond basin, designated locations "A" and "B". Sediments were obtained from four depths at location A [4.5, 6, 16, and 25 ft (1.4, 1.8, 4.9, and 7.6 m)] and two depths at location B [1 and 2 ft (0.3 and 0.6 m)]. Samples were therefore designated as A-4.5, A-6, A-16, A-25, B-1, and B-2. Samples were collected, sieved to pass through a 1-mm screen, and stored at 4°C until analyzed.

The six sediments had a wide range of total metal concentrations (Figure 2). In general, metal concentrations in the sediments decreased as a function of depth (compare A-4.5 through A-25 or B-1 and B-2). A variety of metals occurred at concentrations above background; only those with at least a tenfold decrease as a function of depth were included in Figure 2. The concentrations of copper and zirconium were multiplied by 0.1 so these data would fit in the figure, and thus the actual concentrations of copper and zirconium are ten times higher than the bars shown in Figure 2. Notice the high concentrations of copper, nickel, chromium, uranium, and zirconium in sediments B-1, B-2, and A-4.5. These sediments will be generally referred to in this article as the contaminated sediments.

The radioactive contamination in sediments B-1, B-2, and A-4.5 was discernible upon sampling with a hand-held β,γ-counter. The predominant radionuclides in these sediments were ^{238}U and ^{235}U and their decay products. The concentrations of ^{238}U and ^{235}U are presented in Figure 2. The concentration of ^{238}U was multiplied by 0.1 so the data would fit in the figure; thus the actual concentration of ^{238}U is ten times higher than the bar shown in Figure 2. The high concentrations of uranium, ^{238}U, ^{235}U, zirconium,

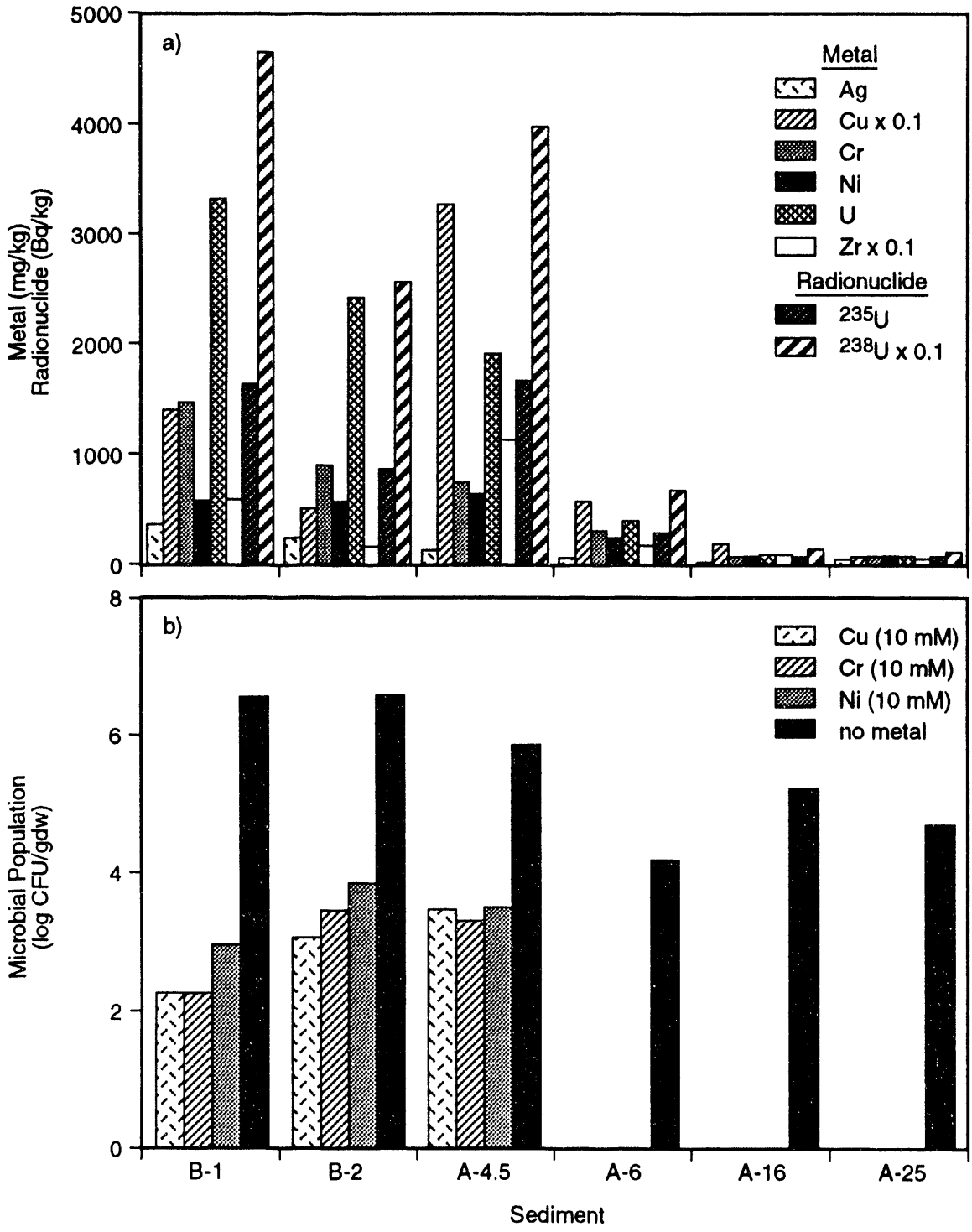

FIGURE 2. Contaminant Concentrations and Microbial Densities. a) Metal and radionuclide concentrations in processing pond sediments. Concentrations of copper, zirconium, and ^{238}U are ten times larger than bars shown. b) Microbial population densities in processing pond sediments. Microbial populations were plated onto 1% PTYG or onto 1% PTYG with cobalt, chromium, or nickel at a concentration of 10 mM.

and copper in selected sediments (Figure 2) demonstrates the previous use of this pond as a waste site for nuclear fuel fabrication facilities.

Viable microbial populations, as demonstrated by growth on the same medium (PTYG), were found in all six sediments (Figure 2). Viable microbial populations enumerated from plates with no additional metal were highest in B-1, B-2, and A-4.5, the sediments most contaminated with metals and radionuclides (Figure 2). Thus viable populations of microorganisms were not reduced in the most contaminated sediments, disproving our first hypothesis. These three metal- and radionuclide-contaminated sediments were also the only ones with microorganisms able to grow on a medium amended with copper, chromium, or nickel at a 10 mM concentration (Figure 2). Thus enhanced metal resistance of the microbial population was apparently selected for by the presence of these metal contaminants, confirming our second hypothesis. It should be noted, however, that the microbial population of metal-resistant microorganisms, as defined by growth on plates containing 10 mM metal, was significantly less than the total population (Figure 2). In some cases the metal-resistant population was less than the total counts by four orders of magnitude (e.g., B-1). So although there was a metal-resistant population, organisms not resistant to metals were also present. This point was also demonstrated by a random survey of metal resistance of isolates that grew on PTYG plates without metals. These randomly selected isolates were tested for their resistance to nickel, copper, and chromium, using metal-impregnated filter disks placed onto inoculated agar; inhibition of growth around the disk was measured. There was no difference in the MIC of copper, chromium, or nickel for isolates from the various sediments. Thus metal resistance was not enhanced in the general microbial population from the contaminated sediments that grew up on the 1% PTYG plates without metals. Statistical analysis of population counts from the metal-amended plates allowed a comparison of average metal resistance for the three contaminated sediments and average metal resistance for the three metals. The population of nickel-resistant microorganisms was significantly higher [3.5 log colony-forming units/gram dry weight (CFU/gdw)] than those for chromium or copper (3.1 and 3.0 log CFU/gdw, respectively). The random testing of isolates from 1% PTYG without metals also showed a higher MIC for nickel (138 μg) than for copper (80 μg) or chromium (46 μg). Sediments A-4.5 and B-2 had similar metal-resistant microbial populations (3.4 log CFU/gdw), while the population in B-1 was significantly less at 2.5 log CFU/gdw.

Because some microorganisms may not grow on our selective medium, we also assayed total microbial biomass and activity in these sediments. The soil microbial biomass, as determined by sediment adenosine triphosphate (ATP) concentration, was significantly higher in the most contaminated sediments (Figure 3). Sediment B-2 had the highest ATP concentration, followed by B-1 and then A-4.5. The three uncontaminated sediments had similar ATP contents but had a significantly lower level than the most contaminated sediments. The microbial activity in the sediments, as determined by ^{14}C-glucose mineralization, was highest in the least contaminated sediments (Figure 3). Sediments A-16, A-25, and A-6 had the fastest rate and greatest amount of ^{14}C-glucose mineralized when the sediments were maintained at native soil moisture content (Figure 3). After the mineralization approached an asymptotic value, fresh glucose was added, along with a nutrient solution to provide both nutrients and moisture, to determine whether either of these was limiting ^{14}C-glucose mineralization. Mineralization rates of ^{14}C-glucose were generally the same before and after the addition of nutrients and water (Figure 3), suggesting that microbial activity in the contaminated sediments was not limited by either nutrients or moisture. Thus the contaminated sediments had a larger biomass but a less active microflora than the uncontaminated sediments. One possible explanation for this inverse relationship between microbial biomass and activity is that the contaminated sediments were located closer to the surface of the dried pond and microorganisms may have infiltrated from shallower uncontaminated sediments. (The surface of the dried pond was covered with a layer of uncontaminated sediment upon closure to prevent air dispersal of contaminated sediments.)

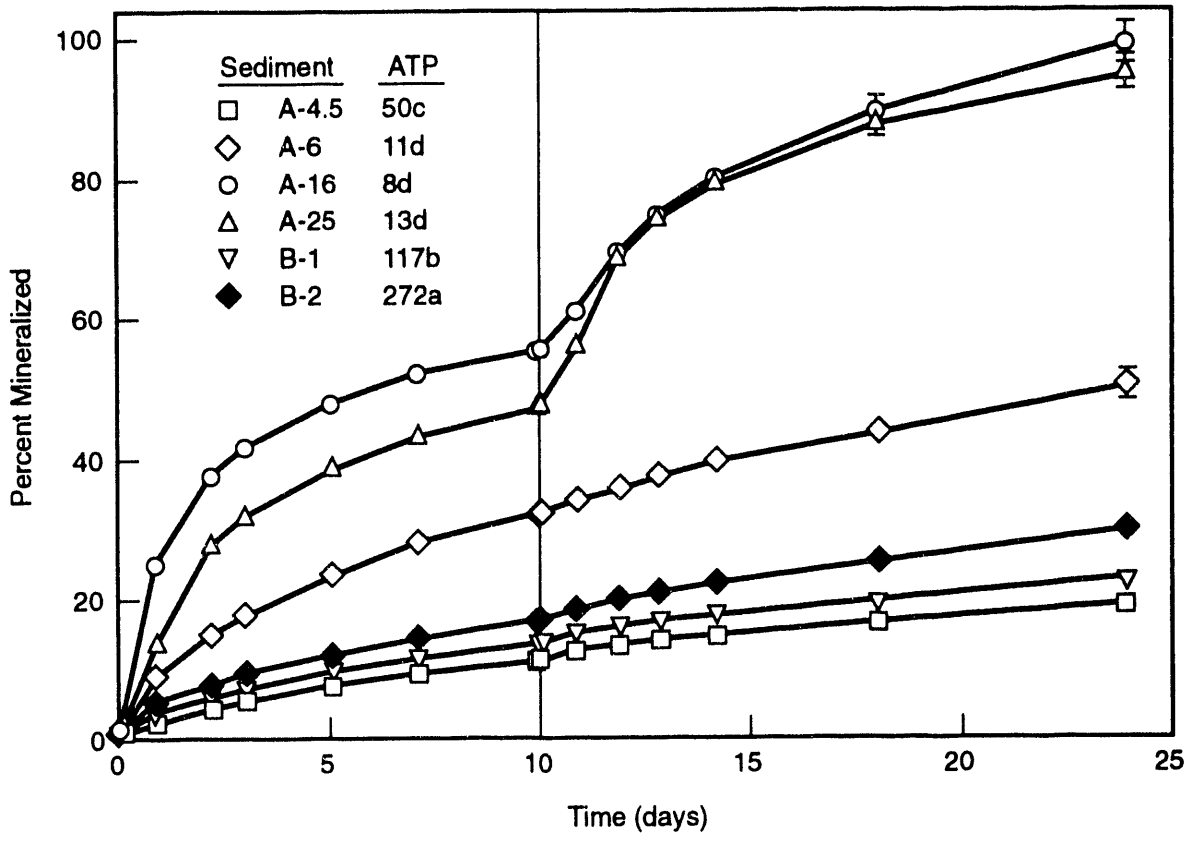

FIGURE 3. Sediment ATP Concentration and ^{14}C-labeled Glucose Mineralization in Various Processing Pond Sediments. The legend lists ATP concentrations as nmol ATP/mg sediment. Means followed by the same letter are not significantly different ($p \leq 0.05$). For the mineralization of glucose, 10 g of sediment was supplemented with 20 μg ^{14}C-labeled glucose (2 mCi/mmol) with the evolved $^{14}CO_2$ being trapped in a vial containing 0.3 M KOH. At day ten, 10 ml of a 0.1X nutrient solution was added to the sediments along with a fresh addition of ^{14}C-labeled glucose. Error bars represent the standard deviations of the means.

The presence of radiation in the sediments A-4.5, B-1, and B-2 (Figure 2) for extended periods suggested that microbial populations in these three sediments might have enhanced radiation resistance. Sediments were weighed into sterile tubes and exposed to γ-radiation from a ^{60}Co source for different times to provide varying levels of radiation exposure. The sediments were then serially diluted and plated (onto 1% PTYG) to determine viable counts for percent survival calculations. There was a wide range of percent survival in the various sediments as a function of radiation exposure (Figure 4). At the 0.1-Mrad dose, the range in survival was from approximately 0.1% in sediment B-2 to 2% in sediment A-25. Only one of the contaminated sediments (B-1) had a percent survival higher than the other sediments at the highest dose (0.25 Mrad). Sediment B-1 also had the highest amount of ^{238}U in comparison to the other sediments (Figure 2). The enhanced survival of microorganisms exposed to radiation in sediment B-1, although significantly higher statistically, was not much greater than the other sediments.

In conclusion, the presence of mixed inorganic contaminants, including various metals and radionuclides, over a long time did not significantly alter viable sediment microbial counts when compared to the less contaminated sediments. Enhanced radiation resistance was found only for the most radioactive sediment, but the enhanced survival was not large compared to the

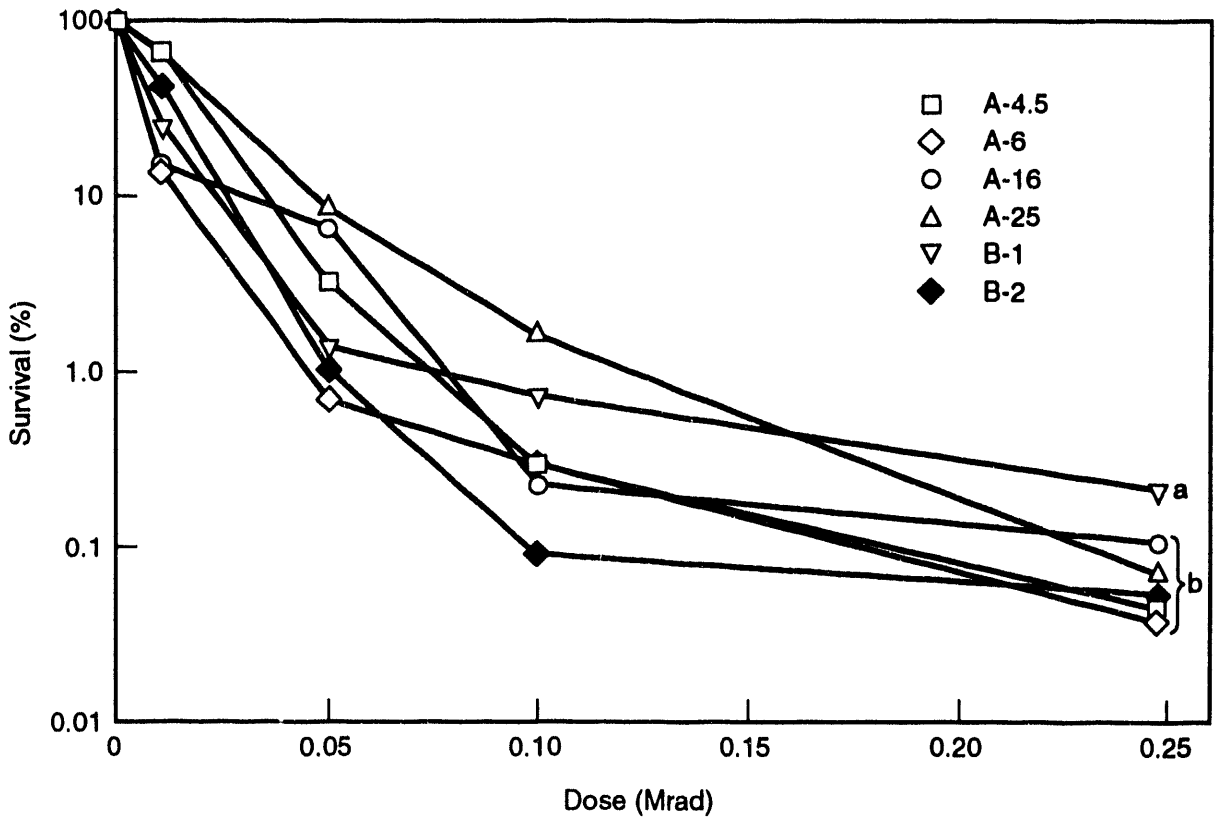

FIGURE 4. Dose Response Curve of Viable Microbial Populations in the Various Processing Pond Sediments to γ-Radiation from a ^{60}Co Source. Sediments were serially diluted after radiation exposure and plated onto 1% PTYG. The last sampling time was statistically analyzed, and points followed by the same letter are not significantly different ($p \leq 0.05$).

other sediments. Metal-resistant microorganisms were found in the most contaminated sediments, but their numbers were much less than the total viable population. Microbial biomass was higher in the contaminated sediments, but microbial activity was lower. Thus although microbial populations were able to survive in the contaminated sediments, they were not as active as in the less contaminated sediments.

Future Research

This project will conclude in FY 1993 with investigations of metal bioaccumulation of strains isolated from the sediments of the 300 Area processing ponds at the Hanford Site. The hypothesis we will test is that microorganisms isolated from metal-contaminated environments will bioaccumulate less metal than isolates from more pristine environments. We will also conduct in-depth mechanistic studies of metal bioaccumulation with a single subsurface spore-forming bacterium. This spore-former was chosen because it bioaccumulated substantial quantities of metals in the screening study and because spore-formers are an important portion of the total platable microbial population in the vadose zone at Hanford (48% are spore-formers). Also, the use of a spore-former will allow us to investigate several stages of growth over short periods, including active growth (log phase), transition to starvation (spore formation), starvation-survival (spores), and resuscitation (spore germination).

Improving the Biodegradative Capacity of Subsurface Bacteria

M. F. Romine and F. J. Brockman

Contributors

R. Reeves (Florida State University) and
D. Balkwill (Florida State University)

The continual release of synthetic materials into the environment by industrial and agricultural sources over the last few decades has resulted in pollution of the subsurface environment. The potential harm this could cause to our health and environment requires that we take the initiative to clean up the contaminated sites. However, such cleanup has been difficult because of the relative inaccessibility of the contaminants resulting from their wide dispersal in the deep subsurface environment, often at low concentrations and in large volumes. As a possible solution for these problems, interest in the introduction of bacteria for *in situ* remediation of contaminated sites has increased greatly in recent years. The selection of a microorganism(s) to apply in such cleanup entails consideration of such factors as

- Metabolic response to abiotic factors, such as pH, temperature, moisture, and texture
- Ability of a microbe to establish itself and survive predation within the indigenous microbial community and to compete effectively for nutrients, which are commonly at suboptimal levels
- Resistance to naturally occurring toxins.

The use of microorganisms isolated from subsurface environments would be advantageous because the organisms are already adapted to the subsurface conditions. Although many natural isolates able to degrade contaminants have been identified, there are still some limitations on their use:

- The rate at which the contaminant is removed is often too slow for timely removal of the pollutant
- Expression of the enzymes involved in degradation often requires the presence of environmental conditions or chemicals that may not be present or that are highly toxic to humans
- To handle mixtures of highly recalcitrant anthropogenic waste compounds requires extensive evolution of catabolic pathways.

These obstacles can be overcome by recruiting enzymes from well-characterized microorganisms, placing the genes for the enzymes under the control of regulatable promoters, and moving the new genetic constructs into diverse groups of subsurface microbes. Therefore, the objectives of this research project are to 1) construct vehicles that enable the transfer of recruited enzymes to subsurface bacteria and allow expression to be controlled by nontoxic and inexpensive external factors, and 2) determine the ability of engineered subsurface bacteria to degrade the target contaminant. The project has been conducted under the auspices of PNL's Environmental Science Center, as part of its basic program of developing new scientific knowledge and concepts for use of natural processes in restoration of the subsurface environment.

FY 1992 Research Highlights

Construction of Plasmids. We have chosen two plasmid vectors to be used as vehicles for the transfer of genes that encode recruited enzymes into selected subsurface isolates. These plasmids, pMMB66EH and pNM185, were chosen because they can be maintained in a wide variety of microorganisms. Each of these plasmids also encodes antibiotic resistance markers (ampicillin and kanamycin resistance, respectively), which will allow us to monitor transfer of the plasmid into the subsurface isolates. Regulatable expression of recruited genes can be achieved by placing these genes behind plasmid-encoded promoters. The pMMB66EH vector carries a ptac promoter originally derived from *Escherichia coli*. This promoter is negatively regulated by the product of the *lacI* gene, which is present on the same vector. Repression of transcription from this

promoter can be relieved by adding the chemical isopropylthiogalactoside (IPTG). The pNM185 vector carries the ptol promoter, which originated from the pWWO plasmid of *Pseudomonas putida* strain F1. This promoter is positively regulated by the product of the *xylS* gene encoded on the plasmid and the coinducers benzoate or *m*-toluate.

Two enzymes, toluene dioxygenase (*tod*) and toluene-4-monooxygenase (*tmo*), were selected as the initial model systems for enzyme recruitment. These enzymes catalyze the degradation of both toluene and trichloroethylene (TCE). The DNA encoding *tod* and *tmo* were recruited from *P. putida* F1 and *P. mendocina* KR1, respectively. Four plasmid vehicles were constructed by cloning each of these enzymes into each of the selected plasmid vectors. The IPTG-regulatable pMMB66EH derivatives are pMY402, which encodes the *tmo* genes, and pMR601, which encodes the *tod* genes. The benzoate- or *m*-toluate-regulatable pNM185 derivatives are pMR404, which encodes the *tmo* genes, and pMR604, which encodes the *tod* genes.

Transfer and Expression of Recruited Enzymes in Subsurface Bacteria. Isolates from the P24 borehole at the Savannah River Site in South Carolina were chosen for this study. Fifty-five subsurface isolates were screened for their inherent resistance to kanamycin and ampicillin. Of the isolates, 29 lacked such resistance and were unable to grow on the antibiotic-containing media, making them suitable for use with our resistance-marked plasmids. Some of these 29 strains are being typed phylogenetically by Reeves and Balkwill at Florida State University. Based on preliminary typing, eight isolates from different bacterial groups were chosen for enzyme recruitment: BO615, *Rhodospirillum rubrum*; BO724, *Arthrobacter globiformis*; BO265, *Alcaligenes eutrophus*; BO445, *Acinetobacter calcoaceticus*; BO669 and BO446, *P. testeroni*; BO259, *P. aeruginosa*; and BO450 (not yet typed).

Cesium-purified plasmid DNA was electroporated into these subsurface isolates. Cells that had received the plasmid were identified by their ability to grow on antibiotic-containing media that they had initially been unable to grow on. Then any newly antibiotic-resistant colonies were tested for presence of the new plasmid DNA by amplifying the *tod* and *tmo* genes by the polymerase chain reaction. As of the end of FY 1992, we have transferred all four plasmid constructs into BO445, BO450, BO265, BO669, and BO259, and transferred pMR604 into BO724 and BO446. No colonies were formed by BO615 after electroporation with any of the plasmids.

Expression of Biodegradative Capacity. Expression of the *tod* and *tmo* genes was monitored by high-performance liquid chromatography (HPLC) analysis of culture supernatants. Cultures grown in the presence of toluene and expressing *tod* or *tmo* would be expected to convert toluene to *cis*-dihydrodiol or *p*-cresol, respectively.

Cultures of strains BO445, BO450, BO265, BO669, and BO259 that contained each of the four plasmids were tested for their ability to degrade toluene. Culture supernatants were collected from cultures that had been grown in minimal media, containing 20 mM lactate and 100 ppm toluene. Identical cultures were also set up in the presence of the inducers, IPTG or *m*-toluic acid, at a final concentration of 1 mM.

p-Cresol produced by strains BO265, BO259, BO445, BO450, and BO669 with plasmid pMR404 (light bar) and pMR404-induced (dark bar) are shown in Figure 1. Levels of dihydrodiol produced by these strains with plasmids pMR601 (open bar), pMR601-induced (solid bar), pMR604 (lightly shaded bar), and pMR604-induced (darkly shaded bar) are shown in Figure 2.

None of the parental strains, which were devoid of these four plasmids, were able to degrade toluene. In addition, expression from pMY402 was not evident in any of these strains. Degradation of toluene by *tmo* was exhibited in four out of five strains and inducible in three of these four strains. Degradation of toluene by *tod* was successful in three out of five strains in the presence of the pMR601 construct and in all five strains carrying the pMR604 construct. Toluene was completely removed from BO445 containing pMR601 (either induced or noninduced) and by BO450 carrying pMR604 (either induced or noninduced).

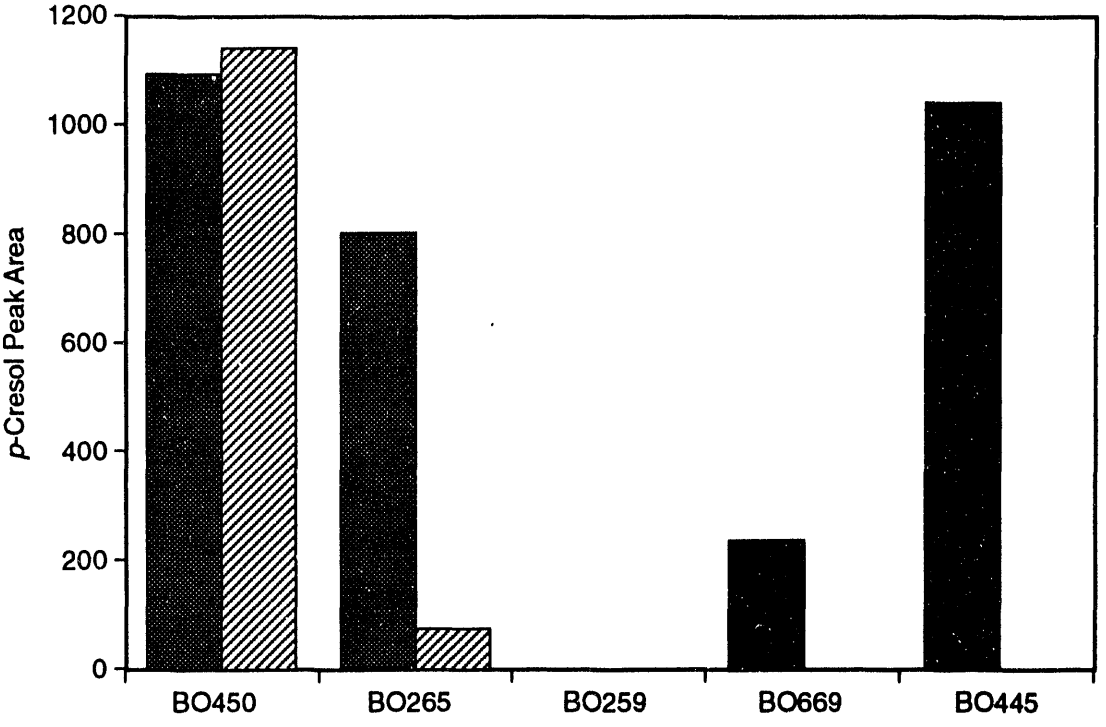

FIGURE 1. Production of *p*-Cresol by Strains Containing a Recruited Toluene-4-Monooxygenase

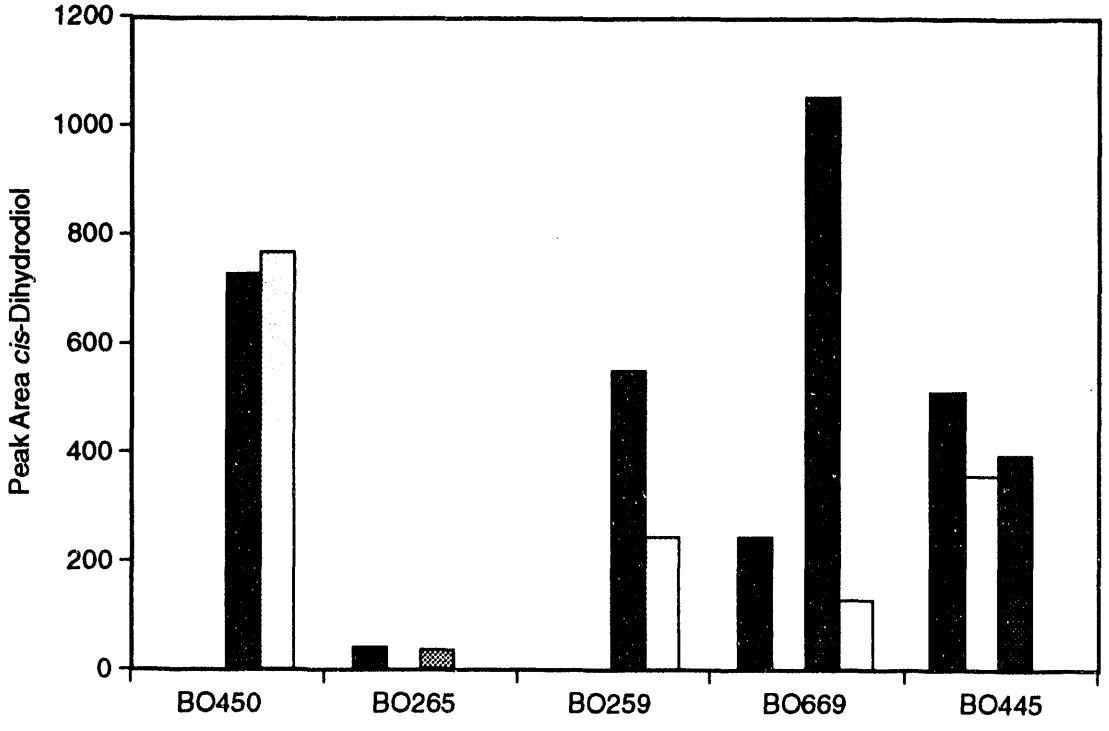

FIGURE 2. Production of *cis*-Dihydrodiol by Strains Containing a Recruited Toluene Dioxygenase

To examine the kinetics of the *tmo* and *tod* enzymes, a time-course assay was also performed with the parent BO450 and derivatives that carried plasmid pMR404 (Figure 3) or pMR604 (Figure 4), using benzoic acid as the inducer. The results indicate that degradation of toluene by *tod* (pMR604) is much more rapid than degradation by *tmo* (pMR404) in BO450. After 21 hours, only 0.25% of the initial level of toluene remained in the supernatant with pMR604, but over 90% was still detectable in the supernatant with pMR404. The parental strain BO450 did not produce a detectable level of either compound; thus both plasmids exhibited a considerable level of constitutive activity.

Future Research

Preliminary results indicate that, in some cases, recruited *tod* and *tmo* enhanced the biodegradative capacity of subsurface bacteria. Additional experiments will test the effects of cell concentration, growth state, and toluene concentration on degradation by the engineered strains and on the ability of these strains to degrade TCE. Strains will then be ready for testing in subsurface sediments and groundwater to assess their survival and their ability to express the genes under environmental conditions.

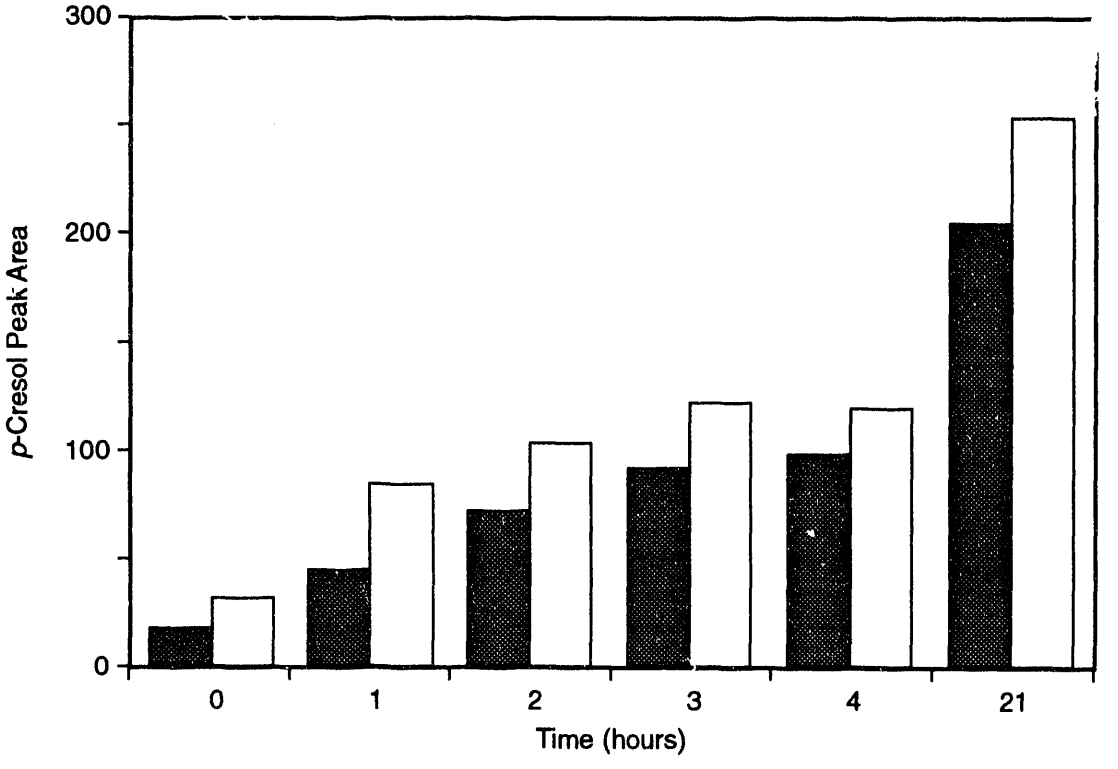

FIGURE 3. Production of *p*-Cresol by BO450 (pMR404)

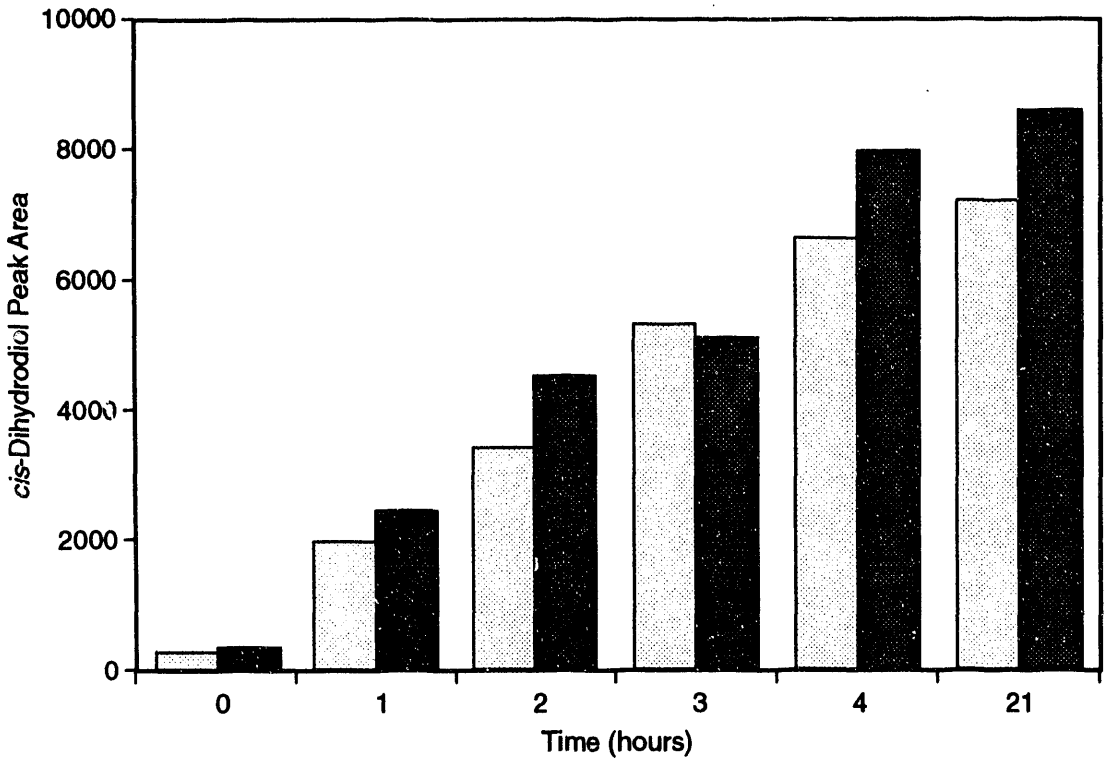

FIGURE 4. Production of *cis*-Dihydrodiol by B0450 (pMR604)

Intermediate-Scale Subsurface Transport of Co-Contaminants

E. M. Murphy, B. D. Wood, T. R. Ginn, F. J. Brockman, R. J. Lenhard, and A. J. Valocchi (University of Illinois)

The natural subsurface environment is often highly heterogeneous in its physical, chemical, and biologic properties. Processes in subsurface environments are complex because of the simultaneous interaction of chemical, microbiological, and hydrologic phenomena. These interacting phenomena determine the distribution and structure of the subsurface microbial community, the evolution of groundwater chemistry, and the migration and fate of solutes. Ultimately, the design of effective remediation strategies depends on our ability to accurately predict the subsurface transport and transformation of contaminants in these complex systems. Previous field experimentation has shown that our predictive ability is limited by 1) a lack of understanding of interacting processes on a mechanistic level, and 2) an inability to scale mechanistic processes from observations in the laboratory to the field. Improving our understanding of mechanistic processes and our ability to scale these processes to relevant field problems can best be addressed by controlled laboratory experimentation in intermediate-scale flow cells. The goals of this project are to identify and test our understanding of interactive mechanisms under controlled laboratory conditions and to develop and test approaches to scaling mechanistic processes to the field.

FY 1992 Research Highlights

During FY 1992, the focus of this project shifted from an emphasis on biodegradation of organic contaminants to testing our understanding of natural interacting processes in the subsurface environment. The reason for this change of focus is that hypotheses arising from field investigations in DOE's Subsurface Science Program are often impossible to test at the field scale. In particular, physical heterogeneity gives

rise to chemical and microbial heterogeneity, often controlling these interacting processes at the field scale. In FY 1992, research was directed to 1) testing our ability to predict large-scale phenomena of solute degradation and transport by incorporating mechanistic microbial processes into a two-dimensional transport model, and 2) the design, premodeling, and background experimental work to address hypotheses on the subsurface biogeochemical carbon cycle. In addition to testing hypotheses relating to the subsurface biogeochemical cycle, we are using intermediate-scale experimentation to determine the effect of natural heterogeneity of groundwater chemistry on microbial transport and distribution and on solute migration. The progress of this work in FY 1992 is summarized in the following sections.

Coupling Microbial Kinetic Processes to Transport. A number of mathematical models have been developed that couple microbial growth kinetics with the transport of biologically active components in groundwater systems. These models can be broadly grouped into two categories: those that include mass-transfer limitations between the fluid phase and the microbes (hereafter referred to as "multiple-phase models"), and those that do not ("single-phase models"). Multiple-phase models define separate biomass and aqueous phases and assume that there is a mass-transfer limitation between them. The result is a set of coupled partial differential equations that describe mass transport in mobile aqueous and immobile biomass phases, as well as the growth of the biomass phase. All multiple-phase models require a mass-transfer coefficient that allows representation of the pore-scale mass-transfer process at the macroscopic scale at which the associated mass-balance equations are valid. Because these mass-transfer coefficients are dependent on geometrical configurations of the biomass and necessarily reflect the effects of averaging the pore-scale mass-transfer process up to the macroscopic scale, it is difficult to interpret them physically.

The second approach assumes that the mass-transfer limitation between the biomass and the aqueous phase can be neglected. This neglect leads to mass-balance equations that are written for a single aqueous phase and do not require the estimation of additional parameters to describe interphase transfer. In fact, for large values of the mass-transfer coefficient, multiple-phase models reduce to a single-phase model.

Microbial Kinetics in Porous Media. In the environment, the growth kinetics of microorganisms are a function of many environmental variables (e.g., nutrient concentrations, pH, temperature, competition with other organisms) and may also be affected by the history of environmental conditions experienced by the organism. However, mathematical descriptions of microbial kinetics in the environment use a substantially reduced set of variables, because exact mechanistic description of microbial processes is generally an intractable problem. In making the mathematical description of microbial kinetics tractable, some empiricism is introduced.

Models used to describe microbial kinetics can be categorized as being either structured or unstructured. Structured models are generally more mechanistic (molecular) and represent physiological changes in the cell by expressing the kinetics in terms of variables that are internal (e.g., concentration of enzymes, DNA, RNA) and external to the cell (i.e., environmental variables). In contrast, unstructured models describe microbial growth as a function of environmental variables only. Application of structured models tends to be somewhat complicated; therefore, models applied to problems in the environment have generally been of the unstructured type.

For applications to groundwater systems, modifications of the unstructured kinetic model proposed by Monod (1949) have been used to describe the specific growth rate as a function of the concentration of one or more limiting nutrients.

In general, the mathematical model used to describe the kinetics of a system should be based on phenomenological considerations. The model should incorporate each of the phenomena that are known or expected to have a significant effect on microbial growth. In addition to the effect of substrate limitation, which is accounted for by such approaches as the Monod model, other effects that may profoundly influence

microbial kinetics include enzyme inhibition, production of metabolic toxins, the occurrence of a lag before substrate degradation can begin, and competition between microbial species. Although there are mathematical methods to describe each of these phenomena separately, no single kinetic model can be generalized to describe microbial growth for all systems.

In the absence of such a single model, we propose the following equations to describe the kinetics of quinoline degradation:

$$\Gamma_{S1} = -kX\,S_1\left(\frac{O}{O+K_{O1}}\right)\lambda \qquad (1)$$

$$\Gamma_{S2} = -\frac{\mu_2}{Y_2}X\left(\frac{S_2}{S_2+K_{S2}}\right)\left(\frac{O}{O+K_{O2}}\right) - r\Gamma_{S1} \qquad (2)$$

$$\Gamma_O = -Xkf_1S_1\left(\frac{O}{O+K_{O1}}\right)$$
$$\lambda - \frac{\mu_2 f_2 X}{Y_2}\left(\frac{S_2}{S_2+K_{S2}}\right)\left(\frac{O}{O+K_{O2}}\right) - \gamma X \qquad (3)$$

where

$S_{1,2}$ = fluid phase concentrations of quinoline and 2-hydroxyquinoline, respectively [M•L^3]
k = first-order reaction rate coefficient [per T]
X = mass of microorganisms attached to solids per unit volume porous medium [M•L^3]
O = fluid phase concentration of oxygen (electron acceptor) as molecular O_2 [M•L^3]
K_{S1} = half-saturation constant for quinoline and 2-hydroxyquinoline [M•L^3]
λ = function accounting for metabolic lag
μ_2 = specific growth rate for microorganisms [per T]
Y_2 = yield coefficient (mass of organisms created per unit substrate consumed)
f_1 = ratio of mass of oxygen consumed per unit mass substrate consumed
f_2 = ratio of mass of oxygen consumed per unit mass substrate consumed
γ = endogenous respiration oxygen utilization coefficient

These expressions are the source/sink terms. In addition, an expression for the growth rate of microorganisms is required:

$$\Gamma_X = X\left(\frac{\mu_2 S_2}{S_2+K_{S2}}\right)\left(\frac{O}{O+K_{O2}}\right) - bX \qquad (4)$$

where b is the microbial decay/endogenous respiration coefficient [per T].

The metabolic lag function λ (Wood and Dawson 1992) is

$$\lambda = 0 \text{ if } \tau < \tau_L$$

$$\lambda = \frac{\tau - \tau_L}{\tau_E - \tau_L} \text{ if } \tau_L \le \tau < \tau_E$$

$$\lambda = 1 \text{ if } \tau \ge \tau_E$$

where τ is the time that microorganisms in a given volume have been in contact with the inducing substrate, τ_L is the lag time, and τ_E is the length of time required to reach exponential growth.

Equation (1) represents the rate of quinoline degradation; Equation (2) represents the net rate of change of 2-hydroxyquinoline (2OHQ, a degradative intermediate of quinoline), which is the sum of the rate of production of 2OHQ from Equation (1) plus the rate of degradation of 2OHQ to carbon dioxide and water. Equation (3) expresses the rate of oxygen uptake from the degradation of 2OHQ, and indirectly from hydrogen ions produced in the quinoline-to-2OHQ step. The last term on the right-hand side of this equation ($-\gamma X$) represents the rate of endogenous respiration and is explained in more detail below. Equation (4) expresses the microbial growth rate as a function of 2OHQ concentration; because no energy or carbon for growth is obtained from the transformation of quinoline to 2OHQ, it is assumed that the microbial growth rate is not a function of quinoline concentration.

Numerical Methods and Model Validation. The numerical methods used to conduct simulations de-couple the transport portion of the equations from the reaction portions, by first solving for the transport with the source/sink term set to zero. The transport equations are solved by a finite-element modified method of characteristics (Chiang et al. 1989), which has the desirable ability to handle large concentration gradients. The concentrations obtained from this step are then used as the initial concentrations for solving the reactions, which are treated as ordinary differential equations and are solved with a second-order, explicit Runge-Kutta method, with time steps that are generally much smaller than those used in transport modeling. This method, in which the reactions are solved separately from the transport problem, is known conventionally as operator splitting (Wheeler and Dawson 1988; Valocchi and Malmstead 1992).

The validity of the microbial kinetic model was tested by comparison of the simulation results to laboratory results. Experiments were conducted in a saturated flow cell [100 cm long (x coordinate) by 10 cm wide (y coordinate) by 20 cm high (z coordinate)] packed with two horizontal sand layers. Advective movement of fluid was in the long (x) direction. The flow cell was packed with a 17-cm-thick, low-conductivity (low-k) layer (0.15 mm sand) overlaid by a 3-cm-thick, high-conductivity (high-k) layer (0.60 mm sand). The initial bacteria inoculation density was $5x10^6$ colony-forming units (CFU) per gram of media in the low-conductivity layer, and 0 in the high-conductivity layer.

For the simulations, the boundary condition at the inlet was a specified concentration, and the boundary condition at the outlet was a zero concentration gradient; concentration values for the inflow boundary and the initial conditions appear in Table 1. Values of the physical parameters used in the simulations appear in Table 2, and kinetic parameters used in Equations (1-4) to conduct these simulations appear in Table 3. The results of model simulations appear as breakthrough curves in Figure 1. These breakthrough curves show the concentrations of quinolin, 2OHQ, and oxygen at a given point as a function of time for locations in the high-k layer (z = 19cm), interface (z = 16 cm), and low-k layer (z = 10 cm).

TABLE 1. Concentrations for Boundary and Initial Conditions

Parameter	Initial Conditions	Simulation Inflow
S_1	20.0 mg/L	20.0 mg/L
S_2	0.0 mg/L	0.0 mg/L
O	9.0 mg/L	9.0 mg/L
X	0 CFU/g	$5x10^6$ CFU/g

TABLE 2. Physical Parameters Used to Model Flowcell

Parameter	Value	Source
θ_w	0.4	Measured
α_l	1.15×10^{-3} m	Measured
α_t	4.50×10^{-4} m	Calculated
k_{high}	1.6×10^{-3} m/s	Measured
k_{low}	1.2×10^{-4} m/s	Calculated[a]
D	1×10^{-9} m^2/s	Bird et al. 1960

(a) Conductivity in the low-k layer (k_{low}) calculated from measured conductivity in high-k (k_{high}) and the ratio of the velocities measured by tracer tests.

The porous media in the flow cell were packed carefully to minimize the influence of hydraulic and microbiologic heterogeneities (other than layering); however, such heterogeneities did occur in the system, and the large volume of the flow cell system contributed substantially to their existence. Although the scatter in the data in Figure 1 is due in part to uncertainty in the analyses of the aqueous-phase constituents, hydraulic heterogeneity within individual layers may also contribute. Furthermore, because the microorganisms were mixed with the porous media in batches, some microbial heterogeneity was inevitable. Microbial heterogeneity would

TABLE 3. Microbial Kinetic Parameters Used to Model Flow

Parameter	Value	Source
k	1.70 per mg/L•d	Measured
K_{O1}	0.02 mg/L	Malmstead 1992
μ_2	1.71 per d	Measured
Y_2	0.35	Measured
K_{S2}	0.05 mg/L	Malmstead 1992
K_{O2}	2.00 mg/L	Malmstead 1992
r	1.12	Calculated
f_1	0.15	Malmstead 1992
f_2	1.50	Measured
g	1.00 per d	Measured
τ_L	0.4 d	Measured; Truex et al. 1992
τ_E	3.0 d	Measured; Truex et al. 1992

lead in turn to heterogeneity in the local reaction rates, which might also cause additional scatter in the observed concentration data.

For the simulations, it was assumed that the initial concentrations of microorganisms throughout the low-k and high-k layers were uniform. Although there were initially no microorganisms in the high-k layer, it was apparent from the breakthrough curves that there was an appreciable number of organisms in this layer when the biodegradation experiment began. We believe that organisms were transported to the high-k layer by advection and dispersion during tracer experiments conducted before the biodegradation experiment. Previous experiments (Truex et al. 1992) and monitoring of the flow cell effluent have shown that at low velocities organisms remain strongly attached to the porous medium. However, during the tracer experiments, velocities in both layers were approximately 45 times greater than during the biodegradation experiments. It is possible that at these higher velocities shear forces were large enough to mobilize organisms, especially from near the hydraulic interface. The actual distribution of organisms in the high-k layer was, therefore, not accurately known at the start of the biodegradation experiment.

At the interface (z = 16 cm), results from simulations match the observed data (Figure 1c, d, and e). The importance of transverse dispersion is particularly evident at this interface (actually within the low-k layer, 1 cm below the high-k layer), where the flux of aqueous components from transverse dispersion greatly affects the shape of the breakthrough curves. The value of the effective transverse dispersivity (α_T) used for these simulations was determined from tracer studies. Simulations of the low-k layer reflected several trends in the observed data. The effects of the endogenous oxygen uptake term in Equation (3) could be seen clearly. The organisms used for the experiment were initially grown on nutrient-rich media, which allowed the organisms to store some carbon. Then if external carbon sources are lacking, this endogenous carbon can be degraded as an energy source to maintain cellular processes; it is such endogenous respiration that causes the oxygen concentration to drop at a constant rate before any quinoline or 2OHQ is present. For the range of oxygen concentrations simulated, a first-order model for endogenous oxygen uptake represented the observed data well.

The effects of microbial lag can also be seen in these simulations. The pulse of quinoline that travels through the low-k layer (Figure 1f, g, and h) is a result of the lag phase. Because some time is required for the organisms in any volume of porous medium to induce the quinoline-degrading pathways once quinoline has been introduced, some quinoline is transported through the volume before degradation begins. Once degradation begins, the quinoline begins to be transformed into 2OHQ. The result is that some of the quinoline initially injected as a front moves through the system as a quinoline pulse. The effect of including the lag phase in simulation can be seen by comparing simulations that account for lag to those that do not. Figure 2 shows the results of such a comparison for the low-k layer at x = 20 cm. The inclusion of microbial lag accounts for the pulse that moves through the system; although all other microbial

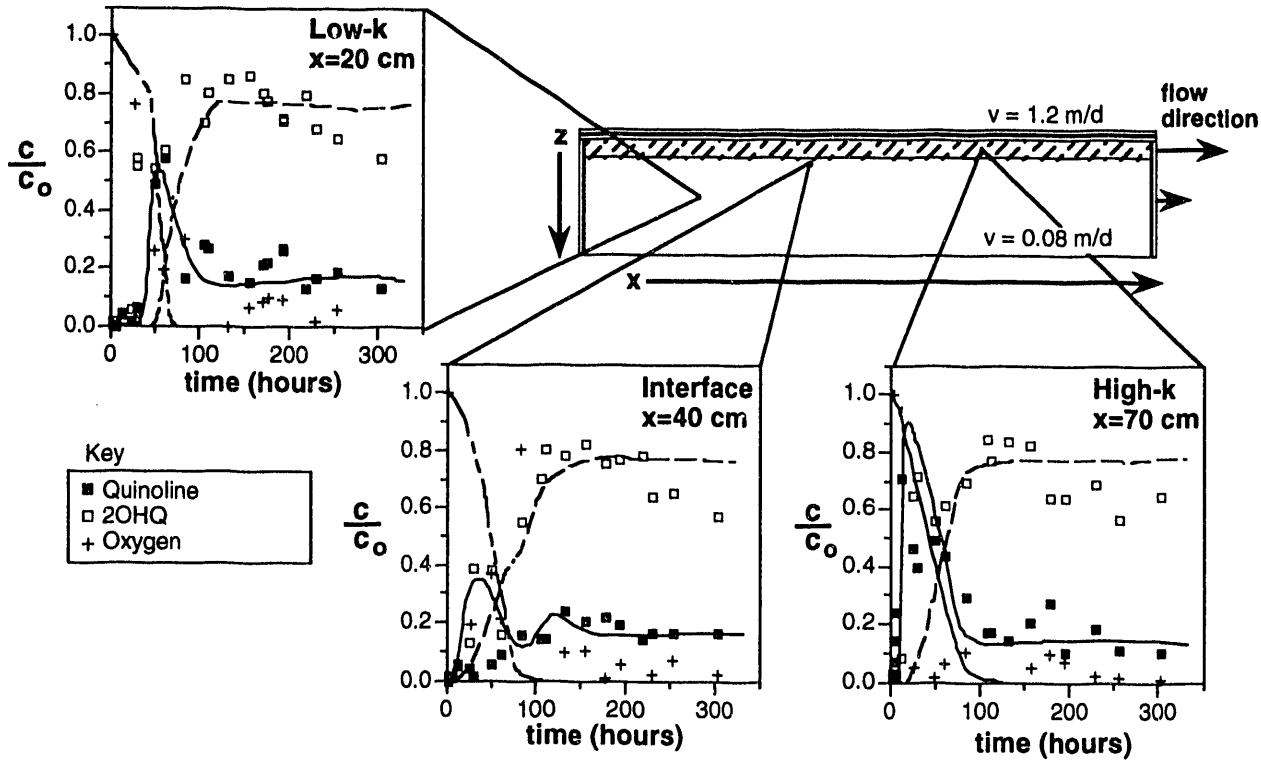

FIGURE 1. Cross Section of Flow Cell Showing Solute Breakthrough Curves for the High-k Layer, Interface, and Low-k Layer

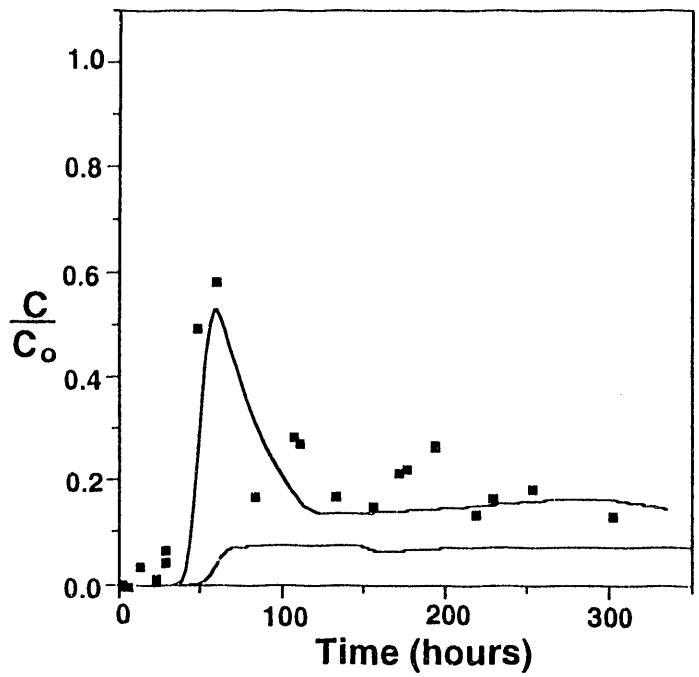

FIGURE 2. Effect of Including Microbial Lag in the Model Fits of Quinoline Degradation. Solid lines represent model fits.

parameters are the same for the two simulations, the case that accounts for lag indicates a higher concentration is maintained for longer times.

Measured and simulated microbial concentrations are compared in Figure 3, which shows a concentration contour plot for a vertical plane along the length of the flow cell. Although the initial concentration of organisms in the high-k layer was not accurately known, the final distributions of organisms for the simulations and observed data match relatively well; the correlation between the concentration at the sampled points and the corresponding simulation was 0.70.

Increased growth in the low-k layer near the hydraulic layer interface was observed. The simulated microbial concentrations also showed this trend, although the simulations show significantly more growth in the high-k layer than was observed.

Discrepancies between the observed data and simulations appear to derive largely from three sources: 1) uncertainty in the initial concentration of organisms in the high-k layer when the biodegradation portion of the experiment was begun, 2) heterogeneities in packing and in initial microbial distribution, and 3) redistribution of organisms in the low-k layer during tracer tests. Some redistribution of organisms in the low-k layer is believed to have occurred, because the final microbial concentrations in portions of the low-k layer were lower than the initial concentration. Although this redistribution did not appear to have much effect on the breakthrough curves, it may explain the apparent increase in microbial concentration near the outlet of the flow cell (Figure 3a).

Results of the simulations suggest that kinetic models developed from batch and small-scale column experiments can be applied on larger

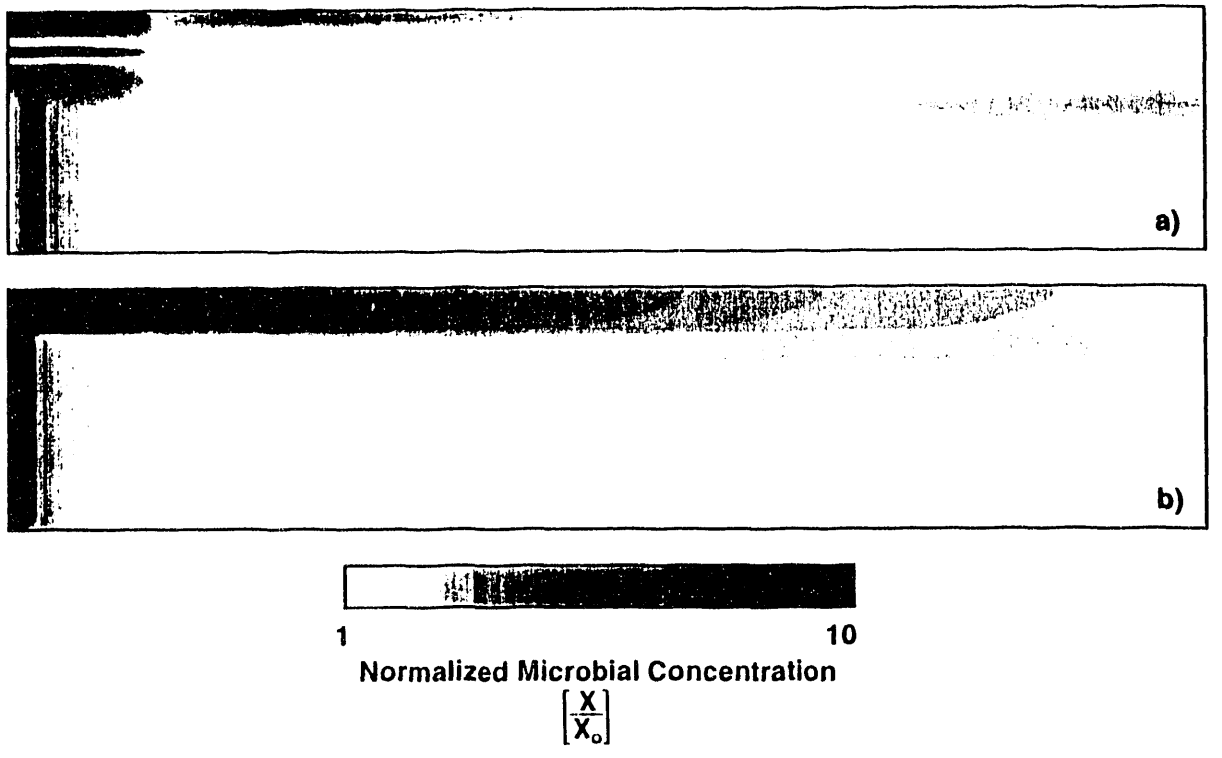

FIGURE 3. Comparison of Microbial Biomass Concentrations in a Cross Section of the Flow Cell: a) Measured concentration, b) Modeled concentration

scales using unstructured (spatially averaged) models to predict the behavior of heterogeneous systems. Thus one kinetic model with a consistent set of parameters could be used to successfully simulate the interaction between transport and reactions in a system with hydraulic heterogeneity. The advantages of this method are that unstructured models are simpler than structured models, are much easier to scale to large field problems, and do not require information about how the microbes are distributed in the subsurface environment. The results also showed the importance of including microbial lag in the simulations and that lateral mass transfer increases microbial activity at the layer interface.

Intermediate-Scale Investigations of Subsurface Biogeochemical Processes. Early in FY 1992, a series of planning meetings were held to develop research questions for intermediate-scale experiments that would address several important issues within the Subsurface Science Program: 1) the effect of spatial heterogeneity on the subsurface biogeochemical cycle (relating to field observations in the Deep Microbiology Subprogram); 2) microbial transport in porous media (to be studied in collaboration with investigators in the Microbial Physiology, Colloids, and Deep Microbiology Subprograms); 3) the role of mineral/chemical heterogeneities relative to the redox potential and transport of chelated radionuclides; and 4) the role of microbial iron reduction relative to the redox potential and transport of chelated radionuclides. The merits of these research issues and preliminary design were reviewed by a group of microbiologists, hydrologists, and geochemists within the Subsurface Science Program. This project will address research issues associated with field studies in the Deep Microbiology Subprogram in FY 1993 and microbial transport issues in FY 1994. The research issues in 3 and 4 are being addressed by the Co-Contaminant Chemistry Subprogram using the intermediate-scale approach, and will not be covered in this review.

Intermediate-Scale Experimentation in Support of Subsurface Science Program Field Hypotheses. Field studies in the Subsurface Science Program have demonstrated heterogeneity in physical, chemical, and microbial characteristics in deep subsurface systems. For instance, aerobic and anaerobic heterotrophic microorganisms were widely distributed throughout sediments from the Atlantic Coastal Plain. Although aerobic heterotrophs were the dominant microorganism in sediments from aerobic groundwater, anaerobic heterotrophs, such as iron- and sulfate-reducing organisms, were also present. This diversity in microorganisms was also reflected in the groundwater chemistry. Anomalously high concentrations of ferrous iron were detected in aerobic groundwaters, suggesting that 1) iron-reducing microorganisms were active in anaerobic microsites within an aerobic aquifer, and 2) mixing between stratified aerobic and anaerobic zones was induced during pumping. Organic-rich lignite was distributed as inclusions within the otherwise sandy coastal sediments, yet the aerobic heterotrophic microorganisms decreased with increasing proximity to these organic-rich inclusions, suggesting that the zones were anaerobic. This subsurface system may represent a classic microbial food chain, in which fermenting microorganisms degrade complex organic matter to simple organic acids that, in turn, serve as organic substrates for anaerobic and aerobic heterotrophs. Ultimately, the distribution of individual microbial species in the subsurface community will be determined by the chemical and physical heterogeneity of the system.

The rate of fermentation of organic acids in microsites and the density of such anaerobic microsites determine the spatial distribution of respiring microorganisms. The microsites, by their very nature, are anaerobic because the inclusions represent low-k flow zones. Therefore, two processes interact to influence the spatial distribution of microorganisms: 1) the rate of fermentation of organic acids in microsites, and 2) the distribution and concentration of organic acid substrate controlled by this complex physical flow field. The processes that have led to the distribution of microorganisms in the Atlantic Coastal Plain sediments cannot be determined by the scale of the field sampling, which is limited by several factors: 1) sampling through a vertical plane was one dimensional, 2) the density of sampling was low relative to the scale of the heterogeneities, and 3) the distribution of cell numbers in oligotrophic environments is often not correlated with cell

activity. For such reasons, process-level studies of the effects of chemical and physical heterogeneity on the structure of microbial communities can best be addressed under controlled laboratory conditions in intermediate-scale flow cells. The use of intermediate-scale experimentation with coupled transport/biodegradation models allows us to validate and apply quantitative bounds to these processes.

Physical Aspects of Anaerobic Inclusions and Experimental Design. The association of microbial communities with lignitic inclusions in an unconsolidiated matrix implies general design limits on the shape and type of the heterogeneities involved. From the physical perspective, these limits make the heterogeneous conductivity field binary inclusive isotropic; that is, point-symmetric (cubic or spherical) low-k zones are placed within a homogeneous medium.

The central hypothesis that drives the design criteria for physical heterogeneities concerns our ability to separate microbial kinetics and physical transport and to accurately predict microbial dynamics in a heterogeneous medium. Specifically, we hypothesize that the primary vehicle for the cause-effect link from binary inclusive physical heterogeneities to microbial processes is the set of transport processes affecting microsite environmental conditions: solute advection, dispersion, and diffusion. If this hypothesis holds, physical heterogeneity dominates microbial dynamics by means of the transport process. The corollary to this hypothesis is a necessary condition for the cause-effect relation between binary inclusive physical heterogeneity and microbial dynamics. This corollary is that the transport process is driven by physical heterogeneity and can effectively be separated from microbial kinetics.

This hypothesis and its corollary are important and, if they are valid, the understanding of microbial dynamics in the heterogeneous subsurface can be divided into two tractable problems: 1) the determination of microbial kinetics by means of inexpensive batch and column experiments in the laboratory, independent of heterogeneity patterns in the field, and 2) the characterization of the field transport regime (using the host of tools developed for solute transport simulation). If it proves appropriate, this approach would greatly expedite field-scale examination of microbial phenomena, facilitating research into basic questions about the history and fate of microbes in the subsurface. It would also simplify the prediction of biodegradation in complex subsurface systems.

We will test the hypothesis by performing batch experiments to determine the parameters of microbial kinetics in the absence of heterogeneities and carrying out intermediate-scale experiments with and without microbes. Then the microbial kinetics will be joined with high-resolution simulations of the transport regime to predict experimental measurements on multiple scales. If the experimental measurements can be successfully predicted, it will validate the separability hypothesis. On the other hand, if the experimental measurements cannot be predicted, it will give valuable information as to whether it is the model of transport, the microbial kinetics, the upscaling (of either), or the hypothesis of separability that is flawed.

To carry out this study, the scales of the heterogeneities involved must be carefully specified, because they relate to both the expected scales of transport and the scales of measurement. To afford the most general interpretations of the experimental results, the physical design must capture the essential aspects of the heterogeneity pattern while avoiding unnecessary elements that may illuminate specific profiles of transport at the expense of a more general insight into the effect on microbial systems. Bearing these considerations in mind allows design of a representative heterogeneity pattern that is both general to a variety of DOE sites and recognizable as representing a useful class of heterogeneities. These considerations direct the resolution of three major issues for physical design: isotropy, periodicity, and scale.

Isotropy: Because the dominant direction of fluid or gas flow in binary inclusive systems varies widely over sites, there is no clearly preferred orientation for potentially asymmetric low-k zone inclusions. Moreover, anisotropically heterogeneous systems, particularly binary inclusive systems, can often be treated as mathematical

distortions of isotropic systems. Thus the criterion of generality leads us to choose an isotropic design. Extensions from isotropic conditions are achieved simply by making the average separation between inclusions spatially dependent or making the inclusions themselves asymmetric.

Periodicity: Despite the well-known difficulties of applying classical dispersion relations to physically heterogeneous systems, some new theories to represent transport in periodic systems are improvements on classical descriptions, but these theories are as yet novel and untested. To understand and predict transport and microbial dynamics within binary inclusive heterogeneous systems (e.g., in the field) requires that we validate and use a rational description of the transport processes in these systems. To meet this need, these experiments will provide timely and useful data for testing descriptions of transport in such systems. These descriptions include classical, periodic, and nonlocal theories.

Although the specific aspects of heterogeneity periodicity of the planned experiments cannot be determined beforehand, it is possible to address these design questions by means of high-resolution premodeling. Premodeling for periodicity design requires that competing transport descriptions be incorporated into simulators and then that the simulators be operated with different periodicity parameters (e.g., size and separation of inclusions, shape of inclusions, packing orientation of inclusions). The untested transport theories can be used in this premodeling exercise because the heterogeneity field is wholly known and specified. The premodeling can identify those regimes of periodicity parameter values under which the various transport descriptions perform well or poorly. These parameter values can then be used to design the experiments to address specific transport scenarios to investigate the net effect on microbial dynamics.

Scale: In the natural subsurface environment, heterogeneities may occur on multiple discrete or even continuously evolving scales. Figure 4 depicts how a transport parameter such as conductivity might vary as the scale of the measurement of that parameter increases. As depicted, the value of the parameter may be relatively constant for certain sample size ranges (spectral ranges) between the scales of the heterogeneities, and then exhibit noisy fluctuations at the scales of heterogeneities. In the system shown in Figure 4, heterogeneities are on four discrete scales, where the lowest scale corresponds to pore-scale heterogeneity, and the highest scale corresponds to the presence of different geologic strata or facies. The flatter regions where parameter values are relatively constant are known as representative elementary volume (REV) wavelengths.

The problem posed by such multiple-scale heterogeneity is that transport equations are necessarily derived on a specific scale, usually above the pore scale but much smaller than the field modeling scale. Then the application of the model assumes that there are no other scales of heterogeneity between the pore scale and the modeling scale. This assumption typically fails, with varying degrees of damage to the model's predictive capability. The most robust way to treat this problem is to treat all scales of heterogeneity, arriving at the field scale from above and below simultaneously (Figure 4). To do so, first characterize deterministically the heterogeneities existing at or above the modeling scale ("zonation") and incorporate the corresponding zones into the field-scale model. (Zonation refers to the geophysical identification and characterization of field-scale heterogeneous zones, and the incorporation of this information into process models.) Then upscale the transport equation by determining the effect of the middle-scale heterogeneities on the equation that was originally derived.

Upscaling has only recently been recognized as a requisite for understanding (and predicting) transport processes on the field scale. New work has shown that, under certain relatively benign patterns of heterogeneity, the classical equations of transport may not be a suitable framework for simulating transport processes on large scales. With the realization that the old equations will not work, new research on upscaling has focused on stochastic (asymptotic), nonlocal, and heterogeneity-specific transport theories. In light of these developments, a

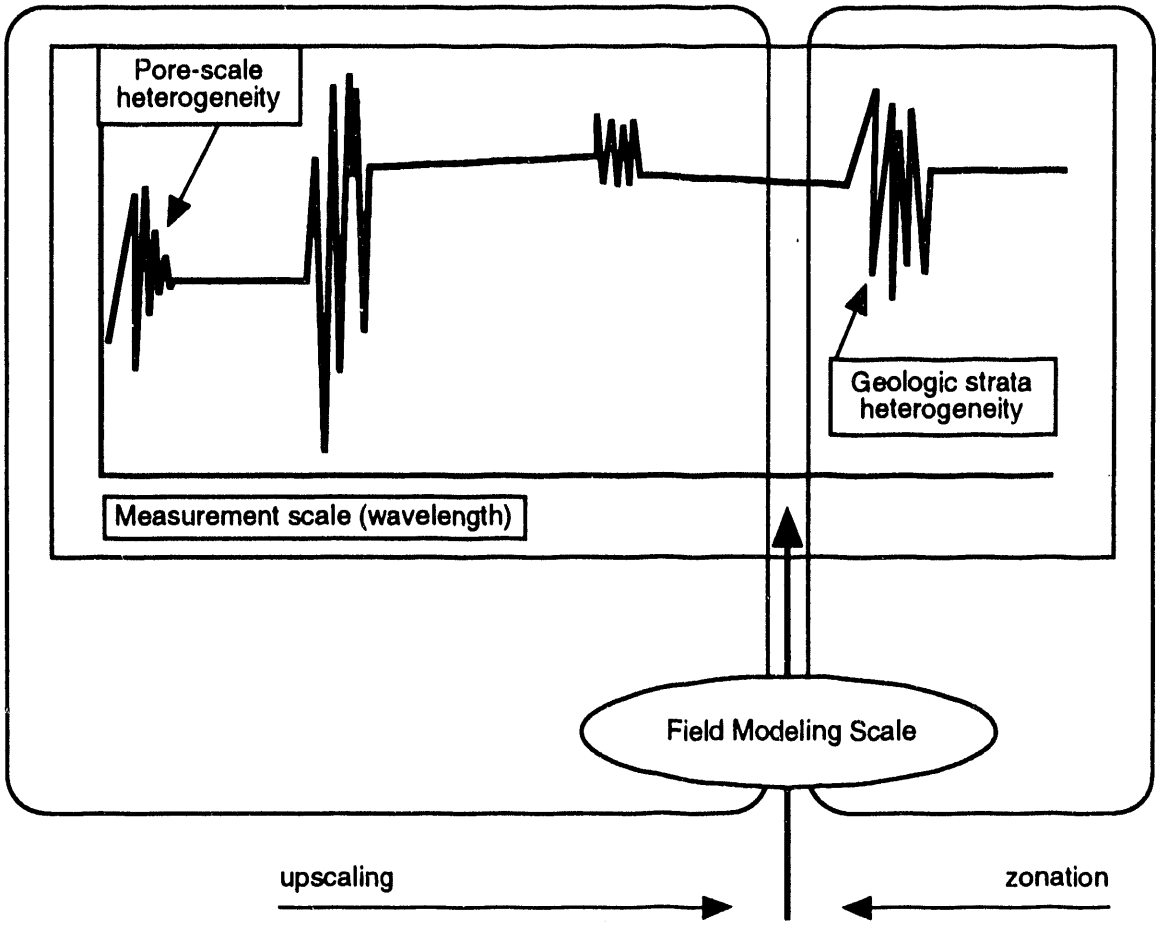

FIGURE 4. Scale of Measurement of Transport Parameters in Heterogeneous Media Ranging from Pore-Scale to Field-Scale Geologic Strata

question arises: given the general pattern of heterogeneity involved in the experiment, what scales of heterogeneity should be involved in the design?

Design Aspects. As a first consideration, the experimental design must address the separability hypothesis. To do so requires that high-resolution measurement and modeling of transport alone be tractable, and that microbial dynamics be measurable within the scale of the heterogeneous inclusions (and matrix) alone. Consequently the inclusions must be larger than a minimum size determined by 1) resolution of the transport modeling capability and 2) the microbial kinetic batch experiments (Figure 5). This approach allows measurement of dispersion and other processes on multiple length scales and, hence, insight into the effect of the heterogeneities on the scaling of the transport processes.

Second, unless the potential for validation of upscaling the observed relations is ensured, the experiments could provide ungeneralizable results. In fact, it can be argued that the principal value of the intermediate-scale experiment is that it affords upscaling validation, albeit on a restricted spectral range. In this case, although the separability hypothesis may hold for a single low-k inclusion, it is not clear that it would hold for a field in which such inclusions are closely packed. As a result, the separability hypothesis itself requires upscaling. This is only possible if the overall experimental volume is much larger than the sizes of the inclusions

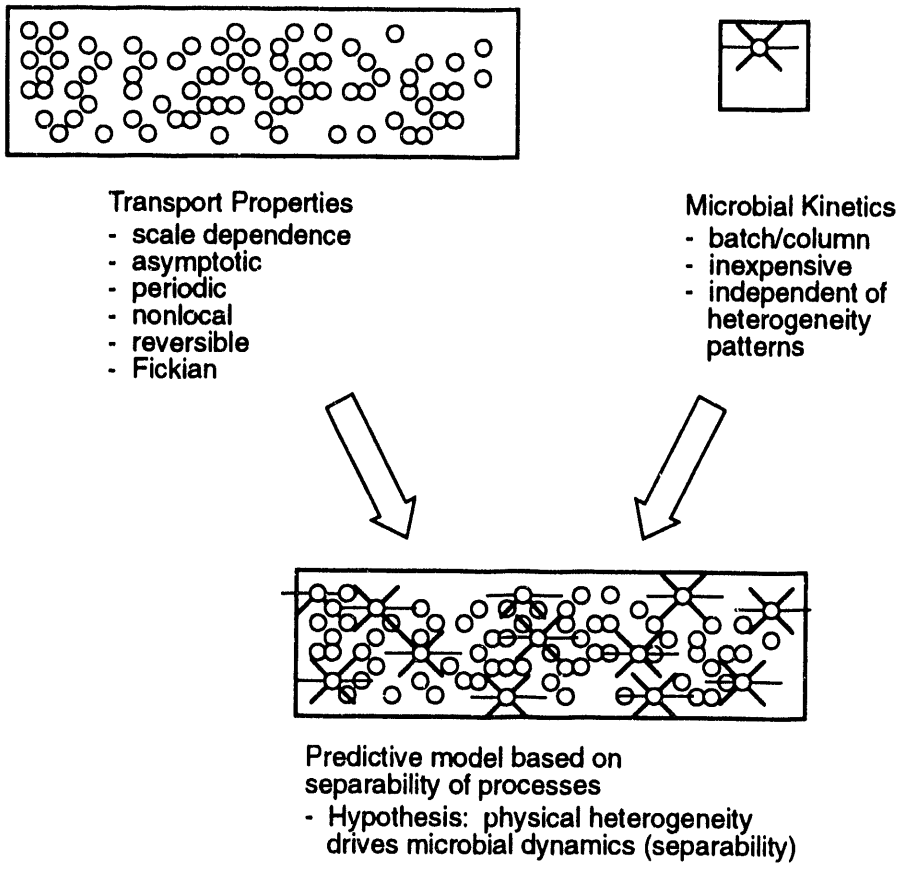

FIGURE 5. Design of Physical System in 1-m Flow Cell Showing Low-k Organic Inclusions

involved, and if measurements are taken on multiple scales. Mathematically, such an approach affords measurement on an REV wavelength, with heterogeneities being restricted to a spectral range well below the experimental domain. Premodeling may be used to determine specific ranges, but dispersion studies indicate that a two-order-of-magnitude difference is desirable. To accommodate this, if the inclusions are spherical with diameters on the order of a few centimeters, then the total flow domain should be on the order of 1 or 2 m (Figure 5).

Addressing the Separability Hypothesis. Restricting the heterogeneities to scales that are small relative to the overall experimental volume has the effect of broadening the total range of measurement scales. It allows assessment of the separability hypothesis on both the scale of the heterogeneity and the scale of the experiment. If the scale of the experiment is large enough to permit REV wavelength measurements of dispersion as well as measurements on the scale of the small inclusions, the data will also afford testing of scale-dependent transport theories, including periodic, stochastic asymptotic, and nonlocal theories. The broad range of measurement scales also allows analysis of microbial data on multiple scales. Larger-scale measurements of microbial populations can be used to cross-check the results of batch experiments that were used to determine microbial kinetics originally. Larger-scale comparative measurements of solute breakthrough (e.g., comparing experiments with and without microbes) makes it possible to assess the use of such measures as proxy measures of microbial activity at larger scales.

Experimental Design with Microorganisms. This experimental design has multiple levels of complexity, ranging from an environment of

respiring aerobic microorganisms in the transmissive matrix only to an environment of competition between aerobic microorganisms in the transmissive matrix and anaerobic respiring microorganisms in the low-k inclusions. The spatial distribution of respiring microorganisms in heterogeneous systems is controlled by 1) the distribution and concentration of organic acid substrate, which is controlled by the complex physical flow field; 2) the rate of fermentation of organic acids in microsites; and 3) competition between the aerobic and anaerobic microorganisms. The goal of the experiments with microorganisms is to determine the levels of contribution of each of these controlling factors.

For the initial experiments with only a single microbial species, the respiring microorganism selected is *Pseudomonas cepacia* 3N3A strain, an aerobic heterotroph isolated from the Middendorf aquifer in South Carolina. In the experiments, 3N3A is initially evenly distibuted throughout the high-k matrix. Although 3N3A tends to adhere to the matrix readily, its final distribution in this heterogeneous system reflects a combination of convective processes (i.e., the induced flow field) and the concentration of substrate (which is controlled by the heterogeneous flow .field). Initially, the rate of substrate flux (release of organic acids to represent fermentation reactions in the subsurface environment) is constant. In subsequent experiments, the rate of organic acid production is varied to determine the effect of fermentation rates on microbial distribution.

The most complex experiments contain two respiring microorganisms, the 3N3A strain and *Geobacter metalloreductans* GS-15, a heterotrophic iron-reducing microorganism that is an obligate anaerobe. Within this microbial community structure, 3N3A and GS-15 compete for the same electron donor (i.e., organic acid) and the organic acids are produced in the low-k anaerobic inclusions. Because GS-15 is anaerobic, it can reside closer to the source of organic substrate (i.e., the fermenting organisms) than 3N3A, and may have a proximity advantage. However, GS-15 is also dependent on 3N3A to keep the concentration of oxygen low around the anaerobic organic microsite.

The discrete microsites in this flow cell create complicated flow and pressure fields, affecting the distribution of an organic substrate in the absence of biodegradation (Figure 5). The following research questions are being addressed:

- Does the density of microsites control the spatial distribution of a surrounding microbial community by affecting the flux of nutrients and electron acceptors?

- What rate of fermentation (or production of organic acids) is necessary to support both an anaerobic heterotroph microbial community and an aerobic heterotroph community in a system analogous to the Savannah River Site?

- Do anaerobic heterotrophs have a spatial advantage over the aerobic heterotrophs in the structure of the microbial community? Can the spatial advantage of proximity to the carbon source give a species a competitive advantage by shortening the generation time?

Future Research

The intermediate-scale approach will continue to be used to investigate complex research questions encompassing interacting microbial, chemical, and hydrological processes. The major emphasis is on testing hypotheses that arise from field studies, but that cannot feasibly be tested at the field scale. The future direction of this project will be closely linked to research issues in microbial origins and microbial transport.

References

Bird, R. B., W. E. Stewart, and E. N. Lightfoot. 1960. *Transport Phenomena.* John Wiley & Sons, New York.

Chiang, C. Y., M. F. Wheeler, and P. B. Bedient. 1989. "A Modified Method of Characteristics Technique and a Mixed Finite Element Method for Simulation of Groundwater Solute Transport." *Water Resources Research* 25:1541-1549.

Malmstead, M. J. 1992. *Modeling Oxygen-Dependent Biodegradation of Quinoline in Batch and Column Systems.* Master's Thesis, University of Illinois, Urbana-Champaign, Illinois.

McMahon, P. B., and F. H. Chapelle. 1991. "Microbial Production of Organic Acids in Aquitard Sediments and Its Role in Aquifer Geochemistry." *Nature* 349:233-235.

Monod, J. 1949. "The Growth of Bacterial Cultures." *Annual Review of Microbiology* 3:371-393.

Valocchi, A., and M. Malmstead. 1992. "Accuracy of Operator Splitting for Advection-Dispersion-Reaction Problems." *Water Resources Research* 28:1471-1476.

Truex, M. J., F. J. Brockman, D. L. Johnstone, and J. K. Fredrickson. 1992. "Effect of Starvation on Induction of Quinoline Degradation for a Subsurface Bacterium in a Continuous-Flow Column." *Applied and Environmental Microbiology* 58:2386-2392.

Wheeler, M. F., and C. N. Dawson. 1988. "An Operator-Splitting Method for Advection-Diffusion-Reaction Problems." In *MAFELAP Proceedings VI*, ed. J.A.S. Whiteman, pp. 463-482. Academic Press, New York.

Wood, B. D., and C. N. Dawson. 1992. "Effects of Lag and Maximum Growth in Contaminant Transport and Biodegradation Modeling." In *Proceedings of the IX International Conference on Computational Methods in Water Resource Modeling* 2:317-324.

Subsurface Microbial Processes

J. K. Fredrickson, F. J. Brockman, and T. O. Stevens

Contributors

D. Balkwill (Florida State University), T. Kieft (New Mexico Institute of Mining and Technology), B. N. Bjornstad, P. E. Long, J. P. McKinley, T. Phelps (Oak Ridge National Laboratory), S. A. Rawson, D. Ringelberg (University of Tennessee), S. Nierzwicki-Bauer (Rensselaer Polytechnic Institute), D. White (University of Tennessee), and J. M. Zachara

In recent years, there has been increasing interest in the microbiology of the deep terrestrial subsurface. Core samples have been recovered from a number of boreholes at depths to 2,800 m below ground surface and subjected to microbiological analysis. A diverse array of microorganisms has been detected in these samples from both aquifer and vadose zone environments. This interest is driven in part by the need to estimate the potential for bioremediation of subsurface contaminants, but other studies have focused on understanding the basic ecology of this little-studied portion of the biosphere.

In particular, groundwater quality is a major environmental issue for DOE, the nation, and the world, and it will become increasingly important as reliance on this water source continues. Microbial transformation of organic and inorganic contaminants has been shown to be a potential mechanism for remediating and stabilizing contaminants in soils and shallow aquifers. However, while there is scientific information on the types and activities of microorganisms that exist in these systems, little is available for deep systems, from 50 to 1,000 m. The work reported in this article is a continuation of research that has been ongoing since the early exploratory stages of DOE's Deep Subsurface Microbiology Research Program. DOE operates a number of sites where dispersed contaminants are present at depths to several hundred meters. At the sites in the arid western United States, thick vadose zones can act as contaminant reservoirs for the saturated zone. There is currently little information about the diversity and activity of microbial populations that may reside in the unsaturated zone. It is the objective of this project to improve the current understanding of the microbiology of these environments.

There are several fundamental questions regarding the microbiology of deep subsurface saturated zones, including the source of energy for the organisms that reside there and the geochemical and geophysical controls on their *in situ* growth and metabolic activities. A number of research hypotheses have been formulated to develop a thorough understanding of the ecology

of microorganisms in deep subsurface environments, focusing on the physical, geological, and chemical properties controlling their presence and activities. We believe this information to be essential for predicting contaminant fate and developing biological remediation strategies. Finally, the origins of microorganisms in deep subsurface environments are not well understood. However, it is clear that in deep, oligotrophic subsurface environments where electron donors are scarce, microorganisms must be capable of maintaining cell integrity for extended, and in some cases even geologic, time periods.

The goal of this research project is to investigate the ecology of microorganisms in deep subsurface environments, focusing on factors that control the composition and distribution of these microbial communities and their respective metabolic activities. Ultimately, an improved understanding of the fundamental ecology of subsurface microorganisms that will contribute to an improved predictive capability is expected.

FY 1992 Research Highlights

In FY 1992, the focus of this research project was on 1) investigating mechanisms that control the distribution and activities of microorganisms in the vadose zone and 2) initiating a **GE**ochemical-**M**icrobial-Hydrological **EX**periment (GEMHEX) to evaluate certain hypotheses regarding the geochemical and hydrological factors that control the presence and activity of subsurface microorganisms.

This article is not a comprehensive summary of all research activities over the past year, but rather provides examples of key results and their implications.

Effect of Storage on Microbial Community Structure and Activity in a Subsurface Paleosol. Deep vadose zone sediments at arid western sites, such as the Hanford Site, are harsh environments for microorganisms, because nutrient input from moisture recharge is essentially absent and the availability of sediment-associated nutrients to microorganims is very low due to limited moisture. The result is starvation conditions. However, the majority of sites at Hanford that are candidates for *in situ* bioremediation have been impacted in the recent past by artificial recharge from site operations. Therefore, knowing the impact of artificial recharge on subsurface microbial communities is important for assessing the potential for using indigenous microflora for *in situ* biorestoration of contaminanted subsurface environments.

In an earlier study (Brockman et al. 1992), we described the microbiology of a stratigraphically defined paleosol (a surface soil that had been buried in the geological past) at one location that had been impacted by artificial moisture recharge and at a second location that was not impacted. In that study, sediment from the center of the core was removed for microbiological characterization, resulting in disturbance of the material before it was stored. Although immediately after sampling microbiological parameters at both locations were similar, storage of the sediment affected by artificial recharge resulted in log2 to log4 increases in culturable microorganisms. However, there was little change in the microbiological properties (Figure 1). Similar storage-induced increases in culturable microorganisms and other microbiological parameters have since been observed in other Hanford Site deep vadose zone samples affected by artificial recharge.

The effects of disturbance and of oxygen concentration were identified as factors likely to control the storage-induced changes in microbiology. Disturbance could increase nutrient availability by redistributing cells and liquid- and solid-phase nutrients and by increasing gaseous exchange. Removal of sediments from the subsurface and storage in the laboratory would result in exposure to a greater oxygen concentration and diffusion rate. Therefore, the objectives of this study were 1) to further examine the paleosol impacted by artificial recharge to determine the mechanisms controlling the storage-induced changes in microbiology and 2) to use molecular methods to further characterize the changes in community structure during storage.

A 1-m by 1-m intact block of paleosol was removed from the White Bluffs, 0.5 m behind the face of a recent landslide scarp. In the laboratory, the sediment was aseptically cut into small blocks about 5 cm on a side, and groups of 7 blocks were distributed to each of 48 jars

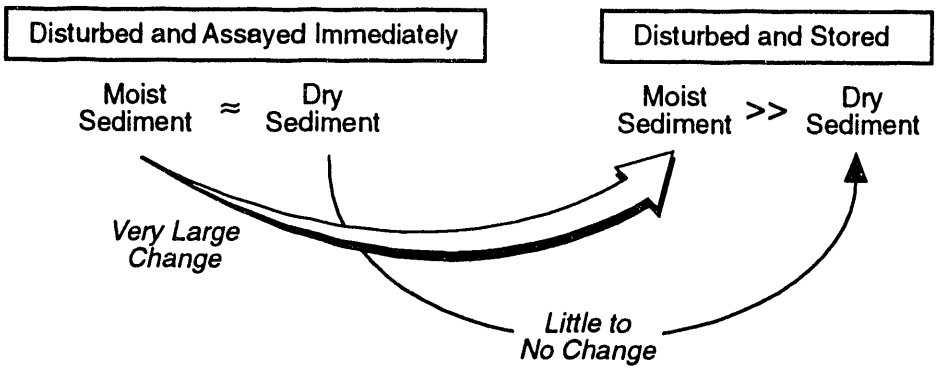

FIGURE 1. Representation of the Microbiological Properties of a Subsurface Paleosol before and after Storage. The paleosol was sampled at a location impacted by artificial recharge (moist sediment) and at a nearby unimpacted location (dry sediment).

(336 blocks). An equivalent number of blocks were aseptically crushed and the sediment passed through a 2-mm screen. The homogenized sediment was then distributed to another 48 jars. Both the intact and homogenized sediments were stored at 15°C under atmospheric (21%), reduced (4.5%), and microaerobic (0.5%) oxygen concentrations. After storage of sediment for 3, 5, 9, 16, and 32 weeks, triplicate jars were sacrificed for each of the six treatments, and microbiological parameters were measured. (The remaining jars were used in geochemical analyses.)

As storage time increased, heterotrophic bacteria able to grow on 1% peptone-trypticase-yeast extract-glucose (PTYG) medium increased more rapidly and to a greater extent in the homogenized sediment than in the intact sediment (Figure 2). However, even in the intact sediment increases were quite large, suggesting that a factor other than homogenization *per se* was involved. Diffusion of oxygen into the sediment blocks is likely to be the primary controlling factor responsible for the increased numbers of heterotrophic bacteria. Analysis of population densities among the jars at different oxygen concentrations showed that statistically greater populations were present in microaerobic incubations than in standard oxygen incubations in the intact sediments at the later timepoints (9, 16, and 32 weeks). In the homogenized sediments, microaerobic and/or reduced oxygen incubations produced statistically greater populations than did standard oxygen incubations at 5, 9, and 32 weeks. These results indicate that the indigenous bacteria are adapted to microaerobic conditions.

The total number of cells, as measured by acridine orange direct counts (AODC), did not increase substantially in two-thirds of the treatments, and increases in culturable microorganisms were 20 to 300 times greater than increases in AODC in the remaining one-third of the treatments. Phospholipid fatty acid (PLFA) concentrations, an alternative measure of total biomass, showed a similar pattern. The PLFA concentrations after storage (1.0-12.5 pmol/g sediment) were rarely greater than immediately after sample acquisition (4.5 pmol/g sediment). Thus, increases in biomass were very small relative to increases in the culturable population. The increases in the culturable populations may be due to 1) biomass turnover (i.e., multiplication of specific microorganisms that are able to utilize dead and dying cells), 2) resuscitation of microorganisms that had been dormant or otherwise unable to grow immediately following sample acquisition, or 3) a combination of the two processes.

Phospholipid signature biomarkers were used to determine whether major components of the microbial community changed with increasing storage and with the different treatments. Similar clusters were observed when either the homogenized sediments or the intact sediments

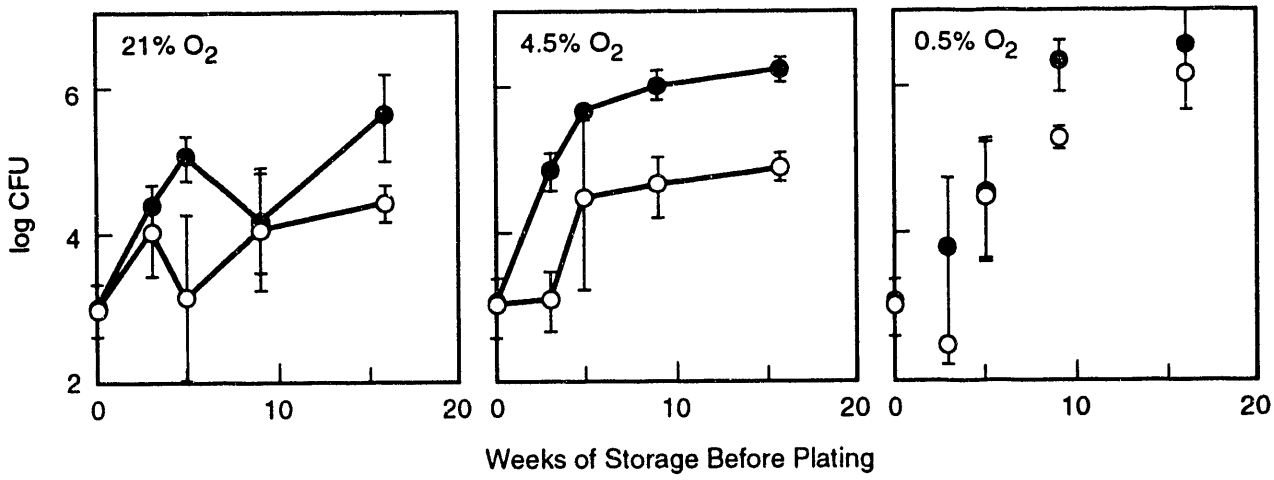

FIGURE 2. Colony-Forming Units (CFU) in Homogenized (closed circles) and Intact (open circles) Sediments Stored under Atmopheric (21%), Reduced (4.5%), and Microaerobic (0.5%) Oxygen Concentrations

were analyzed. Sediments stored for 3 weeks and 5 weeks at microaerobic and reduced oxygen conditions, and all timepoints at the standard oxygen condition, formed cluster 1. Principal component analysis showed that a fungal signature biomarker, monoenoic PLFA, was a major component in defining cluster 1. Sediments stored for 9, 16, and 32 weeks at microaerobic and reduced oxygen conditions formed cluster 2. Terminally branched PLFA, a signature biomarker for Gram-positive microorganisms, was the major component in defining cluster 2. Terminally branched PLFA was present at concentrations 6 to 11 times greater in the intact sediment, and 3 to 5 times greater in the homogenized sediment than it had been immediately following sample acquisition. These data indicate that Gram-positive microorganisms displaced portions of the original community at the later timepoints under microaerobic and reduced oxygen concentrations. However, shifts in signature biomarkers, as for AODC and total PLFA, were small relative to the increases in culturable populations.

Rate constants for ^{14}C-glucose (3 μg in 10 μl water/g moist sediment) mineralization to $^{14}CO_2$ increased by 3 to 7 times as compared to immediately following sample acquisition. Lag times for ^{14}C-glucose mineralization decreased with increased time of storage prior to the addition of substrate (Figure 3). Decreased mineralization lag times may result from either colonization of regions of the sediment that were not initially colonized or resuscitation of microorganisms that had initially been dormant or otherwise unable to grow immediately following sample acquisition. Lag times at 3 weeks were statistically lower than the initial lag time for the homogenized sediments. In contrast, in the intact sediments lag times were not (with one exception) statistically less than the initial lag time until 9 weeks. After 32 weeks of storage, both rate constants and lag times were similar for homogenized and intact sediments. These results show that the intact sediments responded slower than the homogenized sediments but eventually reached a similar endpoint, suggesting that oxygen diffusion into the intact sediment blocks strongly controls the microbial response to substrate addition.

Microbial production of carbon dioxide in the absence of exogenous substrate makes it possible to measure the effect of the various treatments on microbial utilization of sediment organic matter. Immediately following sample acquisition, sediment was placed in gas-tight vials and incubated at 25°C for various lengths of time, and then the headspace was analyzed by gas chromatography. Carbon dioxide concentrations were statistically greater than background concentrations in all treatments after 14 weeks incubation (Figure 4). However,

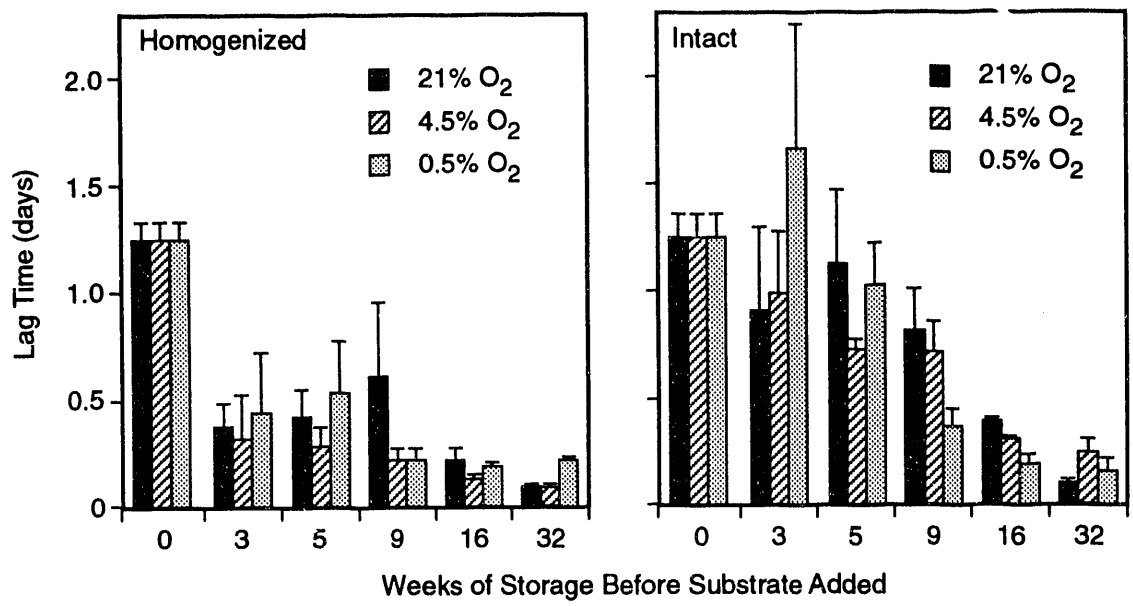

FIGURE 3. Lag Times for Glucose Mineralization in Homogenized and Intact Sediments Stored under Atmospheric (21%), Reduced (4.5%), and Microaerobic (0.5%) Oxygen Concentrations

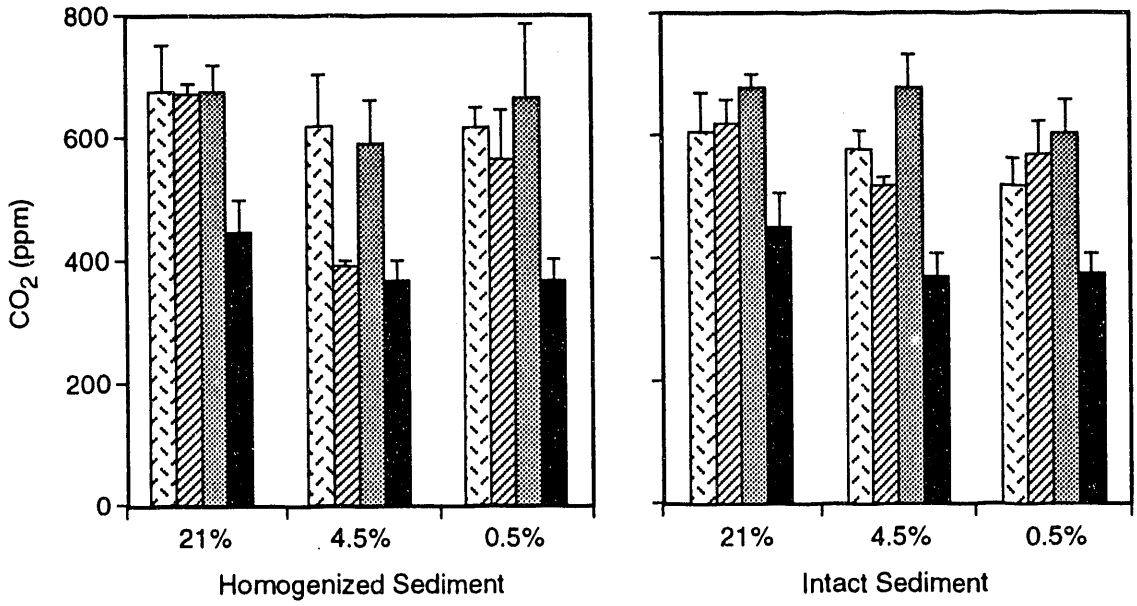

FIGURE 4. Carbon Dioxide Evolved by Sediments Incubated under Atmospheric (21%), Reduced (4.5%), and Microaerobic (0.5%) Oxygen Concentrations after 14 Weeks (dashed), 24 Weeks (hatched), and 49 Weeks (dotted). Background concentrations are shown by solid bars.

statistical differences between treatments were rare, and carbon dioxide concentrations did not increase with increased incubation. The amount of sediment organic matter utilized by microorganisms in the sediments reached a maximal value by 14 weeks and was similar for both the homogenized and the intact sediments. These results correspond with the large increases in culturable heterotrophs observed over the first 16 weeks (Figure 2). These results also corroborate the results obtained when ^{14}C-glucose was added to sediments; that is, oxygen diffusion, not homogenization, appears to be responsible for the increase in microbial activity.

In summary, greater numbers of culturable microorganisms were present at the lower oxygen concentrations, indicating that the microbial community is initially adapted to microaerobic conditions. However, the microbial community was able to rapidly adapt to the higher-oxygen concentrations. Numbers of culturable microorganisms and rate constants and lag times for glucose mineralization indicate that oxygen diffusion into the sediment is likely to be the mechanism that controls the storage-induced change in microbiology. Although homogenization of the sediment results in faster response times for mineralization of added substrate and can result in greater populations, improved oxygen diffusion (rather than redistribution of cells and liquid- and solid-phase nutrients due to physical mixing) is the primary controlling factor. These conclusions are favorable for bioremediation activities that attempt to stimulate microbial activity *in situ*, because they indicate that moist sediments containing very low culturable populations can be successfully stimulated by addition of oxygen.

Spatial Heterogeneity and Density Dependence of Terrestrial Subsurface Microbiological Populations. We have recently completed experiments to investigate the centimeter-scale spatial variability of total bacterial numbers in subsurface sediments. In both subsurface microbial ecology studies and studies of bioremediation treatability, samples are often assayed for a variety of microbial types and chemical properties. Unfortunately, spatial heterogeneity can complicate the comparisons of these measures. When performing such multiple assays on a soil or sediment sample, it is common to thoroughly homogenize the sample to reduce the inherent variability of the sample and allow all assays to be performed on similar material. Microorganisms in soils, however, are often distributed in microcolonies that may be tightly associated with soil crumbs or particles. Depending on the patchiness of this distribution, homogenization might do little to decrease intersample variability. Our data showed that, for similar population sizes, bacterial distributions are much more heterogeneous in subsurface sediments than in surface soils. The investigations also showed that a surprisingly large fraction of subsurface bacterial populations exhibit density-dependent growth, a property that complicates the interpretation of many standard microbiological assay techniques.

In this project, we tested the effect of homogenization on the variability of plate-count numbers in surface soil and subsurface sediments. Cores of buried paleosols or of surface soil were collected and pared aseptically. The cores were divided longitudinally and one half of the core was subjected to thorough homogenization. From both treatments, 8 to 12 subsamples of 1 cm^3 were removed and the number of culturable bacteria was counted by standard plate-count techniques. Coefficients of variability were calculated, as shown in Table 1. Although the mean numbers of bacteria were approximately equal in the two types of sample, the variability was consistently much greater in the subsurface sediments, indicating that the distribution was much more patchy. Homogenization reduced this variability somewhat in all samples, but typically by less than two times, and intersample variability remained high in subsurface samples. The data would suggest that microorganisms are distributed in discrete microcolonies to a much greater extent than in surface soils.

Another phenomenon can be seen in these data (Table 1). The mean number of bacteria growing on agar plates was consistently lower (by an order of magnitude) in homogenized subsurface samples. In surface soil samples, homogenization had little or no effect on plate-count populations. Mixing is generally assumed to increase

TABLE 1. Numbers and Variability of Microorganisms in Homogenized and Unhomogenized Samples

	Coefficient of Variability		log Mean CFU[(a)]/g		
Sample	homogenized	not homogenized	homogenized	not homogenized	*p*-value[(b)]
Surface	4.26	8.64	5.2	4.9	0.0002
Surface	2.86	3.89	5.3	6.3	0.51
Surface	2.73	4.02	5.0	5.0	0.33
Surface	1.65	3.45	5.7	5.5	0.0014
Paleosol	38.3	45.2	3.3	4.5	0.0046
Paleosol	18.5	25.7	3.8	4.9	0.0082
Paleosol	4.9	7.3	4.8	5.2	0.0002

(a) CFU = colony-forming units.
(b) *p*-value refers to statistical significance.

plate counts, because breaking up microcolonies increases the number of propagules; however, in this experiment all samples were subjected to the same amount of mechanical mixing, with the only difference being the volume of the amount homogenized. Thus, the differences in means were due only to redistribution of cells within the sample. Given a patchy distribution, this should result in a lower density of cells than in the unhomogenized samples. Density dependence was also observed in a number of other subsurface samples from boreholes at the Hanford Site and Idaho National Engineering Laboratory (INEL), as shown in Table 2. In these cases, during routine plate counts, low dilutions of the samples produced confluent growth of bacteria or colonies "too numerous to count," while one tenfold dilution yielded no growth at all. Thus, density-dependent growth appears to be a general trait of subsurface bacteria.

Density dependence has been observed for a number of different bacterial species and can be caused by a number of different mechanisms. In general, density dependence occurs when bacteria grow in a hostile environment that must be altered locally for the organisms to grow. Examples include organisms that create gradients of pH or oxygen concentration in their immediate vicinity, organisms that must excrete extracellular enzymes or other remote-acting substances, and organisms that form multicellular structures. Our current observations are unusual in that they indicate that a large fraction — sometimes all — of the bacterial communities are density dependent in the subsurface environment. Another of our observations offers a possible explanation: in all INEL borehole samples with density-dependent growth, microaerophilic organisms were detected. High densities of these organisms might be required to draw oxygen concentrations down to levels that the individual cells could tolerate. This raises the question of whether density-dependent growth is a laboratory artifact caused by insufficient approximation of the microbial habitat by the culture medium, or whether it is a significant ecological phenomenon. In either case, a previously unknown property of subsurface organisms has been delineated.

Development of a Bacteriological Culture Medium Optimized for Enumeration of Subsurface Aerobic Heterotrophic Bacteria. Viable plate-count techniques to enumerate microorganisms in environmental samples suffer from an inherent selectivity that results from the choice of culture medium and conditions. Microbiologists have long noted the discrepancy between the population size of microorganisms that can be observed by direct microscopic observation and the population size as determined by viable plate-count techniques. This discrepancy can be attributed to two general factors: 1) the inherent inability of cells to form visible colonies on agar (e.g., because they are stressed or nonviable), and 2) inappropriate culture conditions.

TABLE 2. Density Dependence in Plate Counts of Subsurface Bacteria. Numbers in each successive dilution should decrease by approximately ten times, except in the case of density dependence.

Description	Plate-Count Numbers in Each Dilution				Density Dependence	Microaerophiles
	10 E-1	10 E-2	10 E-3	10 E-4		
Basalt	0	0	0	0	-	nd[a]
Sediment	19	0	0	0	-	nd
Basalt	0	0	0	0	-	-
Basalt	0	0	0	0	-	-
Sediment	tntc	0	0	0	+	nd
Fracture faces	0	0	0	0	-	nd
Basalt	0.6	0	0	0	-	+
Sediment	0	0	0	0	-	-
Sediment	tntc	0	0	0	+	+
Rubble	8.7	0	0	0	-	+
Basalt	0	0	0	0	-	-
Rubble	0	0	0	0	-	+
Sediment/rubble	tntc	0	0	0	+	+
Clay/rubble	0	0	0	0	-	-
Sediment/rubble	1.3	0	0	0	-	-
Sediment	tntc	tntc	375	nd	nd	nd
Sediment	tntc	tntc	tntc	0	+	+
Sand	0	0	nd	0	nd	nd
Sand	0	0	0	0	-	nd
Sand	0.3	0	0	0	-	nd
Sand	0	0	0	0	-	nd
Gravel	0	0	0	0	-	nd
Gravel	0	0	0	0	-	nd
Gravel	0	0	0	0	-	nd
Paleosol	tntc	0	0	0	+	nd
Paleosol	tntc	0	0	0	+	nd
Paleosol	tntc	0	0	0	+	nd
Gravel	0	0	0	0	-	nd
Gravel	0	0	0	0	-	nd
Paleosol	14.5	1	nd	nd	-	nd
Paleosol	94	1.5	nd	nd	(+)	nd
Paleosol	13.5	2	nd	nd	-	nd
Paleosol	9.5	0	nd	nd	-	nd
Paleosol	2.5	0	nd	nd	-	nd

(a) nd = not done.

It is an axiom of microbiology that *all* culture media are selective. Many well-characterized heterotrophic microorganisms can regulate their interior environment to allow for growth under a range of nutrient regimes. However, the range of conditions that allow for growth of subsurface microorganisms is not well known. While recognizing that a universal medium is not likely to be attainable, we attempted to maximize the plate-count numbers from subsurface samples by optimizing a culture medium for terrestrial subsurface bacteria.

A Plackett-Burman experimental design was used to test the significance of the effects of 13 possible medium parameters. These parameters and the rationale for selecting them are listed in Table 3. This experimental design allows simultaneous screening of large numbers of variables and indicates whether varying a particular parameter will have a significant effect on the dependent variable. Its main drawback is that two-factor interactions are confounded.

Subsurface sediment samples were obtained from a variety of boreholes and buried paleosols, as well as nearby surface soils. As shown in Table 3, no parameter led to a significant increase in plate-count numbers in all samples; however, several factors consistently had positive effects, where these effects were significant. The most effective medium ingredients were activated charcoal and vitamin supplements. Activated charcoal was selected because of its ability to scavenge forms of oxygen, such as superoxide and peroxide radicals, that are toxic to microorganisms, and that are assumed to be the toxic factors limiting microaerophilic bacteria. Vitamins are metabolic cofactors that have a high metabolic cost to produce and so might not be maintained in starved subsurface cells.

Based on our results, a new medium, "Optimized Plate Count Agar" (OPCA), was formulated and tested on a variety of subsurface samples. As shown in Table 4, OPCA yielded significantly higher counts than other standard media used in the Subsurface Science Program research. Thus this medium formulation should provide a better tool for future subsurface investigations.

Geochemical H_2 Generation as an Energy Source for Subsurface Microbiological Ecosystems. The presence of microorganisms in the deep terrestrial subsurface environment has been established at a number of different geological settings and depths. Some studies have shown that true ecosystems can exist in the subsurface environment, in which microorganisms are metabolically active, albeit at very low rates, and interact with their physical environment (Stevens et al., in press; Chapelle and Lovley 1992). These microorganisms may have descended from populations present during deposition of the geological formations, or they may have been transported by aquifer flow, or some combination of these two possibilities may be true. In any case, if subsurface populations are metabolically active, they must have an external energy source. There are also several possible origins for such an energy source. Organic carbon could have been laid down with the sediments, resulting in "fossil" carbon. Organic carbon could also have been transported from the surface through the movement of groundwater. Finally, geochemical energy could originate from abiological sources, such as geothermally produced hydrogen or methane gas. Given that many subsurface ecosystems appear to contain very little organic carbon, and transport is often limited, geochemical energy sources may be predominant in very deep strata. In our FY 1992 research, we have discovered a geochemical source of hydrogen that may drive microbial ecosystems in the deep confined aquifers beneath the Hanford Site and elsewhere.

A variety of anaerobic microorganisms are present in the aquifers that are confined within and between the layered basalt flows in the Pasco Basin of southeastern Washington (Stevens et al., in press). Geochemical evidence gathered during the Basalt Waste Isolation Project suggests that these organisms are metabolically active on a regional scale (Figure 5), even though very little organic carbon is present in the layered basalt flows. Recent field work has shown that hydrogen gas is dissolved in these aquifers in concentrations 1,000 times higher (0.9 to 7 μm) than had been expected in subsurface aquifers (Lovley and Goodwin 1988). Historical data show that hydrogen can make up

TABLE 3. Significance and Relative Effect of Variables in Different Subsurface Samples. Values are relative percentage of plate-count numbers at the "high" versus the "low" setting of the variable (100 = no effect, < 100 = negative effect, > 100 = positive effect). (+ = significant positive effect at $p = 0.1$ level, - = significant negative effect at $p = 0.1$ level, 0 = no significant effect at $p = 0.1$ level.)

Variable	Hanford Surface	Ringold #1	Ringold #2	Ringold #3	Ringold #6	Ringold #7	YakBar 1335	INEL Surface	INEL Water	INEL Cartridge
Vitamins	144, 0	229, +	227, +	5, 0	147, 0	140, 0	220, +	102, 0	161, 0	226, +
Dummy	57, 0	100, 0	121, 0	59, 0	134, 0	102, 0	108, 0	124, 0	107, 0	115, 0
Complex	161, 0	87, 0	87, 0	809, 0	185, 0	92, 0	90, 0	104, 0	111, 0	139, 0
Dummy	47, 0	62, -	101, 0	1646, 0	64, 0	211, +	140, 0	122, 0	530, 0	101, 0
Fatty Acids	210, 0	76, -	139, +	11259, 0	202, 0	134, 0	84, 0	100, 0	66, 0	121, 0
Glucose	129, 0	296, +	154, +	177, 0	124, 0	217, +	95, 0	83, 0	175, 0	44, -
Glutamate	53, 0	87, +	68, -	83, 0	122, 0	151, 0	120, 0	103, 0	179, 0	169, +
Water Potential	17, 0	36, -	50, -	132, 0	128, 0	78, 0	29, -	29, -	46, 0	25, -
Dummy	280, 0	113, 0	105, 0	73, 0	63, 0	71, 0	69, 0	57, 0	10, 0	101, -
Ammonium	48, 0	48, -	120, 0	1523, 0	54, 0	225, +	126, 0	209, 0	260, 0	73, 0
pH	72, 0	15, -	39, -	155, 0	75, 0	35, 0	57, 0	180, 0	103, 0	411, +
Plate Type	57, 0	15, -	73, -	14, 0	18, -	35, -	87, 0	102, 0	25, 0	164, +
Temperature	210, 0	101, 0	79, 0	67, 0	71, 0	59, -	72, 0	41, -	27, 0	122, 0
Charcoal	182, 0	298, +	3365, +	116, 0	224, 0	219, +	704, +	171, 0	464, 0	181, +
Trace Elements	117, 0	190, +	222, +	8, 0	260, 0	110, 0	139, 0	70, 0	78, 0	54, -

TABLE 4. Comparison of Plate Counts on 1% PTYG Medium and OPCA Medium

Sample	log Cells on PTYG	log Cells on OPCA
Ringold 1	2.97	3.35
Ringold 2	0	4.39
Ringold 3	0	0
Ringold 7	1.82	2.65
INEL cart	5.01	5.58

>4 mole % of the gases dissolved in some Hanford groundwaters, although actual concentrations were not determined (Early et al. 1986). We suggest that dissolved hydrogen gas may be the energy source that drives microbiological activity in the confined aquifer ecosystem.

Recently, hydrogen generation was observed during the course of routine well-drilling activities undertaken by the Subsurface Science Program at the Hanford Site. Investigations in our laboratory demonstrated that hydrogen gas was generated from interactions between water and basalt rocks, such as those present in the confined aquifer system. Taking place at room temperatures and pressures, these reactions may be a ready source of energy for microorganisms in basaltic aquifers. Samples of a well-characterized basalt formation were crushed to a 0.5- to 2-mm size range. Metal particles derived from the crushing apparatus were removed. Aliquots of the basalt samples were added to 18 Ω deionized water in gas-tight tubes. Headspace samples were removed by syringe and analyzed by gas chromatography with thermal conductivity detection. The identity of gases was then confirmed by mass spectrometry. Hydrogen evolution could be detected within minutes, and it continued for over two weeks (Figure 6). Hydrogen production was several times greater in samples with Hanford

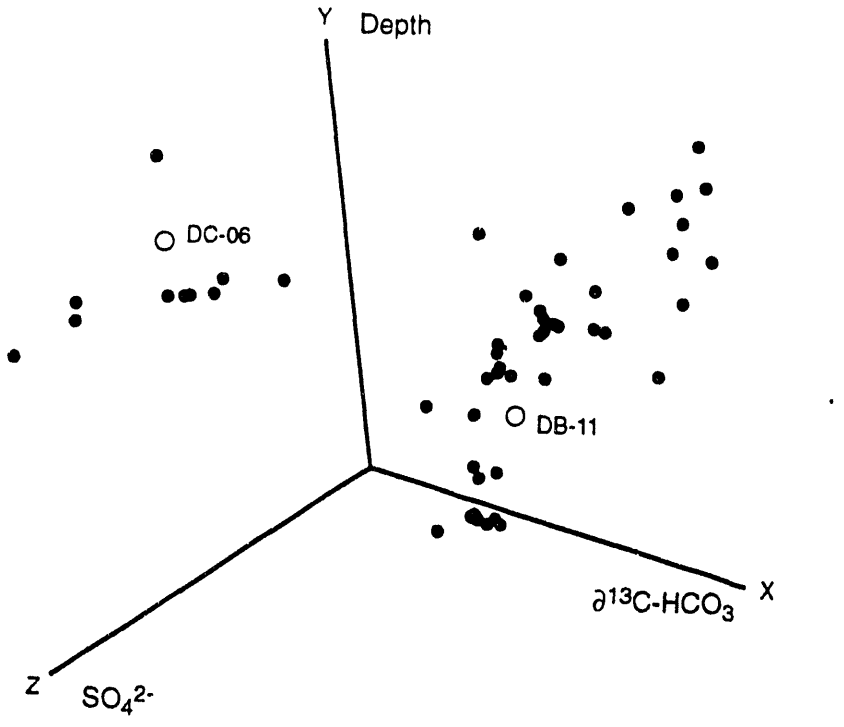

FIGURE 5. Stable Carbon Isotope Signatures Showing Microbial Influence on Confined Aquifer Groundwaters. Increasing $\partial^{13}C$ with depth shows CO_2 consumption by methanogenic bacteria. Anomalously low values in the presence of sulfate indicate oxidation of organic matter by non-methanogenic bacteria. These predicted bacterial types were confirmed by microbiological tests in representative wells.

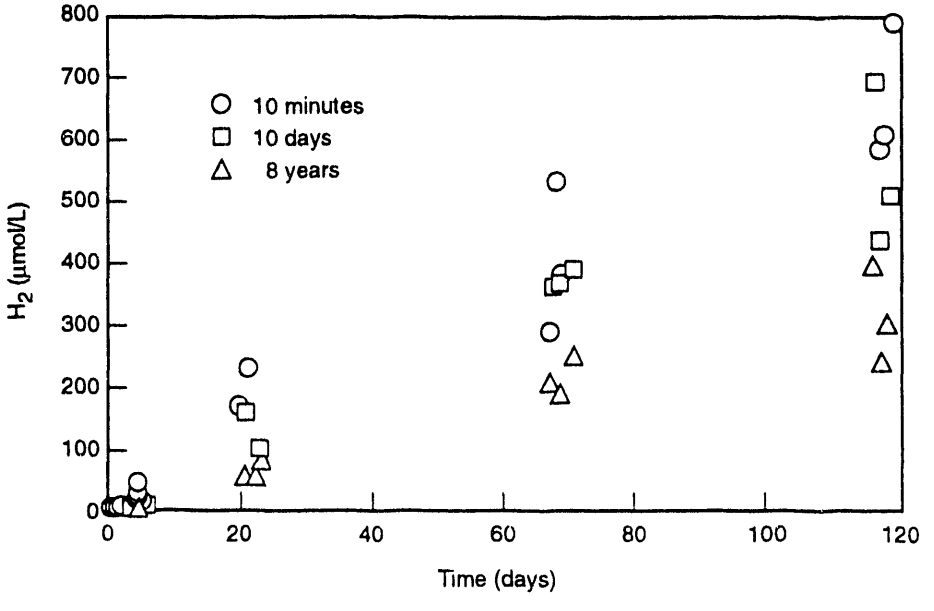

FIGURE 6. Hydrogen Production by Basalt/Water Interactions. Tubes contained 2 g crushed basalt and 10 ml anaerobic water. Water added after 10 min of air exposure of crushed rock, 10-day air exposure, and 8-year air exposure.

groundwater than in deionized water. Subsequent experiments demonstrated that the reaction rate was dependent on carbon dioxide concentration, and that this dependence was independent of simple pH effects (Figure 4).

The chemistry of basalt/water interactions is complex, and the exact mechanism of hydrogen generation has not yet been determined, although several mechanisms have been proposed in the literature. To date, the only other report of hydrogen generation by water/rock interactions at room temperature involved pure quartz and granite (Kito et al. 1982). That study attributed the reaction to formation of $Si^{\cdot}$ and $SiO^{\cdot}$ radicals by mechanical cleavage of silica bonds, and subsequent reaction of these radicals with water. If this were the mechanism, we reasoned that fresh fracture faces would be necessary for hydrogen generation. We therefore repeated the basalt/water experiment using basalt samples of various ages, i.e., samples that were crushed minutes before the addition of water, several weeks before addition, and 6 to 8 years before the experiment. All samples were from the same reference outcrop. Although there appeared to be some difference in rates, hydrogen production was observed in all samples, even those in which the fracture faces were several years old. There were apparent differences in secondary mineral production with aged fractures, and those are currently being analyzed. The results of this experiment suggest that free radicals are unlikely to be required for generation of H_2 from basalt water interactions. More detailed mechanistic studies are planned for the future.

GEMHEX. This integrated geochemical, microbiological, and hydrological experiment, which is described in more detail in the article that follows, was designed to increase our current understanding of subsurface microbial-geochemical-hydrological process interactions. The broad objectives of this experiment were to further define 1) spatial heterogeneity of microbial populations in saturated subsurface sediments and 2) the geochemical and physical controls on community size, diversity, and metabolic activity. The scientific hypotheses that were developed were an outgrowth of the knowledge gained from exploratory research at the Savannah River Site, INEL, and the Hanford Site from prior phases of the DOE's Subsurface Science Program's Deep Microbiology Subprogram. The specific hypotheses are based on observations of previously sampled core material:

1) Hydraulic conductivity and sedimentary grain properties related to porosity and pore structure will control the size and activity of microbial populations (convective/diffusive flux).

2) Variations in iron valence/mineralogy with depth through the sediment profile will reflect transitions between a) microbial dissimilatory reduction of iron(III) as a terminal electron acceptor and b) biological/chemical oxidation of iron(II).

3) Microbial growth and metabolic activity in saturated lacustrine/fluvial sediments will be phosphorous limited, but that in paleosols will be O_2 limited.

This third hypothesis was developed as part of this project and is described here. Hypotheses 1 and 2 were developed by investigators in other projects and therefore will not be described. In oligotrophic aquatic environments, phosphorous and organic carbon are the principal nutrients limiting bacterial growth. During previous DOE studies of aquifers of the southeastern coastal plain, including the Middendorf aquifer, inorganic phosphorous (P_i) in groundwater was shown to be at or below analytical detection limits, whereas dissolved organic carbon and nitrogen were present in concentrations that could sustain low levels of bacterial production. At Hanford, P_i in groundwater from the unconfined aquifer is also at or below analytical detection limits (0.5 mg/L). At the pH (approximately 7.5-8.0) and calcium concentration (40 mg/L) of the groundwater, the maximum soluble P_i level would be 10^{-6} - 10^{-10} M (i.e., 1-100 μg/L), depending on the solubility-limiting solid phase. The higher solubility value occurs when hydroxylapatite is the controlling solid phase. Other phases and mechanisms may also influence the concentration of dissolved P_i, such as precipitation of metastable calcium, aluminum, and iron phosphates, and sorption to ferric oxides. Therefore, we hypothesized that soluble P_i is the

primary factor limiting microbial growth and metabolism in the nonpaleosol sediments. In addition, the physiology of the microbiota will reflect phosphorus starvation, and geochemical and mineralogical properties that control solution P_i will reflect the microbial distributions.

At the Hanford Site, the Basal Ringold paleosol is characterized by fine texture and an apparently low permeability. Low permeability will limit both the movement of microorganisms into the paleosol from adjacent nonpaleosol sediments and the diffusion of O_2 from the surrounding sediments. Given that paleosols are ancient soils, we hypothesize that the original microflora would have been dominated by aerobic heterotrophs; with increasing distance into the paleosol, the microbial community will be dominated by aerobic heterotrophs, and metabolism and growth will be limited primarily by the diffusion of O_2 (Brockman et al. 1992). Experiments with an analogous, although considerably younger, vadose zone paleosol from the Upper Ringold indicate that viable microbial populations and metabolic activities increase with mixing and exposure to atmospheric O_2. This increase occurs even without the addition of exogenous nutrients, suggesting that nutrients are not the primary factor limiting growth and metabolism. It is likely that aerobic metabolism will be even more limited in the Basal Ringold paleosol because the diffusion of O_2 through water is much less than through air. Therefore, we hypothesize that 1) the microbial community will grade from being predominantly anaerobic and facultative to being predominantly aerobic, and 2) microbial activity will be limited by O_2 diffusion with increasing depth from the Lower Ringold lacustrine-Basal Ringold paleosol contact.

To test this hypothesis will require analyses of geochemical, mineralogic, physical, and microbiological properties of sediment cores and manipulative experiments. Samples for analyses have been taken with increasing density at and near the boundary between the Lower Ringold and Basal Ringold units (i.e., the lacustrine-paleosol contact). Manipulative experiments have been conducted with a subset of these samples (the experiments are labor intensive and therefore costly). Microbiological measurements of cored sediments rely on the use of classical enrichment techniques for measuring aerobic, facultative, and anaerobic heterotrophic microbial populations and the use of PLFA and direct microscopic counts as measurements of total microbial biomass. Specific functional groups, including spore-formers, apatite-solubilizers, and $CaCO_3$-precipitating organisms are also being measured. In addition, 16S rRNA-targeted DNA probes for broad phylogenetic groups are being used to gain additional information on the composition of microbial communities and their metabolic state. To assess the metabolic activity and degree of phosphorus starvation of the microbiota, several types of activity measurements are being made. Basal aerobic and anaerobic metabolic activity is being assessed by measuring both ^{14}C-acetate incorporation into lipids and mineralization of mixed ^{14}C-labeled substrates. If microorganisms are phosphorus-starved, they will possess high-affinity uptake systems for P_i. To assess this, we are measuring the ability of the microbial community to assimilate phosphorus by adding $^{32}PO_4$ to sediments and measuring the rate of P_i incorporation into lipids and DNA. Alkaline phosphatase activity is also being measured. In manipulative experiments, whole sediments are being amended with P_i, apatite, organic carbon, inorganic nitrogen, or combinations of these, or are left unamended. Sediments have been incubated and metabolic activity and growth have been measured using mixed ^{14}C-acetate incorporation into lipids, ^{3}H-thymidine incorporation into DNA, and mineralization of ^{14}C-labeled substrates.

The GEMHEX focused on a defined 20-m interval in the Lower and Basal Ringold Formation on the Hanford Site. This interval spanned a variety of physical, chemical, and geological properties. Core material for the GEMHEX was obtained by deepening the Yakima Barricade Borehole, which lies in the western part of the Hanford Site where the subsurface has not been contaminated by past site operations. Planning, collection, and analysis of samples and hypothesis testing were part of a multidisciplinary effort that is expected to reach a new level of understanding of microbial function in the subsurface environment.

Details of stratigraphy and sampling are presented in the article that follows. In addition to their extensive geochemical and physical measurements, microbiological measurements were made on the series of core samples by investigators from other universities and national laboratories. The microbiological analyses focused on those characteristics critical to testing of the hypotheses listed above, including

Microbial Biomass/Community Structure
- Direct microscopic counts
- Phosphoester-linked fatty acids
- Biolog community assay
- Direct observation/scanning electron microscopy

Culturable Microorganisms
- Most probable numbers, plates for functional groups
  - Aerobic heterotrophs
  - Iron reducers
  - Iron oxidizers
  - $CaCO_3$ precipitators
  - Spore-formers
  - Apatite-dissolvers
  - Sulfate-reducing bacteria
  - Fermenters
  - Methanogens

Metabolic Activity
- ^3H-thymidine incorporation into DNA
- ^{14}C acetate incorporation into lipids
- ^{14}C-labeled substrate mineralization
- Iron-oxidizers/reducers
- $^{32}PO_4$ incorporation

Molecular Analyses
- DNA extraction and probing for functional genes
- 16s rRNA-targeted DNA probes.

In addition to these analyses, experiments were conducted to evaluate whether nutrients or water may be limiting microbial activity in the GEMHEX sediment samples.

Future Research

Effect of Storage on Microbial Community Structure and Activity in a Subsurface Paleosol. Future research will examine the extent to which the dramatic increases in culturability are due to biomass turnover vs. resuscitation of cells that were unable to grow immediately following sample acquisition as a result of long-term starvation in the sediment. Oligonucleotide probes for specific types of microorganisms will be used in conjunction with ^3H-thymidine and $^{32}PO_4$ incorporation into DNA in these studies. Resuscitation of inactive cells, which may have survived since deposition of the sediments millions of years ago, may prove to be an extremely important mechanism for bioremediation of deep vadose zones in arid and semiarid environments.

Spatial Heterogeneity and Density Dependence of Terrestrial Subsurface Microbiological Populations. Additional data from new sampling efforts are currently being developed to extend these observations. So far, these experiments appear to demonstrate two ecological principles of subsurface habitats. First, subsurface bacteria are distributed in highly patchy patterns, probably due to lack of turbation and local extinction in patches where sufficient nutrients are not present. This leads to greater spatial heterogeneity than in comparably sized surface populations. Second, bacteria in the subsurface often exhibit strongly density-dependent growth, detectable at the community level. This may be an indication of a physiological adaptation to the subsurface environment.

Development of a Bacteriological Culture Medium Optimized for Enumeration of Subsurface Aerobic Heterotrophic Bacteria. Future work will make use of the new OPCA medium developed in FY 1992.

Geochemical H_2 Generation as an Energy Source for Subsurface Microbiological Ecosystems. The Columbia River flood basalts cover an area of over 163,000 km^2 in the northwestern United States to a depth of several kilometers, and similar formations are found around the world. Given the ready occurrence of hydrogen generation when fractured basalt is wetted, these massive basalt formations can be seen as vast reservoirs of chemical energy that is slowly released as water percolates through fracture and interbed networks. This process is likely to be the basis for a functional microbiological ecosystem wherever microorganisms are able to

penetrate the formation, if sufficient inorganic nutrients are present. In laboratory microcosms, anaerobic microorganisms can be grown to high densities simply by introducing Hanford groundwater to crushed basalt in sealed containers. Future research will elucidate the details of the microorganism/basalt/water interactions and their relevance to the ecology of the subsurface environment. The evidence to date suggests that the basaltic aquifers may contain a non-photosynthesis-based ecosystem, which might be similar in some ways to the systems in deep ocean trenches and may contribute to global carbon cycling.

GEMHEX. The GEMHEX analyses and experiments were in progress at the time of this report but will be presented in detail in next year's annual report.

References

Brockman, F. J., T. L. Kieft, J. K. Fredrickson, B. N. Bjornstad, S.-M. W. Li, W. Spangenburg, and P. E. Long. 1992. "Microbiology of Vadose Zone Paleosols in South-Central Washington State." *Microbial Ecology* 23:279-301.

Chapelle, F. H., and D. R. Lovley. 1992. "Competitive Exclusion of Sulfate Reduction by Fe(III)-Reducing Bacteria: A Mechanism for Producing Discrete Zones of High-Iron Ground Water." *Ground Water* 30:29-36.

Early, T. O., M. D. Mitchell, and G. D. Spice. 1986. *A Hydrochemical Database for the Hanford Site, Washington.* Basalt Waste Isolation Project Document Number BWI-DP-061-Rev. 1, Rockwell Hanford Operations, Richland, Washington.

Kito, I., S. Matsuo, and H. Wakita. 1982. "H_2 Generation by Reaction Between H_2O and Crushed Rock: An Experimental Study on H_2 Degassing from the Active Fault Zone." *Journal of Geophysical Research* 87(B13):10789-10795.

Lovley, D. R., and S. Goodwin. 1988. "Hydrogen Concentrations as an Indicator of the Predominant Terminal Electron-Accepting Reactions in Aquatic Sediments." *Geochimica et Cosmochimica Acta* 52:2993-3003.

Stevens, T. O., J. P. McKinley, and J. K. Fredrickson. "Bacteria Associated with Deep, Alkaline, Anaerobic Groundwaters in SE Washington." *Microbial Ecology* (in press).

An Integrated Geochemical, Microbiological, and Hydrological Experiment (GEMHEX) at Hanford: Experimental Design, Sample Acquisition, and Preliminary Results

P. E. Long, S. A. Rawson, J. K. Fredrickson, and J. M. Zachara

Contributors

B. N. Bjornstad, E. L. Hardin (University of Arizona), J. P. McKinley, T. Kieft (New Mexico Institute of Mining and Technology), and T. O. Stevens

In FY 1992, four projects in PNL's Environmental Science Research Center and DOE's Subsurface Science Program have focused on the planning, experimental design, sample acquisition, and sample analysis for an integrated **GE**ochemical, **M**icrobiological, and **H**ydrological **EX**periment (GEMHEX) at the Hanford Site. This experiment is designed to increase our current understanding of the interactions between subsurface microbial, geochemical, and hydrological processes. The broad objective of the GEMHEX is to further define 1) the spatial heterogeneity of microbial populations in saturated subsurface sediments and 2) the geochemical and physical controls on their community size, diversity, and metabolic activities. The scientific hypotheses developed for the GEMHEX are an outgrowth of the knowledge gained from prior research at the Savannah River Site (SRS) and from the Deep Microbiology Subprogram of the Subsurface Science Program at the Idaho National Engineering Laboratory (INEL) and the Hanford Site. The GEMHEX required that pristine subsurface materials with broad variations in physical and chemical properties be collected over a short vertical interval. Core material for the GEMHEX was obtained by deepening the Yakima Barricade Borehole, which lies in the western part of the Hanford Site (Figure 1). The focus of the GEMHEX was an 18-m interval in the Lower and Basal Ringold Formation that exhibits the desired range of

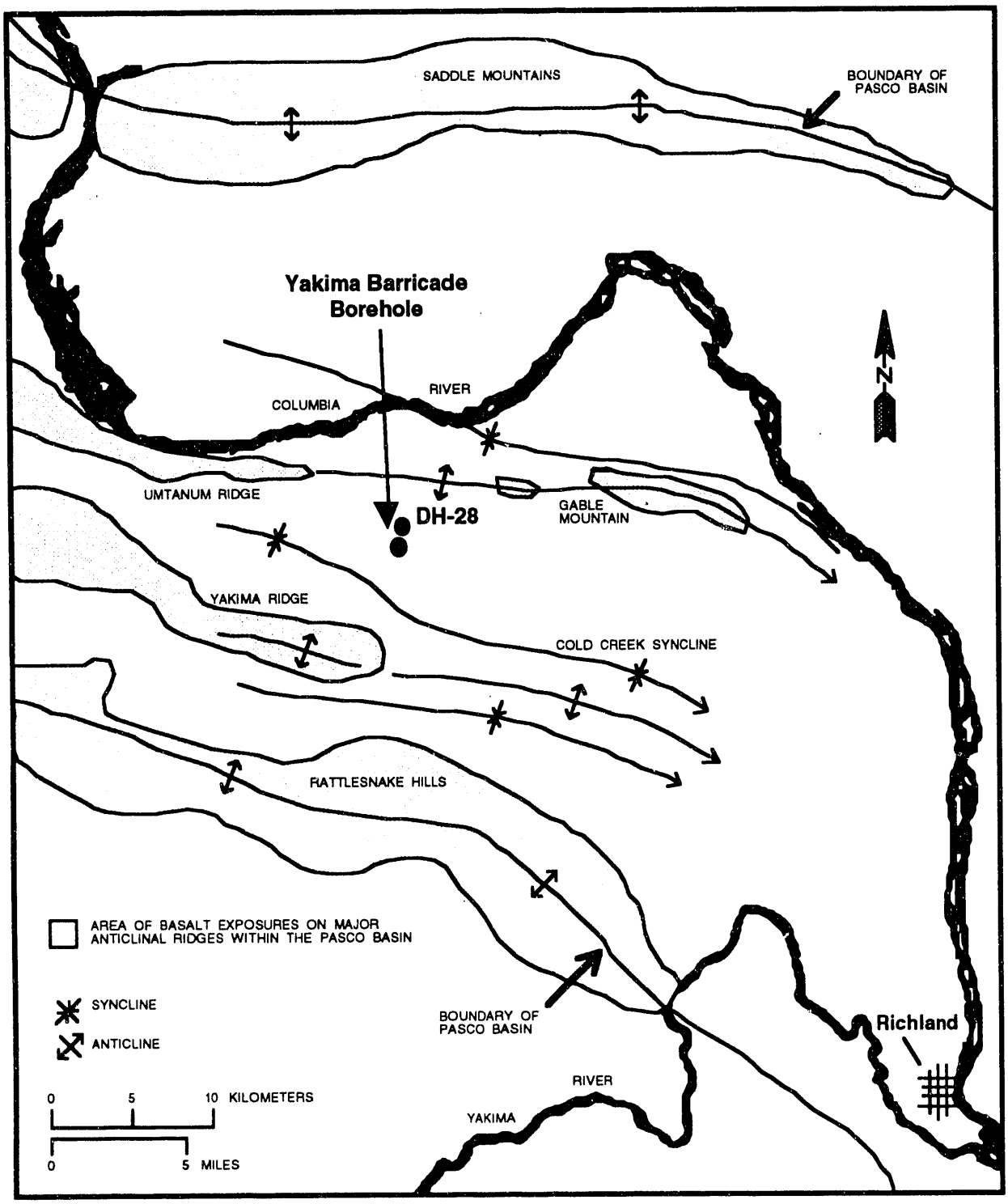

FIGURE 1. Location of the Yakima Barricade Borehole

geologic characteristics. The interval included a sequence of coarse-grained sandy gravels grading upward into a fine-grained paleosol, which was overlain by fine-grained laminated lacustrine sediments and sandy gravels. The interval sampled was thus a relatively fine-grained sequence sandwiched between two coarse-grained, highly transmissive zones.

In this paper, we summarize the scientific rationale for GEMHEX, the hypotheses that are being tested, and the highly successful sample acquisition phase of GEMHEX. Sample analyses are currently under way, with only limited and preliminary results available.

The transport and persistence of contaminants in subsurface environments may be strongly influenced by microbial metabolic processes. The nature, rate, and direction of these processes are in turn strongly influenced by chemical and physical properties of the subsurface environment. Therefore, understanding the physical and chemical variables that control the diversity, abundance, and activity of subsurface microorganisms is critical for the development of *in situ* technologies to remediate contaminants in deep subsurface environments.

The purpose of the geoscience research conducted by the Deep Microbiology Subprogram is to evaluate the geologic, chemical, and hydrologic conditions that influence the distribution of microbes in subsurface environments at depths down to several hundred meters. Samples from a borehole at Hanford and one at INEL (Long et al. 1990) provide a basis for preliminary comparisons with results from earlier samples taken at the SRS (Balkwill et al. 1989; Fredrickson et al. 1989). Relationships among key physical and chemical properties and microbiologic characteristics are being evaluated and used to address a series of hypotheses (Balkwill and Wobber 1989; Brockman et al. 1992; Kieft and Rosacker 1991; Long et al. 1991). The eventual goal is to predict the types, abundance, and activities of microbes in the subsurface environment from physical, chemical, and geological information. To date, research at the western arid and semiarid sites has focused principally on the vadose zone. Resolving our questions required that we extend the Yakima Barricade Borehole to obtain samples from the saturated zone.

FY 1992 Research Highlights

Objectives of GEMHEX Research at the Hanford Site. The central objective of the GEMHEX is to determine the influence of physical and chemical properties on microbial abundance, diversity, and function. To accomplish this objective, observations must be made at a scale relevant to the microbial and geochemical processes involved (i.e., the centimeter scale). At the Yakima Barricade Borehole, samples were collected from a continuous subsurface interval of approximately 18 m over which lithology and chemical and physical properties vary significantly.

The GEMHEX research has the following specific objectives:

- Determine the effects of centimeter-scale features (e.g., bedding planes, mineralogy, or localizations of organic matter) on microbial occurrence, numbers, type, and activity, and then identify the chemical and physical environments (habitats) that favor growth or preservation of microorganisms in sediment cores

- Determine the physical and chemical features and processes occurring in paleosols that result in differences between paleosols and non-paleosols in population size and activity of subsurface microorganisms

- Determine the relationships among relevant solid phase properties, pore-water geochemistry, groundwater geochemistry, and the dominant microbial functional groups.

Meeting these objectives will increase understanding of the physical and geochemical influences on subsurface microbial communities and make it possible to compare their relationships at different DOE sites.

Scientific Approach and GEMHEX Research Hypotheses. The GEMHEX research involves a combination of macroscale and microscale

observations and laboratory experiments on intact cores and core segments obtained from the unconfined aquifer at Hanford. Cored sediments for the GEMHEX were collected starting at the contact between the Lower and Basal Ringold units and extending into the Basal Ringold unit (Figure 2). Analyses of these sediments are focused on 1) paleosols and the sediments overlying and underlying them and 2) microbiological and geochemical dynamics across a semiconfining layer with complex lithologic features.

A drill core of the Ringold Formation from a borehole (DH-28; Figure 1) located approximately 1 km from the Yakima Barricade Borehole shows two well-developed paleosols within the Basal Ringold unit (Figure 2). The uppermost paleosol is the thicker (approx. 10 m) and is capped by fine-grained lake sediments of the Lower Ringold. Directly below the contact with the Lower Ringold sediments, the paleosol displays massive to blocky pedogenic structures that include root casts and calcareous stringers. The lower paleosol is approximately 7 m thick and is capped by a coarse-grained gravel. It also contains pedogenic structures, such as root casts and animal burrows.

A 18-m-thick sequence of lacustrine sediments, paleosols, and fluvial sediments within the Lower and Basal Ringold units (Figure 2) was selected as the target zone for the GEMHEX for several reasons. First, evidence from previous sampling in the unsaturated zone at Hanford suggested that greater numbers of culturable microorganisms are present within paleosol units than in other fluvial sediments (Brockman et al. 1992; Long et al. 1991). With an intact core across an interval of interest, it is possible to examine microbial properties of paleosols and sediments as a function of distance from a sedimentary contact. Second, it has been suggested that total organic carbon has a major influence on the total numbers of microorganisms within different hydrogeologic regimes. Based on previous observations of core material, it appears that paleosols may be a source of organic carbon for both aerobic and anaerobic microbial populations. Third, the paleosol sequence and associated fine-grained lacustrine sediments function as a semiconfining layer within Hanford's unconfined aquifer and so provide an excellent opportunity to evaluate linked geochemical and microbiological processes throughout an interval where gradients in nutrients, electron acceptors, and pH are expected.

In addition to depicting the stratigraphy in the GEMHEX sampling interval, Figure 2 also shows the hypothesized relative numbers of microorganisms and ratio of anaerobic to aerobic microorganisms, based on general considerations of subsurface geochemical conditions.

The overall working hypothesis for the GEMHEX is that the distribution and activity of microorganisms across heterogeneous subsurface sedimentary units is governed by aqueous fluxes of organic carbon, oxygen, and phosphorous, which in turn reflect differences in formation structure, permeability, and mineralogy.

Specific scientific hypotheses are as follows:

1. The abundance and activity of aerobic heterotrophic bacteria are greatest in sediments where aqueous concentrations of oxygen and dissolved organic carbon are optimized by spatial variability in permeability and pore structure.

2. Variations in iron valence or in mineralogy across sedimentary units reflect transitions between microbial dissimilatory reduction of iron(III) as a terminal electron acceptor and biological or chemical oxidation of iron(II).

3. Microbial abundance and metabolic activity and the physiological state of phosphorous assimilatory systems are governed by soluble phosphorous and the ability of solid phases in different sediments to replenish phosphorous.

The GEMHEX research is organized based on the evaluation of these three hypotheses. Analyses of core samples are designed to test the hypotheses and therefore include evaluation of the geological and sedimentary structures that may control fine-scale variations in microbial communities. Sampling on the scale of a few centimeters, as has been done for selected cores, permits direct comparison with microbial measurements in the unsaturated zone that

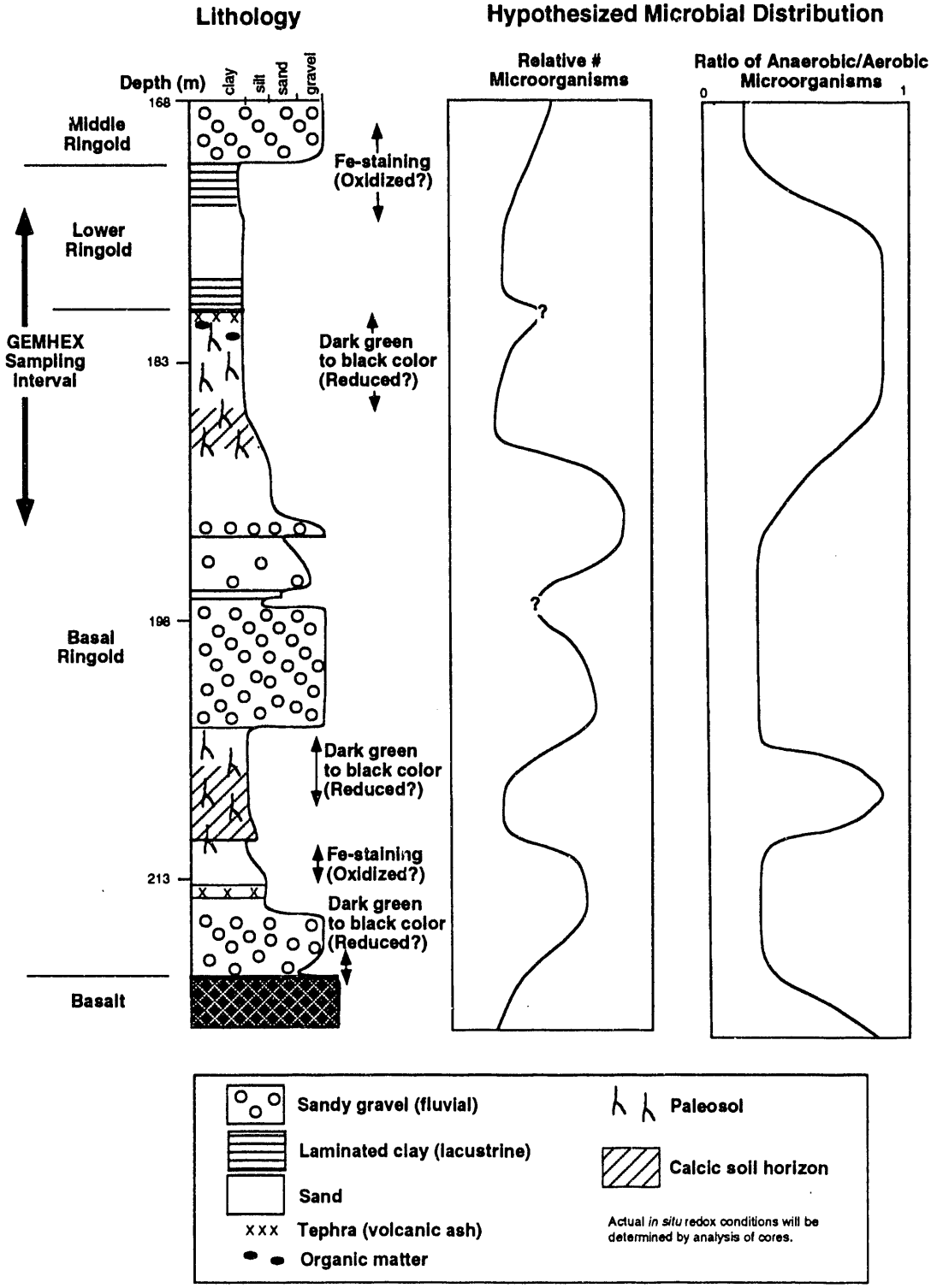

FIGURE 2. Predicted Stratigraphy (based on DH-28 core logs) and Microbial Characteristics of the GEMHEX Interval. Interpretation of oxidation-reduction (redox) conditions is uncertain because it is based on the color of the core. Actual *in situ* redox conditions will be determined by analysis of cores.

showed heterogeneity on a scale of a few centimeters or less. It was expected, however, that microbial communities would be more active in the saturated zone than in the vadose zone and that therefore heterogeneities in microbial abundance and activity would be less pronounced in the saturated zone than in the unsaturated zone.

Hypotheses 1 and 2 are discussed in detail below. Hypothesis 3 is discussed in the preceding paper by Fredrickson and others.

Hypothesis 1: Results from prior research in southeastern coastal plain sediments indicated that the greatest biomass and most active aerobic heterotrophic microbial populations were associated with coarse-grained aquifer sediments. In contrast, formations with a higher proportion of silts and clays (i.e., aquitards) exhibited fewer viable microorganisms and less activity than coarse-grained sediments (Fredrickson et al. 1989). These results suggested that greater microbial abundance would be associated with more permeable zones. The continued survival and metabolism of bacteria in sediments depends on the flux of nutrients and metabolic by-products to and from attached or planktonic cells within pores. Furthermore, for bacteria to move into and colonize sediments, pore throats (the interconnections between pores) must exist and be at least the size of cells (0.5 to 1 μm). Therefore, we hypothesized that the abundance and activity of aerobic heterotrophic bacteria in the sediments sampled for the GEMHEX would reflect the effects of formation permeability and pore structure on nutrient fluxes in the different sedimentary units, regardless of whether microorganisms have been present *in situ* since deposition of the sediments or were transported to their present location later.

Despite the lack of a rigorous theoretical description of the relationship between the dynamics of microbial populations and the dynamics of nutrient transport, the relationship has been explored through use of classical advective-dispersive theory based on the continuum model of a porous medium (e.g., Molz et al. 1986; Kindred and Celia 1989). The advective-dispersive theory describes flow and transport processes related to formation permeability, dispersivity, and solute adsorption. However, this approach requires that the issue of scale dependency be addressed explicitly, because permeability and dispersivity are represented by volume-averaged measurements. Therefore, to test the hypothesis, it was necessary to measure physical properties of permeability and pore structure at the same scale as microbial abundance and activity.

Microbial abundance and activity are usually measured on the scale of centimeters. One of the few physical properties that can be measured at the centimeter scale is the grain size distribution, which is related to formation porosity and permeability (Davis 1969; Doyen 1988; Raffensperger and Ferrell 1991). The grain size distribution controls the total porosity and pore geometry of the formation, thereby influencing the local advective flux within pores. Therefore, if porosity is a controlling factor for microbial distribution, microbial numbers can be expected to be greater in well-sorted sediments than in poorly sorted sediments. Pore geometry also affects the numbers of viable microorganisms because it directly controls the space available for colonization by microorganisms. The diameter of pore throats may be a limiting factor in how well microorganisms can move between pores. In pores with smaller mean diameter, local advective flux through the formation is also reduced, because of flow resistance.

Other properties of sedimentary grains, such as grain shape (roundness) and texture (roughness), are expected to affect the attachment and detachment of microorganisms to and from grains within pores. Grain roughness may be an important determinant in the types of grains to which microorganisms attach. The specific surface area of the grains plays a role in formation permeability by causing frictional resistance in fine-grained sediments, which have greater surface areas than medium-grained sediments. Specific surface area also influences the ratio of adsorbed to free water within a pore and, depending on grain surface and the microbial surface chemical characteristics that control adsorption, may influence the transport and location of microorganisms within pores.

Permeability, although it cannot be directly measured at the centimeter scale, controls the relative importance of advective and diffusive transport of nutrients within the formations. In highly permeable layers, such as well-sorted sands and gravelly sands ($K_{sat} = 10^{-2}$ to 10^{1} cm/s), advective transport is expected to dominate within the formation, and similar microbial types are expected to occur throughout the formation. In less permeable formations (Ksat $\leq$ 10^{-3} to 1.0^{-5} cm/s), diffusion-limited transport of nutrients is expected to result in a variation of microbial types along a spatial gradient perpendicular to the sedimentary bedding.

Flux of a specific nutrient or metabolite is controlled by both its concentration in solution and its transport in the solution phase by advection and diffusion. Given that concentrations of major nutrients in pristine subsurface sediments are very low, often near analytical limits, transport will be the dominant factor controlling nutrient availability to microorganisms at a distance from the nutrient source. Near the nutrient source, transport may not limit nutrient availability; instead constant solubilization of nutrient combined with rapid uptake by microorganisms may maintain low nutrient concentrations. The GEMHEX is expected to establish which of these processes actually dominate in different parts of the subsurface environment.

The hypothesis is being tested in several ways. First, the relationship of particle size distribution statistics (mean, median, standard deviation, skewness, kurtosis) and porosity to total microbial biomass and metabolic activity is being determined. Microbial numbers are being measured by plate counts of viable aerobic, microaerophilic, and anaerobic bacteria, as well as by measurement of phospholipid ester-linked fatty acid (PLFA) concentrations. Microbial activity is being measured by ^{14}C acetate incorporation in lipids, mineralization of ^{14}C substrates, and microautoradiography of individual cells. Heterogeneity and diversity of microbial distributions on a range of scales from a few to tens of centimeters and in different size fractions will be examined using DNA extraction and PLFA data. The advantage of using DNA extraction and the PLFA techniques is that, unlike standard plate-count techniques, they can be applied to the appropriate range of sample sizes. Multivariate statistical analysis of the relationships between physical properties and the microbial abundance/activity at the centimeter scale will be conducted.

These analyses are expected to show that numbers of microorganisms are greater and metabolic activities higher in well-sorted sands than in poorly sorted sediments, such as gravelly sands and muds. The greatest numbers or activities of microorganisms are expected to be associated with particles in the silt to fine sand size range, because this range optimizes surface area while maintaining a reasonably high local permeability. The relationship between numbers of microorganisms and grain size should be observable within beds as thin as several centimeters. Sampling at smaller scales is expected to reflect either more or less random sample-to-sample differences in microbial numbers within individual beds or the effects of factors other than grain size, such as localized (centimeter-scale) concentrations of organic carbon.

Similarly, the relationship between the sediment physical structure and the occurrence of microorganisms is being established by examining the pore geometry (surface porosity in horizontal and vertical directions, spatial dimensions of pore throats, and pore volumes) using image analysis of thin sections of intact, undisturbed core via petrographic microscopy and scanning electron microscopy. Greater numbers of microorganisms [as measured by acridine orange direct counts (AODC)] and higher levels of metabolic activity are expected in medium- to coarse-grained sediments in which the pore space is well-connected (i.e., where effective porosity is high) and where the average diameter of pores exceeds approximately 1.0 μm; lower numbers are expected to be associated with fine-grained sediments with low effective porosity.

Finally, horizontal and vertical permeability and diffusion coefficients in intact core segments are being measured. The permeability (or, as a proxy, the grain size distribution) is expected to relate to the spatial distribution of microorganisms within the formation. Greater numbers of microorganisms and higher levels of metabolic activity are expected in the more permeable

formations adjacent to fine-grained sedimentary beds. Dissolved organic carbon diffuses out of fine-grained layers, whereas oxygen advects within more permeable layers as partially oxygenated water. At some position adjacent to the fine-grained unit, conditions are expected to be optimal for growth of aerobic heterotrophic bacteria. Thus we also expect to find a spatial relationship (perpendicular to the sedimentary layering) between O_2 or dissolved organic carbon and microbial activity.

Alternatively, the boundary between high- and low-permeability layers may, by itself, create an ecological niche that favors microbial growth. This phenomenon has been observed in intermediate-scale experiments conducted at PNL's Subsurface Experimental Research Facility (SERF) and has been explained as being caused by mechanical mixing of nutrients at the layer interface rather than by diffusion from within dissolved-organic-carbon-rich fine-grained layers. Increased microbial abundance adjacent to the fine-grained sequence (e.g., a paleosol) could result from either mechanical mixing or diffusion, and determining the vertical spatial distribution of microorganisms alone will not permit a distinction between these two alternatives. It may be possible to distinguish between the alternatives by directly measuring O_2 and dissolved organic carbon or by predicting O_2 and dissolved organic carbon concentrations with the aid of a detailed numerical model of mass transfer and microbial processes across and along layer interfaces. Upon well completion at the Yakima Barricade Borehole in FY 1993, measurement of porewater concentrations of O_2 and dissolved organic carbon will be attempted at boundaries between coarse- and fine-grained sedimentary units. Permeability data and transport parameters (such as diffusion coefficients) will be used to simulate expected O_2 and dissolved organic carbon concentrations, and the results will be compared to observed O_2 and dissolved organic carbon values as well as to microbial abundance and activity.

Hypothesis 2: Because the unconfined groundwaters at Hanford contain low concentrations of electron acceptors other than O_2, such as NO_3, and because the sediments are enriched in basalt fragments and in ferromagnesian minerals of basaltic provenance, it is hypothesized that the deep microbiological community within and surrounding the semiconfining layer formed by the paleosol-lacustrine sequence are intimately associated with the cycling of oxidized and reduced forms of iron and manganese.

Microorganisms are known to use iron in electron donor/electron acceptor reactions. Microbial dissimilatory reduction of iron(III) is an important mechanism by which organic carbon is oxidized in anoxic environments including groundwaters. Although the aqueous concentration of iron(III) maintained by the solubility of iron(III) oxide solid phases at neutral pH is low and insufficient to support microbial oxidation of organic carbon, biological reduction of iron(III) has nonetheless been observed. There is evidence that iron(III)-reducing microorganisms can reduce certain forms of solid phase iron(III), including poorly crystalline iron oxides and layer silicates containing isomorphically substituted iron(III). Thus, in anoxic near-neutral environments, the microbial oxidation of organic carbon can be linked directly to the reduction of solid phase iron(III), which may remain as a structural constituent (in layer silicates) or be released as aqueous iron(II).

When anaerobic waters containing iron(II) come into contact with O_2, iron(II) is chemically reoxidized to iron(III), at a rate that depends on the pH and pO_2. In some environments, so-called "iron-bacteria," many of which are in the genus *Gallionella*, can gain energy for growth from the oxidation of iron(II). Because iron(II) chemically oxidizes on contact with O_2-saturated waters, the habitat of these microorganisms is confined to environments where iron(II) is chemically stable. Characteristics of these are low O_2 (0.1 - 1 mg/L), low temperature (8-16°C), circumneutral pH (6-8), and low organic carbon (<12 mg/L). Thus, pristine subsurface environments are potential habitats for iron(II)-oxidizing bacteria. In fact, *Gallionella* is often found in wells and near the water table in regions where the groundwater is anoxic.

Thus, it is hypothesized that dissimilatory reduction of iron(III) occurs within the confining zone where O_2 is limited as a result of microbial respiration and low permeability/diffusivity of the porous media. It is further hypothesized that

iron(II) from dissimilatory iron(III) reduction migrates by convection or diffusion from anoxic zones to microaerobic zones, where it is biologically reoxidized to iron(III). Visual observation of archived Basal Ringold cores revealed a transition zone textured with intermittent bands of iron oxides grading into clayey silts where iron is either reduced or depleted. These observations formed the basis for and lend credibility to the hypothesis.

Testing this hypothesis relies on measurements of

- iron-reducing and iron-oxidizing bacteria using classical enrichment and most-probable-number (MPN) methods,
- speciation of iron aqueous and solid phase valences via ion chromatography, titrimetry, or Mössbauer spectroscopy,
- labile forms of iron(II) and iron(III) via selective chemical extraction.

Attempts are being made to document whether the concentrations of iron(III) oxide particle coatings increase in zones of iron-oxidizing bacterial activity, and whether aqueous iron(II), $FeCO_3$, and structural iron(II) concentrations in layer silicates increase where iron-reducers are found.

Enrichments for iron-reducers include a range of electron donors and acceptors, including relevant iron(III)-containing solids. Where possible, 16S rRNA-targeted DNA probes for genera known to carry out these transformations are being employed for direct microscopic enumeration of these groups. In addition, manganese-reducing bacteria, sulfate-reducing bacteria, and fermentors are also being enumerated. Some iron-reducing bacteria are also known to reduce sulfate, and fermentors are required for primary degradation of complex organic carbon to various fermentation products, such as acetate, propionate, butyrate, formate, and H_2, which are in turn metabolized by iron(III)-reducing bacteria. Microbial iron(III) reduction in sediments is estimated by amending sediments with fermentation products and iron(III) and measuring rates of reduction.

In addition to the geochemical measurements described above for iron in pore waters and the associated sedimentary material, other analyses have targeted the identity of macroscopic, crystalline iron solid phases. Vanadate titrations were performed to assess the global oxidation-reduction (redox) potential of the sediments, and other relevant measurements were made to establish a conceptual geochemical model of redox processes within the confining layer. Other electron acceptors (including O_2, NO_3, and SO_4) were routinely measured on all pore waters and relevant solutions.

Drilling and Sampling Process and Stratigraphic Results. Deepening of the Yakima Barricade Borehole was initiated in late spring of 1992 and completed on October 30, 1992. Cable-tool drilling methods were used to deepen the borehole from the water table to the top of basalt bedrock. Samples were obtained using a heavy-duty split-spoon device. Sample quality was quantified with the use of both particulate and chemical tracers. A total of 33 samples were collected over a depth range of approximately 18 m. Sample locations and lithology are shown in Figure 3. Note that the entire section is a few meters deeper and thicker than had been predicted from data from DH-28 (Figure 2). This difference is apparently due to the fact that DH-28 is closer to the crest of the Umtanum Ridge anticline than is the Yakima Barricade Borehole. The observed increase in thickness and deptn was expected but its magnitude was greater than anticipated.

The detailed stratigraphy of the GEMHEX interval from the bottom up is as follows: The base of the sequence is a fluvial muddy sandy gravel that is clast supported and exhibits well-rounded iron-stained clasts. The unit is poorly sorted. Calcic concretions were observed at the top of the unit. Overlying the gravel is an olive to yellowish brown sandy silt, silty sand, or sand layer approximately 4 m thick. This fluvial unit is micaceous and well sorted, and it shows weak cross laminations and graded beds. The sand grades upward over a meter or so into a paleosol sequence that consists of dark greenish/bluish gray clay, silt, and sand that is bioturbated and weathered and contains white pedogenic carbonate nodules and stringers. The top 0.5 m of the paleosol is a well-developed, dark brown layer

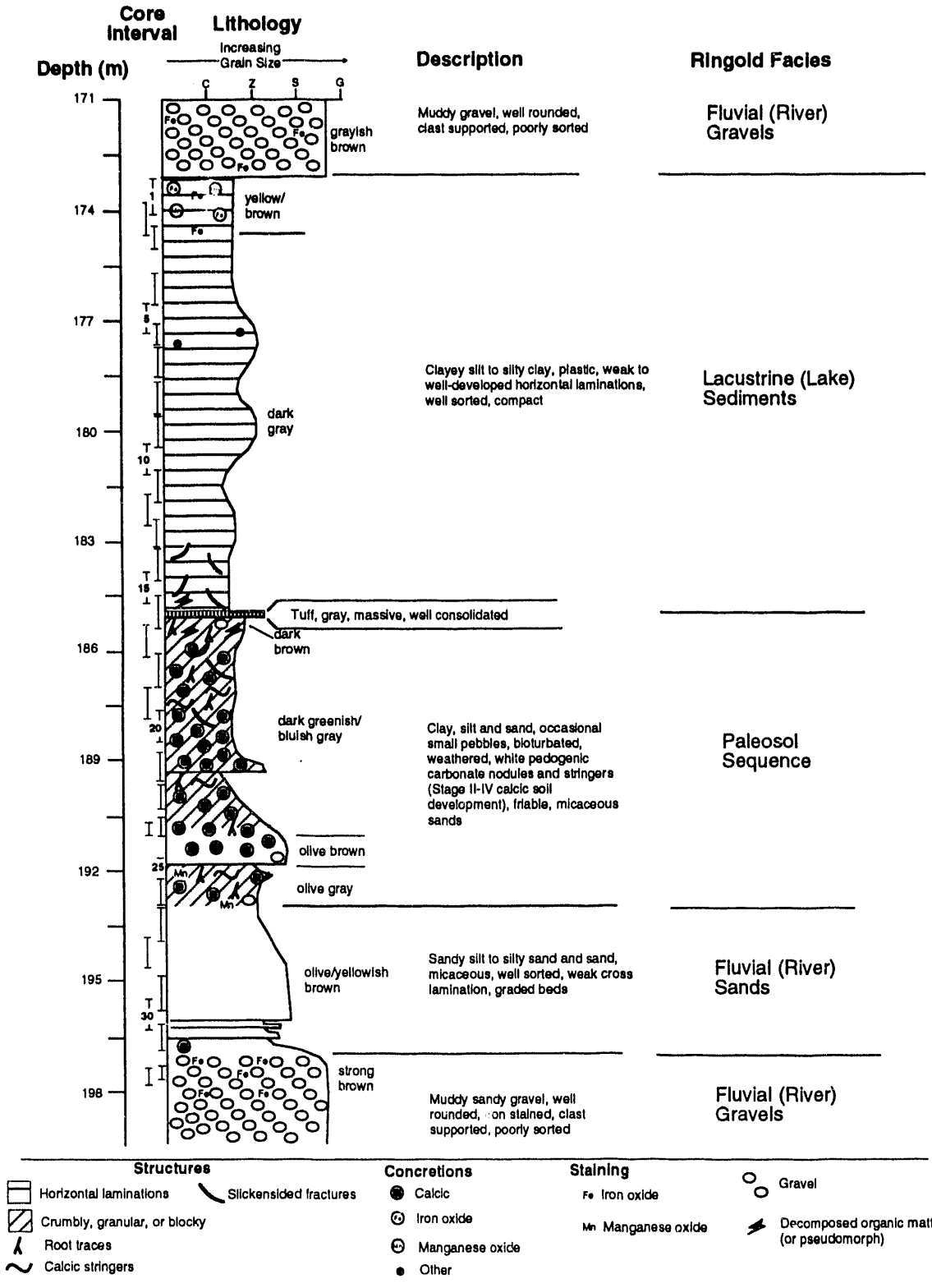

FIGURE 3. Detailed Stratigraphic Section and Split-Spoon Sample Locations for the GEMHEX Interval

suggestive of an Ah horizon. The total thickness of the paleosol sequence is approximately 9 m. The paleosol is overlain by a reddish gray volcanic tuff several centimeters thick. The tuff is fine grained, massive, and well consolidated and impressions of organic matter (e.g., twigs) show clearly in its base. The top half of the GEMHEX interval consists of 13 m of lacustrine clayey silt to silty clay. The bulk of the lacustrine unit is dark gray and exhibits weak to well-developed horizontal laminations. The unit is well sorted and has a compact but semiplastic consistency. At the base of the unit, organic matter and slickensided fractures occur. In the upper 2 m of the unit, the color is yellow-brown and iron staining, iron concretions, and manganese concretions are apparent. The GEMHEX interval is capped by grayish brown fluvial muddy gravel. The texture is well-rounded and poorly sorted with a clast-supported fabric. Iron staining is common.

The following key facets of the geology are being considered in testing of the hypotheses:

- Fluvial gravels above and below the GEMHEX interval are strongly to moderately iron stained. The upper 2 m of the lacustrine sediments directly underlying the gravels at the top of the GEMHEX interval are light-colored and iron-stained, and they contain iron oxide and manganese oxide nodules and concretions. In contrast, the underlying lacustrine sediments are dark gray.

- Subvertical fractures occur in the lower part of the lacustrine sediments. These fractures may enhance the local permeability of this part of the interval.

- The occurrence of a layer similar in appearance to an organic-rich A horizon at the top of the paleosol could provide a potential carbon and microbe source that might influence adjacent microbial communities if such materials are important to subsurface microbial ecology. If the overlying volcanic tuff is well-colonized, it suggests that both nutrients and microorganisms are readily transported the few centimeters across the paleosol-tuff interface.

- The contrasting permeabilities and perhaps nutrient levels between the paleosol and the underlying sand layer are expected to provide a key test of Hypothesis 1. Interplay among permeability, nutrient levels, and original microbial abundance in the paleosol will be particularly interesting in this part of the GEMHEX interval.

- Each of the units described above represents specific depositional, weathering, and diagenetic environments that must be considered when testing the hypotheses. For example, the contrasting origins, mineralogies, and permeabilities of the lacustrine sediments and the sand indicate that initial microbial abundances were different, evolution of the pore-water chemistry was different, and the total water flux through the sediments may have differed by orders of magnitude. The occurrence of the tuff at the contact between the paleosol (representing subaerial conditions) and the lacustrine sediments (representing slow lake sedimentation) may indicate a relationship between the volcanic episode resulting in the tuff and a change in the base level for the drainage system. For example, volcanic activity in the Cascade Range may have caused the level of the ancestral Columbia River to change, thus initiating a change from soil development to lacustrine sedimentation. Volcanism or tectonism of that magnitude may also have altered other factors, such as the pH of precipitation, or it may even have perturbed existing precipitation patterns.

Overall, the GEMHEX sampling was highly successful. From each 0.6- or 0.9-m-long split-spoon sample, a few kilograms of pristine material was typically available for subsampling. Each split-spoon sample was systematically subsampled, as illustrated in Figure 4. Analyses of samples were planned to provide the key data needed to test Hypotheses 1 through 3.

Sample Collection and Sample Processing. Decisions regarding the collection, processing, and disposition of GEMHEX samples were made by consensus of the team of GEMHEX principal investigators: geologists Phil Long and Shirley

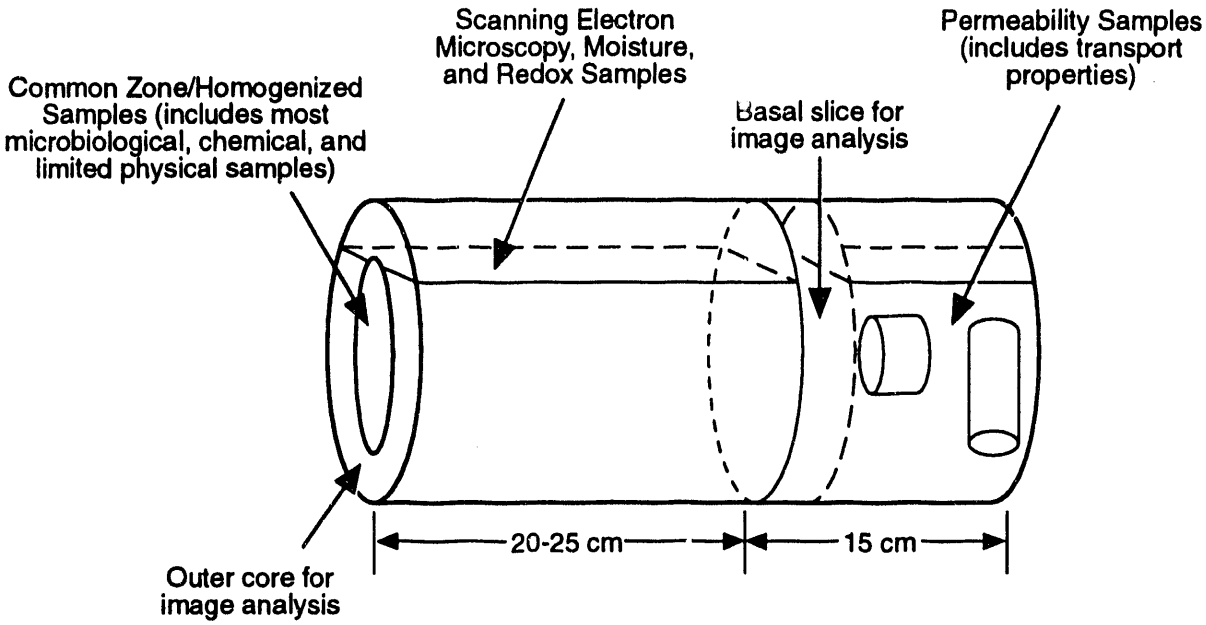

FIGURE 4. General Scheme for Subsampling of Split-Spoon Cores

Rawson or their designee, microbiologists Jim Fredrickson and Todd Stevens or their designee, and geochemists John Zachara and Jim McKinley or their designee.

We originally planned to collect 20 to 25 samples. The greater-than-expected thickness of the GEMHEX interval resulted in a total of 33 samples, 27 of which were common samples.

For each sample, a decision was made to designate it as either 1) a common sample, 2) an interface sample, 3) a heterogeneity sample, 4) a "limited" sample, or 5) an unusable sample. The sample types are defined below, with general guidance on the criteria for sample selection and identification. The criteria were agreed upon by key GEMHEX participants for use in identifying areas within each core for sampling. It was assumed that 0.9-m-long core barrels would be used and would provide approximately 0.6-m lengths of usable material for various investigations. The diameter of the split-spoon cores was 10 cm; these cores were pared for the microbiology and chemistry investigations.

Common samples were core samples that were processed to allow all three GEMHEX hypotheses to be addressed using materials from a single core interval. Some 27 common samples were collected. The common samples were typically 25-cm sections from selected locations in the core. The 25-cm sections were visually homogeneous and representative of the dominant lithology in the core segment. They were generally collected from the middle to lower third of the core barrel to minimize potential contamination. Targeted zones were those that generally satisfied the above criteria and that displayed visual evidence of 1) iron oxidation (red staining) or iron reduction (black, blue, or green) or 2) organic matter, such as root casts or lignite pieces.

Attempts were made to obtain uncontaminated common samples of Middle Ringold gravels. These attempts were largely unsuccessful. It is virtually impossible to obtain gravel samples that are physically intact using the split-spoon sampling method. We were, however, able to obtain limited quantities of these materials for microbiological analyses.

Interface samples were pairs of samples that were closely spaced across a major lithologic interface (e.g., gravel/lacustrine or paleosol/sand interface). Collection of at least two such

samples was planned from each of six to eight cores exhibiting clear transitions in chemical, physical, or lithologic properties. The two samples from each core were to be taken from above and below the interface in order to characterize the changes occurring across the contact. Target samples included, but were not limited to, 1) the lacustrine to paleosol contact, 2) the paleosol to fluvial transition region, and 3) apparent boundaries between oxidized and reduced zones.

Heterogeneity samples were single core segments that were divided for analysis at multiple sampling scales (e.g., 5, 20, 80, or 160 g). The intent was to obtain two whole cores for a detailed heterogeneity study, based on sectioning normal to the core axis. No common samples would be taken from these cores. One core would be selected as exhibiting generally homogeneous properties (like the common samples, perhaps a paleosol), and the other as containing visual heterogeneities, such as varves or regular layers of iron oxide staining (i.e., as observed in the upper lacustrine sequence). Approximately 43 subsamples were to be analyzed per heterogeneity sample core using a limited set of microbiological, chemical, and physical techniques. During the GEMHEX sampling, however, only one interface sample (lacustrine-paleosol contact) and one heterogeneity sample (lacustrine sediments) were collected.

Limited samples were those for which homogeneous or uncontaminated materials were insufficient to meet the criteria for other samples but from which useful (intact and/or uncontaminated) samples could be extracted. These materials were processed and distributed at the discretion of the team of principal investigators.

Unusable samples were samples that were physically, chemically, or microbiologically compromised, such that they were not usable for GEMHEX purposes. The team of principal investigators identified such samples at the earliest possible point in the collection process, and the samples were not processed further except for use in special projects or in general geologic characterization.

Alternative sampling approaches were occasionally used (e.g., drive-barrel sampling), but when they were used, sample selection was more difficult because the samplers lacked a removable liner.

Characterization of GEMHEX Samples. Samples from each of the sample locations within the GEMHEX sampling interval are currently being intensively characterized to test Hypotheses 1 through 3. The physical, chemical, and mineralogic analyses being performed at each of the sampling points are listed in Table 1.

For certain analyses (e.g., permeability), it is not possible to obtain suitable samples at all sample points. On these cores, the hypotheses will be tested based on other analytical techniques, such as grain size distribution and its empirical relationship to permeability.

Most sample analyses are still in progress; it is premature to draw conclusions regarding the three GEMHEX hypotheses. However, some of the geohydrologic data were collected during drilling, and results are discussed below. Only limited geochemical and microbiological results are available at the time of writing. The data from geohydrologic, geochemical, and microbiological analyses are discussed briefly below, but major conclusions will be deferred and published in subsequent annual reports and scientific papers.

GEMHEX Geohydrology. Aquifer responses to the GEMHEX drilling and sampling were evaluated to provide data on the geohydrologic conditions in the Yakima Barricade Borehole, because knowledge of the geohydrology is required for assessing the nutrient fluxes to the GEMHEX sampling interval.

To estimate the hydraulic conductivity, borehole-scale hydraulic measurements were made during the deepening of the Yakima Barricade Borehole. Two drawdown tests were conducted, at 161 and 162 m below the surface. The rate of borehole recovery was observed after bailing was conducted to collect water samples. Because the Yakima Barricade Borehole is nearly fully cased at all times, when the borehole is bailed,

TABLE 1. Physical, Chemical, and Mineralogic Analyses[a]

Analysis	Individual Responsible
Physical Property Analyses	
Grain size distribution	B. N. Bjornstad, S. Birnbaum
Direct microbial association with size fraction (aseptic sieving)	S. A. Rawson, S. Birnbaum
Specific surface	S. A. Rawson
Bulk density	S. A. Rawson
Particle density	S. A. Rawson
Porosity (ϕ)	B. N. Bjornstad
Permeability, k_s	S. A. Rawson
Image analysis of pore structure	P. E. Long
Transport properties (diffusion coefficients for O_2)	S. A. Rawson
Pore throat sizes (mercury porosimetry)	S. A. Rawson
Definition of sedimentary units	B. N. Bjornstad
Chemical and Mineralogic Analyses	
Expressed pore water and groundwater:	
Major/minor cations and anions	J. P. McKinley
Nutrient ions (nitrogen, phosphorous)	J. P. McKinley
Electron acceptors [O_2, SO_4, NO_3, manganese, iron(II), iron(III)]	J. P. McKinley
Dissolved organic carbon, dissolved inorganic carbon	J. P. McKinley
Fermentation products when possible (acetate, formate, butyrate, propionate)	J. P. McKinley
Stable isotopes (hydrogen, oxygen, carbon, nitrogen, sulfur)	E. M. Murphy
H_2 (if reducing conditions prevail)	J. P. McKinley
Solids:	
Extractable iron and manganese (amorphous, crystalline)	J. P. McKinley
Total organic carbon, nitrogen, phosphorous	J. P. McKinley
Iron(II)/iron(III) (in solid phases)	J. M. Zachara
Manganese oxidation state (in solid phases)	J. M. Zachara
Reduction capacity (CrO_4^{5-} titration)	J. M. Zachara
$CaCO_3$	J. P. McKinley
Mineralogy (X-ray diffraction, scanning electron microscopy-energy dispersive spectroscopy)	S. A. Rawson, S. Birnbaum
Petrography (diagenetic mineralogy)	B. N. Bjornstad
Phosphate mineralogy in weathered basalt cobbles	P. E. Long
Phosphate solubility factors	J. P. McKinley
Extractable forms of phosphate	
-Labile P_i (isotope dilution)	J. P. McKinley
-P fractionation	J. P. McKinley

(a) Associated microbiological analyses are described in the paper by Fredrickson and others, this volume.

water inflow occurs only at the bottom. The recovery data were obtained by monitoring the water level after a period of about 2 hours during which the hole was bailed about once every 2 min, at an average rate of 3.56×10^{-4} m^3/sec (5.6 gpm). The error bars on the time base and initial water-level measurements are about 60 sec and 0.03 m. Drilling produced a borehole slurry that was significantly more dense than groundwater; consequently there is a discrepancy between water levels measured during drilling and after bailing. As a result, no water-level measurements were possible during bailing, and the full extent of drawdown could not be quantified. This effect can contribute to underestimation of formation conductivity, although the recovery data analyzed here were acquired when the borehole fluid was relatively clean. The borehole depth was nominally 162 m during testing, which was within the thick but variable gravelly unit above the Lower Ringold Formation. The recovery data from the 162-m depth were acquired after two borehole volumes were bailed. Fluid clarity was improved markedly, so borehole water levels were taken as indicative of formation heads. Testing was attempted at about 161 m, just below a sandy interval a meter or two thick, but very slow recovery was observed and the 161-m test was abandoned.

Because of the cased configuration of the borehole, recovery of the borehole with time was analyzed using expressions for both cylindrical flow in a confined aquifer (Papadopulos and Cooper 1967) and spherical radial flow expressions (Carslaw and Jaeger 1959). Cylindrical flow could be important if the formation is relatively impermeable or anisotropic at the location of the test and if there are conduits for axial flow behind the casing (extending the length of the test interval). Recovery curves calculated for cylindrical flow indicated a transmissivity of 4×10^{-4} m/sec at 162 m (Figure 5). A small value for storativity ($S = 10^{-4}$) was used for these calculations because the interval was short, the drawdown was slight, and the well was subjected to pressure cycling by surging during cable-tool operations.

Spherically radial flow could be important if the formation is relatively uniform, highly conductive, and isotropic, or if axial flow behind the casing is impeded. The first test observations at 161 m indicated that flow behind the casing was indeed restricted; there was evidently no connection behind the casing to gravels above this level, and therefore the tests at 162 m did not communicate directly with gravels above 161 ft. The results of the first test indicate that at a scale of 0.6 to 0.9 m or more, the flow potentials are hemispherical, and a spherical radial flow model could be warranted. A spherical radial flow model yielded the recovery curves plotted in Figure 6. The curves were recomputed with different values for K, a, and Ss; none fit the data any better than those shown, so spherical flow divergence does not appear to be important for the 162-m test.

There are several limitations on the applicability of these results. First, cable-tool drilling in the Yakima Barricade Borehole produced a heavy slurry, which caused the measured water level to be lower than the actual formation head. This uncertainty must be considered during evaluation of the drawdown results. Static water level rose in the casing when the hole was bailed to remove slurry, as a result of fresh groundwater inflow. Water level also rose because of settling during a hiatus in drilling operations; however, density measurements of the slurry near the base of the hole indicated little tendency for significant settling within a few days.

The water-level measurements reported here are referenced to the static water level measured after a weekend hiatus of about 60 hours. Error associated with the measured drawdown values could be as much as 0.2 m. If that is the case, the data points on Figures 5 and 6 would be plotted lower by 0.2 m. Replotting these data would change the recovery curve from something closely resembling cylindrically radial flow to something partway between cylindrical and spherically radial flow.

Second, the flow geometry of the 162-m recovery test was uncertain and the relative error on

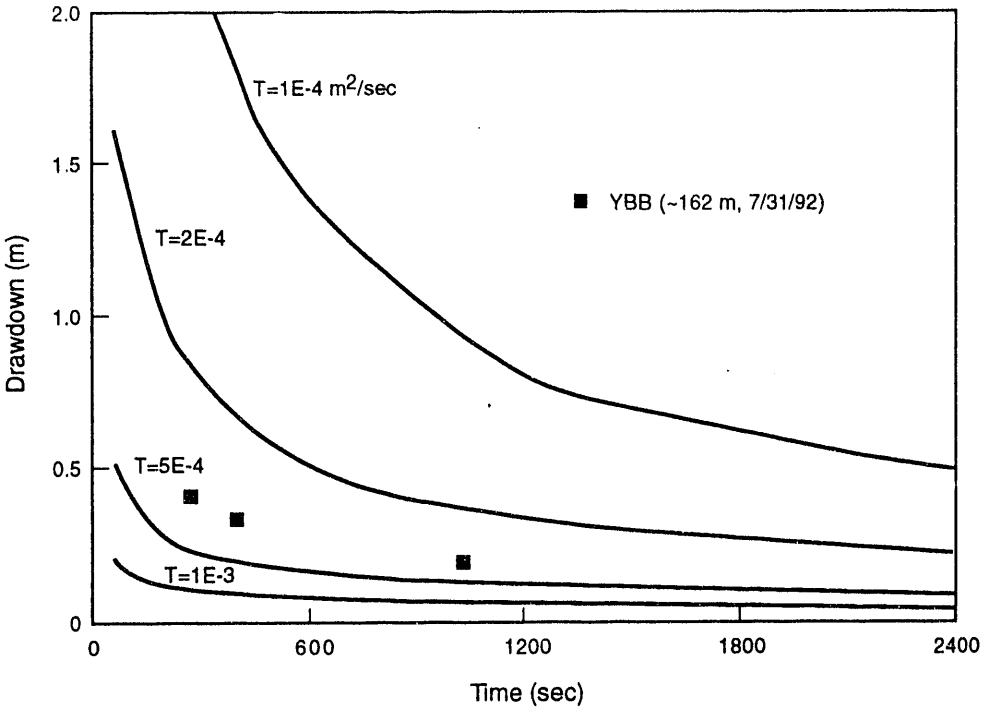

FIGURE 5. Recovery Curves Based on Cylindrical Flow Response to Drawdown in the 162-m Test. Solid symbols representing recovery of the formation indicate a transmissivity (T) of 4 x 10^{-4} m^2/sec.

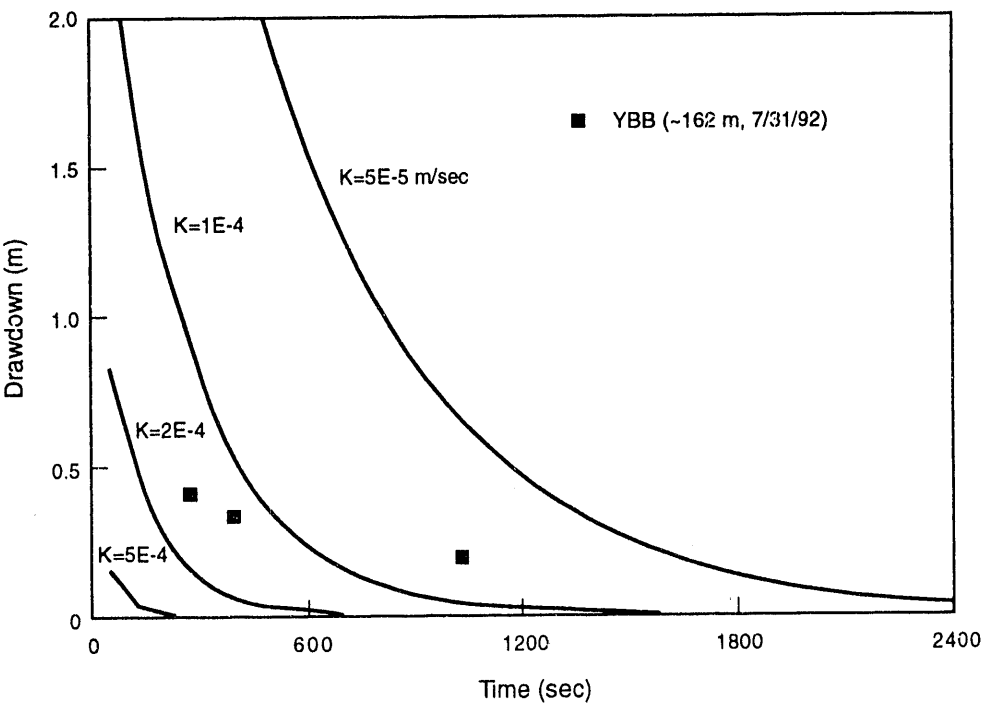

FIGURE 6. Recovery Curves Based on Spherically Radial Flow Response to Drawdown in a Spherical Cavity Connected to a Cylindrical Casing in the 162-m Test. Solid symbols indicate that the spherically radial flow model is not applicable to the formation at 162 m.

the thickness could be as much as 50%. Consequently, the interpretation was limited to end-member flow models. Additional modeling could include partial penetration and the effect of confining boundaries, but these effects would not be distinguishable from the effects of flow geometry or the effects of small-scale heterogeneity, given the currently available test data. The flow regime appears to be cylindrically radial, and the apparent transmissivity is approximately 4×10^{-4} m^2/sec. Hydraulic conductivity could range from 4×10^{-4} to 8×10^{-4} m/sec, if the interval length was as small as 0.5 m.

Data were collected from a variety of sources to explicate the well-bore hydrology and assess nutrient flux. Sources of information on hydraulic conductivity in the Yakima Barricade Borehole include published results of irrigation well tests and pumpage, geophysical logs, and the 162-m drawdown recovery test, which are plotted together in Figure 7. The Fair–Hatch and Repsold-derived curves display estimates of hydraulic conductivity derived from porosity and lithology data extracted from geophysical logs obtained from the same sedimentary sequence in DH-28 and adjusted to match field data for hydraulic conductivity. More drawdown/recovery test data are needed to reduce the arbitrariness of the adjustment of the estimated hydraulic conductivity profiles. The proposed hydraulic conductivity profile plotted in Figure 7 is intended to respect the major features of the adjusted profiles, at 3-m resolution, and to do so in round numbers, for the purpose of flux modeling across the GEMHEX interval.

Although modeling of nutrient fluxes must await groundwater chemistry results from the completed Yakima Barricade Borehole well, these profiles of vertical distribution of hydraulic conductivity show the wide range of variability in physical properties (three to four orders of magnitude) over short vertical distances within the GEMHEX interval. Completion of laboratory-scale physical property analyses and multilevel water sampling within the well will allow further quantification of the estimates made to date.

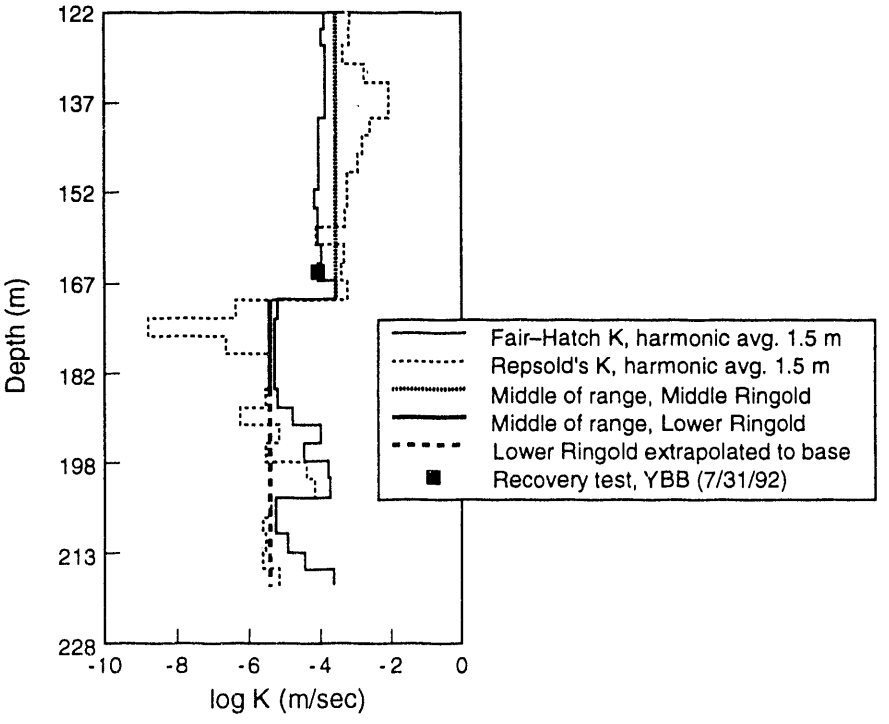

FIGURE 7. Comparative Hydraulic Conductivity Profiles, Plotted with Constraint Data and Adjusted Profiles Based on Geophysical Logs. The adjusted profiles were calculated from the harmonic mean of data in 1.5-m intervals, and the proposed profile is specified on 3-m intervals.

Preliminary Geochemical Results. Geochemical measurements made during the period of sampling have demonstrated some key characteristics of the deep unconfined aquifer:

- Oxidizing or microaerophilic conditions may exist throughout the GEMHEX sampling interval and probably extend to or near the top of the basalt. This conclusion is based on redox measurements of expressed pore water and on downhole measurements performed using a commercially available multisensor device.

- There do not appear to be significant differences in reductive capacity between obviously oxidized (iron oxide-stained) sands or silts on the one hand and dark-colored silts and clays on the other. This conclusion is based on measurement of reductive capacity of 1:1 sediment:water mixtures.

- Highly reduced conditions (-400 mV) exist within the borehole slurry during drilling. These conditions are apparently the result of interaction of borehole fluids with newly created fracture surfaces that expose ferrous iron cations. Subsequent reactions result not only in highly reducing conditions but also in the hydrolysis of water to produce detectable gaseous hydrogen. The presence of hydrogen presented a minor safety issue during borehole drilling, but it has more important implications for microbial ecology of subsurface locations where reducing conditions occur naturally. Even minor hydrogen production could provide a significant energy source for microorganisms.

In general, the groundwater geochemistry of the GEMHEX interval appears to be consistent with measurements on samples from wells within a few kilometers of the Yakima Barricade Borehole. Additional information on redox conditions in the GEMHEX interval awaits completion of solids analyses currently in progress.

Preliminary Microbiological Results. Microbiological results are still very preliminary. Available data, primarily on aerobic microorganisms, indicate that microbial abundance and activity are relatively low in the GEMHEX interval. Acridine orange direct counts (AODC) show that in the bulk of the samples, observable microbial numbers are too low to detect (Figure 8). Moreover, AODC suggests that the abundances are greatest and most consistent in the lacustrine sediments, the inverse of the predicted results (Figure 2). The interpretation of these results is currently far from clear, especially considering that the data set is incomplete. Nonetheless, it can be speculated that the subsurface microbial community in the GEMHEX sampling interval has largely exhausted its energy sources, particularly in the areas of relatively high permeability where groundwater flux has made the complete oxidation of available reduced carbon possible. In low-permeability zones, such as the lacustrine sediments, lower groundwater flux has limited the availability of oxygen and thus the rate at which aerobic microorganisms have been able to oxidize available reduced carbon. Reduced carbon in the lacustrine sediments thus continues to support a very low level of microbial life in the lacustrine sediments. If this hypothesis holds, then organic carbon should be measurably different in the oxidized and unoxidized parts of the lacustrine sediments. Based on the geohydrologic results, future calculations of nutrient flux in the various parts of the GEMHEX interval should also be consistent with the concept of high-permeability zones being exhausted of available nutrient sources.

Future Research

The planning, experimental design, sample acquisition, and initial sample analysis for the GEMHEX have been highly successful. Preliminary results suggest that the conclusions we will finally draw from the GEMHEX may be different from those predicted in the hypotheses. Nonetheless, the principal objective of enhancing our understanding of subsurface microbial processes will be well served by the GEMHEX.

Borehole completion at the Yakima Barricade Borehole is currently in the final stages of design and should be complete by early March 1993. During this phase, screened casing will be installed in the saturated zone of the Ringold Formation. For each intact core zone interval, samples of bulk formation waters will be taken with a multilevel sampler that uses dialysis

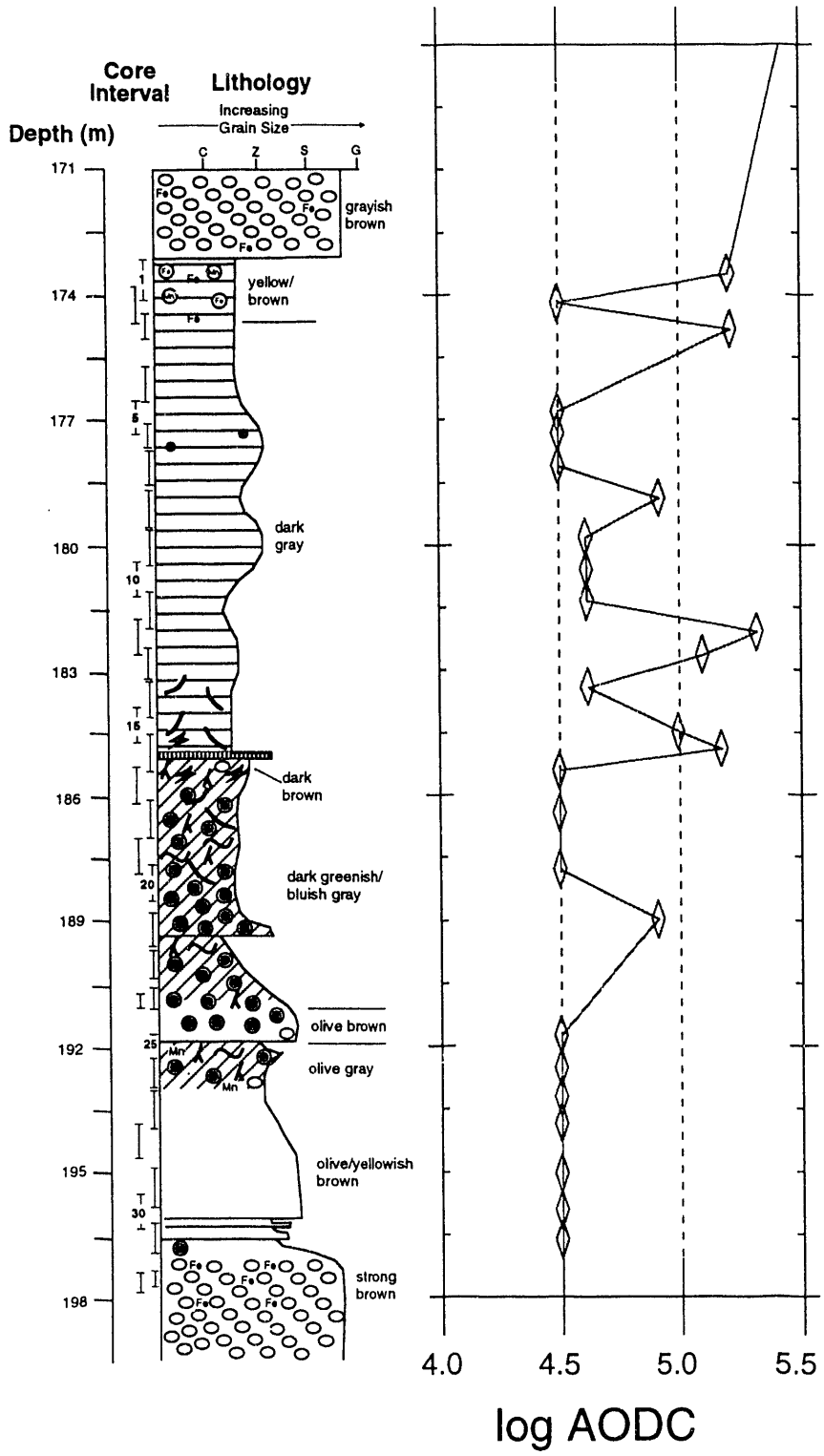

FIGURE 8. Acridine Orange Direct Counts Plotted Against Depth and Stratigraphy of the GEMHEX Interval

membrane cells to determine equilibrium aqueous concentrations in the borehole (Ronen et al. 1986, 1991). The samples collected will provide formation water chemistry to correspond with each GEMHEX solid sample and thus provide a comparison to water chemistry obtained from pore waters. Use of multilevel samplers to determine *in situ* hydraulic gradients and flow rates is also being evaluated.

Installation of the well screen will also allow us to conduct an additional experiment, to evaluate the potential *in situ* colonization of microorganisms within the lacustrine sediments or other subsurface horizons. Sterilized sediments will be suspended in the borehole and allowed to "equilibrate" and be colonized by the free-floating microbial population (Hiebert 1991). The organisms that colonize these sediments will be compared (using molecular and physiological approaches) with microorganisms obtained from the original sediments to determine the degree to which the two populations overlap. This experiment is primarily designed to support testing of Hypothesis 3 (on phosphorous limitation), by providing additional insight into the active microbial types present in the zone of the GEMHEX cores.

References

Balkwill, D. L., and F. J. Wobber. 1989. *Subsurface Science Program Deep Microbiology Transitional Program Plan*. DOE/ER-0328, U.S. Department of Energy, Washington, D.C.

Balkwill, D. L., J. K. Fredrickson, and J. M. Thomas. 1989. "Vertical and Horizontal Variations in the Physiological Diversity of the Aerobic Chemoheterotrophic Bacterial Microflora in Deep Southeast Coastal Plain Subsurface Sediments." *Applied Environmental Microbiology* 55:1058-1065.

Brockman, F. J., T. L. Kieft, J. K. Fredrickson, B. N. Bjornstad, S.-M. W. Li, F. W. Spangenberg, and P. E. Long. 1992. "Microbiology of Vadose Zone Paleosols in South-Central Washington State." *Microbial Ecology* 23:279-301.

Carslaw, H. S., and J. C. Jaeger. 1959. *Conduction of Heat in Solids*. Oxford University Press, London.

Davis, S. N. 1969. "Porosity and Permeability of Natural Materials." In *Flow Through Porous Media*, ed. R.J.M. DeWiest, pp. 54-89. Academic Press, New York.

Doyen, P. M. 1988. "Permeability, Conductivity, and Pore Geometry of Sandstones." *Journal of Geophysical Research* 93(B7):7729-7740.

Fredrickson, J. K., T. R. Garland, R. J. Hicks, J. M. Thomas, S.-M. W. Li, and K. M. McFadden. 1989. "Lithotrophic and Heterotrophic Bacteria in Deep Subsurface Sediments and Their Relation to Sediment Properties." *Geomicrobiology Journal* 7:53-66.

Hiebert, F. 1991. "SEM Study of Bacteria-Mineral Interactions in Microcosms that Model the Shallow Subsurface." *Geological Society of America Abstracts with Programs* 23:A-290.

Kieft, T. L., and L. L. Rosacker. 1991. "Application of Respiration-Based and Adenylate-Based Soil Microbiological Assays to Deep Subsurface Terrestrial Sediments." *Soil Biology and Biochemistry* 23:563-568.

Kindred, J. S., and M. A. Celia. 1989. "Contaminant Transport and Biodegradation, 2. Conceptual Model and Test Simulations." *Water Resources Research* 25:1149-1159.

Long, P. E., S. A. Rawson, F. S. Colwell, G. J. Stormberg, J. K. Fredrickson, D. L. Balkwill, and F. J. Wobber. 1990. "Progress of Sample Acquisition for the Deep Microbiology Program, U.S. Department of Energy." *EOS* 71:1326.

Long, P. E., J. K. Fredrickson, E. M. Murphy, S. A. Rawson, J. P. McKinley, F. J. Brockman, and B. N. Bjornstad. 1991. "Geohydrologic and Geochemical Controls on Subsurface Microorganisms in the Late Cenozoic Sediments, South-Central Washington." *Geological Society of America Abstracts with Programs* 23:A377.

Molz, F. J., M. A. Widdowson, and L. D. Benefield. 1986. "Simulation of Microbial Growth Dynamics Coupled to Nutrient and Oxygen Transport in Porous Media." *Water Resources Research* 22:1207-1216.

Papadopulos, I. S., and H. H. Cooper, Jr. 1967. "Drawdown in a Well of Large Diameter." *Water Resources Research* 3:241–244.

Raffensperger, J. P., and R. E. Ferrell, Jr. 1991. "An Empirical Model of Intrinsic Permeability in Reactive Clay-Bearing Sands." *Water Resources Research* 27:2835-2844.

Repsold, H. 1989. *Well Logging in Groundwater Development*, Volume 9. International Contributions to Hydrogeology Series, International Association of Hydrogeologists, Verlag Heinz Heise, Hanover, Germany.

Ronen, D., M. Margaritz, E. Almon, and A. J. Amiel. 1986. "Anthropogenic Anoxification ('Eutrophication') of the Water Table Region of a Deep Phreatic Aquifer." *Water Resources Research* 23:1554-1560.

Ronen, D., M. Margaritz, and F. J. Molz. 1991. "Comparison between Natural and Forced Gradient Tests to Determine the Vertical Distribution of Horizontal Transport Properties of Aquifers." *Water Resources Research* 27:1309-1314.

Pore-Water Chemistry in a Deep Aquifer System at the Hanford Site, Washington

J. P. McKinley

This project conducts research into the relationship between subsurface water chemistry and microbial activity. Included within this area are geochemical investigations conducted in collaboration with projects investigating subsurface microbial processes and hydrogeologic and geochemical controls on microorganisms in subsurface formations. Activities in FY 1992 included 1) analysis and interpretation of pore-water and solid-phase chemistry of samples collected from the vadose zone at the Yakima Barricade Borehole at the Hanford Site in FY 1991, 2) collection and analysis of pore water and associated solid samples from the saturated zone (the unconfined aquifer) at the Yakima Barricade Borehole, 3) introduction and analysis of aqueous-phase tracers at the Yakima Barricade Borehole, and 4) investigations of short-term geochemical variations within the Yakima Barricade Borehole in relation to observed occurrences of hydrogen gas.

FY 1992 Research Highlights

Analysis and Interpretation of Vadose-Zone Samples. Drilling in the vadose zone at the Yakima Barricade site reached the unconfined aquifer at 99.7 m. Samples collected above that depth were generally too dry to yield water for direct analysis and were leached using deionized water to allow estimation of pore-water compositions. Samples were also collected for the measurement of gravimetric moisture content and bulk chemical properties by several methods, including bulk chemistry by proton-induced X-ray emission (PIXE) analysis and wet chemical digestion assays of total nitrogen and phosphorous and of organic and inorganic carbon. Results from these tests were compared to microbiological results for the same samples.

Comparisons of chemical information with microbiological data were limited to log colony-forming unit (CFU) numbers derived from cultures grown aerobically on 1% peptone-trypticase-yeast extract-glucose (PTYG) medium. To facilitate comparisons incorporating data from a number of microbiologists, the mean of all available 1% PTYG results was computed and compared with chemical data. This method of comparison was thought to partially mitigate an inherent sampling problem: the samples used for chemical measurements and microbiological measurements did not generally originate from the same part of a given core sample. For certain analyses, the chemical measurement samples had to be of large volume and had to originate outside the lithologic boundaries selected for microbial sampling. Samples for PIXE and digestion assays required much less mass for successful analysis and were taken generally within the microbial sampling interval, but not as subsamples of the homogenized sample distributed for microbiological analysis. Chemical samples therefore represented average compositions of a potentially heterogeneous core interval and were compared to microbiological subsamples originating at differing places within that core.

Despite the sampling difficulties inherent in chemical-microbial comparisons, some microbial dependence on chemical environment could be inferred. Figure 1 illustrates the relationship between gravimetric moisture content and the abundance of aerobic bacteria. Figure 2 shows a subordinate relationship between solid phase phosphorous and microbial abundance. Although microbial abundance and gravimetric moisture are smoothly correlated, total phosphorous is correlated with abundance only above a threshold moisture value. These relationships suggest that moisture is more important than phosphorous, either as a necessary element of the microbes' environment or as a limiting factor in transporting phosphorous to phosporous-limited microbial communities.

Collection and Analysis of Pore Water and Associated Solid Samples from the Saturated Zone (the unconfined aquifer) at the Yakima Barricade Borehole. Drilling and sampling within the saturated zone at the Yakima Barricade Borehole was begun in the spring of 1992. This phase of investigation included cable-tool drilling through Ringold Formation sediments to the top of basalt at approximately 230 m. Within this overall interval was an intensively sampled interval of approximately 18 m, encompassing lacustrine sediments and a paleosol unit grading into sandy sediments below.

Although these sediments were water saturated, they were very fine-grained (a large fraction of each lithology consisted of clay minerals), and expression of water from them using standard methods was impossible. A small volume of water was removed from each specimen by ultracentrifugation (under a subcontract to Washington State University at Tri-Cities). Samples obtained from the "common" interval (from which samples were distributed to microbiologists in the Deep Microbiology Subprogram of the Subsurface Science Program) were processed under inert atmosphere. In most cases it was possible to extract 6 to 12 ml of pore water from 160 g of sediment using this method. Careful allocation of expressed water has allowed analysis for the following analytes on all but a few low-volume samples: cations, anions including bromide and ClO_4, dissolved oxygen, pH, inorganic and organic carbon,

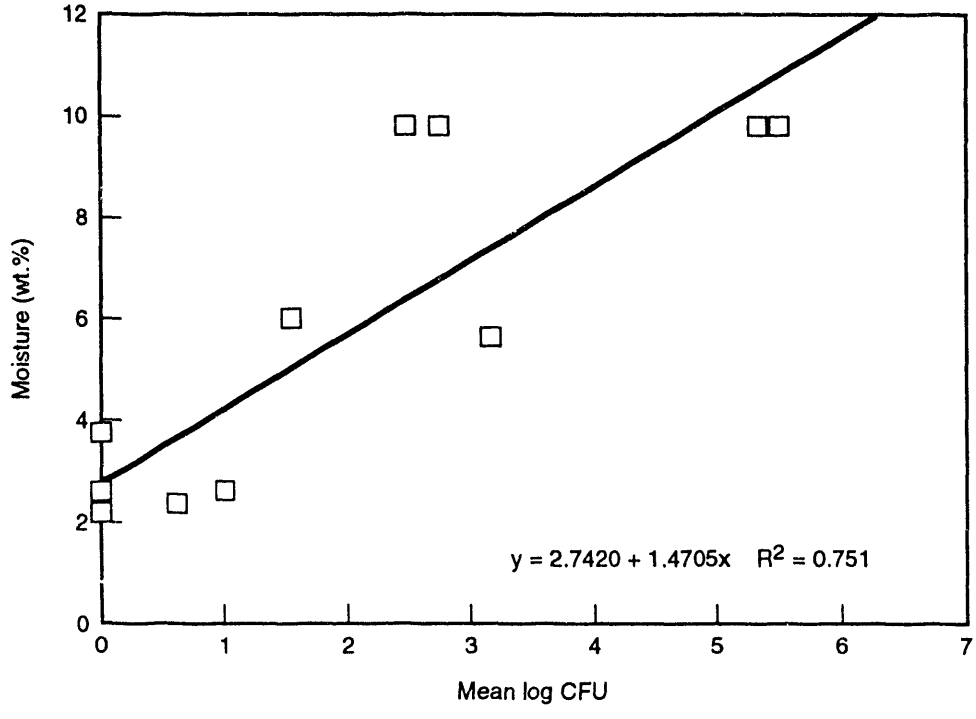

FIGURE 1. Mean log CFU versus Moisture

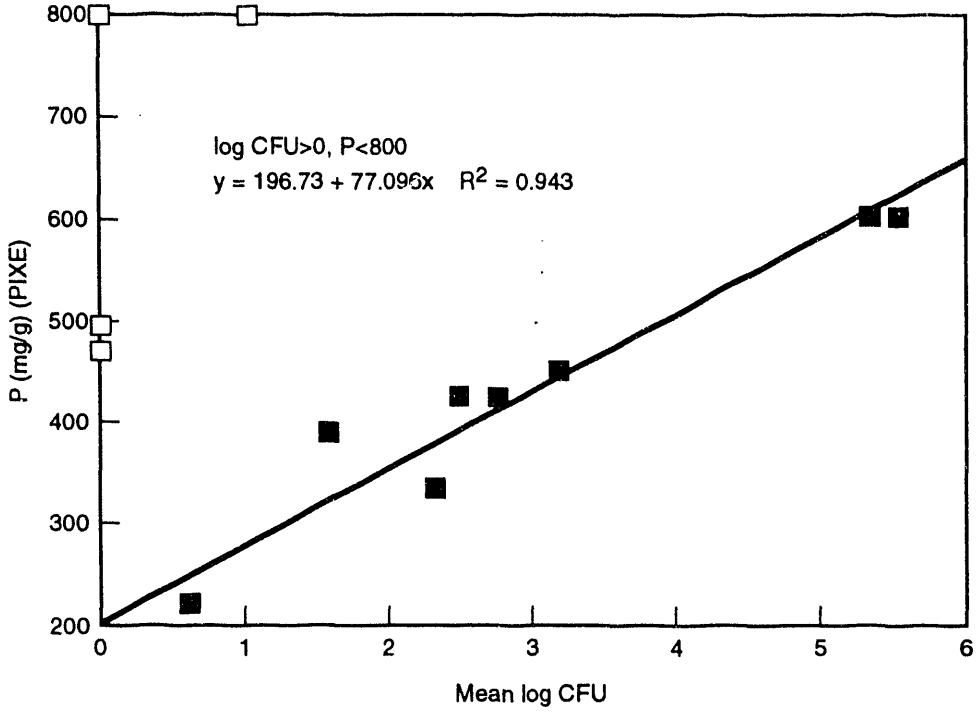

FIGURE 2. Mean log CFU versus Phosphorous above Water Table

iron(II/III), sulfate/sulfite, nitrate/nitrite, ammonium, and orthophosphate. In addition to pore-water analysis, pH and reducing capacity (measured by platinum electrode) of 1:1 slurries of solid samples were determined.

Downhole conditions during drilling were measured by deployment of a sonde purchased for that purpose, and through the use of a downhole sampler. Both instruments were monitored and controlled from the ground surface. The sonde produced temporal information on variation in downhole temperature, pH, dissolved oxygen, oxidation-reduction (redox) conditions, and depth (changes in depth were observed during pumping and as water levels within the casing changed as a function of drilling).

Measurements of solid-phase chemistry, particularly iron phase and phosphorous content, are still under way. When they are complete, overall geochemical conditions within the borehole will be integrated with microbiological results to produce an evaluation of chemical microbial interactions over a short but heterogeneous stratigraphic section.

Introduction and Analysis of Aqueous-Phase Tracers at the Yakima Barricade Borehole. As in previous drilling projects in the Deep Microbiology Subprogram, chemical tracers were used in the Yakima Barricade Borehole to determine the extent of contamination of samples during drilling and removal. Bromide was introduced as an indicator of chemical contamination from within the borehole. In the saturated zone, bromide was introduced by maintaining an approximately constant concentration of KBr in the borehole slurry enclosed within the steel casing. Frequent measurement of bromide concentration in the slurry by ion-selective electrode was followed by addition of appropriate amounts of bromide stock solution, if necessary, to maintain bromide concentrations at the desired level. Muds attached to the split-spoon drilling device were collected as a means of directly measuring background concentrations of the tracer, as were borehole slurry samples (collected just prior to or just after sample collection). Preliminary results for a subset of pore-water samples indicate that there was some infiltration of bromide into samples, generally at a level that was less than 1 mg/L, negligible in

comparison to the borehole level of approximately 200 mg/L.

In the saturated zone, there was an additional sample contamination problem in the form of water added to the Lexan core barrel liner prior to sampling. This water was separated from the core sample by a core marker sealed against the liner; it was a necessary component of the sampling system because of the pressure differential inherent in sampling below the water table. To determine infiltration of this core-liner water into the sample, a separate tracer was required; $NaClO_4$ and microspheres were added for this purpose. The microspheres were counted by microbiologists participating in this project. Perchlorate concentrations were determined via ion chromatography of expressed pore waters. Preliminary results from a subset of samples indicated very little (or undetectable) concentrations of ClO_4 within pore waters.

Investigations of Geochemical Variation within the Yakima Barricade Borehole Steel Casing. The concentration of flammable gas within the steel casing used at the Yakima Barricade Borehole was observed to rise during drilling and resulted in a small explosion within the casing during welding operations. Therefore, drilling procedures were modified to prevent a recurrence of this event, and careful and frequent monitoring of the borehole gases' approach to a standard "lower explosive limit" were initiated. Identification of the gas involved was undertaken using gas sample tubes and eventually gas chromatograph-mass spectrometry determined that hydrogen gas (H_2) was present within the borehole casing. Field investigations to determine the source of this gas were initiated.

Two possibilities for the origin of H_2 in the Yakima Barricade Borehole were considered. The first was that hydrogen gas was being generated within the casing as a result of interaction between crushed rock fragments and groundwater, and the second was that groundwater welling into the casing contained dissolved hydrogen that was degassing as it entered the borehole, causing a concentration of hydrogen gas in the well's gaseous headspace. These possibilities were evaluated in part through downhole monitoring of aqueous composition.

To evaluate the reactivity and evolution of aqueous compositions within the casing, the sonde was lowered after the borehole had been bailed to remove stagnant water, and fresh formation water was equilibrated with the atmosphere by repeated downhole trips by the bailer. The sonde was allowed to stand within the well for 36 hours, during which time dissolved oxygen, temperature, pH, Eh, conductivity, and depth were monitored. The results of this monitoring for Eh are shown in Figure 3. Beginning at an Eh of +200 mV, the borehole redox state declined over a period of 13 hours to an Eh of -275, where it remained for the duration of the test. These results suggested that reactions within the casing were responsible for hydrogen gas generation, but did not rule out the possibility that hydrogen gas originated from within the formation and was concentrated in the well casing.

The composition of formation water, particularly its dissolved oxygen content and Eh, were determined by lowering the sonde to the bottom of the borehole, after which a submersible pump was lowered into the water column above it. By pumping water from the top of the water column within the casing while monitoring water composition at the bottom of the casing, the Eh and dissolved oxygen content of formation water could be measured directly, as it flowed into the borehole to replace water removed by pumping. This test was conducted after partial bailing of the borehole; water composition was monitored at 1-min intervals for a period of 1 hour. Results of pumping and monitoring are shown in Figure 4. Borehole conditions were at an Eh of approximately +90 mV and 0.15 mg/L dissolved oxygen at the beginning of pumping; as fresh water entered the casing, these values rapidly changed to formation conditions of +190 mV and 4.85 mg/L, respectively. An independent measure of dissolved hydrogen gas in formation water removed after pumping ceased did not detect hydrogen gas. Hydrogen gas therefore appears to have been generated within the well casing by reaction of rock fragments with water.

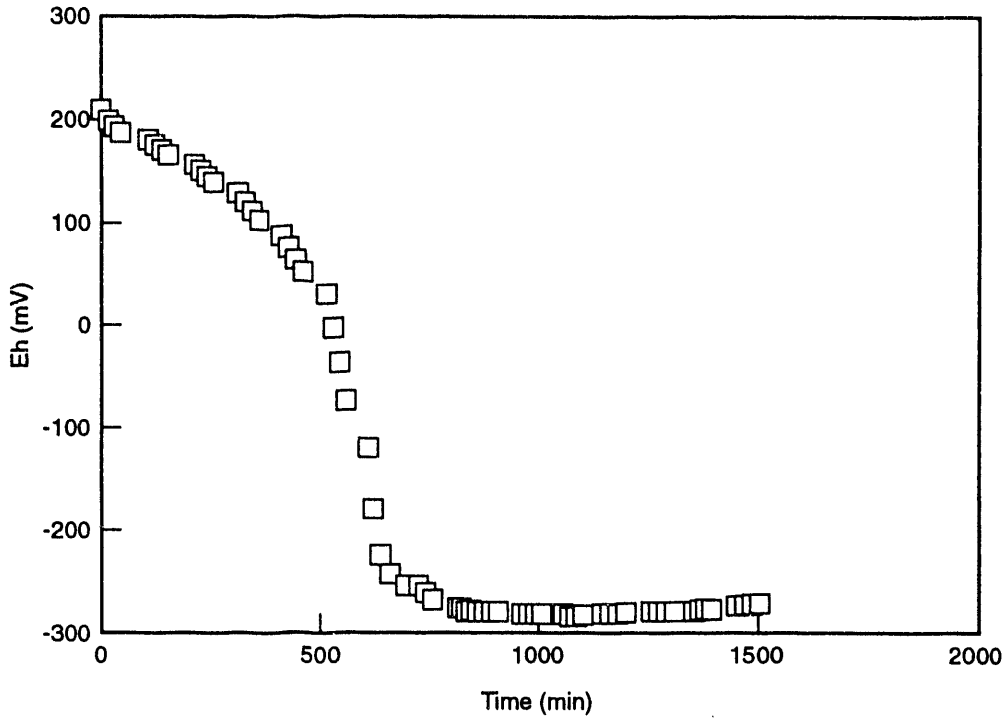

FIGURE 3. Eh versus Time in Casing, after Bailing

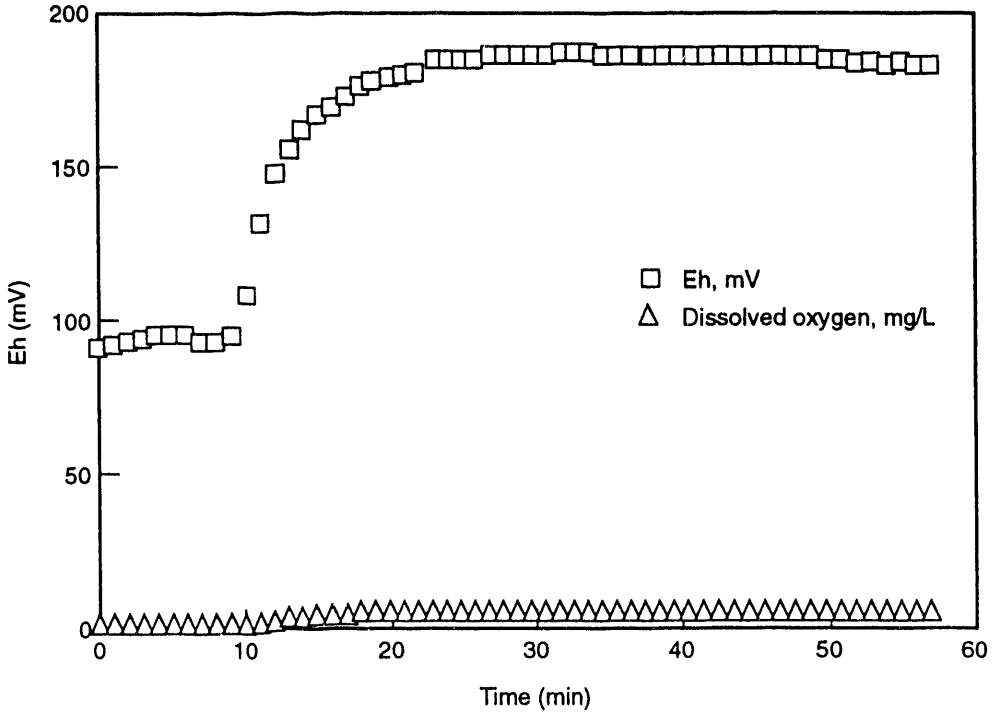

FIGURE 4. Eh and Dissolved Oxygen at Bottom of Yakima Barricade Borehole during Pumping

Microbial Transport/Origin in Subsurface Systems

E. M. Murphy, J. A. Schramke, B. D. Wood, and D. Janecky (Los Alamos National Laboratory)

The origin and transport of microorganisms in deep groundwater systems is poorly understood and as yet we lack the scientific approaches necessary to study microbial transport over regional time and distance scales (time scales ranging from hundreds to hundreds of thousands of years and distance scales ranging from tens to hundreds of kilometers). It is difficult to extrapolate from results of studies of microbial transport using traditional tracer techniques (which have been applied over distances generally <10 m and over times ranging from days to a few months) to regional groundwater flow paths, where the longer time scales may have a significant impact on transport. Microbial transport is affected by both physical and biological processes: advection, dispersion, filtration, exclusion, adsorption/adhesion, chemotaxis, growth/decay, and adaptation. The importance of these processes will vary along the time and distance scales. For example, at regional scales, biological processes (such as adhesion, growth/decay, chemotaxis, and adaptation) may play a more dominant role in microbial transport than physical processes (such as exclusion and filtration). The physical processes of advection and dispersion will likely be important regardless of the scale, but they are especially dominant where the groundwater has a high linear velocity.

In an aquifer, groundwater chemistry changes in a predictable manner as a result of mineral dissolution and precipitation. Along a regional groundwater flow path, oxygen decreases, pH and ionic strength increase, and temperature increases with the geothermal gradient. An increase in pH has been shown to increase microbial mobility, and increasing ionic strength retards movement of the microorganisms by decreasing the thickness of the double layer, thus promoting sorption. As oxygen decreases along a groundwater flow path, other electron acceptors become dominant, exerting selective pressure on the microbial community through growth/decay and adaptation. Thus changing geochemical properties alter microbial mobility and attest to the problem of extrapolating results on microbial transport from short-term tracer tests to regional groundwater flow paths.

Much of the existing information on microbial transport comes from laboratory column and field tracer experiments, but the study of microbial transport at regional scales requires non-traditional approaches. Understanding the processes that create and sustain a microbial community at any point along a groundwater flow path is critical to our understanding and prediction of microbial transport at the regional scale. Appropriate research approaches include determining the age of groundwater by radioactive isotopes, evaluating microbial respiration processes using stable isotopes, evaluating geochemical evolution along a groundwater flow path, and determining microbial phylogeny by techniques from molecular biology. Although no single approach will provide a definitive answer, in combination these approaches may produce compelling evidence of regional microbial transport.

FY 1992 Research Highlights

The focus of this exploratory research project is on geologic information that addresses regional microbial transport, such as groundwater dating, fractionation of stable isotopes by microbial respiration, and geochemical evolution of groundwater. The progress of this work is summarized in the following sections, which are not intended to be comprehensive.

Field Studies at the Savannah River Site. Microorganisms present in deep Atlantic Coastal Plain sediments affect the geochemical evolution of groundwater and its chemical and isotopic composition, yet the factors controlling their origin, distribution, and diversity are poorly understood. The evolution of the groundwater chemistry, the fractionation of stable carbon isotopes, and the groundwater age are all indicators of the inorganic and microbial reactions occurring along a given flow path from groundwater recharge to groundwater discharge. For the Savannah River Site (SRS), we analyzed tritium, ^{14}C, and groundwater chemistry along three flow paths of the Middendorf aquifer in South Carolina.

The ^{14}C ranged from 89 percent modern carbon (pmC) in the recharge zone to 9.9 pmC in the distal borehole; the $\delta^{13}C$ remained relatively constant at about -22‰, suggesting microbial oxidation of organic carbon. Carbon isotope analyses of particulate organic carbon from core sediments and groundwater chemistry were used to model the carbon chemistry using a geochemical reaction path model (PHREEQE, Parkhurst et al. 1980) with a subroutine to account for carbon isotopes (CSOTOP, Cheng and Long 1984). The primary reactions occurring along this groundwater flow path were silicate weathering and the oxidation of organic matter by iron reduction. Silicate weathering is responsible for increasing pH, calcium, and potassium. Because quartz, plagioclase, K-feldspar, kaolinite, illite, lignite inclusions with associated FeS(s) and organic sulfur, and smectite have been reported for the Middendorf Formation, the reactions that were modeled included oxidation of lignite; dissolution of gypsum, K-feldspar, and $Fe(OH)_3(a)$; precipitation of calcium-nontronite, gibbsite, and FeS(s); ion exchange; and dissolution or precipitation of chalcedony. The modelled reaction paths used only minerals that have been observed in the Middendorf Formation, with the addition of gypsum.

Although the Middendorf groundwater chemistry was modeled as a homogeneous system, the subsurface system is actually physically and chemically heterogeneous. Aerobic heterotrophs dominated the microbial community; however, the zones with the highest organic content (in the form of lignite inclusions) contained relatively low concentrations of aerobic heterotrophic microorganisms (Figure 1). When the lignite oxidized, pH fell and ferrous iron and sulfate rose. These observations suggest that complex organic matter is degraded by a microbial food chain, along which fermenting microorganisms produce simple organic acids that are in turn used in aerobic and anaerobic respiration (Figure 1). Indeed, in addition to aerobic heterotrophs, iron- and sulfate-reducing microorganisms, nitrifying microorganisms, and sulfur-oxidizing microorganisms were identified in the aquifer sediments. The presence of lignite inclusions and the diverse aerobic and anaerobic microorganisms suggested that sulfate may be produced by the oxidation of reduced sulfur, FeS(s), or organic sulfur (either abiotically or by sulfur-oxidizing bacteria) (Figure 1). Use of these phases as sulfur sources in the model resulted in good agreement between the modeled and observed pH and concentration of dissolved ions (Table 1; Murphy et al. 1992).

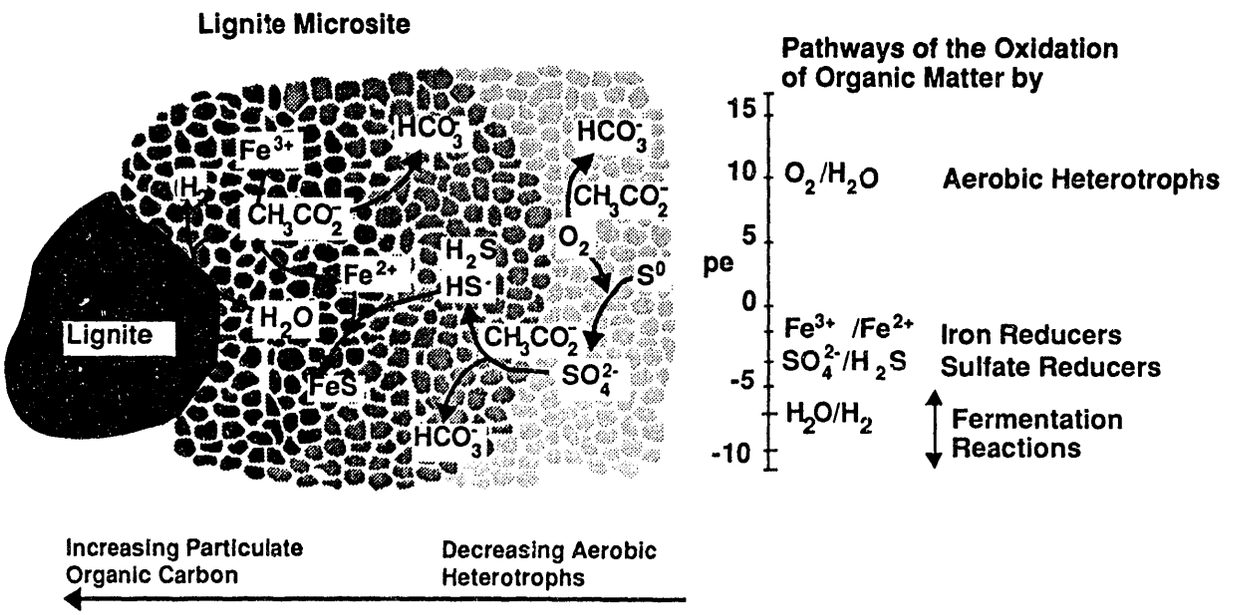

FIGURE 1. Microbially Mediated Reactions Occurring near Anaerobic Microsites

The groundwater ages obtained using ^{14}C ranged from modern to 11,500 years before present (yBP) (Table 1). The highest frequencies of occurrence, numbers, and diversity of aerobic and anaerobic bacteria were found in boreholes near the recharge zone, where the calculated ages were <1000 yBP. The transport of microorganisms from the recharge zone may be responsible for this distribution, as well as the distribution of electron acceptors necessary to support this diverse community of bacteria. The presence of both aerobic heterotrophs and anaerobic sulfate- and iron-reducing bacteria in the core sediments suggested that anaerobic microsites must exist throughout this otherwise relatively aerobic aquifer. Groundwaters in the recharge zone exhibited nearly saturated oxygen concentrations, but those decreased along the flow path, and anaerobic conditions were approached approximately 50 km from the recharge area (Figure 2).

Microbial respiration rates were calculated based on a model in which the increase in dissolved inorganic carbon is attributed to the respiration of organic carbon (Figure 2). Groundwater age was used to calculate the respiration rate, where $CO_2 = m_{CO2}(age^{-1})$. Based on the groundwater age, the respiration rates ranged from 4.3×10^{-4} to 3.5×10^{-6} mmol/L per year. The highest respiration rate was found in the flow path that had the youngest groundwater age (Figure 2). We speculate that a higher metabolic activity in younger groundwaters may relate directly to a predominantly surface origin for the microorganisms found in boreholes near a recharge area. A greater diversity of microorganisms could be maintained by the availability of a wide range of electron acceptors in those groundwaters close to the recharge zone. By the time that the groundwater residence time in the Middendorf aquifer exceeds several hundred years, it is likely that the electron acceptors necessary for supporting a diverse microbial community are depleted.

Iron Speciation and Fractionation in the Middendorf Aquifer. A zone of high dissolved iron (>1 mg/L) caused by the activity of iron-reducing bacteria was present in groundwaters from the Middendorf aquifer. However, there should be virtually no ferrous iron in these groundwaters because the dissolved oxygen concentrations were above 4 mg/L. If the iron in these samples was indeed ferrous, it would indicate that the well is drawing water both from aerobic and low-dissolved-iron horizons and from anaerobic high-dissolved-iron horizons. To resolve this issue, groundwater samples were collected from four boreholes along one groundwater flow path at the SRS (Table 2). Total iron, ferrous iron, and dissolved oxygen were measured immediately in the field using Hach AccuVac™ glass ampules. Field measurements confirmed that almost all of the dissolved iron was in the form of ferrous iron [iron(II)]. As predicted from the pH of the groundwater, the ferrous iron oxidized to ferric iron in the sealed containers within 8 to 12 hours after collection (Eary and Schramke 1990).

Iron-reducing bacteria play an important role in the biogeochemical carbon cycle and in the evolution of groundwater chemistry. Fractionation of stable iron isotopes will largely depend on the iron reactions taking place in the microbial cell and the forms of iron minerals in the environment before and after cell reaction. Ferric iron serves as a terminal electron acceptor and this reaction may be either enzymatic or nonenzymatic (i.e., reduction may be an indirect effect of microbial respiration). In nature, mos* nonenzymatic reduction processes are insignificant, with a few notable exceptions: 1) production of hydrogen sulfide by sulfate-reducing bacteria, which may reduce ferric to ferrous iron before precipitating ferrous sulfide, and 2) reduction of ferric iron by formate, a metabolic product of a number of bacteria. Nonenzymatic reduction of iron would not result in isotope fractionation. When ferric iron is reduced as a terminal electron acceptor in respiration, the process is called dissimilatory iron reduction. Relatively large quantities of iron are consumed in dissimilatory reduction, which is likely to be the cause of the high ferrous iron concentrations in the Middendorf aquifer. The reaction for the oxidation of organic matter by iron-reducing bacteria is written as

$$CH_2O + 4Fe(OH)_3 + 7H^+ \rightarrow$$

$$4Fe^{2+} + HCO_3^- + 10\ H_2O$$

TABLE 1. Summary of Measured and Modeled Results of Groundwater Geochemistry Using the PHREEQE/CSOTOP Model. Unless otherwise specified, gypsum was used as the sulfur source and concentrations are in mmol/kg.

	Rainwater to Aiken		Aiken to P-24		Rainwater to C-10	
	measured	modeled	measured	modeled	measured	modeled
Temperature	19.2	19.2	22.3	22.3	27.1	27.1
pH	5.00	5.00	5.96	5.96	6.9	6.9
pe	9.65	14.08	3.41	3.41	2.35	-3.18
$\delta^{13}C$ (‰)	-22.3	-22.4	-21.0	-21.0	-21.4	-21.4
^{14}C (pmC)[a]	88.6	87.9	36.5	36.5	9.9	39.6
age[b]	1,000	modern	8,330	8,330	19,100	11,500

	Aiken to P-28				Aiken to P-29			
		modeled				modeled		
	measured	FeS(s)	S(s)	Gypsum	measured	FeS(s)	S(s)	Gypsum
pH	5.49	5.49	5.48	5.49	5.53	5.54	5.53	5.53
pe	5.98	-2.18	-1.83	5.91	6.00	-2.29	-2.28	6.49
$\delta^{13}C$ (‰)	-21.3	-21.89	-21.75	-21.75	-21.3	-21.6	-21.56	-21.1
^{14}C (pmC)[a]	74.8	83.62	81.95	81.95	75.2	80.07	79.67	74.38
age[b]	2,400	920	750	750	2,360	520	480	modern
Ca-feldspar	--	0.00358	0.03540	--[b]	--	--	0.00197	--[b]
K-feldspar	--	0.00767	0.00767	0.00767	--	0.00197	0.00690	0.00690
Na-feldspar	--	0.02090	0.02090	--	--	0.00690	0.01620	--
Lignite	--	0.08580	0.08580	0.08580	--	0.00080	0.03670	0.03670
FeS(s)	--	0.01290	--	-0.03700	--	0.03670	--	0.00920
$Fe(OH)_3$(a)	--	0.03080	0.02390	0.51576	--	0.03710	0.07740	0.52533
Gypsum	--	--	--	0.04989	--	-0.04530	--	0.04625
Ca-nontronite	--	--	--	-0.21727	--	--	--	-0.21939
S(s)	--	--	0.01290	--	--	--	0.03710	--
Ion Ex. Na/Ca[c]	--	NC	NC	-3.572	--	NC	NC	-3.515
Ion Ex. Na/Mg	--	NC	NC	NC	--	-3.211	-3.211	-3.208
Fe (mg/L)	4.35	4.35	4.35	4.35	2.50	2.47	1.37	2.52

(a) The measured value of ^{14}C activity (AMS) of the final well in the reaction path. The modeled ^{14}C value, Qa_o, results from non-decay processes along the flow path.

(b) Under the measured values, the age is uncorrected for carbon reactions in the soil zone and aquifer (i.e., a_o is assumed to be 100 pmC); modeled groundwater age was calculated using Qa_o from PHREEQE/CSOTOP, corrected for carbon sources and sinks along the flow path.

(c) Calculated from observed Na and Ca concentrations $\left[\log\left(\alpha_{Na}^2/\alpha_{Ca}\right)\right]$.

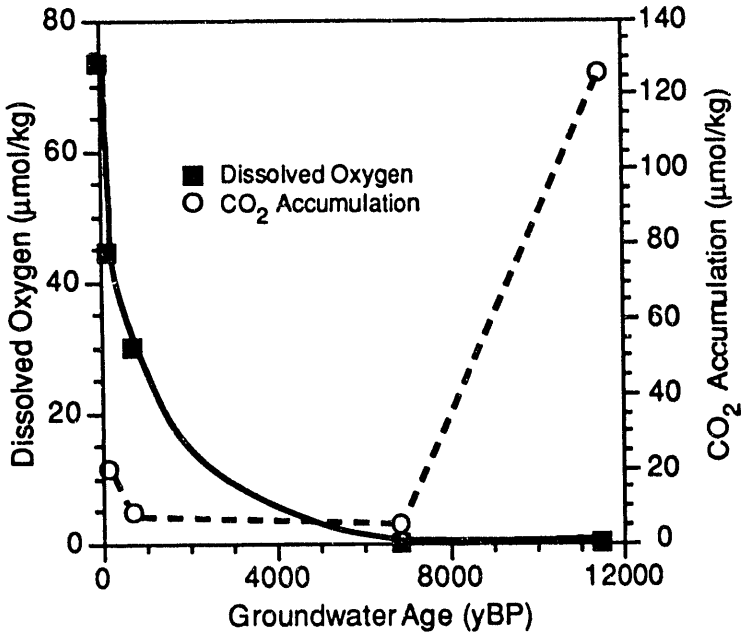

Flow Path	Groundwater Age, yBP	O_2 Consumption Rate, nmol/kg/y	CO_2 Accumulation[a] Rate, nmol/kg/y	CO_2 Respiration Rate, mmol/L/y
P-29	~200[b]	145	107	4.3×10^{-4}
P-28	750	57	12	4.9×10^{-5}
P-24	6,900	11	1	3.5×10^{-6}
C-10	11,500	6	11	4.5×10^{-5}

(a) Based on measured microbial biomass.
(b) 50 years < groundwater age < 500 years.

FIGURE 2. Decrease in Dissolved Oxygen and Accumulation of Carbon Dioxide along a Flow Path in the Middendorf Aquifer That Is Delineated by Groundwater Age. Microbial respiration rates calculated from these values are shown in the inset.

TABLE 2. Dissolved Iron Concentrations in Groundwaters from the Middendorf Aquifer

Sample Name	pH	Fe(II), mg/L	Fe_{Total}, mg/L	Dissolved Oxygen
P26-TA	6.41	4.35	4.41	300 µg/L
P29-TA	5.41	1.66	1.80	6.4 mg/L
P28-TA	5.40	3.07	3.08	3.8 mg/L
P24-TA	5.94	4.38	4.72	--

Although it is unknown whether stable iron isotopes are fractionated during dissimilatory microbial iron reduction, the relative abundances of stable iron isotopes in the environment are quite distinct: ^{54}Fe = 5.82% and ^{56}Fe = 91.66%. Several investigators have shown that the extent of microbial reduction of iron decreases with increasing crystallinity of the Fe (III) form; that is, amorphous iron hydroxides are reduced much more readily than crystalline iron oxides and are the preferred terminal electron acceptor. This behavior may result because 1) less crystalline forms of iron are more soluble, 2) less crystalline forms have greater surface area, or 3) in the absence of solubilizing ligands, direct contact between the bacteria and the ferric solid is necessary for iron reduction to proceed.

Information on the reaction pathway of dissimilatory iron reduction is incomplete, possibly

because specific reaction steps vary among different species of iron-reducing bacteria. Myers and Nealson (1990) showed that cellular energy can be generated from iron reduction. Arnold et al. (1986) postulated that dissimilatory iron reduction is coupled to bacterial electron transport and that the maximum iron reduction rates (in the presence of a solubilizing iron ligand) are determined by dehydrogenase activity or dissipation of proton motive force. These researchers also found that the rates of iron reduction were not limited by mass transport across the hydrodynamic boundary layer. Diffusion across that layer was rapid compared to the observed rate of reduction. Neither of these past studies addressed the rate-controlling step in the reduction sequence of amorphous ferric hydroxide that may lead to the fractionation of iron isotopes.

Although evidence of a specific reaction pathway that may lead to the fractionation of iron isotopes is lacking, if iron fractionation in environmental systems is demonstrated, then the actual mechanism may be similar to dissimilatory sulfate reduction. By analogy to microbial sulfate reduction, evidence suggests that there is an enzyme, referred to as iron reductase, that is responsible for iron reduction in the cell. Sulfur isotopes fractionate during sulfate reduction because of the kinetics of the rate-controlling step, which is the cleavage of the first sulfur-oxygen bond. Because a chemical bond involving a heavy isotope has lower vibrational frequency than the equivalent bond with the light isotope, the bond with the heavy isotope is stronger than that with the light isotope, resulting in a rate-dependent fractionation of sulfur isotopes. In a closed system, if the sulfate-reduction reaction goes to completion, no fractionation will be evident. However, in an open system, the kinetics of the rate-controlling step will lead to the fractionation of sulfur isotopes. As is the case for sulfate, the use of iron hydroxide or iron oxides in dissimilatory iron reduction may require the cleavage of an iron-oxygen bond, leading to the fractionation of iron isotopes. In sulfur, the lighter isotope, ^{32}S, is the more abundant; in iron the heavier isotope is more abundant. If the rate-controlling step in iron reduction is cleavage of the iron-oxygen bond, then microbial fractionation would result in increased abundance of $^{54}Fe(II)$, the lighter and less abundant isotope of iron, in the aqueous phase. Solid iron compounds would become enriched in the heavy isotope as a result of this process.

The complex environmental chemistry of iron in subsurface systems and the role of microorganisms in the iron cycle led researchers at Los Alamos National Laboratory (LANL) to develop a mass spectrometric technique to measure iron isotopes. The fractionation of iron isotopes has broad applicability to isotope hydrology studies, especially at sites where the influence of iron-reducing bacteria on the biogeochemical cycle in groundwater is significant. The fractionation of iron isotopes may eventually be used to determine the presence and *in situ* respiratory activity of iron-reducing bacteria and define the complex interaction of these bacteria with the subsurface microbial community.

Filtered groundwater samples were collected from the Middendorf aquifer in South Carolina and sealed immediately in 1-L glass bottles for stable iron isotope measurements. Groundwater samples were shipped to LANL for iron isotope analyses. Sediment samples were collected from cores from the same Middendorf boreholes. The cores were sampled selectively for high-iron zones near the level of the well screens. Crystalline and amorphous iron were extracted from the sediments using dithionite-citrate and hydroxylamine, respectively. The concentrations of crystalline and amorphous iron in the sediments are shown in Table 3. With the exception of sample P28-765-A, the amorphous iron was usually only a small percentage of the total extractable iron in the sample. The total extracted iron varies directly with total iron as determined by proton-induced X-ray emission (PIXE) analysis. Because microbial activity results in the high ferrous iron concentrations in the Middendorf aquifer, iron isotopes will be determined in both the dissolved and solid forms to determine whether isotope fractionation has occurred. These iron isotope analyses have not yet been completed.

INEL Modeling Results. The chemistry of water samples collected from wells along flow paths at the Idaho National Engineering Laboratory (INEL) are being modeled using the geochemical

TABLE 3. Extracted Crystalline and Amorphous Iron from Middendorf Sediments and Total Iron Determined by Proton-Induced X-ray Emission (PIXE) Analysis

Sample Number	Crystalline Fe, μmol/g	Amorphous Fe, μmol/g	Total Iron Extracted, μmol/g	Total Iron (PIXE), μmol/g
P24-982-A	6.75	1.86	8.61	96.5
P24-998-A	826.82	2.05	828.87	1290.3
P26-972-A	14.32	4.82	19.14	61.3
P28-765-A	218.80	162.11	380.91	480.5
P28-775-A	44.92	1.34	46.26	81.3
P29-664-A	391.06	0.41	391.47	484.5
P29-676-A	93.16	0.43	93.59	177.2
Blank	0.01	0.0		

reaction path codes NETPATH (Plummer et al. 1991) and PHREEQE/CSOTOP, in an effort to 1) examine changes in the groundwater chemistry along flow paths on and near INEL that may have influenced the composition of the microbial community, 2) determine the sources of the groundwater at the different well sites and, hence, potential sources of microorganisms, and 3) use ^{14}C to determine the age of the groundwater at INEL, with specific emphasis on the age of the groundwater at the borehole drilled by the Deep Microbiology Subprogram of DOE's Subsurface Science Program.

The Snake River Plain aquifer underlying INEL is an unconfined aquifer in basalt flows and interbedded sedimentary formations. The general direction of groundwater flow in the eastern Snake River Plain aquifer is from the northeast to the southwest (Figure 3). At INEL, a certain amount of groundwater flow also comes from the northwest and north because of the Little Lost River and Birch Creek drainage basins. Flow velocities in the aquifer average approximately 3 m/d (Robertson et al. 1974), resulting in an estimated hydrodynamic residence time on the order of 250 years (Wood and Low 1986). Groundwater recharge in the vicinity of INEL can occur as a result of 1) groundwater flow from the northeast and the tributary basins to the north and northwest; 2) infiltration from the Big Lost River, which flows onto INEL from the southwest; and 3) infiltration of precipitation (Robertson et al. 1974). It is also possible that geothermal water from formations below the Snake River Plain aquifer may enter the aquifer, although, based on a water-budget analysis for the eastern Snake River Plain aquifer, Wood and Low (1988) believed the contribution from geothermal water was negligible. Wood and Low (1988) calculated the contribution of infiltrating precipitation to the groundwater in the eastern Snake River Plain aquifer to be approximately 10%.

In late 1990, PNL sampled groundwater in the Snake River Plain aquifer from wells located at INEL and from wells north of the site (Figure 3). The wells were selected to avoid any possible influence of INEL operations on the water composition. Measurements of pH, dissolved oxygen concentrations, specific conductivity, and water temperature were carried out in the field. Laboratory analyses on the water samples included major and minor cations by inductively coupled argon plasma atomic emission spectroscopy (ICAP-AES); anions by ion chromatography; dissolved organic carbon and dissolved inorganic carbon; alkalinity; ^{14}C; tritium; $\delta^{13}C$; δD; $\delta^{18}O$; and $\delta^{34}S$.

The wells were classified as belonging to flow paths based on the available information about groundwater flow at INEL and general trends in groundwater composition (Table 4). Changes in groundwater chemistry along the flow paths are likely to be caused by reaction of the groundwater with the basalt and sedimentary interbeds: dissolution of olivine, labradorite, pyroxene, halite, and anhydrite; oxidation of pyrite; and precipitation of smectite, calcite, and silica. In addition to changes in groundwater chemistry caused by reaction with the aquifer solids,

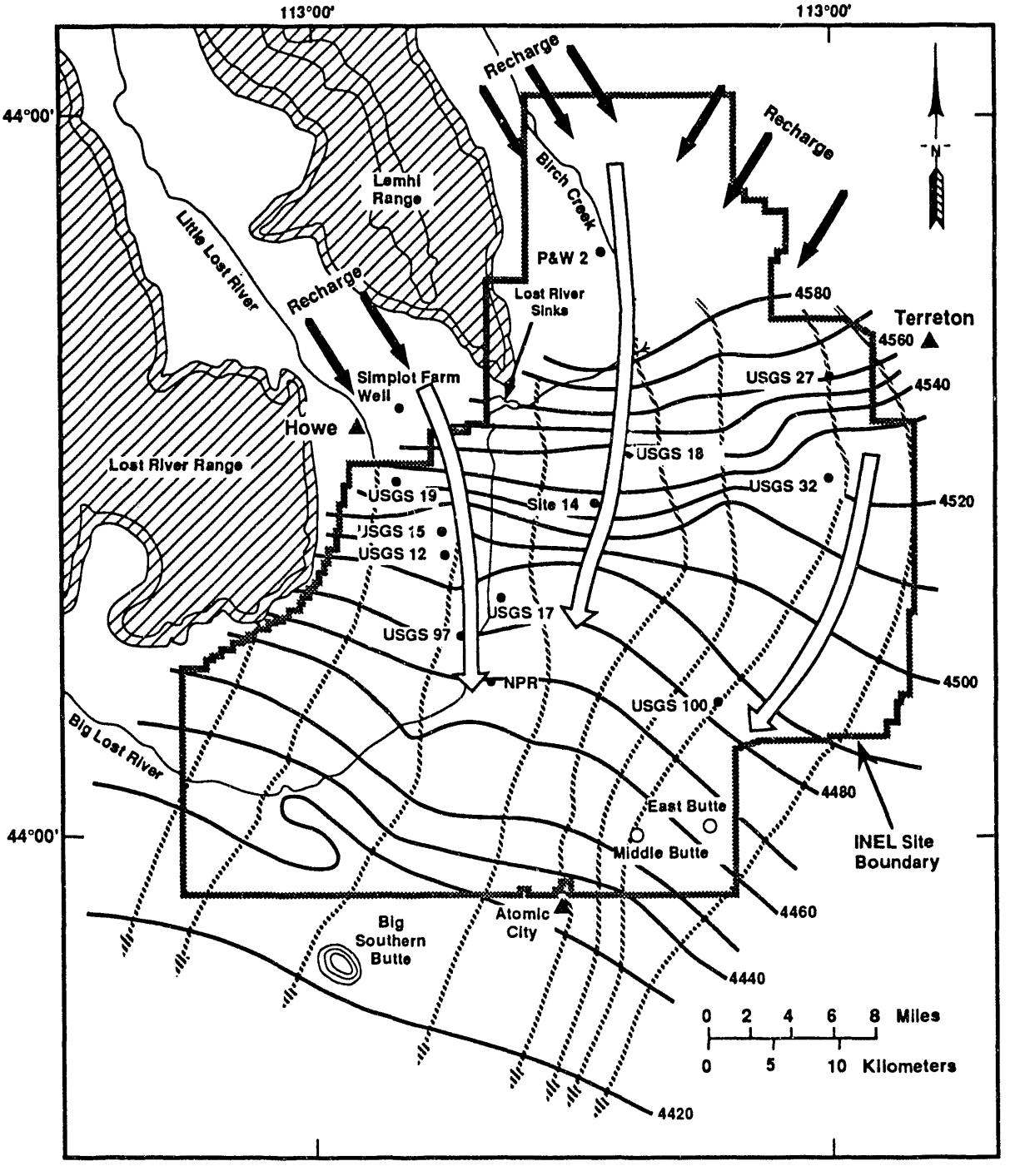

FIGURE 3. Potentiometric Map of the Snake River Plain Aquifer. Arrows represent groundwater flow paths.

TABLE 4. Organization into Flow Paths of Wells Sampled at INEL

Flow Path 1	Flow Path 2	Flow Path 3
Simplot Farm	P&W 2	USGS 27
USGS 19	USGS 18	USGS 32
USGS 15	Site 14	USGS 100
USGS 12		
USGS 97		
USGS 17		
NPR		

chemical changes may also be caused by mixing between groundwaters from various sources.

Along flow path 1, groundwater samples obtained from wells USGS 19, USGS 15, and USGS 12 are most likely derived from groundwater flow that originated in the Little Lost River drainage and, possibly, from infiltrating precipitation. Well USGS 15 was much deeper than the other wells in flow path 1, so differences in water chemistry between USGS 15 and other wells may be the result of changes in water chemistry with depth rather than the changes in water chemistry along the flow path. The water from the Simplot Farm well showed relatively high SO_4^{2-}, Cl^-, and NO_3^- concentrations. These elevated concentrations may be attributed to irrigation recharge, because of the well's location on the Simplot Farm. Based on well locations, groundwater from wells USGS 97, USGS 17, and NPR could be influenced by 1) infiltration from the Big Lost River, 2) underflow from the Birch Creek drainage, 3) underflow from the Little Lost River drainage, 4) underflow from the northeast, and 5) infiltrating precipitation.

Of the wells in flow path 2, water obtained from all three wells could be influenced by underflow from the Birch Creek drainage, by groundwater from the northeast, and by infiltrating precipitation. Along flow path 3, groundwater from wells USGS 27 and USGS 32 is likely to be influenced by groundwater flow from the northeast and by infiltrating precipitation. In addition to these sources of groundwater, samples from well USGS 100 may be influenced by underflow from the Birch Creek drainage. Water samples from well USGS 32 were quite cloudy, which may indicate problems with the well.

Based on the information about potential reactions and groundwater sources, reaction-path and mixing calculations for some of the flow path segments were carried out at PNL in FY 1992. Because for most flow path segments there are a number of potential groundwater sources, reaction-path and mixing models were developed for each possible set of groundwater sources.

The approach taken to modeling the geochemistry along the flow paths can be illustrated by the calculations carried out for the flow path from the Simplot Farm well to NPR. In this calculation, the sources of the groundwater at NPR were assumed to be flow from Simplot Farm and infiltrating precipitation. The infiltrating precipitation was equilibrated with calcite and chalcedony in an open system under the conditions listed in Table 5 using the geochemical code PHREEQE/ CSOTOP. The resultant solution was then mixed in a closed system with groundwater from the Simplot Farm well. The model values that were obtained with NETPATH using these assumptions are listed in Table 5. The model provides an excellent match to the observed changes in major element chemistry, $\delta^{13}C$, $\delta^{18}O$, and $\delta^{34}S$. The minerals included in the model have all been observed in the aquifer. Other possible sources for groundwater at NPR are being investigated, including well P&W 2 (which may be representative of the Birch Creek drainage), the Little Lost River (rather than the Simplot Farm well, for the reasons cited above), and the Big Lost River, which in the past flowed onto INEL.

The approach outlined above is being carried out for the flow path segments represented by the wells in Table 1. At present, about one quarter of the potential flow path segments have been modeled. It is anticipated that the modeling work will be completed in FY 1993.

Future Research

In FY 1993, research will focus on the study of microbial transport and origin in the Cold Creek recharge area at the Hanford Site upgradient from the Yakima Barricade Borehole. The purpose of the Cold Creek study is to test molecular techniques that will be used to determine

TABLE 5. Reaction-Path and Mixing Model for the Flow Path Segment from Simplot 1 Farm Well to NPR

Constraints: Aluminum, Calcium, Carbon, Chloride, Magnesium, Potassium, Silica, Sodium, Sulfur, $\delta^{18}O$

Isotopic Data: pyrite $\delta^{34}S$ = -8 (Wood and Low 1988)
anhydride $\delta^{34}S$ = 15 (Wood and Low 1988)
infiltrating snowmelt $\delta^{18}O$ = -16.56[a]

Data for soil gas in equilibrium with infiltrating precipitation.

Value	Source
log P_{CO2} = -3.00	Rightmire and Lewis 1987
$\delta^{13}C$ = -15	Rightmire and Lewis 1987
^{14}C = 100 pmc	pre-bomb

Phases	Amount Reacted, mmoles/L[b]
Albite (dissolve only)	0.0
Anorthite (dissolve only)	0.88794
Calcite	-1.37297
Forsterite (dissolve only)	0.0
Gibbsite	1.29453
Gypsum/anhydrite (dissolve only)	0.13593
SiO_2	3.14877
K-feldspar (dissolve only)	0.05383
Pyrite (dissolve only)	0.0
Ca-montmorillonite	0.0
Mg-montmorillonite	-0.94707
Na-montmorillonite	-0.39117
NaCl(s)	0.21836
% Simplot Farm	37.5
% infiltrating precipitation	62.5

Parameter	Computed	Measured
$\delta^{13}C$	-8.53	-8.67
^{14}C	86.68	61.74
$\delta^{34}S$	9.29	9.59
$\delta^{18}O$	-17.7	-17.7
age (years)	2805	--

(a) From weighted average of values of $\delta^{18}O$ for snow, measured by Rightmire and Lewis (1987). The weighted mean $\delta^{18}O$ value obtained was -20.2. The snowmelt was evaporated to 78.5% of the original amount, and Rayleigh fractionation calculations resulted in a value of -17.82 for the remaining snowmelt.

(b) Positive value indicates dissolution, negative value indicates precipitation.

microbial origins in a well-controlled field site. Vadose zone recharge rates in semiarid zones like the Hanford Site may range from 0.01 mm per year (at the Yakima Barricade Borehole) to 7.4 cm per year at unvegetated, sandy sites near the Columbia River. Vertical recharge from precipitation at the Yakima Barricade Borehole is negligible; therefore microorganisms in the saturated sediments must have originated from 1) deposition of the original sediments, 2) vertical transport after the last catastrophic flood (~13,000 years ago), or 3) transport from the recharge zone. The rate of microbial transport in the recharge zone of the unconfined aquifer is unknown but expected to be slow. Therefore, the basis of this study is comparative, and evidence of microbial transport will depend largely on molecular techniques to determine the relatedness of microbial species along unsaturated flow paths. The effect of the changing chemical environment on the selection of microbial species within the microbial community will also be determined.

References

Arnold, R. G., T. M. Olson, and M. R. Hoffmann. 1986. "Kinetics and Mechanism of Dissimilative Fe(III) Reduction by *Pseudomonas*-sp-200." *Biotechnology and Bioengineering* 28:1657-1671.

Cheng, S.-L., and A. Long. 1984. "Implementation of Carbon Isotope Subroutine to Computer Program PHREEQE and Their Application to C-14 Ground-Water Dating." In *Hydrology and Water Resources in Arizona and the Southwest, Proceedings of the 1984 Meetings of the Arizona Section, American Water Resources Association and the Hydrology Section, Arizona-Nevada Academy of Science* 14:121-135. Arizona-Nevada Academy of Science, Tucson, Arizona.

Eary, L. E., and J. A. Schramke. 1990. "Rates of Inorganic Oxidation Reactions Involving Dissolved Oxygen." In *Chemical Modeling in Aqueous Systems II*, eds. D. C. Melchior and R. L. Bassett, pp. 379-396. ACS Symposium Series 416, American Chemical Society, Washington, D.C.

Murphy, E. M., J. A. Schramke, J. K. Fredrickson, H. W. Bledsoe, A. J. Francis, D. S. Sklarew, and J. C. Linehan. 1992. "The Influence of Microbial Activity and Sedimentary Organic Carbon on the Isotope Geochemistry of the Middendorf Aquifer." *Water Resources Research* 28(3):723-740.

Myers, C. R., and K. H. Nealson. 1990. "Iron Mineralization by Bacteria: Metabolic Coupling of Iron Reduction to Cell Metabolism in *Alteromonas putrefaciens* Strain MR-1." In *Iron Biominerals*, eds. R. B. Frankel and R. P. Blakemore, pp. 131-149. Plenum Press, New York.

Parkhurst, D. L., D. C. Thorstenson, and L. N. Plummer. 1980. *PHREEQE: A Computer Program for Geochemical Calculations*. USGS Water-Resources Investigations Report 80-96, U.S. Geological Survey, Reston, Virginia.

Plummer, L. N., E. C. Prestemon, and D. L. Parkhurst. 1991. *An Interactive Code (NETPATH) for Modeling Net Geochemical Reactions along a Flow Path*. USGS Water-Resources Investigations Report 91-4078, U.S. Geological Survey, Reston, Virginia.

Rightmire, C. T., and B. D. Lewis. 1987. *Hydrogeology and Geochemistry of the Unsaturated Zone, Radioactive Waste Management Complex, Idaho National Engineering Laboratory, Idaho*. USGS Water Resources Investigations Report 87-4198, U.S. Geological Survey, Idaho Falls, Idaho.

Robertson, J. B., R. Schoen, and J. T. Barraclough. 1974. *The Influence of Liquid Waste Disposal on the Geochemistry of Water at the National Reactor Testing Station, Idaho: 1952-1970*. USGS Open-File Report OF 73-0238, U.S. Geological Survey, Idaho Falls, Idaho.

Wood, W. W., and W. H. Low. 1986. "Aqueous Geochemistry and Diagenesis in the Eastern Snake River Plain Aquifer System, Idaho." *Geological Society of America Bulletin* 97:1456-1466.

Wood, W. W., and W. H. Low. 1988. *Solute Geochemistry of the Snake River Plain Regional Aquifer System, Idaho and Eastern Oregon*. USGS Professional Paper 1408-D, U.S. Geological Survey, Washington, D.C.

Subsurface Organic Fluid Flow

C. S. Simmons, R. J. Lenhard, T. R. Ginn, and J. W. Cary

The research in this project concerns the movement of organic liquid contaminants and their volatile vapors in the subsurface environment. The knowledge gained from this basic research into physical mechanisms is intended to assist DOE in remediating sites contaminated with organic fluid contaminants. Such organic fluids are known to migrate either as liquids that are immiscible with water or as a gas phase. These liquid and gas phases eventually dissolve into the groundwater as a result of interphase mass-transfer processes and thus contaminate the underground water resources.

The research in FY 1992 focused on 1) the capillary retention of organic liquids in sandy porous media, 2) the movement of trichloroethylene (TCE) vapors in a large laboratory flow cell, and 3) the fingering intrusion behavior of a non-spreading organic liquid, as represented by a model mineral oil. We are obtaining answers to scientific questions that are important to predicting the migration of organic fluids (liquid and gas) in the subsurface. In particular, we are determining the extent to which hysteresis behavior in three-phase flow (flow of immiscible water, organic liquid, and air) influences movement. We are also testing the hypothesis that density-driven advective flow of vapor contributes to the dispersal of volatile organic liquids. Like TCE, carbon tetrachloride, which has been found beneath the Hanford Site, is such a mobile vapor. As we began in our experiments in FY 1991, we are attempting to better understand and quantify unstable infiltration behavior of a certain class of organic liquids that were sometimes used in the processing of nuclear materials.

Organic Liquid Retention Behavior and Hysteresis

In FY 1992, investigations continued measuring and predicting the retention of liquids in porous media as a function of fluid pressures and prior hydrologic conditions. Emphasis was placed on measuring the retention of fluids in three-phase, air-nonaqueous phase liquid (NAPL)-water fluid systems. Fluid retention by capillary forces has long been known to be a nonunique function of fluid pressures (i.e., fluid content-pressure relations are hysteretic). The volumetric retention of fluids in the pore spaces will differ depending on whether fluids are draining or imbibing, and this difference could have important implications for predicting the subsurface distribution of NAPLs.

To investigate fluid retention properties, water content in two-phase (air-water) and three-phase (air-NAPL-water) fluid systems was measured as a function of fluid pressures for water draining and imbibing paths. The total liquid content in a three-phase (air-NAPL-water) system was also measured as a function of fluid pressures for total liquid draining and imbibing paths. Measurements were conducted in a specially designed experimental cell capable of measuring fluid retention in three-phase fluid systems. The experimental apparatus, which is shown in Figure 1, consists of sleeves with alternating treated and untreated porous ceramic rings on their inner surfaces. Two rings were chemically treated to render them hydrophobic so that the NAPL could extend continuously from NAPL-filled pores within the porous medium packed in the cell to a NAPL pressure-measuring device located outside the retention cell. The untreated ceramic rings maintained a continuous aqueous phase from water-filled pores within the porous medium to an aqueous-phase pressure-measuring device located outside the cell. The gaseous phase within the porous medium was always in contact with the atmosphere and, hence, its pressure was assumed to be atmospheric (i.e., zero gage pressure).

The measurements involved draining water from an initially water-saturated porous medium, thus creating a two-phase (air-water) system, and then later adding NAPL to create a three-phase (air-NAPL-water) fluid system. The results from the water measurements are shown in Figure 2, and the results from the total liquid measurements are shown in Figure 3, where two-phase (air-water) measurements are shown as open squares and three-phase measurements are shown as closed diamonds. Successive measurements are connected via broken lines in both figures.

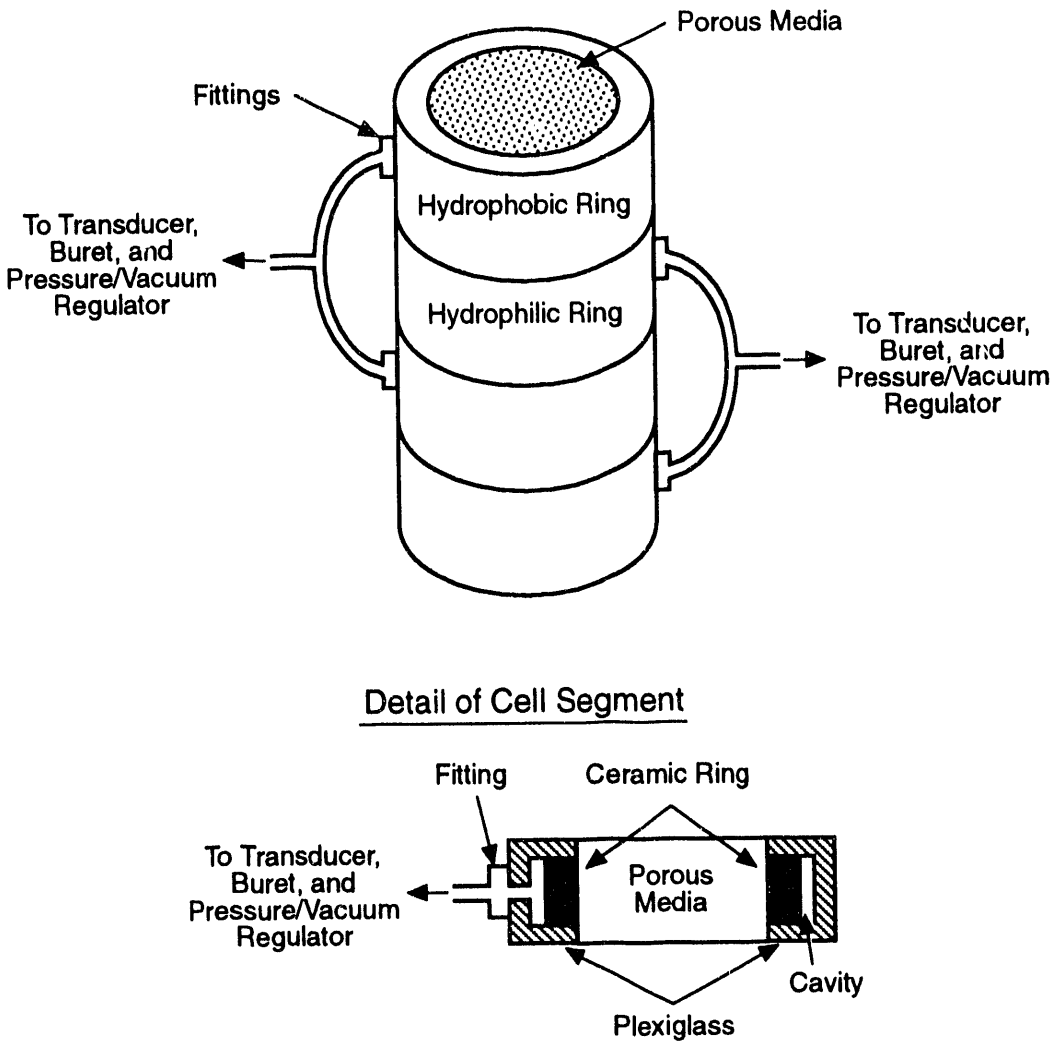

FIGURE 1. Experimental Apparatus to Measure Multiphase Saturation-Pressure

The fluid retention measurements were conducted not only to characterize hysteretic retention behavior, but also to 1) investigate how to scale fluid content-pressure relations among different fluid systems and 2) evaluate a predictive fluid content-pressure model that accounts for hysteretic effects. Thus the vertical axes in Figures 2 and 3 are scaled capillary pressure heads, where the scaled capillary head is the product of a scaling factor and the appropriate capillary head. The fluid-system scaling procedure and theory have been discussed by Lenhard and Parker (1987); we will not discuss fluid scaling theory in detail here. However, the scaling procedure used for Figures 2 and 3 yielded a smooth transition as the fluid system went from a two-phase (air-water) to a three-phase system. In particular, note the smooth continuation of the wetting scanning path in Figure 3 as the fluid system changed from a two- to a three-phase system.

The data shown in Figures 2 and 3 were used to test the ability of a published hysteretic fluid retention model to simulate multiphase fluid retention behavior. This retention model was first published in 1987 (Parker and Lenhard 1987) and later refined (Lenhard et al. 1989).

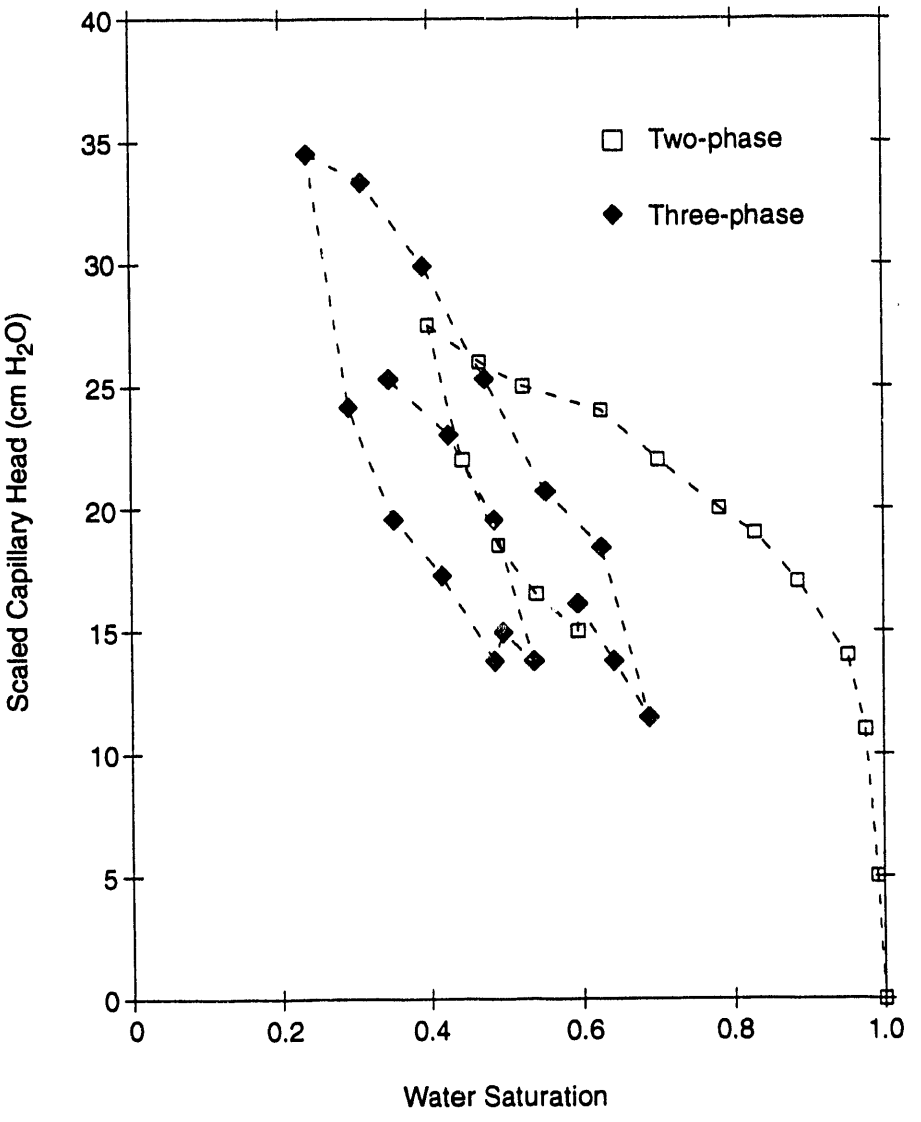

FIGURE 2. Experimental Two- (Open Squares) and Three-Phase (Closed Diamonds) Water Saturations Measured for the Water Saturation Path History (Lenhard 1992).

The effects of both contact angle hysteresis and fluid entrapment are considered in the model. In the model, parameters that are required to predict fluid-retention behavior include 1) parameters that describe the porous medium pore-size distribution (i.e., retention parameters), 2) fluid-system scaling factors, and 3) parameters that reflect the maximum amount of air that can be entrapped by air-water and air-NAPL interfaces and the maximum amount of NAPL that can be entrapped by NAPL-water interfaces in the porous medium. To obtain these values, retention parameters were best-fit to the air-water data only, scaling factors were best-fit to the three-phase data, and fluid entrapment parameters were measured in similar porous media using only two-phase fluid systems.

Figures 4 and 5 show how well the model was able to capture the experimental data shown in Figures 2 and 3, respectively, with the modeling results shown as solid lines. Note the close agreement between the experimental fluid-retention data and the modeling results. In Figure 4, very good agreement was obtained for the water-saturation path history, and in

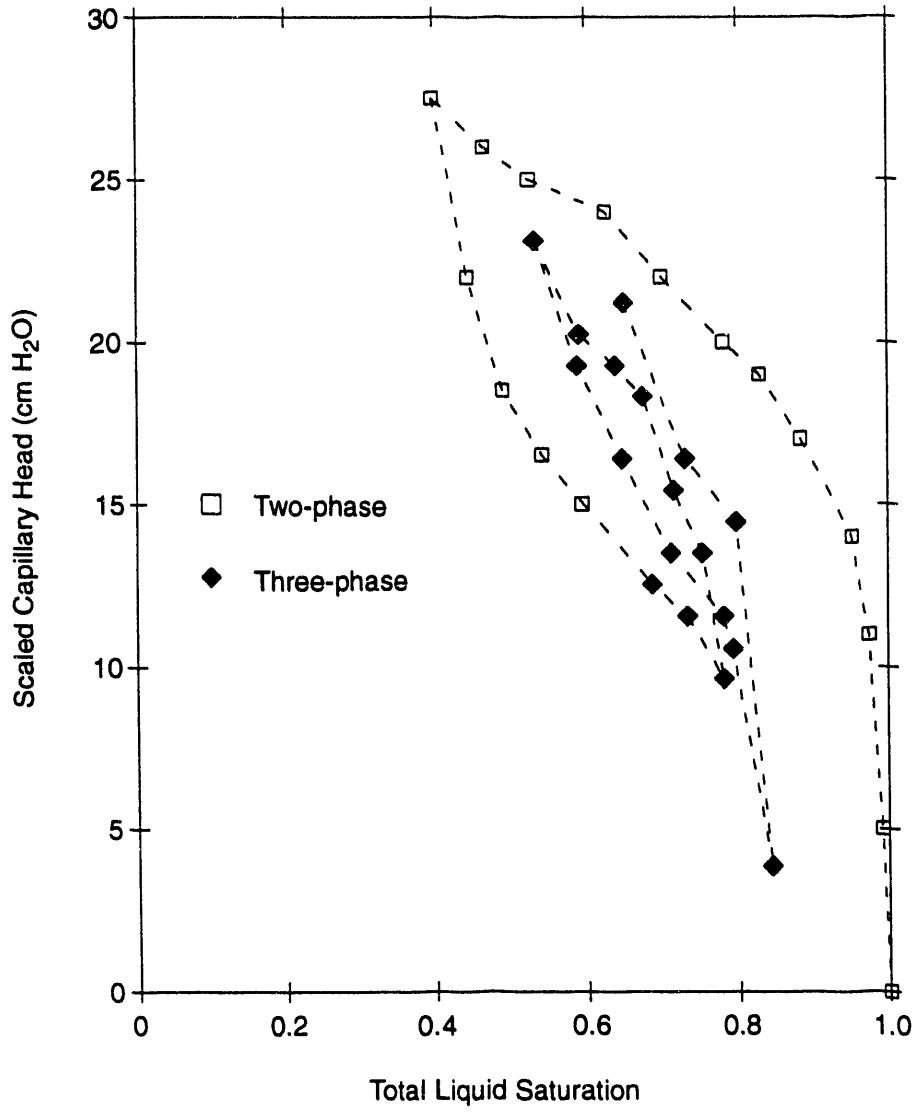

FIGURE 3. Experimental Two-Phase Water (Open Squares) and Three-Phase (Closed Diamonds) Total Liquid Saturations Measured for the Total Liquid Saturation Path History (Lenhard 1992)

Figure 5, very good agreement was obtained for the total-liquid-saturation path history.

Our investigations show the importance of considering hysteretic effects when attempting to predict the distribution of NAPLs in contaminated porous media. The ability to accurately model multiphase fluid-retention behavior can greatly improve predictions of the fate of NAPLs in the subsurface environment. For example, the volume of NAPL that may become trapped below the water table can be accurately predicted, which is very important for assessing the potential for contaminants to move with flowing groundwater.

The investigation is primarily examining the retention of fluids in porous media when fluid movement has ceased. However, to accurately forecast the fate of subsurface contaminants, the transient behavior of fluids in porous media must also be understood. To predict transient fluid flow in porous media, relations between fluid contents and pressures must be known, as

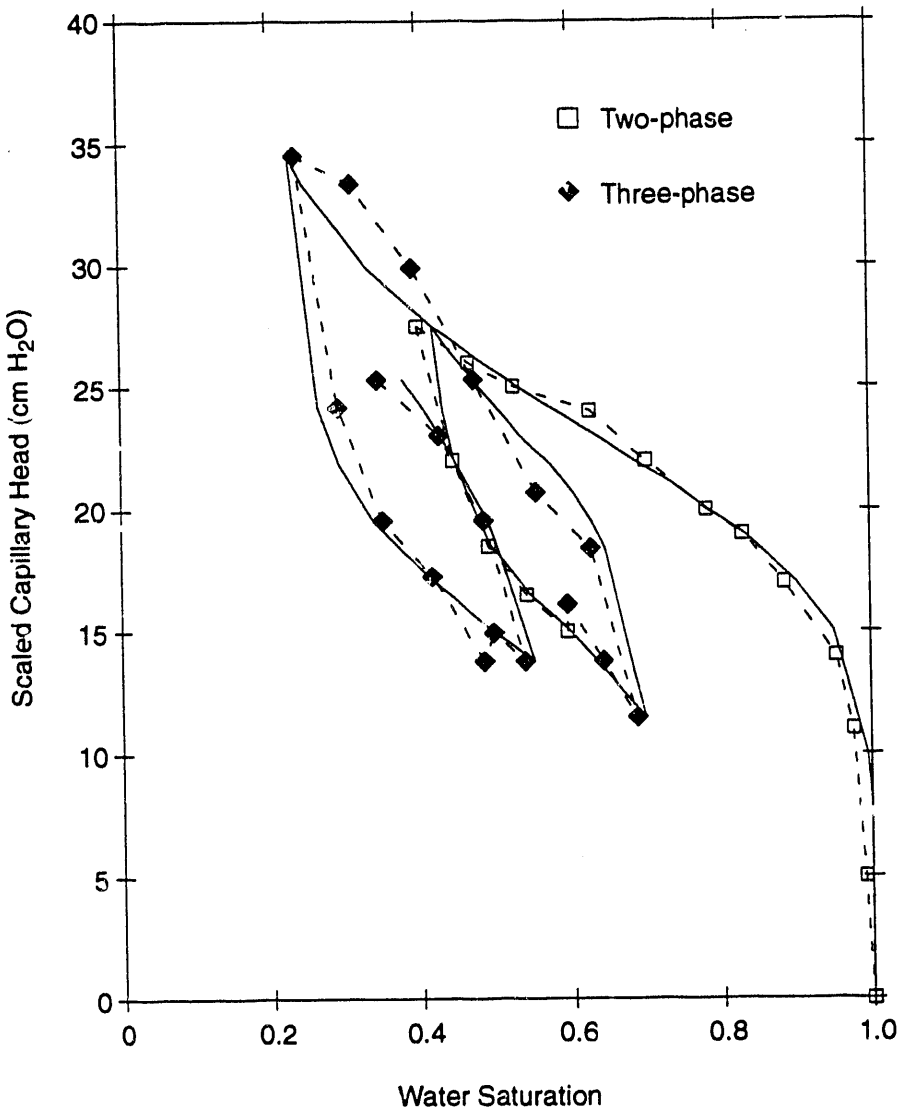

FIGURE 4. Comparison of Experimental (Broken Lines) Water Saturation Path Histories to Modeling Results (Solid Line)

must relations between fluid contents and relative permeabilities. Therefore, a study was initiated to evaluate whether hysteretic relations among fluid contents, pressures, and relative permeabilities are necessary for forecasting transient fluid flow when wetting and drying saturation paths are likely to occur. This initial study focused on a two-phase (air-water) fluid system because it is more difficult to conduct transient measurements in a three-phase (air-NAPL-water) system.

The approach was to compare nonhysteretic and hysteretic modeling results to a transient air-water experiment, where the water-table elevation was made to fluctuate in a one-dimensional flow cell, to produce wetting and drying saturation paths. In the experiment, water contents were measured temporally and nondestructively with a radiation attenuation apparatus at seven locations. The experiment was initiated by lowering the water table in a water-saturated porous medium; this was followed by raising,

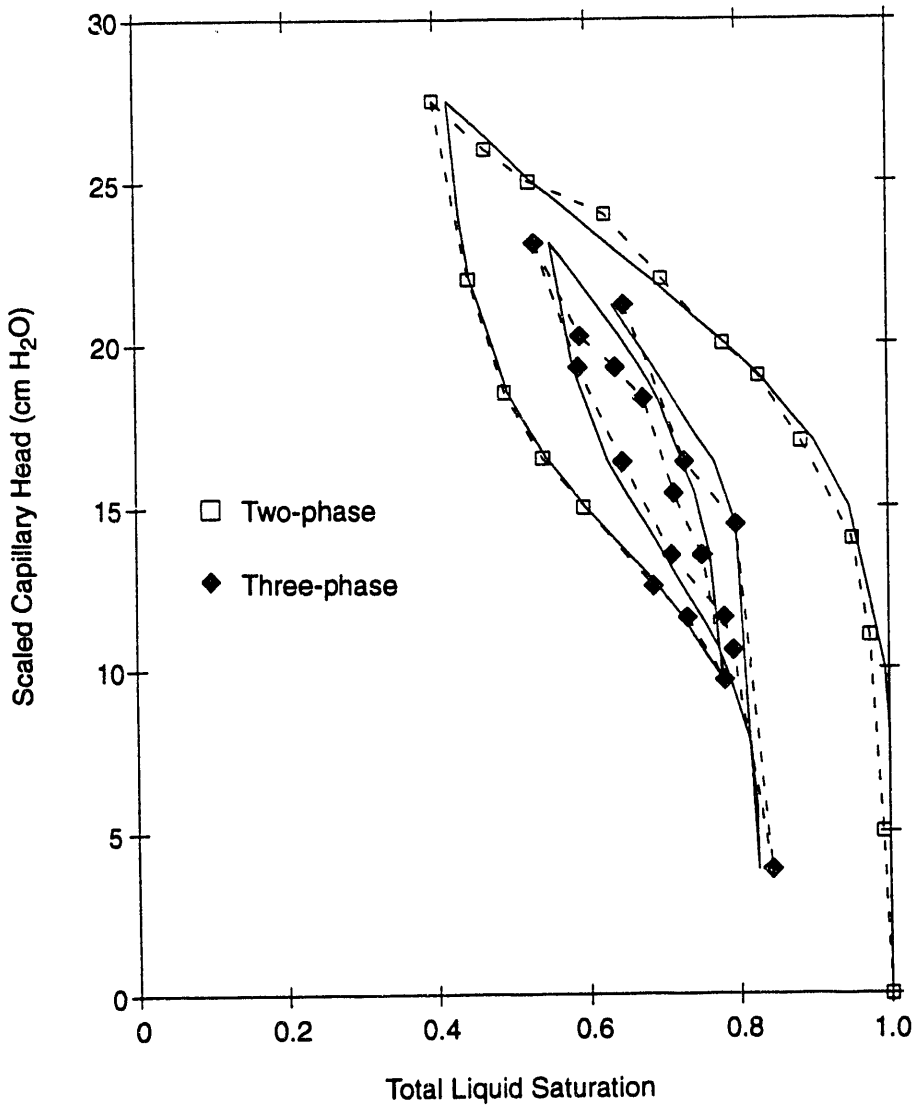

FIGURE 5. Comparison of Experimental (Broken Lines) Total Liquid Saturation Path Histories to Modeling Results (Solid Line)

lowering, and again raising the water table to prescribed elevations. This sequence of water-table adjustments was intended to produce two wetting and two drying saturation paths. To predict these paths, we used retention parameters that reflected the first lowering of the water table. For hysteretic fluid flow simulations, the only other parameter that was needed was the maximum amount of air entrapped by air-water interfaces. This parameter was estimated from fluid content-pressure measurements that had been obtained in similar porous media.

Figure 6 shows the experimental data and modeling results for one of the seven measurement elevations. The experimental data are shown as closed diamonds, the hysteretic modeling results are shown as a solid line, and the nonhysteretic modeling results are shown as a broken line. The hysteretic simulation closely matched the measured water contents, whereas the nonhysteretic simulation deviated markedly from the observed data. From this study, it appears that when predicting transient fluid flow, hysteresis in relations among fluid contents, pressures, and

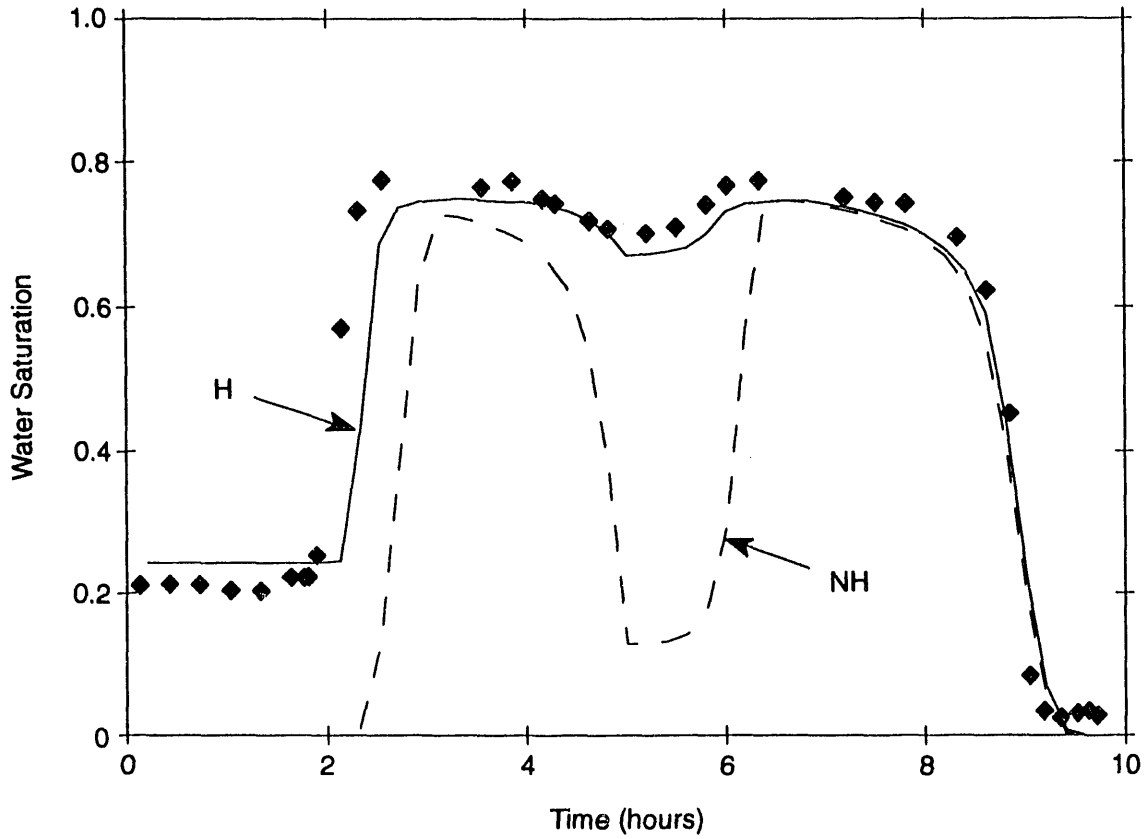

FIGURE 6. Comparison of Measured (Solid Symbols) and Simulated Hysteretic (H - Solid Line) and Nonhysteretic (NH - Broken Lines) Water Saturations for the 60-cm Measurement Location (Lenhard et al. 1991).

relative permeabilities should be considered. If hysteresis is ignored, erroneous fluid content predictions may result.

These studies suggest that the factors that cause hysteresis among fluid content-pressure-relative permeability relations must be considered to accurately predict the subsurface retention and movement of fluids. This requirement can have important implications for predicting the fate of NAPLs in the subsurface. For example, to accurately assess the migration of chemicals that have partitioned from a NAPL to groundwater, the subsurface NAPL distribution must first be predicted. If that NAPL distribution is erroneous, then subsequent NAPL transport predictions are also likely to be erroneous. An accurate assessment of the distribution of NAPLs, which are the source from which hazardous chemicals dissolve, is needed before an accurate prediction of the transport of these chemicals via groundwater can be made.

TCE Vapor Movement in a Sand Medium

In FY 1992, we conducted a novel large-scale laboratory experiment to observe the movement of TCE vapor in a 2-m-long by 1-m-high cell filled with sand in record time (about 450 hours). However, design and construction of the flow cell (shown in Figure 7) took many months. The walls of the flow cell are metal-bar-reinforced plastic sheet with 55 sample ports protruding through. The entire flow cell is sealed with a lid that is vented to atmospheric pressure through a filter capture system designed to contain the overflowed TCE vapor. During the experiment, TCE vapor was evolved from an internal chamber containing an open dish of volatilizing TCE liquid. The TCE vapors emanated downward from an

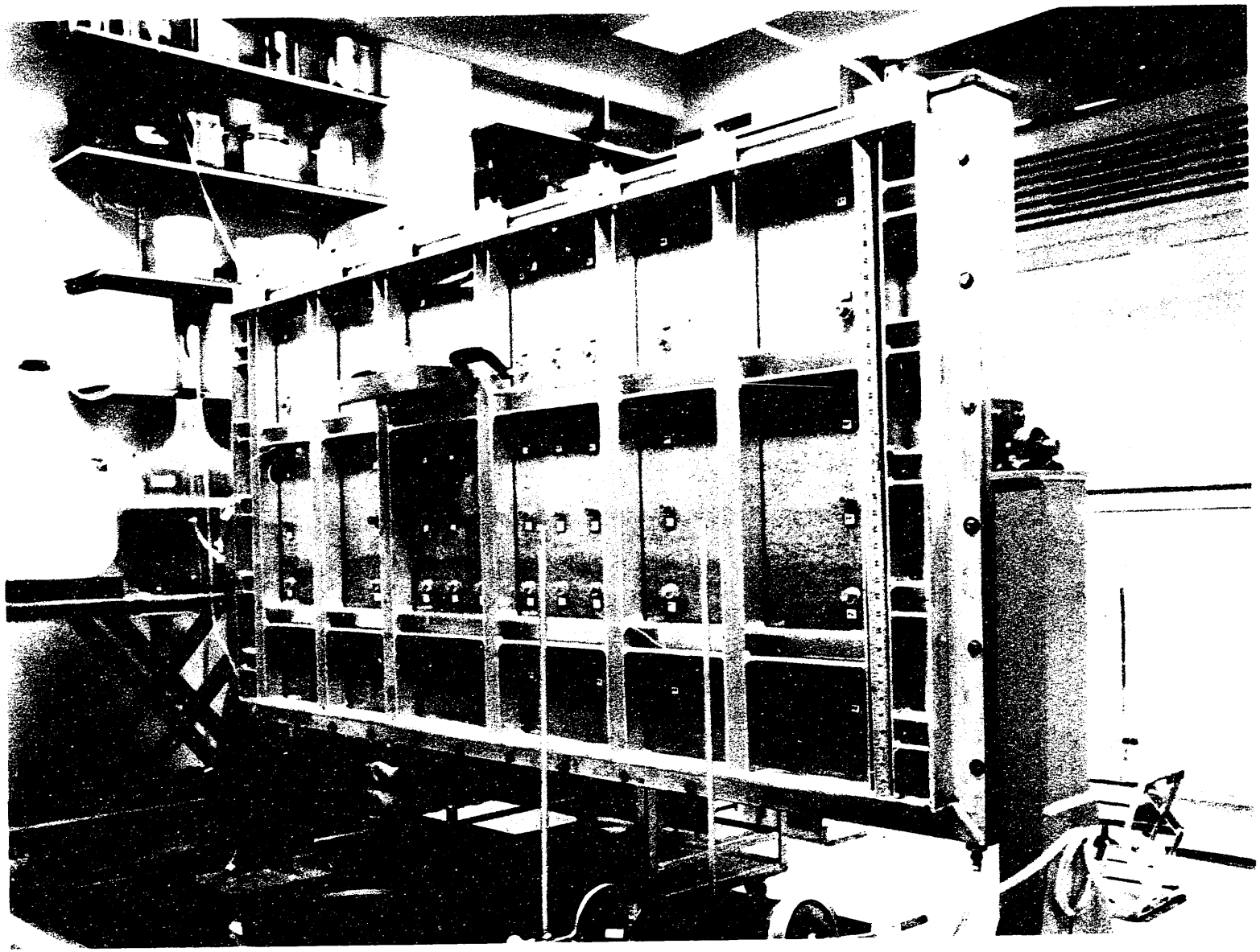

FIGURE 7. Photograph of the Flow Cell. The TCE supply chamber was inside and above the tray clamped to the outside. In this experiment, a small flask outside in the tray supplied the TCE vapor entering through a single port. The darker region of sand seen through the clear plastic wall, with its boundary between the second and third lines of sample ports from the bottom, is the saturated zone, which was maintained with the water supply bottle seen to the left of the cell. Saturated water flow was from left to right. The TCE vapor moved through the unsaturated zone above. In the front is an activated-carbon-filter tube used to remove overflow TCE vapor from the top of the sealed cell. This tube vented the flow cell to the outside and maintained atmospheric pressures throughout the cell.

8-cm by 7.5-cm rectangular opening in the chamber into the sand medium below. The 7.5-cm dimension was the thickness of the flow cell. Movement of the TCE vapor was monitored as if it were two-dimensional, without regard for the small thickness of the cell. The TCE vapor concentrations in the air filling the pores in the sand were measured by extracting small samples (25 μl) from the sample ports with a gas-tight syringe. The rubber-septum-covered sample ports can be seen in Figure 7. The TCE concentration in each sample was quantified by measurements made using a gas chromatograph (GC) with a highly sensitive electron capture detector (ECD type). A TCE sample was introduced into the GC by first injecting the sample into a closed vial of hexane liquid solvent, which dissolved and held the TCE for injection into the GC's analysis column. By using this instrumentation, it was possible to accurately measure TCE concentration over a four-order-of-magnitude range down from its saturated concentration in air.

The vapor concentration was measured only in the unsaturated zone, which extended about 55 cm below the sand surface. There were 37 sample ports in this unsaturated zone; 2 ports went into the TCE supply chamber and the remaining 18 entered the saturated zone below the maintained groundwater table. During the experiment, samples of water were taken directly from the saturated zone and analyzed for dissolved TCE concentration using the GC after a water-extraction step. Thus, the experiment also provided direct measurements of how rapidly TCE dissolves and enters a saturated groundwater zone.

A typical two-dimensional histogram of TCE vapor concentration on the grid is shown in Figure 8, for samples taken 6 hours after the first TCE introduction into the cell. Because TCE samples are taken at slightly different times from each port, values have been interpolated for a single time from the time series of measurements. (Note that the port at depth 0 cm and distance 70 cm is in the supply chamber.) After 6 hours, TCE concentration outside and below the supply chamber was actually somewhat greater than inside. A typical contour plot of the evolving gas plume is shown in Figure 9 for the same gas distribution. (The region devoid of contour lines is the supply chamber's location.) After two days, the TCE concentration (in grams per liter of gas volume) was a substantial fraction of its saturated value in the chamber, as seen in Figure 10. Figure 11 is the associated contour plot of concentrations.

Arrival of the TCE gas throughout the cell was examined from the concentration breakthrough curves for each sample port. Figure 12 shows the history for the source, the port directly below the entry region and the deepest port directly below. There was first an increase and then a decrease in concentration, followed by a build-up to a high, nearly saturated vapor concentration, which prevailed for nearly 120 hours. Concentration in the sand lags behind the source level. But at depth, the oscillation of concentrations is essentially attenuated. This oscillation of the source is not yet explained, inasmuch as the supply dish should have provided a constant amount by volatilization. Moreover, the temperature was constant and the atmospheric pressure was maintained uniformly throughout the supply chamber and the flow cell volume, as indicated by a manometer reading in the supply chamber. Thus there was no excess pressure in the chamber to drive gas out into the surrounding sand. However, the density of the gas (both air and TCE vapor) in the chamber may have contributed to gravity-driven advective downward flow. Moreover, the dissolution of TCE into the water phase may have contributed to a diminished concentration in the air at about 24 hours until the water became saturated and gas flowed steadily out at nearly the saturated vapor value. In any event, the source of TCE exhibited an unexpected dynamic behavior rather than a steady increase in concentration to reach a maximum saturated vapor concentration. After about 120 hours, the TCE supply concentration gradually reduced, to reach a minimum after 300 hours. It was determined that after 300 hours the supply of TCE liquid had vanished.

The breakthrough curves for TCE vapor concentrations along vertical grid lines that are distant from the source, e.g., at 0 and 135 cm, are similar enough to indicate that there was no gradation of vapor density with depth. Directly around the vapor source where concentrations are greatest, however, there is asymmetry in the pattern

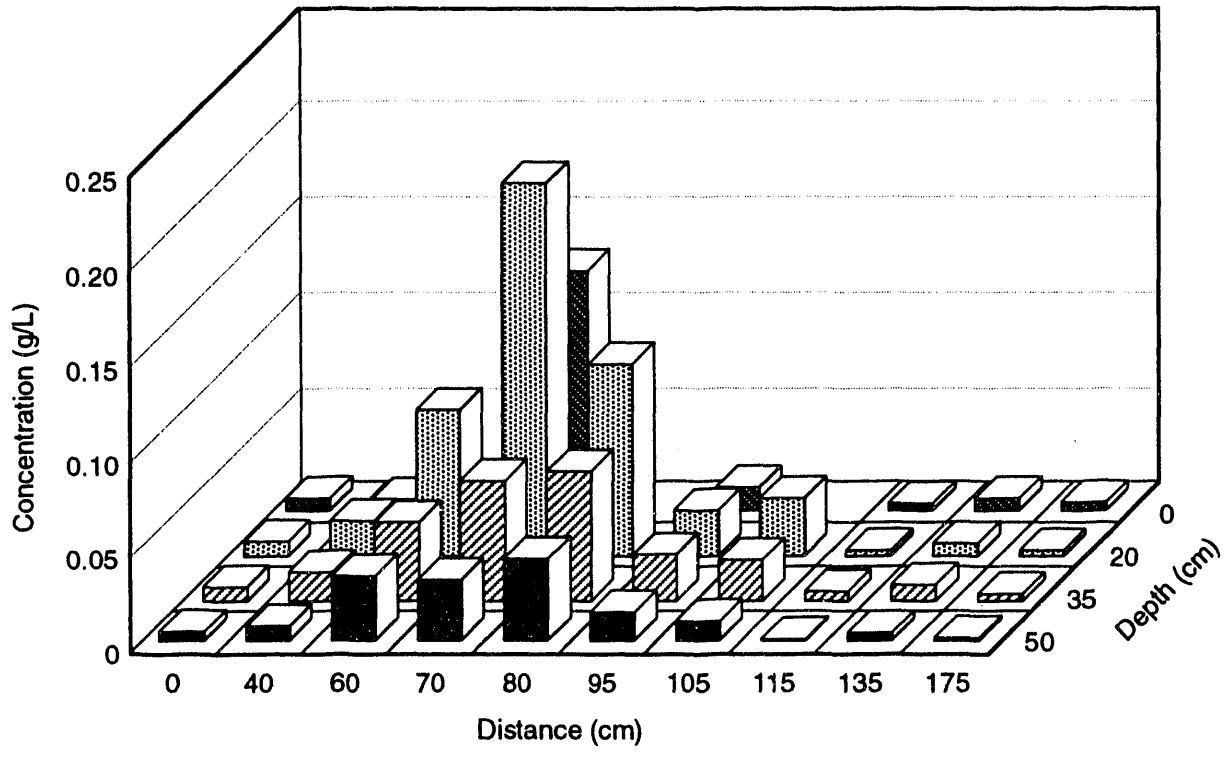

FIGURE 8. Histogram of TCE Concentrations Measured after 6 Hours. Concentration is in grams of TCE vapor per liter of gas volume, which is mostly air. The coordinate grid used to locate the sample ports is shown. The distance and depth are not on a linear scale.

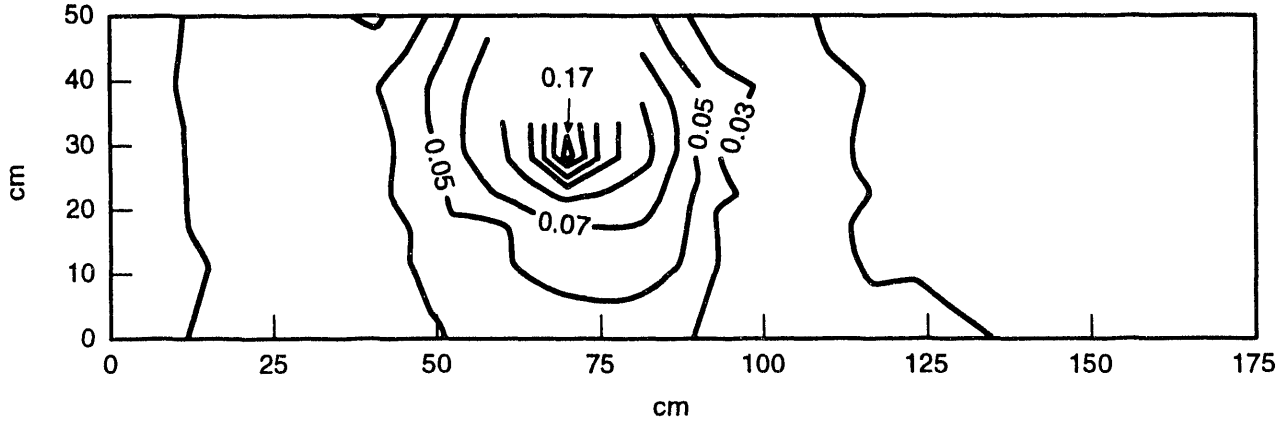

FIGURE 9. Contour Plot of TCE Vapor Concentration (in grams/liter) after 6 Hours. The distances and height from the bottom line of sample ports in the vadose zone are in centimeters. Note that the TCE supply was located to the left of a vertical center line, about 70 cm from the left side. This afforded a greater distance for the TCE to move right in the same direction as water flow in the saturated zone.

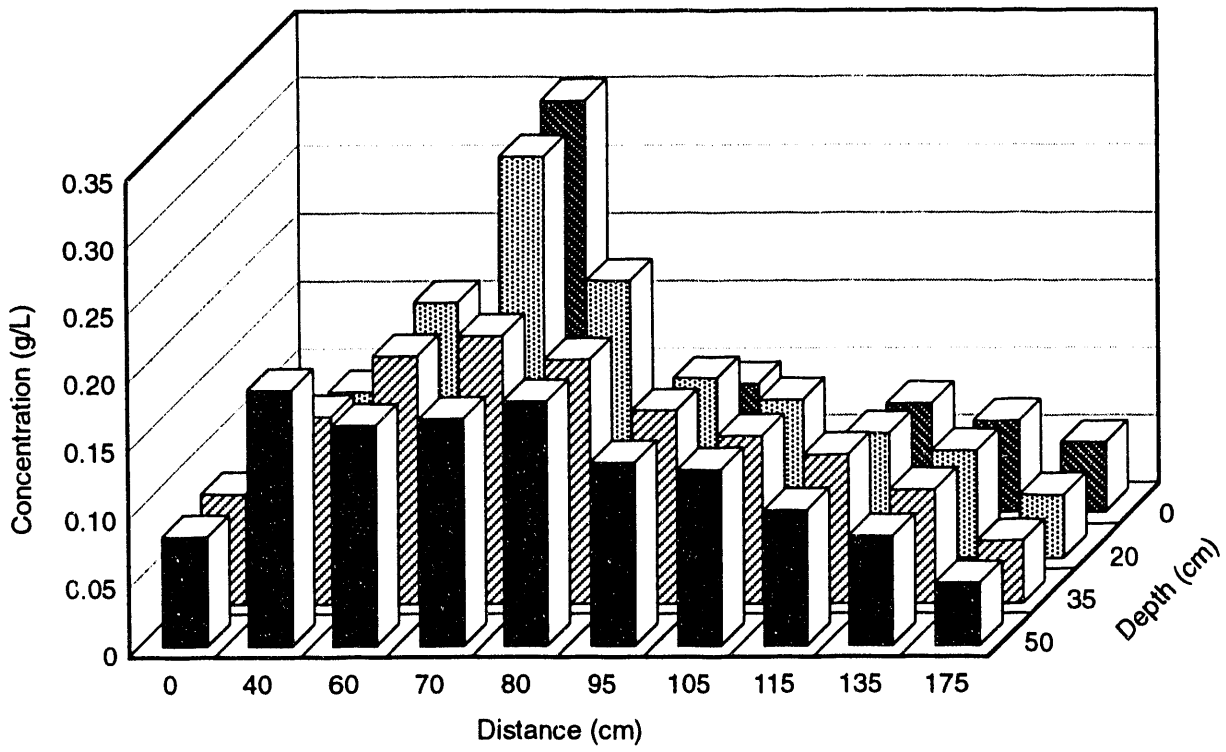

FIGURE 10. Histogram of TCE Concentrations after 48 Hours

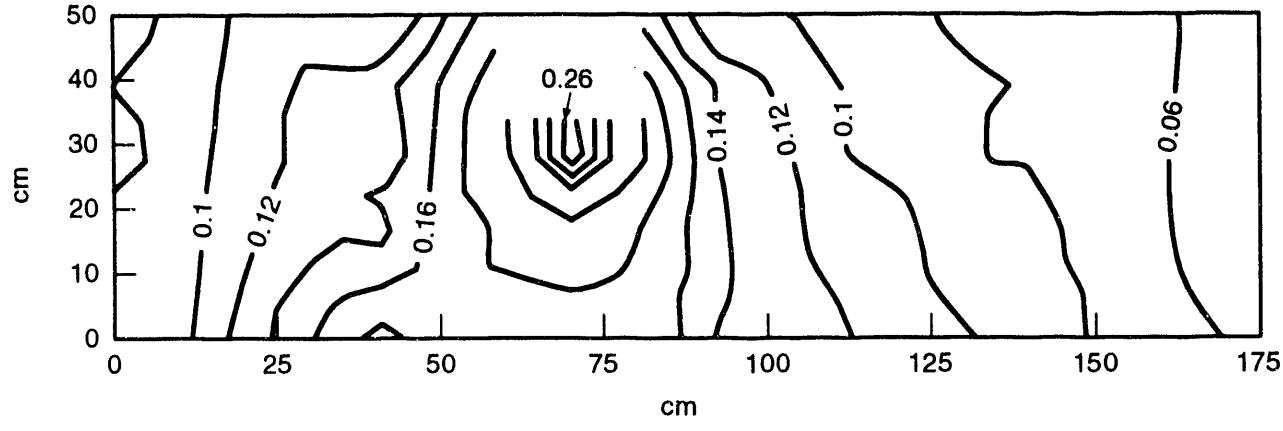

FIGURE 11. Concentration Contour Plot of TCE Vapor after 48 Hours

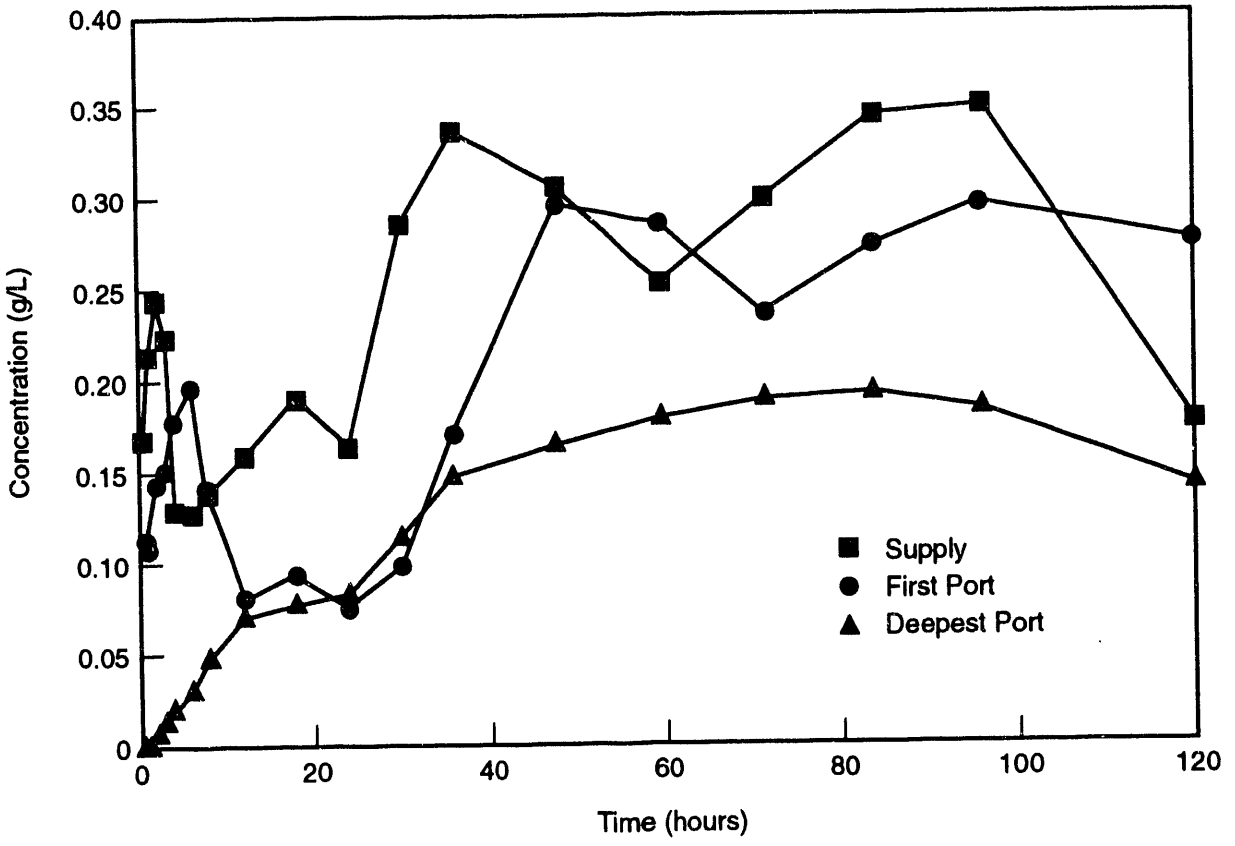

FIGURE 12. TCE Vapor Concentration (grams/liter) Depending on Time for the Supply Chamber, the Port Directly Below, and the Deepest Port. Supply concentration oscillates before attaining a nearly steady value between 30 and 100 hours.

of TCE concentrations to the right and left and below. Figure 13 shows that, between 15 and 40 hours, port #1 (20 cm below the source) had greater concentrations than ports #4 and #5, at about the same distance to the right and left of the source. At greater distance (about 30 cm below the source), port #6 had greater concentration than ports #9 and #10, which were similar distances to the right and left, from 40 hours up to 100 hours, as seen in Figure 14. Thus, it appears that the TCE vapor plume is elongated downward, and not symmetric, as would be expected with solely diffusive movement from the source. The deviation in TCE concentration, however, is not large: it is only about 0.04 g/L larger below the source when the values to the sides are about 0.12 - 0.14 g/L. Nevertheless, the difference appears to be significant in view of the accuracy of the GC measurements and because the data show a continuous trend over a substantial time. Therefore, it appears that a density-driven effect is exhibited only very near the source.

Unstable Fingering Behavior in a Porous Medium

Results from previous laboratory experiments involving multiphase infiltration events indicated that under relatively general conditions certain contaminants did not move as predicted by classical multiphase theory. In these experiments, channeling or fingering flow developed as specific organic liquids infiltrated through partly saturated porous media (Cary et al. 1989; Simmons et al. 1990). Analysis of the experimental results led to a set of hypotheses regarding the causes for the onset and persistence of channelling flow (Simmons et al. 1990). These hypotheses, relating primarily to the spreading pressure of the organic liquid and the distribution

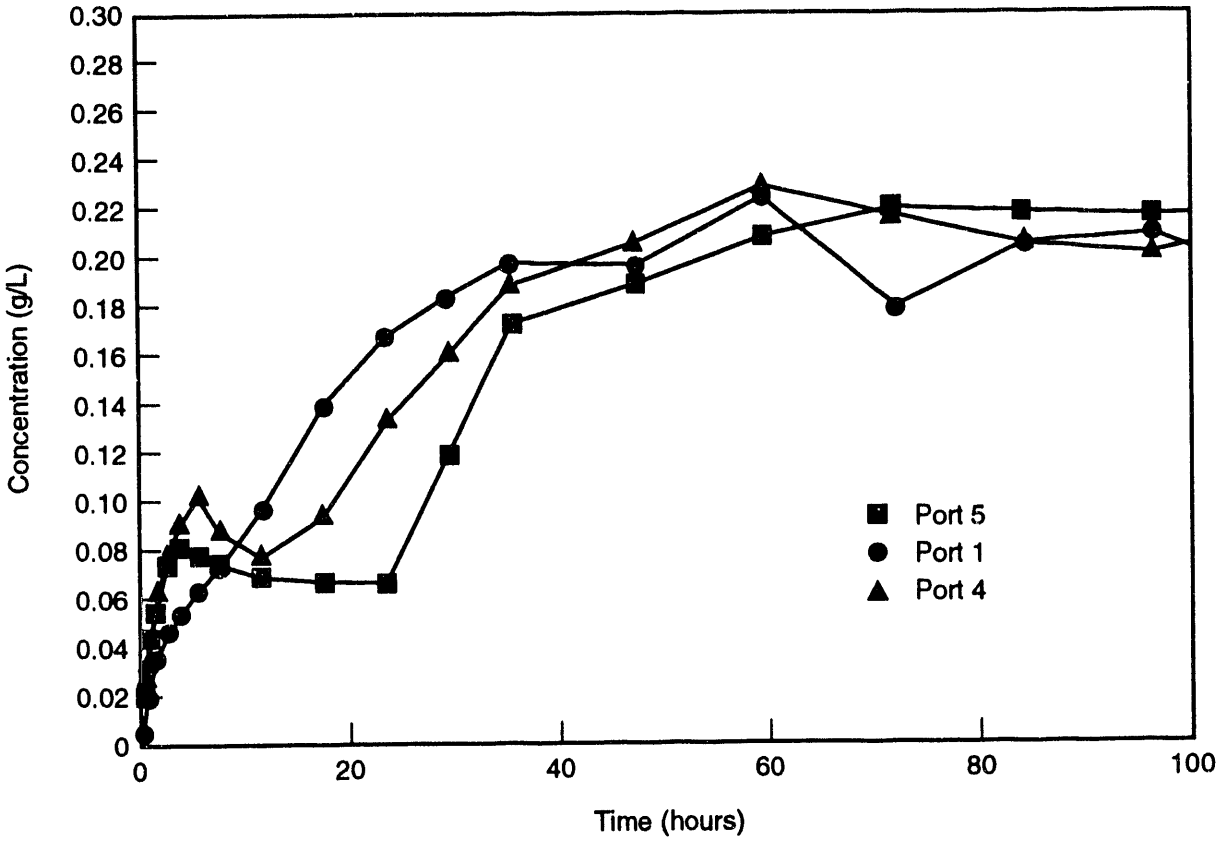

FIGURE 13. Concentration Breakthroughs for Ports #4, #5, and #1. The concentration is greater below the supply than for values in the sample ports to the right and left of the supply.

of pore sizes encountered by the downward-moving organic liquid front, provided a basis for testing the conditions under which classical theory would suffice for prediction of organic fluid flow, and when it would not. One approach to testing these hypotheses requires the development of a means of simulating channeling flow, independent of the restrictions of classical multiphase flow theory. Such computational simulations would not only provide a cost-effective supplement to expensive physical experiments for duplicating channeling flow, but would also afford focused testing of the effects of various physical controls on channeling flow.

Therefore, we conducted a concise review to examine available tools for unconventional simulation of channeling flow and to identify specific approaches for obtaining this capability. This review incorporated and extended the published reviews of Kueper and Frind (1988) and Yortsos (1990). Two valuable approaches were identified: network modeling (e.g., Blunt and King 1991) and random-walk methods to represent diffusion-limited aggregation (e.g., Paterson 1984).

Network models involve a detailed representation of the pore space of a subsurface medium as a fine mesh of interconnected "pipes," and the hydraulics of flow through the network is simulated using the theory of flow through capillaries. This modeling is done on a very fine scale. Rules for flow branching through intersections are determined from physical considerations (such as capillary tensions, gravity, etc.) and are applied to determine which physical aspects control the onset of channeling flow, as observed on the larger scale of the whole network. These models are valuable in examining the scaling hypothesis that flow phenomena on the large scale are dominated by conditions that are in effect at the pore scale.

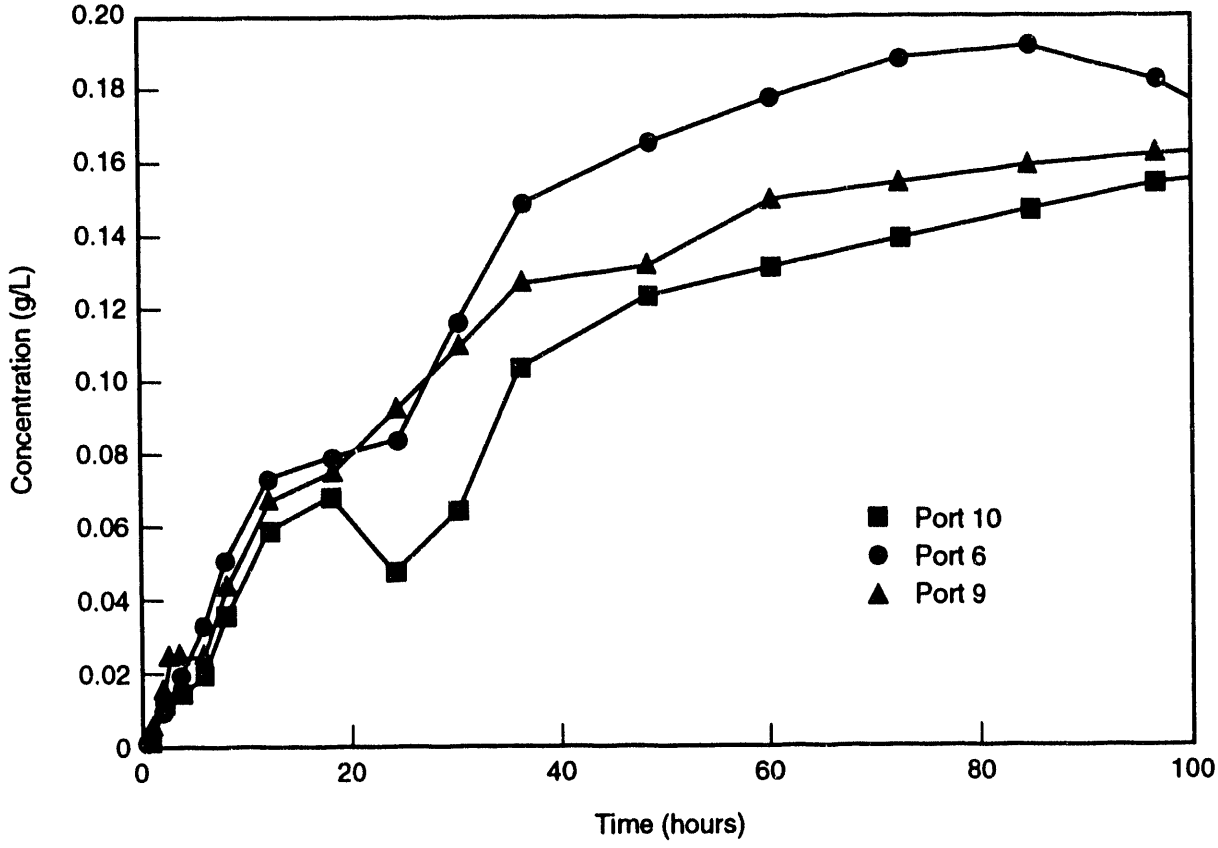

FIGURE 14. Concentration Breakthroughs for Ports #9, #10, and #6. Concentration becomes greater at port #6 (below the supply chamber) than in ports to the right and left of the supply.

Random-walk models, in contrast, provide a very simple way of representing general diffusion phenomena. In these models, the movement of a fluid in a subsurface environment is represented by the displacement of numerous particles whose individual paths are simply a sequence of randomly directed steps. It is well known that properly posed random-walk simulations produce diffusion that is mathematically equivalent to that predicted by classical continuum theory (e.g., Paterson 1984). The advantage of random-walk models over classical continuum diffusion models (Laplace's equation) is that specific physically based rules of motion of the particles may be selectively applied on the very small scale (e.g., Sherwood and Nittmann 1986). This has made it possible for many researchers in disparate fields, such as immiscible fluid displacement, electroplating, and multicomponent gas diffusion, to examine a variety of diffusive processes.

In this work, the random-walk approach was exploited to simulate the evolution of a channeling plume of organic liquid. Plume evolution was represented as the result of two competing processes: pore-specific gravity flow and diffusive spreading. The pore-specific flow component is preferential flow of the organic liquid through only those pores that are larger than a specific threshold (as determined by interfacial tensions), and it is gravity driven. In contrast, diffusive spreading acts in all directions and independently of pore sizes. Simplified renditions of these processes were incorporated as controls on particle paths and were superimposed on a basic random-walk model. This model is a simplified prototype diffusion-limited aggregation (DLA) model, based on Kadanoff's extension of random-walk diffusion for inclusion of fluid interfacial tensions (Kadanoff 1985). Our model expanded on Kadanoff's concepts by incorporating physical aspects of variable spreading

pressures. Controls on the infiltration of a typical non-spreading oil, such as mineral oil, are simulated by amplifying the pore-specific flow component to the magnitude of the diffusional spreading component.

Despite the simplicity of our representation of the physics, a surprisingly good duplication of previous experimental results was achieved. Figure 15 shows a vertical cross section of a mineral oil plume (digitized and color-coded) after infiltration into a cube of unsaturated glass beads (Simmons et al. 1990). Figure 16 shows the results of the DLA simulation of the experiment. The color coding in Figure 16 corresponds to displacement time: red corresponds to the newest part of the plume and blue to the oldest. Figure 16 shows how gravity-griven channelling flow creates an unstable infiltration front, which is then smoothed by diffusional spreading, which lags slightly behind. This pattern is particularly visible in the green "historical channels" in the middle of the plume. General characteristics of the laboratory observations, such as the general shape of the plume, the relative length and width of the channels, and the inclusion of uninvaded bubbles, are all duplicated in the DLA model results.

References

Blunt, M., and P. King. 1991. "Relative Permeabilities from 2-Dimensional and 3-Dimensional Pore-Scale Network Modeling." *Transport in Porous Media* 6:407-433.

Cary, J. W., J. F. McBride, and C. S. Simmons. 1989. "Observations of Water and Oil Infiltration into Soil: Some Simulation Challenges." *Water Resources Research* 25:73-80.

Kadanoff, L. P. 1985. "Simulating Hydrodynamics: A Pedestrian Model." *Journal of Statistical Physics* 39(3/4):267-283.

Kueper, B. H., and E. O. Frind. 1988. "An Overview of Immiscible Fingering in Porous Media." *Journal of Contaminant Hydrology* 2:95-110.

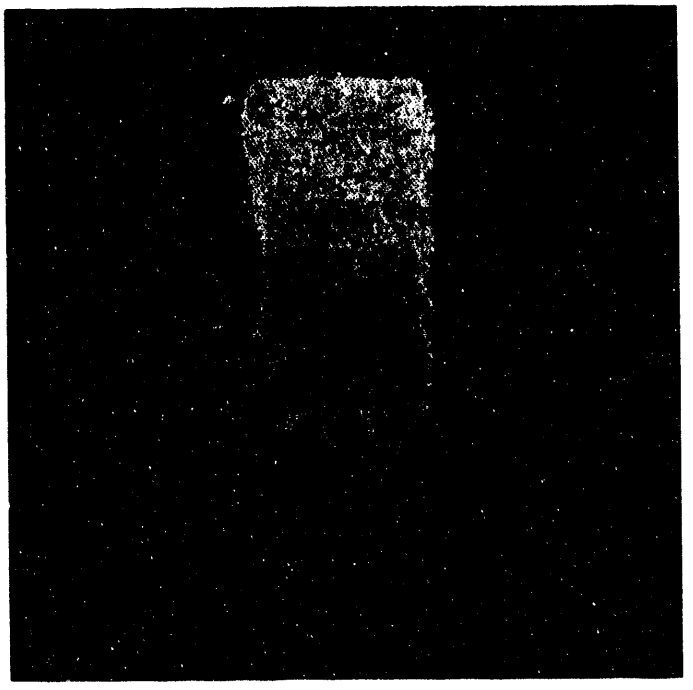

FIGURE 15. Observed Mineral Oil Infiltration

FIGURE 16. DLA Simulation of Mineral Oil Infiltration

Lenhard, R. J. 1992. "Measurement and Modeling of 3-Phase Saturation-Pressure Hysteresis." *Journal of Contaminant Hydrology* 9:243-269.

Lenhard, R. J., and J. C. Parker. 1987. "Measurement and Prediction of Saturation-Pressure Relationships in 3-Phase Porous Media Systems." *Journal of Contaminant Hydrology* 1:407-424.

Lenhard, R. J., J. C. Parker, and J. J. Kaluarachchi. 1989. "A Model for Hysteretic Constitutive Relations Governing Multiphase Flow, 3. Refinements and Numerical Simulations." *Water Resources Research* 25:1726-1736.

Lenhard, R. J., J. C. Parker, and J. J. Kaluarachchi. 1991. "Comparing Simulated and Experimental Hysteretic Two-Phase Transient Fluid Flow Phenomena." *Water Resources Research* 27:2113-2124.

Parker, J. C., and R. J. Lenhard. 1987. "A Model for Hysteretic Constitutive Relations Governing Multiphase Flow, 1. Saturation-Pressure Relations." *Water Resources Research* 23:2187-2196.

Paterson, L. 1984. "Diffusion-Limited Aggregation and Two-Fluid Displacements in Porous Media." *Physical Review Letters* 52(18):1621-1624.

Sherwood, J. D., and J. Nittmann. 1986. "Gradient Governed Growth: The Effect of Viscosity Ratio on Stochastic Simulations of the Saffman-Taylor Instability." *Journal de Physique* 47(1):15-22.

Simmons, C. S., J. F. McBride, R. J. Lenhard, and J. W. Cary. 1990. "Organic Liquid Infiltration into Unsaturated Porous Media." Paper presented at the IAH Conference on Subsurface Contamination by Immiscible Fluids, April 18-20, 1990, Calgary, Alberta.

Yortsos, Y. C. 1990. "Instabilities in Displacement Processes in Porous Media." *Journal of Physics: Condensed Matter* 2:SA443-SA448.

Manipulation of Natural Subsurface Processes: Field Research and Validation

J. S. Fruchter, F. A. Spane, J. K. Fredrickson, C. R. Cole, J. E. Amonette, J. C. Templeton, T. O. Stevens, D. J. Holford, L. E. Eary, J. M. Zachara, B. N. Bjornstad, G. D. Black, and V. R. Vermeul

Under the auspices of DOE's Subsurface Science Program, the use of a field experiment to validate key hypotheses concerning the natural interactions of microbial, chemical, and physical processes was investigated. In FY 1992, the ramifications of such an experiment for *in situ* remediation of subsurface contamination led to the project's being transferred from the Office of Health and Environmental Research to DOE Office of Environmental Restoration and Waste Management. Therefore, recommendations for future research were developed in FY 1992.

The concept underlying the experiments is that the addition of chemical reagents and/or microbial nutrients to the aquifer through an injection well would create chemically reducing conditions in the aquifer, and thus create a permeable geochemical treatment barrier. Such a geochemical barrier could be a powerful tool for future remediation of dispersed contaminants on DOE lands. The reagents and nutrients proposed are those expected to cause only temporary changes to the aquifer chemistry. This approach ensured that additional contaminants would not be added to the aquifer during remediation.

A field injection experiment of this type requires input from a variety of scientific disciplines, including geochemistry, microbiology, and hydrology. The research conducted under the Subsurface Science Program included laboratory studies of the effectiveness of various abiotic reducing agents, characterization of microbial populations and nutrient requirements in Hanford core samples, and hydrologic modeling and visualization experiments to determine the sensitivity of the experiment to natural heterogeneity of the system and to experimental parameters.

The recommended research for continuing evaluation of the feasibility of this approach incorporates consideration of additional chemical reagents and measurements of the ability of dissimilatory iron-reducing conditions to reduce aquifer solids. More detailed computer simulations will optimize reagent dispersal and recovery in the subsurface. Methods that use gradient control to increase reagent residence time in the subsurface will also be investigated.

Successful completion of the field test requires thorough characterization of the field site. Therefore, a three-phase plan for characterization of the hydrophysical, geochemical, and microbiological properties of the field site was also developed.

Numerical Model of Transient Radon Flux Through Cracked Concrete Slabs

D. J. Holford, G. W. Gee, H. D. Freeman, and J. L. Cox

Several researchers have suggested that cracks in concrete floors could be pathways for the entry of significant amounts of radon into buildings (Landman and Cohen 1983; Narasimhan et al. 1990; Schery et al. 1988a; Wilkinson and Dimbylow 1985). Loureiro et al. (1990) used steady-state simulations of advective and diffusive radon transport in soils to demonstrate that diffusion is the dominant mechanism of transport when soil gas permeabilities are less than 1×10^{-12} m^2 (a value typical of a fine sand or silty soil). Because concrete slabs typically have a very low gas permeability, 8.0×10^{-14} to 3.4×10^{-16} m^2 (Rogers et al. 1991), cracks in a concrete floor provide a significant pathway for radon diffusion and advection into houses. Previous work has indicated the importance of barometric pumping in enhancing radon flux from soil (Clements 1974; Duwe 1976; Kraner et al. 1964; Schery and Gaeddert 1982), and that fractures in rock or cracks in soil can result in advective transport that is much larger than diffusive transport (Holford et al., in press; Nilson et al. 1991; Schery et al. 1982; Schery et al. 1988b; Schery and Siegel 1986).

The purpose of the modeling exercise conducted in FY 1992 was to demonstrate how barometric

pumping may enhance radon flux into buildings through cracked concrete slabs. Of interest is how small and widely spaced cracks in concrete must be before their influence is negligible. A unique characteristic of these numerical experiments is that both transient advective (due to pressure gradients) and diffusive (due to concentration gradients) radon transport were simulated. The results of simulations of radon flux from soil through concrete with cracks of different size and spacing and with and without subslab aggregate were compared to radon flux from bare soil.

The transport of radon into houses is governed by the radium content of the soil, as well as its transport properties, diffusion coefficient, permeability, and porosity. These properties are important because radon gas moves both by advection with the bulk flow of liquid and gas in the soil, and by diffusion through liquid and gas in the soil pores. In this project, a finite-element code, Rn3D, has been developed to simulate gas flow and radon transport in porous media by transient advection-diffusion (Holford et al., in press). The code was designed to model the effects of barometric pressure variations on radon transport in soil and other porous media, such as concrete.

FY 1992 Research Highlights

Simulations considering various soil and basement types were conducted to demonstrate the effect of barometric pressure variations on radon transport into basements. A schematic diagram of the model is shown in Figure 1. The depth to the water table was 10 m in all simulations. Sinusoidal pressure variations with an amplitude of 50 Pa and a period of 0.5 h were used in all simulations. Variations in actual barometric pressure can range from an amplitude of a few pascals for periods of minutes to a few hundred pascals over a day. The passage of weather fronts can cause pressure changes on the order of 1,000 to 2,000 Pa (Narasimhan et al. 1990).

Three soil types were considered in the simulations: sand, silt, and clay. Simulations were conducted with bare soil, soil covered by intact concrete, or soil overlain by a cracked concrete slab. Other simulations included a coarse gravel layer underneath the concrete slabs. Properties for all materials used in the simulations are listed in Table 1.

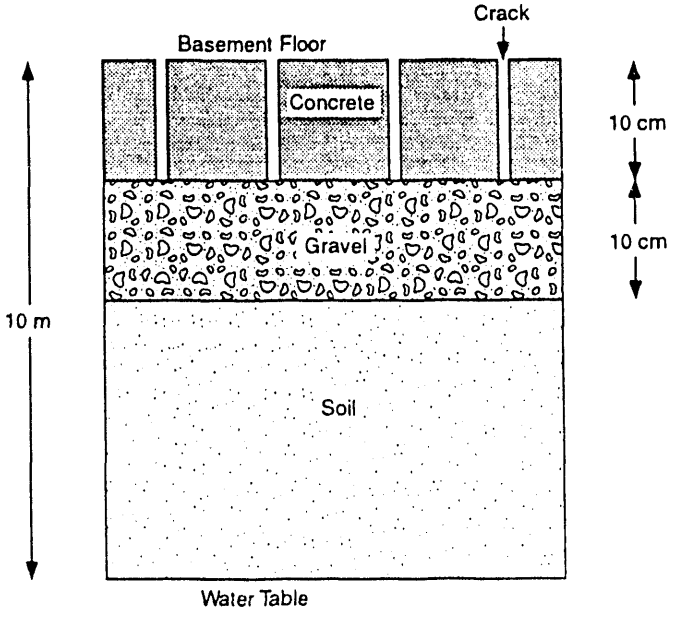

FIGURE 1. Model Diagram for Two-Dimensional Finite-Element Simulation of Radon Flux into a Basement. Simulations were conducted to determine the effect of the 10-cm layers of concrete and gravel on radon flux into a basement.

TABLE 1. Properties of Porous Materials Represented in Simulations

Material	Porosity, m^3/m^3	Permeability, m^2/s	Diffusion, m^2/s	Radium Content, Bq/kg	Radon Emanation Coefficient
Clay	0.56	1.0×10^{-14}	2.0×10^{-2}	35	0.1
Loam	0.45	1.0×10^{-12}	4.0×10^{-2}	35	0.1
Sand	0.35	1.0×10^{-10}	6.1×10^{-2}	35	0.1
Gravel	0.40	3.0×10^{-7}	6.1×10^{-2}	0	0
Concrete	0.25	4.4×10^{-16}	1.3×10^{-3}	0	0

The properties used to represent gravel are typical of sub-slab aggregate (Gadgil et al. 1991). Properties for concrete are typical of new residential dwellings (Rogers et al. 1991). The porosities and permeabilities for the clay, loam, and sand soils are typical values for the respective grain-size classes (Freeze and Cherry 1979; Mualem 1976). Diffusion coefficients were estimated based on typical pore-size distributions for each size class (Nielson et al. 1984) and on the diffusion coefficient of radon in pure air (Bird et al. 1960; Hart 1986). Radium content and emanation coefficients for the three soil types were based on those for soils near Socorro, New Mexico (Schery et al. 1984), and Poamoho, Hawaii (Cotter 1990). Bulk densities for each material were calculated assuming $\rho_b = 2.65(1 - n)$.

Three sets of crack widths and spacing in the concrete slab were considered: 1) crack width = 0.5 cm, spacing = 8 m; 2) crack width = 0.5 cm, spacing = 0.8 m; and 3) crack width = 0.05 cm, spacing = 0.8 m.

Figure 2 shows the transient radon fluxes from bare soils. Because sand has the largest diffusion coefficient, the average radon flux from the sand is larger than that from loam or clay. Also, because sand has the largest permeability, the fluctuations in response to cyclical barometric pressure variations are larger than for either loam or clay. These results indicate that soils with permeabilities less than 1.0×10^{-12} m^2 are relatively unaffected by barometric pressure variations and transmit radon mainly by diffusion. Note the inverse relationship between radon flux and barometric pressure; however, the time lag between radon flux and barometric pressure is shorter for sand because of its higher permeability, which allows pressure changes to propagate faster.

Figure 3 compares radon fluxes from bare sand, sand overlain by a solid concrete slab, and sand overlain by a cracked concrete slab. The flux from the concrete slab with wide (0.5 cm), closely spaced (0.8 m) cracks is significantly larger than the flux from the solid concrete slab. Concrete slabs with smaller (0.05 cm) or more widely spaced (8 m) cracks did not allow the passage of significantly more radon gas than did the solid concrete slab.

Figure 4 compares radon fluxes through a worst-case cracked concrete slab (crack width = 0.5 cm, crack spacing = 0.8 m) for three soil types with and without the presence of 10 cm of gravel beneath the concrete slab. For each soil type, the flux into the basement is slightly less when 10 cm of gravel is placed beneath the concrete slab. The reduction in flux occurs because the gravel layer increases the diffusion length between the top of the soil and the concrete slab; because radon has a short half life of 3.8 days, this increase in diffusion length reduces the flux into the basement. Also, the flux is less with a gravel layer present because the cracks in the concrete slab act as conduits for fresh air to flow into the high-permeability gravel layer during periods of increasing atmospheric pressure, as well as being a conduit for radon gas from the soil during periods of decreasing atmospheric pressure (Figure 5).

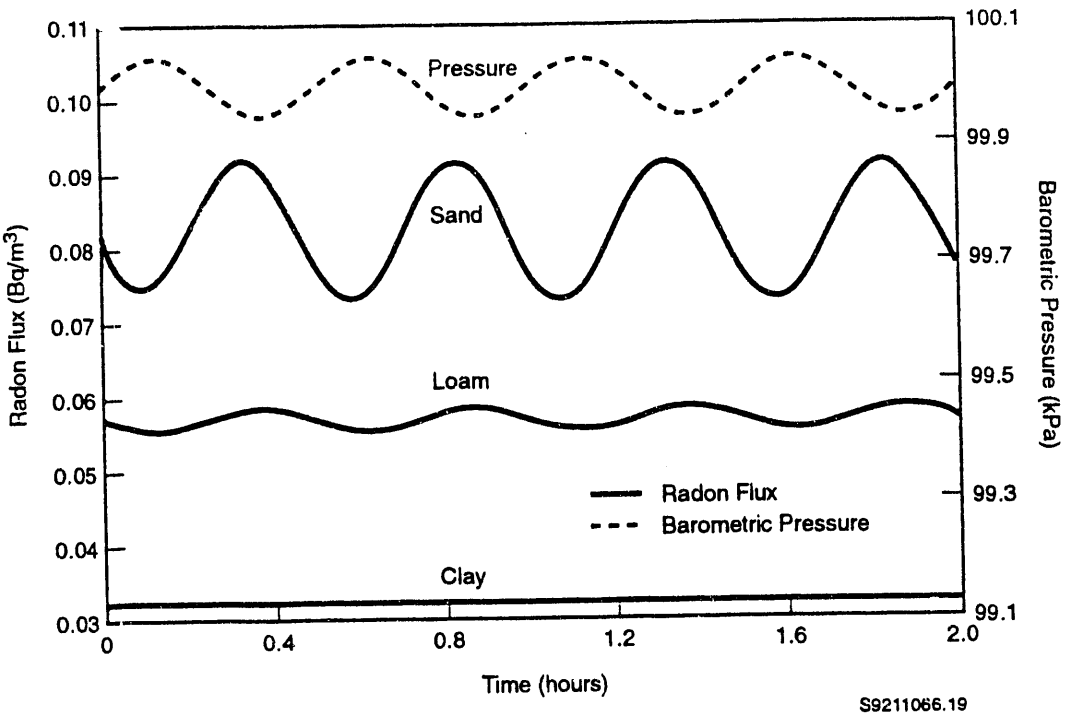

FIGURE 2. Comparison of Transient Radon Fluxes from Three Bare Soils During Cyclical Barometric Pressure Fluctuations. Flux from sandy soil is highest as a result of the soil's higher diffusion coefficient, and the variability of flux from sandy soil is greatest as a result of its higher air permeability.

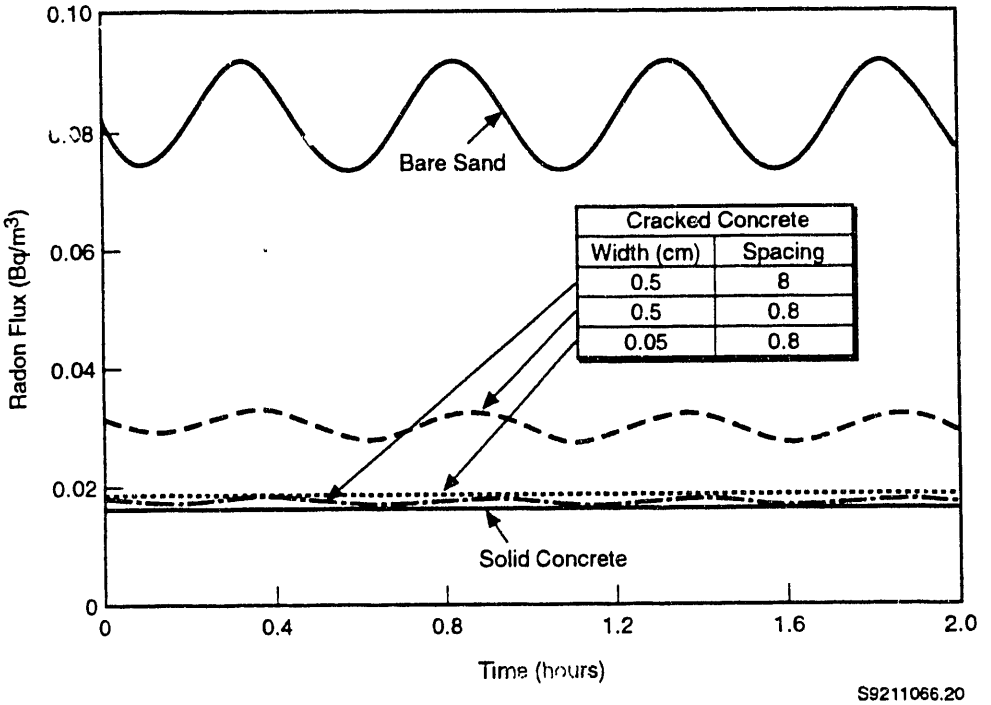

FIGURE 3. Comparison of Transient Radon Fluxes from a Sandy Soil, Sandy Soil Covered by a Solid Concrete Slab, and Sandy Soil Covered by a Cracked Concrete Slab with Cracks of Different Widths and Spacings

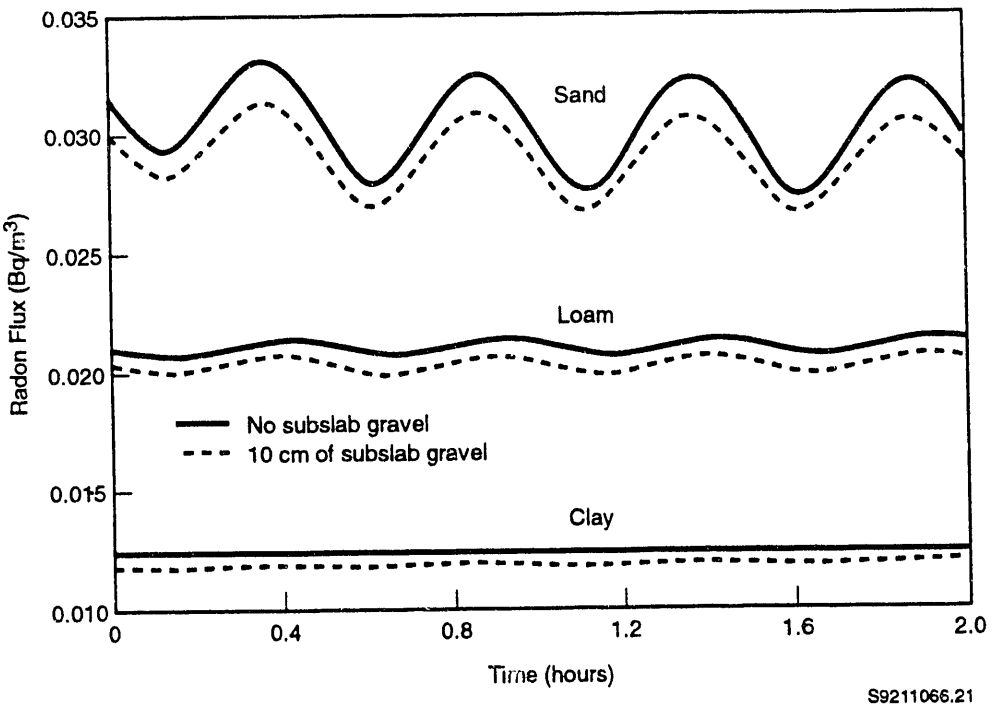

FIGURE 4. Comparison of Transient Radon Flux from Three Soils Covered by a Cracked Concrete Slab (crack width = 0.5 cm, crack spacing = 0.8 m) with and without 10 cm of Gravel Underlying the Slab

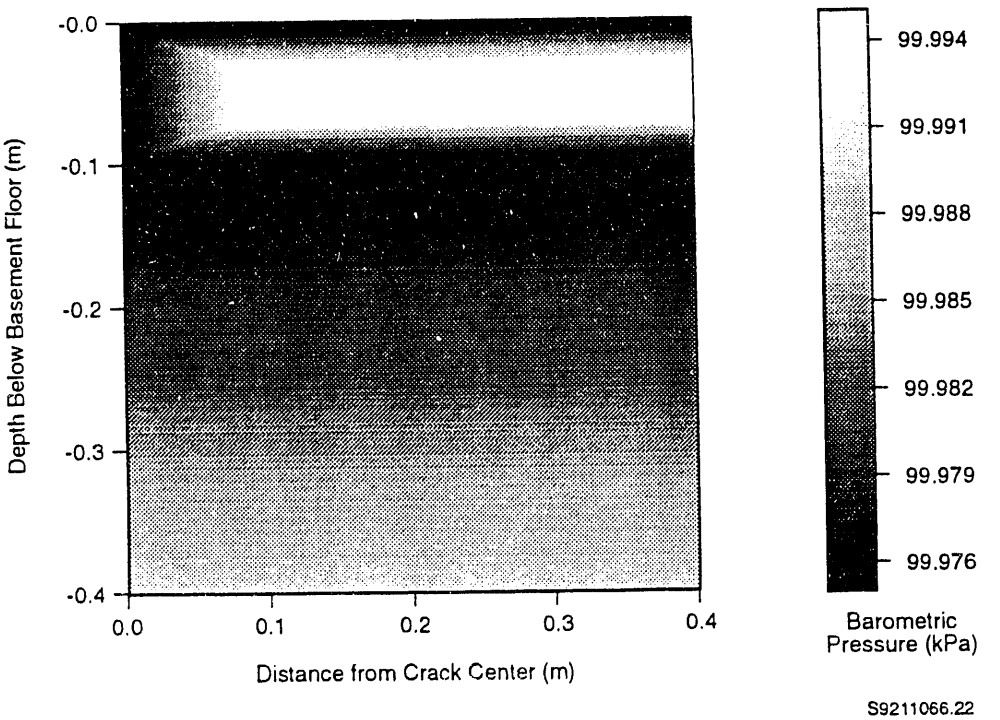

FIGURE 5. Pressure Field at 1.8 hours. At this point, barometric pressure has been decreasing for 0.25 hours. Crack is in upper left corner between the 0- and 0.1-m depths; concrete is from 0 to 0.1 m in depth; gravel is between 0.1 and 0.2 m in depth. Pressure is highest in concrete because of its low permeability; the crack and the gravel layer are high-permeability pathways for decreasing pressure.

Thus this research shows that radon flux into a house can be significantly reduced by sealing cracks in concrete slabs. Although concrete has a very low permeability and diffusion coefficient, cracks can allow the transmission of a significant fraction of the flux that a bare dirt floor would transmit.

Radon flux can be decreased slightly by the presence of a 10-cm gravel layer underlying the concrete slab. Thicker layers of subslab gravel are common and may reduce radon fluxes into houses even further than the 10-cm layer modeled herein.

Future Research

Planned work will study the effectiveness of a subslab ventilation system in reducing radon fluxes into houses. The model would be similar to that shown in Figure 1, but with the addition of a conduit through the concrete into the gravel layer and suction applied to reduce radon concentrations in the gravel layer. This modeling will be based on experimental data that have been collected at houses near Spokane, Washington.

References

Bird, R. B., W. E. Stewart, and E. N. Lightfoot. 1960. *Transport Phenomena*. John Wiley, New York.

Clements, W. E. 1974. *The Effect of Atmospheric Pressure Variation on the Transport of ^{222}Radon from Soil to the Atmosphere*. Ph.D. Dissertation, New Mexico Institute of Mining and Technology, Socorro, New Mexico.

Cotter, J. M. 1990. *Simulated Transport of Radon in Soil Gas*. Master's Thesis, University of Hawaii, Manoa, Hawaii.

Duwe, M. P. 1976. *The Diurnal Variation in Radon Flux from the Soil due to Atmospheric Pressure Change and Turbulence*. Ph.D. Dissertation, University of Wisconsin, Madison, Wisconsin.

Freeze, R. A., and J. A. Cherry. 1979. *Groundwater*. Prentice-Hall, Englewood Cliffs, New Jersey.

Gadgil, A. J., Y. C. Bonnefous, W. J. Fisk, A. Nematollahi, and R. J. Prill. 1991. *Influence of Subslab Aggregate Permeability on Subslab Ventilation Performance*. LBL-31160, Lawrence Berkeley Laboratory, Berkeley, California.

Hart, K. P. 1986. *Radon Exhalation from Uranium Tailings, Volume 1*. Ph.D. Dissertation, University of New South Wales, Kensington, New South Wales.

Holford, D. J., S. D. Schery, J. L. Wilson, and F. M. Phillips. "Modeling Radon Transport in Dry, Cracked Soil." *Journal of Geophysical Research* (in press).

Kraner, H. W., G. L. Schroeder, and R. D. Evans. 1964. "Measurements of the Effects of Atmospheric Variables on Radon-222 Flux and Soil-Gas Concentrations." In *The Natural Radiation Environment*, pp. 161-190. University of Chicago Press, Chicago, Illinois.

Landman, K. A., and D. S. Cohen. 1983. "Transport of Radon Through Cracks in Concrete Slab." *Health Physics* 44:249-257.

Loureiro, C.d.O., L. M. Abriola, J. E. Martin, and R. G. Sextro. 1990. "Three-Dimensional Simulation of Radon Transport into Houses with Basements Under Constant Negative Pressure." *Environmental Science and Technology* 24:1338-1348.

Mualem, Y. 1976. *A Catalogue of the Hydraulic Properties of Unsaturated Soils*. Research Project 442, Technion, Israel Institue of Technology, Haifa, Israel.

Narasimhan, T. N., Y. W. Tsang, and H. Y. Holman. 1990. "On the Potential Importance of Transient Air Flow in Advective Radon Entry into Buildings." *Geophysical Research Letters* 17:821-824.

Nielson, K. K., V. C. Rogers, and G. W. Gee. 1984. "Diffusion of Radon Through Soils: A Pore Distribution Model." *Soil Science Society of America Journal* 48:482-487.

Nilson, R. H., E. W. Peterson, K. H. Lie, N. R. Burkhard, and J. R. Hearst. 1991. "Atmospheric Pumping: A Mechanism Causing Vertical Transport of Contaminated Gases Through Fractured Permeable Media." *Journal of Geophysical Research* 96(B13):21933-21948.

Rogers, V. C., K. K. Nielson, and M. A. Lehto. 1991. *Indoor Radon Entry from Concrete Foundations*. RAE-9127/1-1, Rogers and Associates Engineering Corporation, Salt Lake City, Utah.

Schery, S. D., and D. H. Gaeddert. 1982. "Measurements of the Effect of Cyclic Atmospheric Pressure Variation on the Flux of ^{222}Rn from the Soil." *Geophysical Research Letters* 9:835-838.

Schery, S. D., D. H. Gaeddert, and M. H. Wilkening. 1982. "Transport of Radon from Fractured Rock." *Journal of Geophysical Research* 87(B4):2969-2976.

Schery, S. D., D. H. Gaeddert, and M. H. Wilkening. 1984. "Factors Affecting Exhalation of Radon from a Gravelly Sandy Loam." *Journal of Geophysical Research* 89(D5):7299-7309.

Schery, S. D., D. J. Holford, J. L. Wilson, and F. M. Phillips. 1988a. "The Flow and Diffusion of Radon Isotopes in Fractured Porous Media: Part 1, Finite Slabs." *Radiation Protection Dosimetry* 24:185-189.

Schery, S. D., D. J. Holford, J. L. Wilson, and F. M. Phillips. 1988b. "The Flow and Diffusion of Radon Isotopes in Fractured Porous Media, Part 2, Semi-Infinite Media." *Radiation Protection Dosimetry* 24:191-197.

Schery, S. D., and D. Siegel. 1986. "The Role of Channels in the Transport of Radon from the Soil." *Journal of Geophysical Research* 91(B12):12366-12374.

White, F. M. 1991. *Viscous Fluid Flow*, 2nd ed. McGraw-Hill, New York.

Wilkinson, P., and P. J. Dimbylow. 1985. "Radon Diffusion Modeling." *The Science of the Total Environment* 45:227-232.

Technical Assistance to Coordination of Groundwater Research

S. A. Rawson

This project involves program management assistance to the DOE's Subsurface Science Program. The project was initiated in FY 1992 to provide geochemical and hydrogeological information and advice to the Subsurface Science Program on various areas of groundwater research. Specific research coordination activities performed in FY 1992 included

- technical representation of the Subsurface Science Program on intra- and interagency research committees and task forces
- coordination of the physical, chemical, and microbiological aspects of groundwater research between subprograms of the Subsurface Science Program
- participation in workshops and conferences at which scientific issues pertaining to the Subsurface Science Program are addressed.

The major committee interactions were with those subcommittees that address groundwater concerns for the Committee on Earth and Environmental Sciences (CEES) [part of the Federal Coordinating Council on Science and Engineering Technology (FCCSET)] and the Core Planning Group of DOE's Office of Technology Development (OTD) In-Situ Remediation Integrated Program. During FY 1992, the CEES subcommittee on groundwater completed a document, *Role of Science and Technology in Addressing Four Key National Groundwater Issues*, that was approved by the participating agencies including DOE. The document describes various agency research programs in the areas of assurance of groundwater quantity and quality, remediation of contaminated groundwater, minimization of agricultural contamination of groundwater, and disposal of nuclear waste. Principal investigator Rawson assisted in writing DOE's initial submittals to the report and completing the final DOE-wide submittals, and she represented DOE's basic science programs at monthly interagency committee meetings.

During FY 1992, the CEES subcommittee on groundwater was transformed into the Subcommittee on Water Resources. The charter of the new subcommittee includes all federal research programs conducting non-marine surface water research, water/global change interactions, and groundwater research. Dr. Stephen Ragone, U.S. Geological Survey, and Dr. Steven Cordell, U.S. Environmental Protection Agency, are the chairman and vice-chairman of the subcommittee. Members of the new subcommittee drafted a document entitled *Water Resources: A Research Strategy for Critical National Needs*, which covered several topics that relate to groundwater issues faced by DOE. During FY 1992, several versions of the strategy document were reviewed across DOE programs, and review comments were coordinated and assessed for relevance prior to transmittal to the subcommittee.

The principal investigator represented the Subsurface Science Program research program interests to the Core Planning Group of the DOE/OTD In-Situ Remediation Integrated Program. This group met several times during FY 1992 to develop and implement a program plan describing the technical elements within the In-Situ Remediation Integrated Program. The draft program plan was reviewed in January 1992 and the program objectives were established. The primary objective of the In-Situ Remediation Integrated Program is to manage applied research and development of *in situ* remediation technologies for hazardous waste, radioactive wastes, and mixed wastes in groundwater, soils, and storage tanks at DOE sites. The In-Situ Remediation Integrated Program also coordinates technology development with other parts of DOE, such as the Subsurface Science Program, to avoid duplication of effort and maximize technology transfer to the integrated demonstrations within DOE/OTD. The Core Planning Group for the In-Situ Remediation Integrated Program also established its areas of research focus during FY 1992; it solicited proposals for FY 1993 projects in the areas of *in situ* treatment (destructive or extraction technologies, such as bioremediation or electrokinetics), *in situ* containment, and subsurface manipulation, with subordinate interests in process monitoring and control, and process design and information management.

The principal investigator participated in a number of Subsurface Science Program workshops during FY 1992. The Deep Microbiology Subprogram's "Origins" workshop was held in October 1991. Two guiding hypotheses to explain microbial origins in the subsurface were assessed at the workshop: the *in situ* evolution hypothesis, which focused on the survival of microorganisms in sediments since deposition, and the transport hypothesis, which examined the role of microbial transport in populating subsurface environments. After a series of presentations addressing these two hypotheses, working groups of university and national laboratory scientists discussed these topics; the principal investigator assembled the report for the working group that assessed the *in situ* evolution hypothesis. The findings of both working groups were combined in a program plan for the new Subsurface Science Program initiative in microbial origin, *Origins of Microorganisms in Deep Subsurface Environments, Deep Microbiology Subprogram Phase II Preliminary Plan*.

In April 1992, investigators from the Multicomponent Predictive Modeling Subprogram met in Annapolis, Maryland, to discuss their recent research results and to establish future directions for the subprogram. A representative from DOE's Office of Scientific Computing also attended the meeting to describe DOE's program in high-performance computation. Investigators explored the need for their projects into link more closely with Subsurface Science Program experimental projects; the Subsurface Science Program subsequently realigned the modeling projects into subprograms in which experimental research was being conducted.

The Subsurface Science Program initiated planning for a new subprogram in bacterial transport in FY 1992. The principal investigator coordinated the completion of a draft plan for this new Subsurface Science Program subprogram in collaboration with Dr. Aaron Mills of the University of Virginia. The draft plan was

presented in October 1992, for review and comment by participants in a DOE/OHER workshop entitled "Transport of Bacteria through Porous Media: Field-Scale Experiments." The small workshop included scientists with backgrounds in microbiology, hydrology, geochemistry, and geology. The consensus of the workshop participants was that the emphasis should be on forced-gradient transport experiments in a well-characterized hydrogeologic setting, probably on the east coast.

Other activities conducted as part of this project included peer review of research proposals for the Subsurface Science Program, technical support in long-range program planning, and planning and coordination of subprogram meetings.

Terrestrial
Science

Terrestrial Science

Changes in arid and semiarid landscapes in response to stress are a concern on DOE lands, as well as other sites across the nation. For the future, it will be necessary to predict how natural systems will respond to a variety of factors, not just global climate change, but also contamination and restoration activities, on local to regional scales.

PNL is conducting basic scientific studies of the fundamental mechanisms that control the way ecosystems function. The dynamics of soil nutrients, water, gas flux across interfaces, and energy are being examined to understand how various stresses influence the efficiency with which an ecosystem can process its essential resources. To estimate fundamental ecological properties for landscape-sized areas, quantitative remote-sensing techniques are being developed. Databases are providing new perspectives and methods for resolving environmental problems. Research on sampling and scaling methodology is being conducted to ensure that these new research areas are supported on an appropriate theoretical basis.

Soil Microbial Biomass and Activity of a Disturbed and Undisturbed Shrub-Steppe Ecosystem

H. Bolton, Jr., J. L. Smith (U.S. Department of Agriculture - Agricultural Research Service), and S. O. Link

Disturbance of shrub-steppe soils and alterations in plant cover may affect the distribution, size, and activity of soil microorganisms and their ability to biogeochemically cycle essential nutrients. The spatial distribution of plants in arid ecosystems is not uniform, and "islands of fertility" exist around shrubs and grasses. We would therefore expect the soil microbial populations also to be greater around these shrubs and grasses. Our objective in this project was to determine microbial biomass carbon and nitrogen and the microbial activity of soils under the dominant plant types in the arid shrub-steppe and to compare these properties with those of a soil that was initially shrub-steppe but has become an arid annual grassland since farming ceased in the 1940s. Bolton et al. (1990) showed nitrogen mineralization was similar at these two sites when calculated at the landscape level. Because nitrogen mineralization is a microbially mediated process, microbial biomass should have a similar trend. Thus, our hypothesis for FY 1992 research was that soil microbial biomass calculated for the shrub-steppe on an area basis would be the same as that for the annual grassland.

FY 1992 Research Highlights

Soils were sampled at 0- to 5- and 5- to 15-cm depths beneath sagebrush (*Artemisia tridentata* Nutt.), bluebunch wheatgrass [*Elytrigia spicata* (Pursh) D. R. Dewey], and cryptogamic soil lichen crust at the perennial shrub-steppe site and beneath downy brome (*Bromus tectorum* L.) at the annual grassland site. The *E. spicata* soil sample was used to represent the soil under all perennial grass species present at the perennial shrub-steppe site. Soils were analyzed for chemical and physical properties, including pH, inorganic nitrogen, total nitrogen, total carbon, and bulk density. Biological properties of the soil, including microbial biomass and activity, were also analyzed. Soil microbial biomass was analyzed by chloroform fumigation for microbial biomass carbon (Jenkinson and Powlson 1976) and nitrogen (Myrold 1987) without subtracting respiration from the control soil. Soil microbial activity was estimated both by soil respiration in a Gilson® respirometer with a 0.25% (weight per volume, w/v) glucose addition and by dehydrogenase activity (Tabatabai 1982) with a 0.5% (weight per weight, w/w) glucose addition.

For the calculation of a landscape level of soil microbial biomass carbon and nitrogen (i.e., on an area basis), the percentage cover estimates for these two study sites published by Bolton et al. (1990) were used. The percentage cover for *E. spicata* was taken to be the sum of all perennial grasses present at the shrub-steppe

site, because *E. spicata* was the representative perennial grass species sampled in our study. The standard deviations for the site value of biomass carbon and nitrogen were calculated using the standard deviations from both the biomass values on an area basis and the percentage cover, in a manner typical for propagating errors in computation (Skoog and West 1979). The experimental design was completely randomized, with six replicates for each plant type and for both depths. Fisher's (protected) least significant difference (LSD) at $p \leq 0.05$ was used for treatment mean comparisons (Steel and Torrie 1980). Data are reported on oven-dry (105 °C) soil weight.

With depth from 0-5 to 5-15 cm, soil pH and bulk density usually increased, while inorganic nitrogen, total nitrogen, and total carbon decreased (Table 1). The soil under the soil crust was unusual because pH, inorganic nitrogen, total nitrogen, and bulk density were equal at the two depths. The surface soil in the annual grassland underneath *B. tectorum* had the highest inorganic nitrogen, total nitrogen, and total carbon, and the lowest bulk density of all soils assayed. The surface soil at the perennial shrub-steppe site under *E. spicata* and *A. tridentata* had the same inorganic nitrogen, total nitrogen, and total carbon values, while soil under the soil crust contained significantly less of all three. Thus it appears that the shrubs and grasses in the perennial shrub-steppe create resource islands in the surface soil when compared to the soil crust in the interplant area. However, at the 5- to 15-cm soil depth, soils under *A. tridentata*, *E. spicata*, and the soil crust all had the same values for inorganic nitrogen, total nitrogen, and total carbon, indicating that plant-induced spatial heterogeneities in soil nutrients were limited to the surface soil. Such stratification of soil chemical and physical properties as a function of depth is common in arid ecosystems.

Biomass carbon and nitrogen in the surface soil were highest under *B. tectorum*; soils under *A. tridentata* and *E. spicata* had the same values, and soils under the soil crust had the least (Table 2). All soils had similar biomass carbon and nitrogen contents at the 5- to 15-cm depth. Values of soil microbial biomass carbon and nitrogen at the shrub-steppe and annual grassland sites ranged from approximately 2 to 4 times higher in the surface soil than at the 5- to 15-cm depth (Table 2). This pattern indicates the importance of this surface soil layer (0- to

TABLE 1. Selected Chemical and Physical Properties of Semiarid Soils Collected at 0- to 5- and 5- to 15-cm Depths at the Perennial Shrub-Steppe and Annual Grassland Sites

Plant Cover	Depth, cm	pH	Inorganic N, mg/kg	Total N, mg/kg	Total C, mg/kg	Bulk Density, mg/m^3
Perennial shrub-steppe site						
Soil crust	0-5	6.73cd[a]	4.31c	1500e	4800d	1.32a
	5-15	6.94bc	4.62c	1800cde	2900e	1.37a
E. spicata	0-5	6.65d	7.46b	1900bcd	10700b	1.07b
	5-15	7.01ab	4.96c	1500e	3900de	1.37a
A. tridentata	0-5	7.06ab	7.38b	2200b	11800b	1.31a
	5-15	7.21a	5.18c	1700de	4300de	1.32a
Annual grassland site						
B. tectorum	0-5	6.55d	9.79a	3300a	24300a	0.93c
	5-15	7.22a	5.21c	2100bc	6900e	1.32a

(a) Means in the same column that are followed by the same letter are not significantly different ($p \leq 0.05$, n = 6).

TABLE 2. Microbial Biomass Carbon, Microbial Biomass Nitrogen, Respiration, and Dehydrogenase Activity of Soils at 0- to 5- and 5- to 15-cm Depths at the Perennial Shrub-Steppe and Annual Grassland Sites

Plant Cover	Depth, cm	Biomass C, mg/kg	Biomass N, mg/kg	Respiration[a]	Dehydrogenase[b]
Perennial shrub-steppe site					
Soil crust	0-5	333c[c]	57c	3.14c	18.5c
	5-15	187d	32d	1.01d	8.2d
E. spicata	0-5	759b	127b	9.88b	43.7b
	5-15	251cd	44cd	1.22d	10.7cd
A. tridentata	0-5	811b	141b	9.88b	50.2b
	5-15	271cd	45cd	3.04c	14.1cd
Annual grassland site					
B. tectorum	0-5	1014a	174a	16.00a	80.0a
	5-15	241cd	42cd	2.25cd	18.3c

(a) Microliter O_2 per gram per hour at standard temperature and pressure.
(b) 10^{-2} nmol triphenylformazan per gram per minute.
(c) Means in the same column that are followed by the same letter are not significantly different ($p \leq 0.05$, n = 6).

5-cm depth) for microbially mediated processes, such as nutrient cycling and decomposition. Loss of the surface soil through human or natural disturbance would be detrimental to the functioning of this ecosystem. The values for soil microbial biomass carbon and nitrogen reported here are important because there have so far been very few studies to determine the amount of soil microbial biomass in arid or semiarid ecosystems. Soil microbial biomass carbon values for these arid soils (Table 2) are comparable to those for other terrestrial ecosystems and indicate that the amount of soil microbial biomass may not be a limiting factor for decomposition and nutrient cycling.

Soil microbial activity, as determined by soil respiration and soil dehydrogenase activity, was significantly higher at the soil surface and was definitely influenced by plant cover (Table 2). The highest values were found at the 0- to 5-cm soil depth under *B. tectorum* in the annual grassland, with soils in the perennial shrub-steppe under *A. tridentata* and *E. spicata* having the same values, and soils under soil crust having less. At the 5- to 15-cm depth, soil respiration and dehydrogenase activity approached the same values in all soils.

Soil microbial biomass carbon and nitrogen must be calculated on an area basis to extrapolate biomass estimates from a soil weight basis to the landscape or ecosystem level. The bulk densities of these arid soils (Table 1) were significantly different, making it difficult to compare biomass carbon and nitrogen on a soil dry weight basis for landscape-level interpretations. Therefore, the soil microbial biomass carbon and nitrogen values on a soil mass basis (Table 2) were multiplied by the soil bulk density (Table 1), and values for the two soil depths were summed to estimate soil microbial biomass carbon and nitrogen of soils on a volume basis (per hectare to a depth of 15 cm) (Table 3).

The soil under soil crust had the lowest biomass carbon and nitrogen when calculated on an area basis (Table 3). All other soils had the same values for biomass carbon and nitrogen. The low bulk density of the soil under *B. tectorum* decreased its biomass carbon and nitrogen values on an area basis (Table 3) when compared to values calculated on the basis of soil mass (Table 2). The high bulk density of the soils under soil crust and *A. tridentata* (Table 1) increased their soil microbial biomass carbon and nitrogen values on an area basis and their

TABLE 3. Comparison of Landscape-Level Estimates of Soil Microbial Biomass Carbon and Nitrogen at the Perennial Shrub-Steppe and Annual Grassland Sites

Plant Cover	Biomass,[a] kg/ha	Biomass N,[a] kg/ha	Total Cover,[b] %	Site Biomass C,[a] kg/ha	Site Biomass N,[a] kg/ha
Perennial shrub-steppe site					
Soil crust	476a[c]	81a	41.1 (±19.0)[d]	196 (±98.2)[e]	33 (±16.6)
E. spicata[f]	750b	128b	42.5 (±20.3)	319 (±164.6)	54 (±27.0)
A. tridentata	889b	152b	14.4 (±19.0)	128 (±170.8)	22 (±29.4)
B. tectorum[g]	789b	136b	2.0 (±4.5)	16 (±36.0)	3 (±6.8)
Total			100	659 (±259.2)	112 (±43.8)
Annual grassland site					
B. tectorum[h]	789	136	100	789 (±54.9)	136 (±11.2)

(a) To a depth of 15 cm.
(b) The percentage cover was obtained from Bolton et al. (1990). The percentage cover for *E. spicata* includes all perennial grasses.
(c) Means in the same column that are followed by the same letter are not significantly different ($p \leq 0.05$, n = 6).
(d) Mean ± standard deviation (n = 6).
(e) Standard deviations for the site biomass were computed from the standard deviation for percentage cover and biomass.
(f) The microbial biomass values for *E. spicata* were used as an estimate for all perennial grasses.
(g) *B. tectorum* was predominant, although other grass species were noted.
(h) *B. tectorum* was virtually 100% of the cover at this site.

standing relative to the other soils (Table 3) when compared to values calculated on the basis of soil mass (Table 2).

The percentage plant cover (Table 3) at both the perennial shrub-steppe and annual grassland study sites was used to estimate site values for soil biomass carbon and nitrogen. The perennial shrub-steppe site had a soil crust covering all the interplant areas, while at the annual grassland site *B. tectorum* provided almost 100% of the cover. Site values for biomass carbon and nitrogen were calculated by summing the products of the biomass carbon or nitrogen for each soil multiplied by the percent cover of the corresponding plant species. There was no difference in site values of biomass carbon or nitrogen for the perennial shrub-steppe and annual grassland sites (Table 3), confirming our hypothesis that landscape-level estimates of soil microbial biomass would be the same for the perennial shrub-steppe and annual grassland. The large standard deviations from the percent cover data resulted in a large standard deviation for the landscape estimate of biomass carbon and nitrogen at the shrub-steppe site (±259.2 and ±43.8 from Table 3). If percent cover is treated as a number with no error associated with its measurement, then the standard deviations for the landscape estimate of biomass carbon and nitrogen at the perennial shrub-steppe site become ±77.1 and ±11.3, respectively. Even using these small standard deviations, the landscape-level estimates of biomass carbon and nitrogen at the perennial shrub-steppe and annual grassland sites are the same and are within 1 and 1.1 standard deviations, respectively. Our values of soil microbial biomass carbon and nitrogen (Table 3) are in the middle of the range of values reported for numerous other terrestrial ecosystems [the range for biomass carbon was 110 to 1940 kg/ha and biomass nitrogen ranged from 40 to 496 kg/ha (Smith and Paul 1990)].

The differences observed in soil microbial biomass carbon and nitrogen on both an area (Table 3) and a mass basis (Table 2), and those in soil respiration and dehydrogenase activity (Table 2) for soils at the perennial shrub-steppe site, demonstrate that plant cover determined the amount and activity of soil microorganisms. The spatial distribution of plant species at the shrub-steppe study site resulted in "islands of fertility," where microbial biomass and activity were enhanced. Both shrubs and grasses in this shrub-steppe ecosystem created resource islands, when compared with the soil crust, with enhanced microbial biomass and activity in the upper layer on a mass basis (Table 2) and also enhanced microbial biomass carbon and nitrogen on an area basis (Table 3). The disturbed site, the annual grassland, did not have such "islands" but rather had average values across the whole site.

Future Research

Approaches such as those used here and by Bolton et al. (1990) help determine how several plant types influence soil processes across the landscape. However, because soil samples were obtained directly beneath the dominant vegetation at the shrub-steppe site, we lost information on the transition from one plant type to another. The next approach would involve investigating the transitions from one vegetative type to another, to clarify the extent of these islands of fertility and to provide a better estimate of microbially mediated processes at the landscape level.

References

Bolton, H., Jr., J. L. Smith, and R. E. Wildung. 1990. "Nitrogen Mineralization Potential of Shrub-Steppe Soils with Different Disturbance Histories." *Soil Science Society of America Journal* 54:887-891.

Jenkinson, D. S., and D. S. Powlson. 1976. "The Effects of Biocidal Treatments on Metabolism in Soil. 5. Method for Measuring Soil Biomass." *Soil Biology & Biochemistry* 8:209-213.

Myrold, D. D. 1987. "Relationship Between Microbial Biomass Nitrogen and A Nitrogen Availability Index." *Soil Science Society of America Journal* 51:1047-1049.

Skoog, D. A., and D. M. West. 1979. *Analytical Chemistry*, 3rd ed. Holt, Rinehart, and Winston, New York.

Smith, J. L., and E. A. Paul. 1990. "The Significance of Soil Microbial Biomass Estimates." In *Soil Biochemistry*, Vol. 6, eds. J. M. Bollag and G. Stotzky, pp. 357-396. Marcel Dekker, New York.

Steel, R.G.D., and J. H. Torrie. 1980. *Principles and Procedures of Statistics. A Biometrical Approach*, 2nd ed. McGraw-Hill, New York.

Tabatabai, M. A. 1982. "Soil Enzymes." In *Methods of Soil Analysis Part 2. Chemical and Microbiological Properties*, 2nd ed., ed. A. L. Page, pp. 903-947. Agronomy 9, American Society of Agronomy, Madison, Wisconsin.

Defining Resource Islands Using Multiple-Variable Geostatistics

J. J. Halvorson (NORCUS), J. L. Smith (U.S. Department of Agriculture, Agricultural Research Service), H. Bolton, Jr., and R. E. Rossi (FSS International)

Ecologists are increasingly turning to geostatistics for interpretation of ecological phenomena, in part because they recognize the spatial dependence of their data (Rossi et al. 1992). Geostatistics are a class of applied statistics, developed mainly by mathematical geologists and mining engineers to model spatial characteristics of ore deposits and to provide estimates of ore quantity and quality at unsampled locations. Geostatistics include traditional univariate and bivariate analyses followed by descriptive or diagnostic variography, a process whereby the similarity between samples is determined as a function of their separation distance and direction. Such analyses will often show that neighboring samples are more similar to

each other than samples collected farther apart. This spatial dependence may be modeled and used in a technique known as kriging to predict values for locations that have not been sampled (Isaaks and Srivastava 1989).

Application of geostatistics to ecological data may be somewhat limited because the analyses are typically restricted to a single variable at a time, whereas many ecological phenomena are a function of several independent or correlated variables. For example, in natural systems, identification of phenomena such as prime wildlife habitat or potential plant range may require consideration of the spatial co-occurrence of several biotic and abiotic factors existing at different spatial and temporal scales. In addition to biological and physical constraints, regionalizing concepts, such as population carrying capacity, prime agricultural land, or "high-risk" sites, may also be influenced by human factors like cultural constraints, technological innovation, and trade (Budd 1992). Consequently, to be useful for analyzing the spatial characteristics of many kinds of phenomena, flexible geostatistical methods must be developed to simultaneously integrate and summarize the information for several environmental variables.

Resource islands are an example of an ecological phenomenon that is likely to be most accurately described by more than a single parameter. Resource islands are a well-recognized feature in soils, occurring when plants influence the distribution of resources and biogeochemical processes in the soil in their immediate vicinity. This effect has been documented for a number of soil nutrients and vegetation types.

The objective of this study was to measure resource islands under *Artemisia tridentata* as defined by the integration of several soil parameters. More specifically, we applied existing nonparametric geostatistical techniques with a simple modification to simultaneously describe and model locations in the landscape that met specified multivariate selection criteria. Through the use of nonparametric geostatistics we were able to analyze data sets containing highly variant phenomena and, furthermore, were able to provide risk-qualified estimates of values at unsampled locations (Journel 1983). Although our example concerned small-scale phenomena and a modest number of variables, the technique demonstrated is flexible enough to be applicable to any spatial scale or number of variables.

FY 1992 Research Highlights

The study was conducted at the Arid Land Ecology (ALE) Reserve, located on the Hanford Site in southeastern Washington [see Bolton et al. (1990) for details] following a specific sampling protocol. Briefly, to assess the distribution of soil resources with respect to plant location, cores of surface soil (10.5 cm in diameter by 5 cm deep) were collected at 41 specific locations within five 2-m by 2-m plots, each centered on a mature *A. tridentata* individual. Each sample was analyzed for total inorganic nitrogen (TI-N), water-soluble forms of carbon (H_2O-C), soil microbial biomass carbon (SIR-C), and metabolic quotient (qCO_2) or the amount of CO_2-C produced per unit of SIR-C (Anderson and Domsch 1986; Insam and Haselwandter 1989). In a separate incubation, cumulative soil respiration (MIN-C) was measured for each sample.

Data were analyzed with univariate and nonparametric geostatistics. Nonparametric geostatistics are useful for analyzing data that is skewed or contains outliers. The basis of this approach is a data transformation based on the rank order of the data. The transformation converts a continuous random variable into an indicator or binary random variable (Journel 1983; Isaaks and Srivastava 1989; Rossi et al. 1992). An indicator random variable I(x;z) is a random variable that is coded either 0 or 1 according to whether the underlying continuous variable Z(x) exceeds a specified threshold or cutoff value, z. For this work, we coded data as 0 if $Z(x) \leq z$ and 1 if $Z(x) > z$. Although the indicator transform approach has usually been applied to a single variable, we extended the concept to account for multiple variables. The multiple-variable indicator transform (MVIT) is a method to spatially summarize the information from a number of variables. It is simply an extension of the traditional single-variable indicator transform, whereby a new composite indicator variable is created from the results of several single transformations.

We identified several individual variables that we assumed to represent resource islands, and specified critical threshold levels for each variable. These thresholds were used as a basis for the indicator transformation. For this study, data for five soil parameters (TI-N, H_2O-C, SIR-C, qCO_2, and MIN-C) were indicator-transformed using the local (i.e., within plot) median of each variable as the critical threshold value (Table 1). Each variable at a location was transformed by comparing it to its particular critical threshold value. These indicator-transformed data were analyzed separately and also integrated together to create three new composite variables (or MVITs) of varying complexity. The least restrictive MVIT (COMB3) was coded 1 if any three of the five variables were above the median. The second MVIT (COMB4) was coded 1 if any four of the five variables were coded 1. Our most stringent definition of a resource island (COMB5) required that every variable be found in concentrations greater than the median. Once specified, MVIT data were analyzed just as an individual indicator-transformed variable would be. For this study, we evaluated spatial continuity with "non-ergodic" correlograms (Srivastava and Parker 1989) and estimated the values of soil properties at unsampled locations using ordinary kriging (Isaaks and Srivastava 1989).

As a simple analysis, the sum of individual indicator variables (five total) that met their respective threshold limits was plotted (e.g., Figure 1). Within each 2-m by 2-m plot, we observed a broad range of resource availability, ranging from locations where no variable was greater than the local median (coded 0) through locations where all variables exceeded the local

TABLE 1. Example of Indicator Transformations for Total Inorganic Nitrogen (TI-N), Soil Microbial Biomass-Carbon (SIR-C), Water-Soluble Carbon (H_2O-C), Soil Respiration (MIN-C), and Metabolic Quotients (QCO_2) for Soil Located at Sampling Points X and Y. The critical threshold values used as the basis for the indicator transformation correspond to the median values of each variable calculated for one plot.

X	Y	TI-N, mg/kg dry soil	SIR-C, mg/kg dry soil	H_2O-C, mg/kg dry soil	MIN-C, mg CO_2-C per kg dry soil[a]	QCO_2C, mg CO_2-C per kg SIR-C per day
Untransformed Data						
2.7	18.6	2.2	970	34.5	411	0.043
4.7	18.6	1.1	389	26.9	226	0.028
2.7	18.8	1.8	641	20.6	312	0.029
2.9	18.8	5.6	737	27.3	362	0.026
Threshold Values		1.4	544	28.5	337	0.035
Indicator Transformations						
2.7	18.6	1	1	1	1	1
4.7	18.6	0	0	0	0	0
2.7	18.8	1	1	0	0	0
2.9	18.8	1	1	0	1	0

Multiple-Indicator Transformations		COMB3	COMB4	COMB5
2.7	18.6	1	1	1
4.7	18.6	0	0	0
2.7	18.8	0	0	0
2.9	18.8	1	0	0

(a) 3-week incubation (23°C, dark).

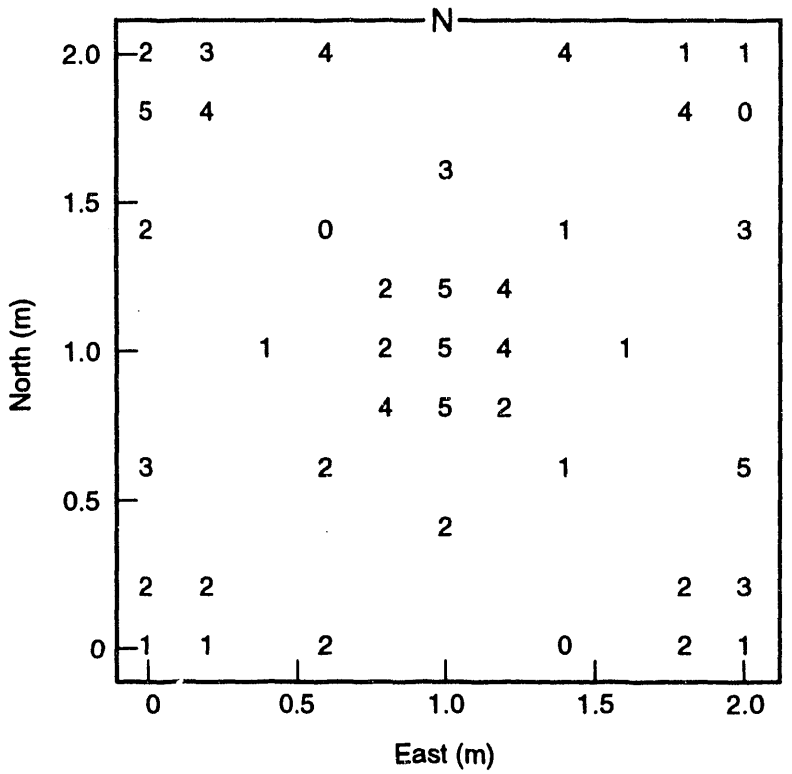

FIGURE 1. The Number of Individual Soil Variables That Were Above the Local Median in the Same Plot as in Table 1. Values have a range from 0 (no variable was greater than the local median) to 5 (all variables were greater than the local median).

median (coded 5). In general, we found that the highest numbers of variables above the local median were congregated in the vicinity of the *A. tridentata* plant, but values near 5 were also occasionally observed elsewhere.

The indicator transform was useful for identifying underlying patterns related to the probability of resource encounter that were otherwise camouflaged by the magnitude of outliers. Figure 2 illustrates differences between continuous, non-transformed TI-N data and indicator-transformed TI-N data for one plot. A posting of the raw untransformed TI-N data (Figure 2a) showed most values were in the range of 1 to 7 mg/kg dry soil, as reflected by mean and median values for TI-N of 3.7 and 2.7 mg/kg dry soil, respectively. However, the 41 individual samples collected in the plot had a range of 0.9 - 17.3 mg/kg dry soil and a coefficient of variation of over 100%. Several locations with large "outliers" were observed in the northeast, northwest, and southeast corners of the plot. The presence of these outliers in a field of lower values resulted in a correlogram for the plot that had short range structure (0.38 m) but high variability (the experimental correlogram value is greater than 1.5 at a lag of 0.34 m) (Figure 2b). The effect of these large values was also strongly expressed as concentration spikes in the map of kriged estimates (Figure 2c). Such spikes obscured any apparent pattern of resources associated with *A. tridentata*.

Indicator transformation of the raw data resulted in a discrete field of 0s and 1s (Figure 2d) based on comparisons to the local median values. The transformation deemphasized the effect of the very large values, since all locations with concentrations greater than 2.7 mg/kg dry soil were coded alike as 1. The correlogram of indicator-transformed data revealed a higher relative

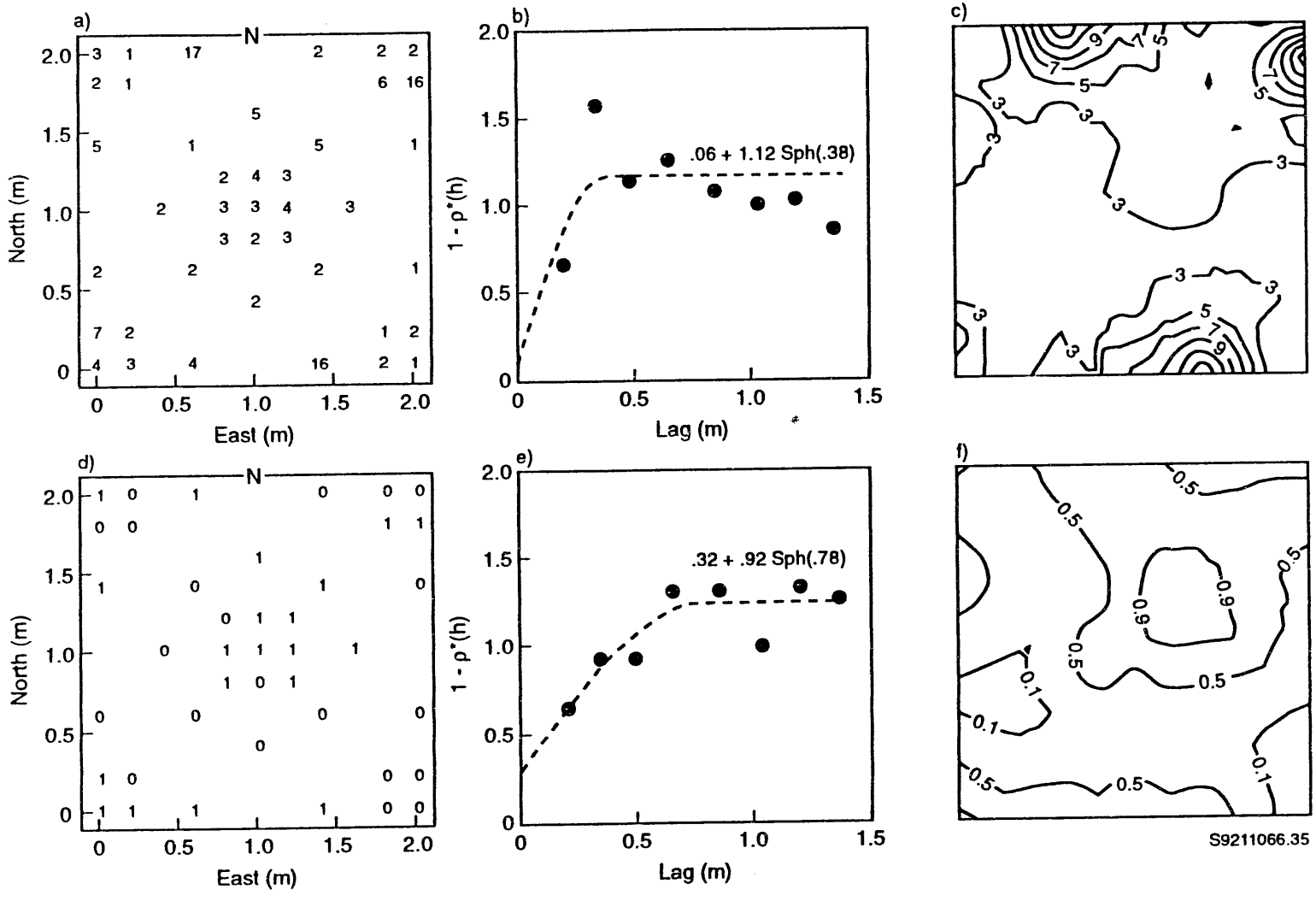

FIGURE 2. Maps and Correlograms. a) Total inorganic N concentrations in soil collected at locations around an *Artemisia tridentata* plant; b) empirical omnidirectional autocorrelogram calculated for the values in a; c) map of kriged estimates calculated with ordinary kriging; d) indicator transformations of TI-N concentration based on the local median value (2.4 mg/kg dry soil); e) empirical omnidirectional autocorrelogram of indicator-transformed data; f) the resulting map of kriged estimates that are equivalent to the probabilities of the value being greater than the local median.

intercept or nugget (0.32) and a longer range (0.78 m) structure than the correlogram for untransformed data (Figure 2e). The map of kriged estimates produced with the indicator-transformed data was also different from the kriged map produced with untransformed values. Unlike Figure 2c, where the highest concentrations were located in the northwest, northeast, and southeast, the map calculated from indicator-transformed TI-N that revealed the region with the highest probabilities for encountering TI-N in concentrations above the median was located closer to the center of the plot, nearer the *A. tridentata* (Figure 2f). Emphasizing the likelihood of encountering "enough" resources, rather than focusing on only the locations of highest concentrations, may change the way in which resource islands are evaluated. The ecological significance of resource distribution may be most related to the probability of encountering them in nonlimiting quantities or quality.

Kriged predictions were also calculated using MVITs (Figure 3). The values in the maps represent the joint probability that the MVIT threshold criteria were met. That is, in the case of COMB5, the probability that all five of the individual indicator soil variables were greater than their local medians. The maps for all plots demonstrated two general phenomena. First, the regionalization of data was inversely related to the number of individual indicators comprised by the MVIT. In general, the more restrictive the MVIT, the fewer locations successfully met the criteria and the smaller the size of the areas with high probability (e.g., 90% or better) for meeting the MVIT criteria. A second conclusion derived from the maps was that resource islands, defined by the conjunction of several soil parameters, were spatially associated with *A. tridentata* (see Figure 3a for a map of plant location). For example, each plot contained regions with at least a 90% probability of meeting the COMB3 criteria (Figure 3b). Each plot also contained areas with high probabilities for meeting the COMB4 criteria, usually in a smaller, localized region beneath *A. tridentata* (Figure 3c). The maps of probabilities of meeting the most stringent set of conditions, COMB5, were mostvariable. One plot (Figure 3d) contained no location with 90% or better probability for an area with all five of the individual indicators above their respective local medians. In the other plots, the areas of highest probability were smaller than those for COMB4 and limited to the center of the plot, under *A. tridentata*.

The MVIT approach integrates the disparate spatial characteristics of individual indicator parameters. The spatial continuity of the resulting single MVIT variable is then more easily analyzed. Unlike some indexes, an MVIT connotes a very specific meaning conditioned on the threshold cutoffs for each individual indicator parameter. This and the ability to consider a potentially unlimited number of variables at different spatial scales simultaneously allows the MVIT considerable flexibility.

References

Anderson T. H., and K. H. Domsch. 1986. "Carbon Assimilation and Microbial Activity in the Soil." *Zeitschrift für Pflanzenernaehring und Bodenkunde* 149:457-486.

Bolton, H., Jr., J. L. Smith, and R. E. Wildung. 1990. "Nitrogen Mineralization Potentials of Shrub-Steppe Soils with Different Disturbance Histories." *Soil Science Society of America Journal* 54:887-891.

Budd, W. W. 1992. "What Capacity the Land?" *Journal of Soil and Water Conservation* 47:28-31.

Insam, H., and K. Haselwandter. 1989. "Metabolic Quotient of the Soil Microflora in Relation to Plant Succession." *Oecologia* 79:174-178.

Isaaks, E. H., and R. M. Srivastava. 1989. *An Introduction to Applied Geostatistics*. Oxford University Press, New York.

Journel, A. G. 1983. "Non-Parametric Estimation of Spatial Distributions." *Journal of the International Association for Mathematical Geology* 15:445-468.

Rossi, R. E., D. J. Mulla, A. G. Journel, and E. H. Franz. 1992. "Geostatistical Tools for Modeling and Interpreting Ecological Spatial Dependence." *Ecological Monographs* 62:277-314.

Srivastava, R. M., and H. M. Parker. 1989. "Robust Measure of Spatial Continuity." In *Geostatistics*, Vol. 1, ed. M. Armstrong, pp. 295-308. Kluwer Academic, Boston.

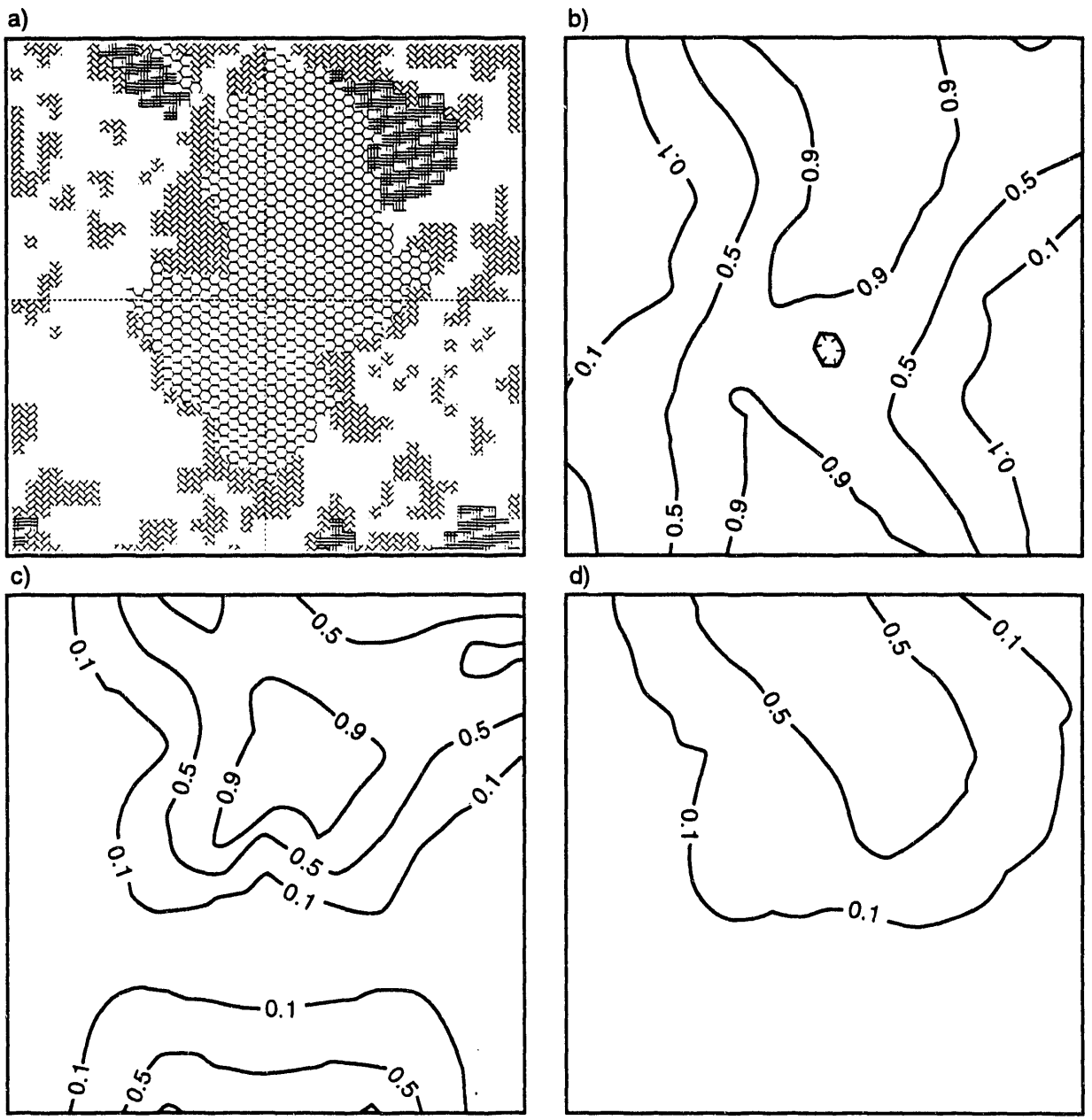

FIGURE 3. Maps of a) Plant Location, and Kriged Estimates of b) COMB3, c) COMB4, and d) COMB5 Probabilities. Vegetation maps indicate the vertical projections of *Artemisia tridentata* (honeycomb pattern), *Elytrigia spicata* (plaid pattern), and other grass species (herringbone pattern) as determined by photographs. Kriged maps were based on omnidirectional correlogram models and calculated from 3-10 neighbors in a 0.6-m search radius. The values portrayed in the maps are the probabilities that samples collected at the specified location will meet the composite criteria.

Changes in Hydraulic Resistance of *Bromus tectorum* under Enhanced Nitrogen and Water Conditions

J. L. Downs and S. O. Link

In arid lands where water is the main factor that limits plant growth, the flow of water through the soil-plant-atmosphere continuum can be a difficult and complex process. Plant resistances to uptake of water from the soil and transport to the stomates are difficult both to separate and to quantify. Because below-ground processes are difficult to study, little definitive knowledge is available concerning the flow of water across the roots and the resistances of the soil-rhizosphere-root water pathway.

Resistance to water flow through the soil to the roots is a function of the soil matrix and the water content of the soil. Resistances across the rhizosphere and root and into the shoot may change with the age of the plant, diurnal cycles, or nutrient availability. These resistances affect the amount of water transpired during the day, as well as the degree to which plants are able to recover from water stress overnight.

Resistances to water uptake and transport were studied for *Bromus tectorum* L., an introduced winter annual grass that dominates old-field communities on the Hanford Site in southeastern Washington. The values for resistance were calculated as a function of the relationship between transpiration and shoot xylem potential under enhanced water and nitrogen conditions, in an attempt to evaluate which factors limit the ability of the plant to absorb and transport water.

FY 1992 Research Highlights

Transpiration and shoot xylem potential were measured on plants growing in old-field communities on the Arid Lands Ecology facility, which is part of the DOE's Hanford Site. The Site lies in the shrub-steppe ecoregion and receives between 15 and 18 cm of precipitation per year, 75% of which arrives between October and March. Twenty circular plots, each 2 m in diameter, were located in the old field. Treatments were randomly assigned--five each for a control (no additional water or nitrogen), additional nitrogen (10 g/m^2), additional water (2x annual winter precipitation), and additional water plus nitrogen. Minirhizotrons and neutron probe access ports were installed in each of the twenty plots in early February.

From April 23 to April 27, transpiration was measured on replicate plants in each treatment using a LiCor 1600 porometer with a cylindrical chamber. Measurements were taken between 7:00 and 10:00 a.m. Xylem potentials were measured before dawn, and each time porometer measurements were made using a Scholander-type pressure chamber. Resistance values were calculated using the relationship $R_h = \Delta\Psi/F$, where F is the transpirational flux and $\Delta\Psi$ is the xylem potential gradient. Neutron probe data were collected twice during a 10-day period at the time of transpiration and xylem potential measurements. Root numbers and distributions were observed in the minirhizotrons using a down-hole miniature video camera.

Examination of predawn xylem potentials indicated that plants receiving additional nitrogen were better able to recover from transpirational stress overnight. These plants were able to recover to xylem potentials of -0.3 MPa, even though measured soil water potentials in the top 45 cm of soil ranged from 2.5 to 3.3 MPa for that treatment. Plants in the control plots were able only to recover to -0.9 to -1.0 MPa overnight (Figure 1a) even under higher measured soil water potentials (-0.8 to -1.1 MPa) in the top 45 cm of the soil profile. Profiles of soil moisture content calculated from neutron probe measurements show higher water contents at depths below 45 cm. These results seem to indicate that plants receiving additional nitrogen were either better able to access soil water, or better able to transport water from the soil to the shoot.

Mean midday xylem potentials of treatments receiving additional nitrogen were lower than midday xylem potentials of the control and water treatments (Figure 1b). Additional canopy biomass resulting from growth under enhanced nitrogen conditions, and thus higher transpirational demand per unit land area, may explain the higher level of water stress. The R_h values calculated at the canopy level are higher for the nitrogen treatment than for the control treatments

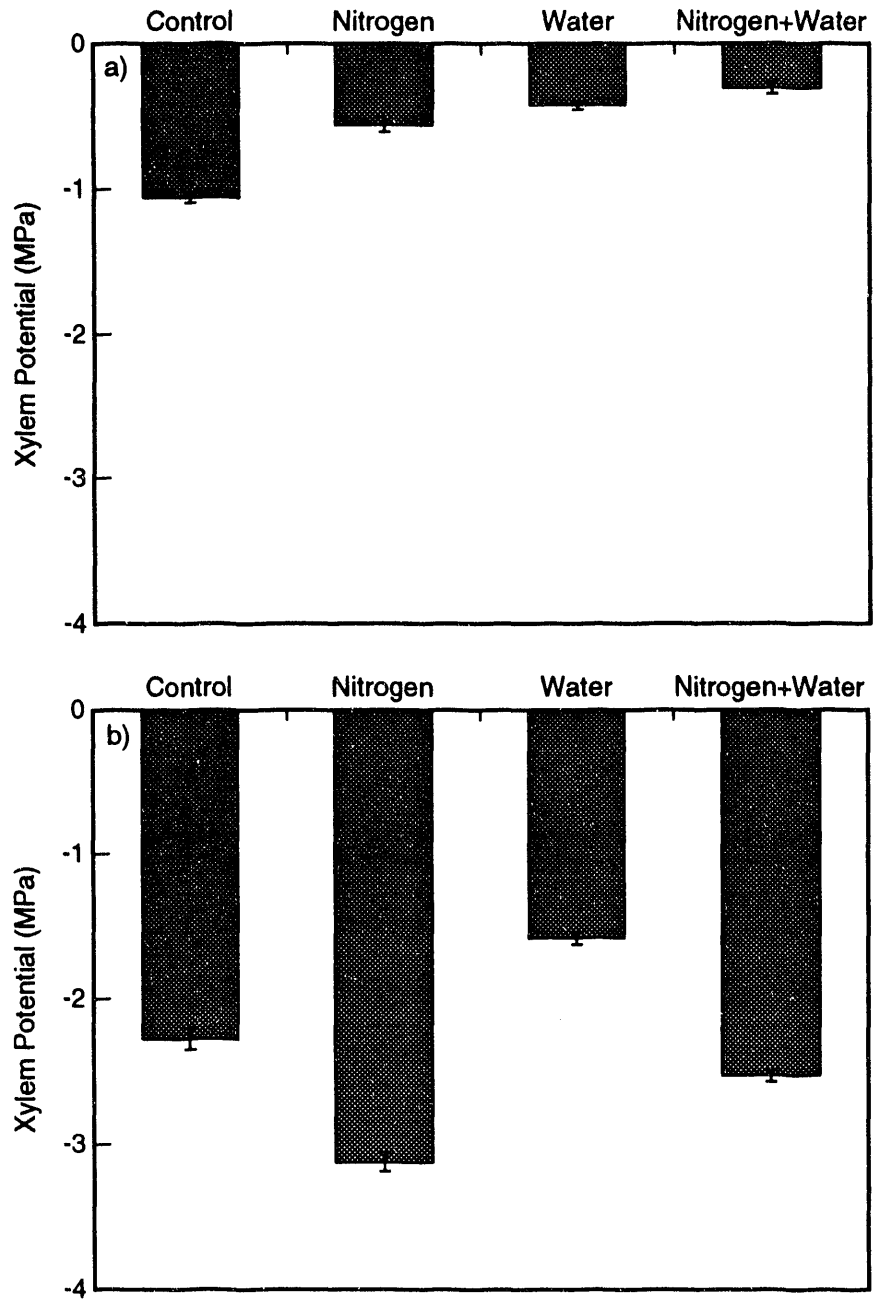

FIGURE 1. Mean Xylem Potentials at a) Dawn and b) Midday

Control R_h values are higher than those calculated for the enhanced water treatment, which in turn are greater than those for the nitrogen + water treatment.

Significant differences in number of roots from 0 to 75 cm below the surface were noted only for the control plants at the 50 to 75 cm depth. Fewer roots were found at depth beneath control plants. The mean number of roots in the profile beneath treatments receiving additional nitrogen, although highly variable, was generally greater than in other treatments. Comparison of the neutron probe soil moisture profiles for the water

and nitrogen + water treatments indicates that plants in the nitrogen + water plot were able to extract more moisture from the profile over the 10-day period.

Future Research

Resistance of *Bromus tectorum* to uptake and transport of water from the soil under field conditions seems to be limited by the resistance of the soil matrix under soil water contents of 0.08 g/g and less. At higher soil water contents, the treatment with nitrogen + water was better able to extract water from the soil and transport it to the shoot. Future work might address the changes in root/shoot ratio that occur under enhanced nitrogen and water conditions.

The Effects of Nitrogen and Water on the Efficiency of Water Use and Nitrogen Use by *Bromus tectorum* in the Field

S. O. Link, H. Bolton, Jr., and J. L. Downs

The limited availability of such resources as nitrogen and water in arid ecosystems strongly influences plant productivity (West and Skujins 1978). Consequently, ecosystem biogeochemical cycling processes, water-use efficiency, and nitrogen-use efficiency are also strongly influenced by the availability of these resources. Resource availability can be affected by human-induced perturbations, such as global warming and air pollution, and by physical disturbance. To better understand how efficiently arid ecosystems process water, carbon, and nitrogen, we have been conducting experiments in the field to determine how such ecosystems respond to increases in water and nitrogen. Developing models of such processes will allow us to hypothesize how the ecosystem will respond to various scenarios of global climate change.

Water-use efficiency generally increases in situations with decreasing water. This means that plants will acquire more carbon for the amount of water lost as water becomes limiting (Fischer and Turner 1978). It has been found that water-use efficiency in cold-desert perennial shrubs and grasses decreased with additional water and increased with increased nitrogen (Toft et al. 1989). The addition of nitrogen in the field has been shown to increase water-use efficiency for the semiarid pinyon and juniper (*Pinus edulis* and *Juniperus monosperma*; Lajtha and Barnes 1991).

Nitrogen-use efficiency (biomass/biomass nitrogen) generally decreases as nitrogen increases (Chapin and van Cleve 1989). The relationship between nitrogen-use efficiency and water has not been studied specifically, but Field et al. (1983) found that chaparral evergreen species from dry sites had lower nitrogen-use efficiency than species from wetter sites. They also observed a negative correlation between water-use efficiency and nitrogen-use efficiency for instantaneous estimates.

We conducted field experiments in FY 1991 to determine the relationship between biomass production and additional nitrogen and water in the annual grass *Bromus tectorum*. We found that biomass production was sensitive to additional nitrogen and water, but only when they were added in combination. We therefore concluded that both resources are limiting for biomass production. The purpose of our FY 1992 work was to determine 1) the long-term relationships between water-use efficiency and nitrogen-use efficiency with additional nitrogen and water, and 2) which resource, water or nitrogen, is more limiting for *Bromus tectorum*.

FY 1992 Research Highlights

Our field site is located in the Lower Snively Field on the Arid Lands Ecology (ALE) Reserve at the Hanford Site. The experimental design involved six levels of water and six levels of nitrogen, with five replicate plots, for a total of 180 experimental units. Each experimental plot was approximately 1 m in diameter. The plots were aligned along six drip-irrigation lines. These lines were randomly placed in the field, with each line representing a different water treatment level. Nitrogen treatment levels were randomly chosen for a total of 30 plots along each irrigation line.

The water treatments were applied on March 6 - 8 and March 18 - 20, 1991. The nitrogen treatments were applied in the last week of February. The natural precipitation (control

water-treatment level) was 13.23 cm from October 1, 1990, until May 30, 1991. For the other five water-treatment levels, added irrigation water was 7.93, 13.75, 17.54, 22.63, and 29.85 cm.

Nitrogen was added as NH_4NO_3 in a 1-L solution of water to achieve the additional nitrogen-treatment levels. An additional unamended liter of water was applied to the control nitrogen treatment plots to maintain comparability among all experimental units. The control level of nitrogen in the top 15 cm of soil was 0.937 g/m^2 (Bolton et al. 1990). The additional nitrogen in the form of NH_4NO_3 yielded nitrogen levels of 3.3, 6.6, 10, 20, and 30 g/m^2 for the other five nitrogen treatment levels.

Plants were harvested over a 2-week period in May. Harvesting was done when the plants were senescing. This stage occurred earlier for the low-water treatments and later for the higher-water treatments. This harvesting plan was followed so that the plants would be harvested at maximum biomass development for all treatments. The harvested area was 0.1 m^2. Plants were placed in plastic bags and returned to the laboratory. The samples were then oven-dried at 55°C for 48 h and weighed.

Nitrogen-use efficiency was computed as the shoot biomass produced divided by total shoot nitrogen. Shoot nitrogen was measured using the Dumas combustion technique on a ground subsample of each experimental unit and is expressed as percent nitrogen.

Water-use efficiency was estimated through the use of carbon isotope discrimination ($^{13}\partial$). Water-use efficiency is linearly correlated with $^{13}\partial$ (Hubick et al. 1986). Thus a low value of $^{13}\partial$ corresponds to a low water-use efficiency. Entire shoots from the harvested lot from all 180 experimental units were analyzed. Dried shoots were ground in a Wiley mill and the $^{13}\partial$ values determined with an isotope ratioing mass spectrometer at the Stable Isotope Facility at the University of Utah, as described by Ehleringer and Cooper (1988).

The model used to describe the relation between total shoot nitrogen and water and soil nitrogen was based on a Michaelis-Menton (rectangular hyperbola) equation, as described by Thornley and Johnson (1990). The relationship between soil nitrogen and total shoot nitrogen is

$$Y = Y_{max}[N/(h + N)] \quad (1)$$

where Y = total shoot nitrogen
Y_{max} = estimated maximum total shoot nitrogen
N = soil nitrogen level
h = a parameter describing the soil nitrogen level that yields a half-maximum total shoot nitrogen.

The relationship between water and total shoot nitrogen is

$$Y = a + bW \quad (2)$$

where W is the water level and a and b are empirical parameters. Total shoot nitrogen as a function of water and nitrogen was predicted by multiplying Equations (1) and (2), as follows:

$$Y = (a + bW)[N/(h + N)] \quad (3)$$

where (a + bW) is now equivalent to Y_{max} as a function of W.

The nitrogen uptake ratio is defined as the ratio of total shoot nitrogen to soil nitrogen.

The model used to describe the relation between total shoot nitrogen and nitrogen-use efficiency was based on an exponential equation. The relationship between shoot nitrogen and nitrogen-use efficiency (NUE) is

$$NUE = a\, e^{(bN)} \quad (4)$$

where a and b are empirical parameters. No relationship between water and nitrogen-use efficiency was apparent.

The model used to describe the relationship between percent shoot nitrogen and water and $^{13}\partial$ is based on exponential equations. The relationship between percent shoot nitrogen and $^{13}\partial$ is

$$^{13}\partial = a\, e^{(b\%N)} \quad (5)$$

where a and b are empirical parameters.

The relationship between water and $^{13}\partial$ is

$$^{13}\partial = a\, e^{(bW)} \quad (6)$$

where a and b are empirical parameters. The $^{13}\partial$ was predicted as a function of water and percent shoot nitrogen by multiplying Equations (1) and (2) with the addition of an interaction term, as follows:

$$^{13}\partial = a\, e^{(bW + c\%N + dW\%N)} \quad (7)$$

where a, b, c, and d are empirical parameters.

The parameters were obtained using nonlinear regression.

Total shoot nitrogen related primarily to the amount of nitrogen added to the soil and secondarily to the amount of water. The relationship between soil nitrogen and total shoot nitrogen [Equation (1)] accounted for 73% of the variation in the data. When water was included, as in Equation (3), the amount of variation explained increased to 85%. The fact that soil nitrogen is the stronger predictor of total shoot nitrogen is apparent by comparing Figures 1 and 2. Figure 1 displays observed and predicted data [Equation (3)] showing the saturation relationship between soil nitrogen and total shoot nitrogen. Soil nitrogen levels above 10.937 g/m^2 do not significantly increase total shoot nitrogen. In contrast, Figure 2 displays the relatively weak relationship between water and total shoot nitrogen. Increasing water does increase total shoot nitrogen. The nitrogen uptake ratio (Figure 3) indicates that nitrogen is taken up by the plant more efficiently when soil nitrogen is at control levels. The nitrogen uptake ratio decreases to less than 1 with increasing soil nitrogen.

Nitrogen-use efficiency decreased with increasing shoot nitrogen (Figure 4) but was not related to water (Figure 5). The predicted curve in Figure 4 was generated from Equation (4).

The carbon isotope ratio, a measure of seasonal water-use efficiency, was largely a function of percent nitrogen and secondarily a function of water. The relationship between percent nitrogen and $^{13}\partial$ [Equation (5)] accounted for 58% of the variation in the data. When water was included [as in Equation (7)], the amount of variation explained increased to 66%. The fact that percent nitrogen is the stronger predictor of $^{13}\partial$ is made apparent by comparing Figures 6 and 7. Figure 6 displays observed and predicted data [Equation (7)] showing the basically linear relationship between percent nitrogen and $^{13}\partial$. As percent nitrogen increases, so does $^{13}\partial$; thus water-use efficiency increases with an increasing percentage of nitrogen. In contrast, the water level had little effect on $^{13}\partial$ (Figure 7). However, even though water was a weak predictor of $^{13}\partial$, $^{13}\partial$ did decrease with increasing water for the control and lowest level of added nitrogen. At higher levels of soil nitrogen, there was no relationship between water and $^{13}\partial$.

The carbon isotope ratio or water-use efficiency was negatively correlated with nitrogen-use efficiency (Figure 8). Plants expressing high water-use efficiency had low nitrogen-use efficiency, and those expressing low water-use efficiency had high nitrogen-use efficiency.

The results of this experiment indicate that nitrogen is more limiting than water for total shoot nitrogen, nitrogen-use efficiency, and $^{13}\partial$ in *B. tectorum*. All of these characteristics were more sensitive to nitrogen than to water.

In our studies, we successfully encompassed the range of nitrogen additions required to define the relationship between total shoot nitrogen and soil nitrogen. Total shoot nitrogen was sensitive to soil nitrogen up to a level of 10.937 g/m^2; above that level there was no effect. Similar relationships have been observed in marsh plants

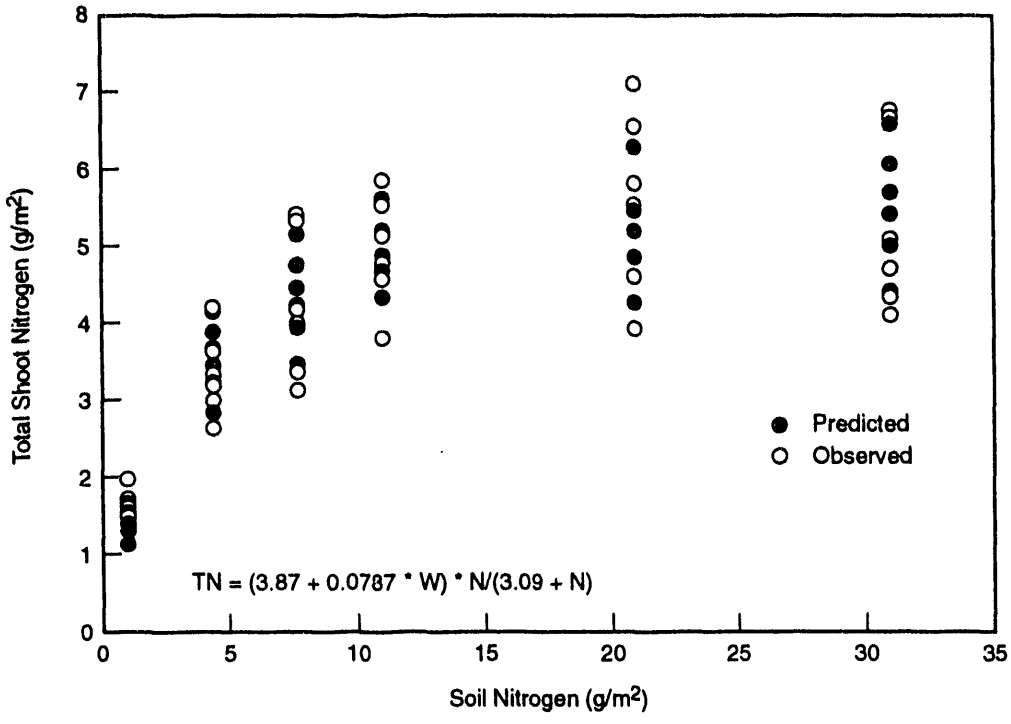

FIGURE 1. The Relationship between Total Shoot Nitrogen and the Predictor Variables (Soil Nitrogen and Water) Displayed against Soil Nitrogen for *Bromus tectorum*

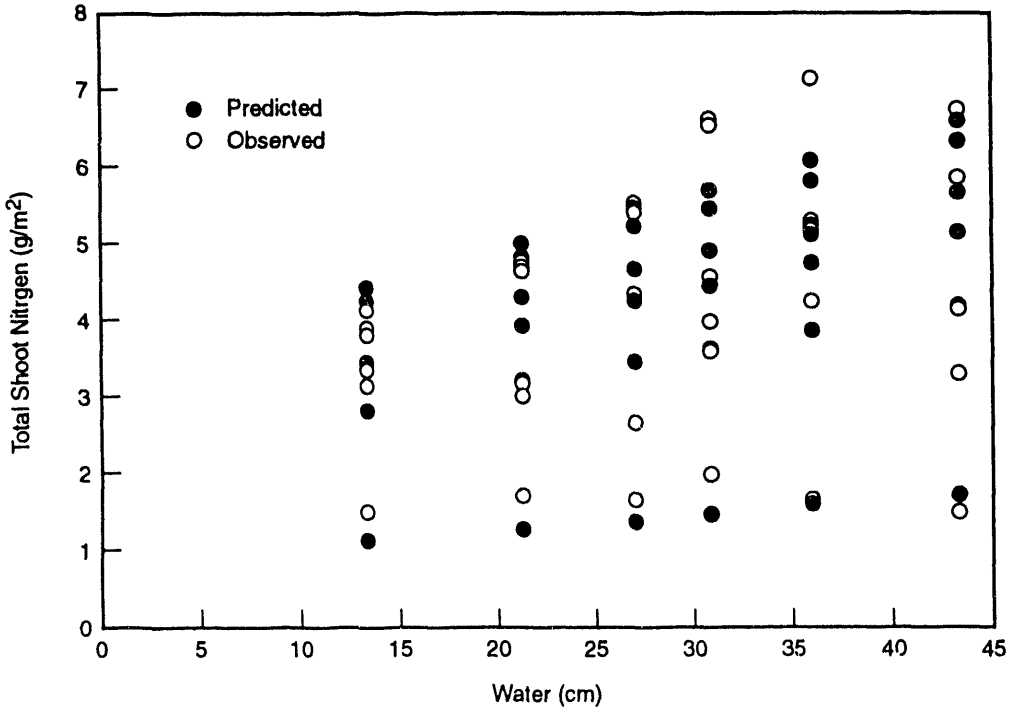

FIGURE 2. The Relationship between Total Shoot Nitrogen and the Predictor Variables (Soil Nitrogen and Water) Displayed against Water for *Bromus tectorum*

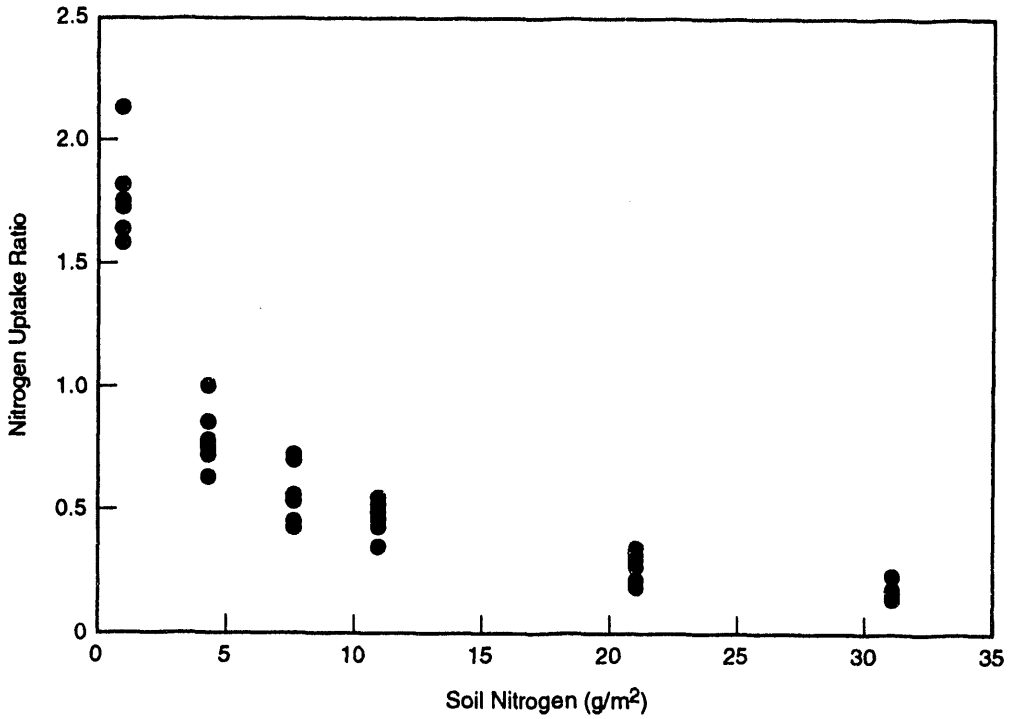

FIGURE 3. Nitrogen Uptake Ratio of *Bromus tectorum* as Function of Soil Nitrogen

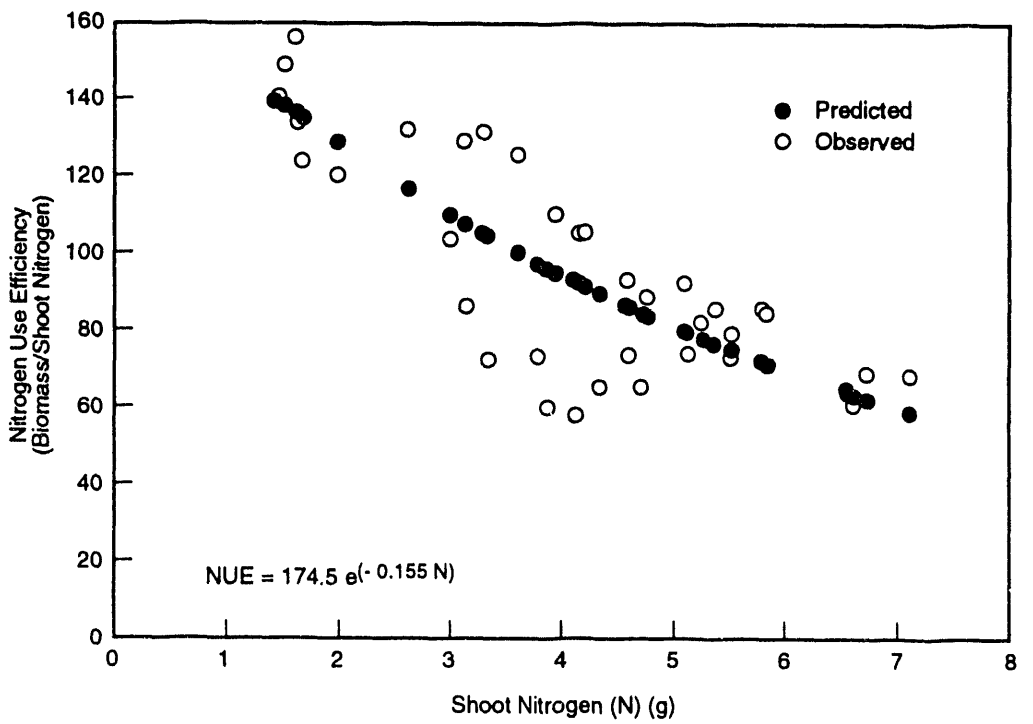

FIGURE 4. The Relationship between Nitrogen-Use Efficiency and Soil Nitrogen for *Bromus tectorum*

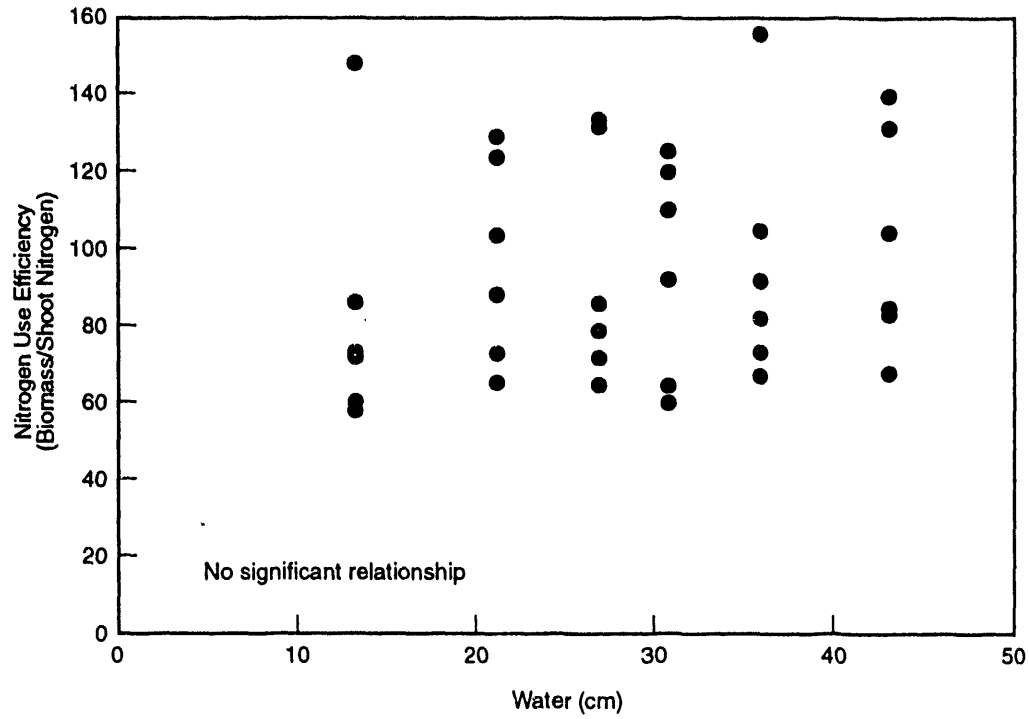

FIGURE 5. The Relationship between Nitrogen-Use Efficiency and Water for *Bromus tectorum*

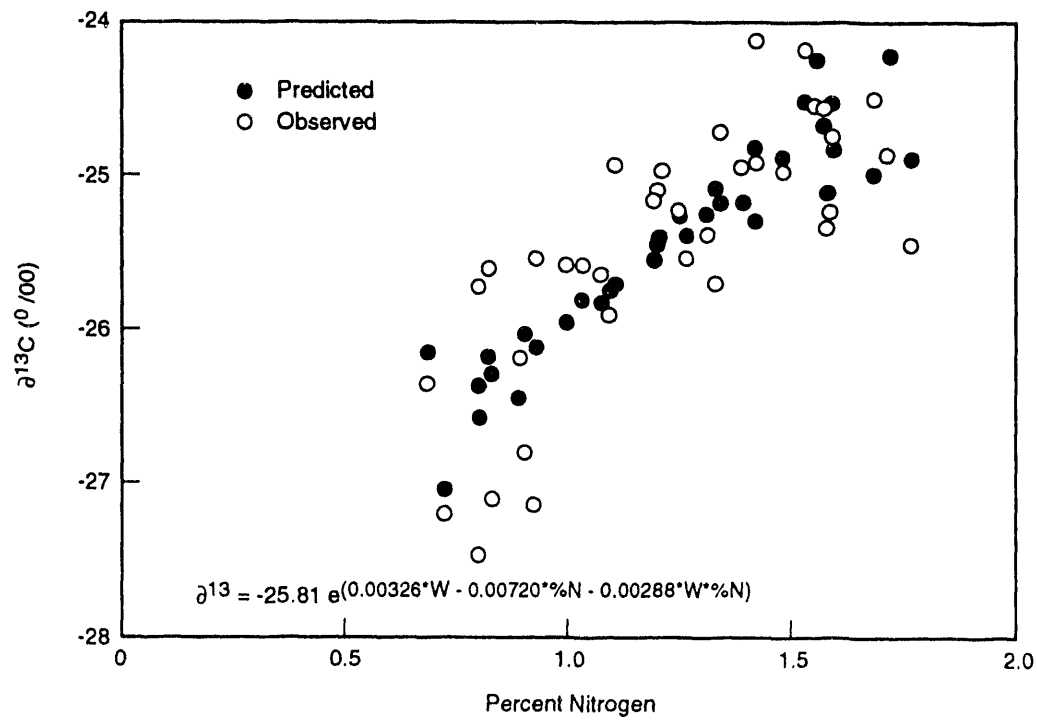

FIGURE 6. The Relationship between $^{13}\partial$ and the Predictor Variables (percent nitrogen and water) Displayed against Percent Nitrogen for *Bromus tectorum*. Water-use efficiency is positively correlated with $^{13}\partial$.

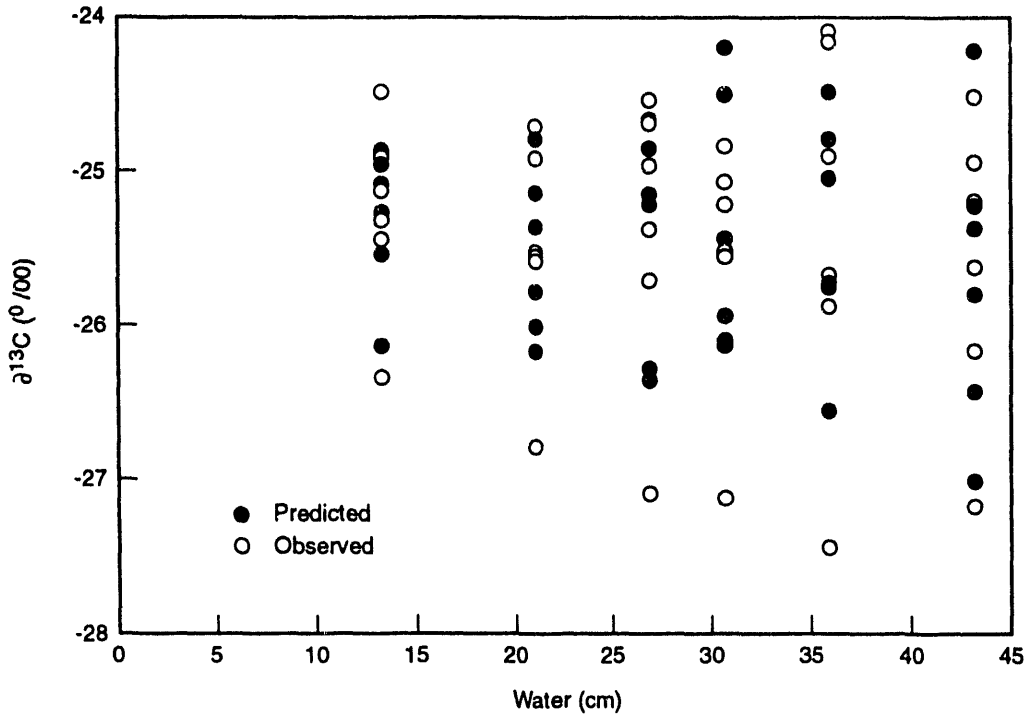

FIGURE 7. The Relationship between $^{13}\partial$ and the Predictor Variables (percent nitrogen and water) Displayed against Water for *Bromus tectorum*. Water-use efficiency is positively correlated with $^{13}\partial$.

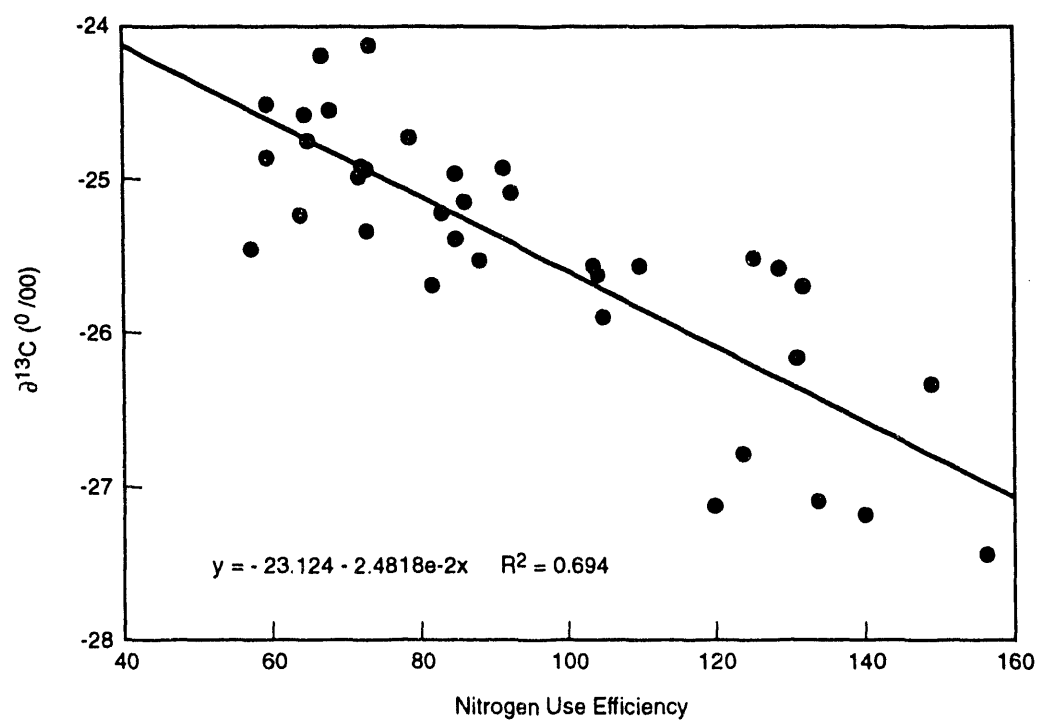

FIGURE 8. The Relationship between $^{13}\partial$ (water-use efficiency) and Nitrogen-Use Efficiency

(Shaver and Melillo 1984). The same effect is further evidenced by the nitrogen uptake ratio. The control values for the nitrogen uptake ratio were greater than 1, suggesting that more nitrogen was taken up by the plant than there was in the soil. This discrepancy can be explained by the fact that the harvest data were collected at the end of the growing season (and thus represented accumulated nitrogen), but the control soil nitrogen level of 0.937 g/m^2 was obtained from one point in time. The season-long control level of soil nitrogen would probably be greater than 0.937 g/m^2 as more nitrogen becomes available during the growing season because of microbial mineralization (i.e., decomposition; Binkley and Vitousek 1989).

Our observation that nitrogen-use efficiency decreases with increasing nitrogen reflects a common plant response (Shaver and Melillo 1984; Chapin and van Cleve 1989). When nutrients such as nitrogen are very limiting, plants are capable of optimizing the amount of carbon gain for nitrogen used. When nitrogen is not limiting, the plant is no longer required to optimize nitrogen usage with respect to carbon gain.

Our most interesting finding was that nitrogen-use efficiency was not influenced by water. There has been little previous research on the influence of water on nitrogen-use efficiency. James and Jurinak (1978) hypothesized that water would influence nitrogen-use efficiency for perennial bunchgrasses. Although our results are for a winter annual, we hypothesize that water's lack of effect on nitrogen-use efficiency reflects the fact that water influences nitrogen uptake and carbon gain equally. As we reported for FY 1991, shoot nitrogen and biomass were significantly related to water.

Water-use efficiency was positively correlated with percent tissue nitrogen and poorly related to water in *B. tectorum*. A similar increase in water-use efficiency with increasing nitrogen has been observed for numerous species, although exceptions have also been found. The positive correlation between water-use efficiency and nitrogen is interpreted as being a consequence of the increase in carbon gain being greater than in the case of stomatal conductance (Toft et al. 1989). Photosynthetic rates are generally positively correlated with leaf nitrogen (Field et al. 1983). Our observation that water-use efficiency was poorly related to water agrees with the conclusion drawn by Toft et al. (1989), that semiarid land plants in general show either no change or an increase in water-use efficiency with decreasing water supply. We found an increase in water-use efficiency with decreasing water at the control and lowest level of added nitrogen, although there was no effect at higher levels of nitrogen.

Our observation that water-use efficiency is negatively correlated with nitrogen-use efficiency is in agreement with observations based on instantaneous data by Field et al. (1983). In contrast to their data, the data for our observations represent factors in effect over the entire life span of *B. tectorum*, and so we conclude that compromises between water-use efficiency and nitrogen-use efficiency are similar at various time scales. Plants limited by nitrogen will preferentially optimize its use (highest nitrogen-use efficiency) but will optimize water use secondarily (lowest water-use efficiency). We hypothesize that such plants will have an accelerated phenological progression to produce viable seed before running out of water and will allocate more carbon to roots to acquire more water. Historically, it has been assumed that plants limited by water will preferentially optimize its use (highest water-use efficiency) and would therefore optimize nitrogen use secondarily (lowest nitrogen-use efficiency). The validity of this assumption is not clear; we found only a poor relationship between water and water-use efficiency. It is likely that all plants developed significant water stress, especially those in the nitrogen-plus-water treatments. With additional nitrogen, plants increased in size and therefore would have used more water. We hypothesize that a significant negative correlation would be found between water-use efficiency and water if we periodically added water to the system to intensify the water treatment effect.

Future Research

One of the values of our experimental design is that equations written to describe the effects of water and nitrogen on resource efficiencies can

be incorporated into ecosystem models for the ALE Reserve. Future research efforts will be made to understand genetic differences with respect to water-use efficiency and nitrogen-use efficiency between co-occurring species at the same location and within species from differing locations. Hypotheses will be developed and tested at the more complex sagebrush-bunchgrass ecosystems common on the ALE Reserve and throughout the arid western United States.

References

Bolton, H., Jr., J. L. Smith, and R. E. Wildung. 1990. "Nitrogen Mineralization Potentials of Shrub-Steppe Soils with Different Disturbance Histories." *Soil Science Society of America Journal* 54:887-891.

Binkley, D., and P. Vitousek. 1989. "Soil Nutrient Availability." In *Plant Physiological Ecology Field Methods and Instrumentation*, eds. R. W. Pearcy, J. R. Ehleringer, H. A. Mooney, and P. W. Rundel, pp. 75-96. Chapman and Hall, New York.

Chapin, F. S. III, and K. van Cleve. 1989. "Approaches to Studying Nutrient Uptake, Use and Loss in Plants." In *Plant Physiological Ecology Field Methods and Instrumentation*, ed. R. W. Pearcy, J. R. Ehleringer, H. A. Mooney, and P. W. Rundel, pp. 185-207. Chapman and Hall, New York.

Ehleringer, J. R., and T. A. Cooper. 1988. "Correlations between Carbon Isotope Ratio and Microhabitat in Desert Plants." *Oecologia* 76:562-566.

Field, C., J. Merino, and H. A. Mooney. 1983. "Compromises between Water-Use Efficiency and Nitrogen-Use Efficiency in Five Species of California Evergreens." *Oecologia* 60:384-389.

Fischer, R. A., and N. C. Turner. 1978. "Plant Productivity in Arid and Semi-arid Zones." *Annual Review of Plant Physiology* 29:277-317.

Hubick, K. T., G. D. Farquhar, and R. Shorter. 1986. "Correlation between Water-Use Efficiency and Carbon Isotope Discrimination in Diverse Peanut (*Arachis*) Germplasm." *Australian Journal of Plant Physiology* 13:803-816.

James, D. W., and J. J. Jurinak. 1978. "Nitrogen Fertilization of Dominant Plants in the Northeastern Great Basin Desert." In *Nitrogen in Desert Ecosystems*, eds. N. E. West and J. J. Skujins, pp. 219-231. Dowden, Hutchinson and Ross, Stroudsburg, Pennsylvania.

Lajtha, K., and F. J. Barnes. 1991. "Carbon Gain and Water-Use in Pinyon Pine-Juniper Woodlands of Northern New Mexico: Field Versus Phytotron Chamber Measurements." *Tree Physiology* 9:59-67.

Shaver, G. R., and J. M. Melillo. 1984. "Nutrient Budgets of Marsh Plants: Efficiency Concepts and Relation to Availability." *Ecology* 65:1491-1510.

Thornley, J.H.M., and I. R. Johnson. 1990. *Plant and Crop Modelling - A Mathematical Approach to Plant and Crop Physiology*. Oxford University Press, Oxford.

Toft, N. L., J. E. Anderson, and R. S. Nowak. 1989. "Water Use Efficiency and Carbon Isotope Composition of Plants in a Cold Desert Environment." *Oecologia* 80:11-18.

West, N. E., and J. Skujins, ed. 1978. *Nitrogen in Desert Ecosystems*. Dowden, Hutchinson and Ross, Stroudsburg, Pennsylvania.

A Survey of Volatile Organic Compounds Emitted from Shrub-Steppe Vegetation

M. D. Wessel, S. O. Link, and R. G. Kelsey
(U.S. Department of Agriculture Forest Service)

Non-methane hydrocarbons (NMHCs) emitted by plants play significant roles in the chemistry of the soil and atmosphere. It has been estimated that as much as 90% of all NMHC is produced by natural sources, the rest coming from anthropogenic sources (Martin et al. 1991). There are many different kinds of NMHC. Of interest to this project are the terpenes, specifically monoterpenes. It is known that barren areas occur

near and under stands of California sagebrush (*Artemisia californica*), an emitter of monoterpenes. These barren areas are caused in part by an allelopathic interaction (Kelsey et al. 1978; Kelsey and Everett, in press). Specifically, some monoterpenes emitted by California sagebrush can inhibit the germination and growth process of other plants, thus preventing their growth near the shrub (Kelsey and Everett, in press). Such allelopathic toxicity may occur for any plant that emits monoterpenes or other NMHC.

Non-methane hydrocarbons also affect the atmosphere. Isoprene and terpene emissions are responsible for 39% of global carbon monoxide production and are precursors to volatile organic acids (Mooney et al. 1987; Lamb et al. 1987). However, the effects of monoterpenes in the atmosphere are not all negative. For instance, these compounds represent a significant sink for low-level ozone (Mooney et al. 1987).

It is important to understand how natural NMHC may function in soil biology and in the atmosphere as pollutants or mediators of pollution. To investigate these processes further, it is necessary to have a broad knowledge of the different types of NMHC being produced and their sources. This study was conducted to determine what volatile NMHCs are emitted by dominant plants found on the Arid Lands Ecology (ALE) Reserve on the Hanford Site.

Plant samples were collected from the ALE site. We investigated *Artemisia tridentata* (big sagebrush), *Grayia spinosa* (hopsage), *Sisymbrium altissimum* (tumble mustard), *Chrysothamnus nauseosus* (rabbitbrush), *Agropyron spicatum* (bluebunch wheatgrass), and *Bromus tectorum* (cheatgrass). Big sagebrush and bluebunch wheatgrass were transplanted into pots for transport to the laboratory in Corvallis, Oregon. All other samples were cut from each plant in the field, placed in plastic bags, and transported to Corvallis on ice.

Subsamples of each plant were weighed (approximately 0.5 g) into headspace vials, sealed with a rubber septum, and allowed to stand at 60°C for 1.5 hours. A locking airtight syringe was used to remove 1 ml of headspace vapor from the vial. After the volume was compressed to 0.5 ml, it was injected into a Hewlett Packard 5890 Series II gas chromatograph (GC) equipped with a mass spectroscopic (MS) detector. The compounds were separated on a J&W Scientific DB-1 capillary column, 0.25-mm inside diameter by 30 m long, with 0.25-μm film thickness. Other GC conditions include an initial oven temperature of 50°C for 2 min, then increasing at 30°C/min up to 160°C, where it was held for 5 min. The injection port temperature was 150°C, and the transfer line and detector temperatures were both 230°C.

The compounds present in each sample were identified by comparing their mass spectra with those found in the Registry of Mass Spectral Data (Stenhagen et al. 1974). For compounds found in the headspace vapors of big sagebrush, the order of elution off the GC column was compared with the order reported by Kelsey et al. (1983). Mass spectra for irregular monoterpenes found in big sagebrush were compared to those reported by Epstein et al. (1976). Blank injections were run periodically to ensure that there was no residual contamination in the syringe from previous samples.

Four of the six species analyzed produced significant quantities of NMHC (Table 1). There were no detectable NMHCs in the two grass species analyzed. Most of the NMHC compounds identified were monoterpenes. The two that were not were methacrolein, an oxidized derivative of isoprene, and 3-butenyl isothiocyanate, which is probably species-specific for mustards.

The vegetation found in desert ecosystems can play a major role in the chemistry of the soil surrounding the plant. For instance, big sagebrush emits monoterpenes that actually discourage the germination and growth of competing vegetation (Kelsey and Everett, in press; Bradow and Connick 1990). The monoterpenes emitted also reduce nitrogen fixation by algae in the soil (Kelsey and Everett, in press). In a sense, the monoterpenes act as natural herbicides. As a result, these plants create a favorable growing environment for themselves, by reducing competition for soil nutrients and water in their immediate vicinity. The role of allelopathy in the ecological interactions of species growing at the ALE site has not yet been

TABLE 1. NMHC Identified in the Headspace Vapors of Six Plant Species Collected at the ALE Site

Plant	Compounds Identified
Big sagebrush	methacrolein[a] α-pinene camphene artemiseole (arthole) 1,8-cineole santolina epoxide methyl santolinate camphor
Hopsage	artemiseole (arthole) 1,8-cineole
Tumble mustard	3-butenyl isothiocyanate
Rabbitbrush	α-pinene β-pinene α-phellandrene β-phellandrene
Bluebunch wheatgrass	None detected
Cheatgrass	None detected

(a) Non-monoterpene compound.

studied. But, based on studies in other areas, there is a strong probability that NMHCs do function as allelopathic agents between some species occurring on the ALE Reserve.

In recent years, the abundance of cheatgrass and bunchgrass at the ALE site has risen greatly. This rise is in part a result of fires that have destroyed big sagebrush, rabbitbrush, and hopsage. In response to this disturbance, cheatgrass and bunchgrass have quickly invaded and replaced the shrubs as the dominant species. The absence of big sagebrush and its herbicidal chemicals in the burned areas may have allowed cheatgrass to become dominant (Kelsey and Everett, in press). The greater abundance of cheatgrass increases the chance of fires and reduces the diversity of plant species within the community, both undesirable changes.

It is not known how the increase in cheatgrass and bunchgrass is affecting the local atmosphere. However, given that these grasses produce lower levels of NMHC than big sagebrush and rabbitbrush do, large measurable changes are anticipated. It is possible that NMHCs emitted from vegetation are actually strong greenhouse gases. In sandy deserts with little or no vegetation, nighttime temperatures are relatively cool. In contrast, in areas like the ALE site, which have more vegetation, nighttime temperatures are relatively warm. The cause may be NMHC emissions in these areas (Hayden 1991).

To determine the effects of changes in the relative abundances of the plant species found at the ALE site will require considerably more research. Currently, we are developing ion mobility spectrometry (Hill et al. 1990) to measure the concentrations of NMHCs in the atmosphere. Also under way is the development of ion mobility spectrometry for use in measuring real-time rates of NMHC flux from plant species found at the ALE site.

References

Bradow, J. M., and W. J. Connick, Jr. 1990. "Volatile Seed Germination Inhibitors from Plant Residues." *Journal of Chemical Ecology* 16:645-666.

Epstein, W. W., L. R. McGee, C. D. Poulter, and L. L. Marsh. 1976. "Mass Spectral Data for Gas Chromatography-Mass Spectral Identification of Some Irregular Monoterpenes." *Journal of Chemical Engineering Data* 21:500-502.

Hayden, B. P. 1991. "Greenhouse Gases, Deserts and Desertification." *Supplement to Bulletin of the Ecological Society of America* 72:138.

Hill, H. H., Jr., W. F. Siems, R. H. St. Louis, and D. G. McMinn. 1990. "Ion Mobility Spectrometry." *Analytical Chemistry* 62:1201A-1209A.

Kelsey, R. G., and R. L. Everett. "Allelopathy." In *Management of Grazing Lands: Importance of Plant Morphology and Physiology to Individual Plant and Community Response*, eds. D. J. Vedunah and R. E. Sosebee. The Society for Range Management, Denver, Colorado (in press).

Kelsey, R. G., T. T. Stevenson, J. P. Scholl, T. J. Watson, Jr., and F. Shafizadeh. 1978. "Chemical Composition of the Litter and Soil in a Community of *Artemisia-tridentata* ssp *vaseyana*." *Biochemical Systematics and Ecology* 6:193-200.

Kelsey, R. G., W. E. Wright, F. Sneva, A. Winward, and C. Britton. 1983. "The Concentration and Composition of Big Sagebrush Essential Oils from Oregon." *Biochemical Systematics and Ecology* 11:353-360.

Lamb, B., A. Guenther, D. Gay, and H. Westberg. 1987. "A National Inventory of Biogenic Hydrocarbon Emissions." *Atmospheric Environment* 21:1695-1705.

Martin, R. S., H. Westberg, E. Allwine, L. Ashman, J. C. Farmer, and B. Lamb. 1991. "Measurement of Isoprene and Its Atmospheric Oxidation Products in a Central Pennsylvania Deciduous Forest." *Journal of Atmospheric Chemistry* 13:1-32.

Mooney, H. A., P. M. Vitousek, and P. A. Matson. 1987. "Exchange of Materials between Terrestrial Ecosystems and the Atmosphere." *Science* 238:926-932.

Stenhagen, E., S. Abrahamsson, and F. W. McLafferty. 1974. *Registry of Mass Spectral Data*, Vol. 1. John Wiley & Sons, New York.

Data Management for the Arid Lands Ecology Reserve and the Environmental Research Park, Hanford Site

S. L. Thorsten and M. A. Simmons

The Arid Lands Ecology (ALE) Reserve and the encompassing Environmental Research Park at the Hanford Site have provided the foundation for several long-term ecological studies. Data sets for salmon (starting in 1948), Canada geese (since 1953), wintering bald eagle/ waterfowl populations (since 1961), and climatological data (since 1944) represent a few of the longest-running studies. Although these data were generally collected to answer specific research questions, now, because of the length and consistency of the records, the data can be used to answer broader questions relating to the maintenance of species, environmental restoration, and land management. To make the data accessible and to maintain continuity of the long-term monitoring studies, a computerized method of storage and retrieval was necessary.

In 1992, the Terrestrial Sciences Section at PNL therefore developed a database program that is capable of archiving, retrieving, and manipulating these data. The *Ecological Data Manager* (EDM) program was created on the Apple MacIntosh using software that is transportable across platforms. It was designed to fit readily into the researchers' established procedures of data collection, analysis, and documentation, while also being user-friendly. Flexibility of the PNL-developed software gives the program the ability to accept a wide variety of data (e.g., statistical, locational, archaeological, descriptive).

The main EDM program provides access to the raw data by individual record. Associated documentation of the focus and methods of each study is contained in the Study Summary.

The Study Site file provides locations of study sites and pertinent topographical features, as well as general information on the history, climate, geography, flora, and fauna. Those studies that now incorporate geographical information system (GIS) technology may store their visual identification records, as well as other relevant photographic records. An example of such images is shown in Figure 1. Companion files contain information on investigators, authors, and publications.

Currently, data from Hanford are being used in studies of wintering bald eagle habitat, shrike nesting locations, and home ranges of deer and elk. The database has also been used to assist the Washington State Department of Wildlife and the DOE Richland Field Office in their land use decisions.

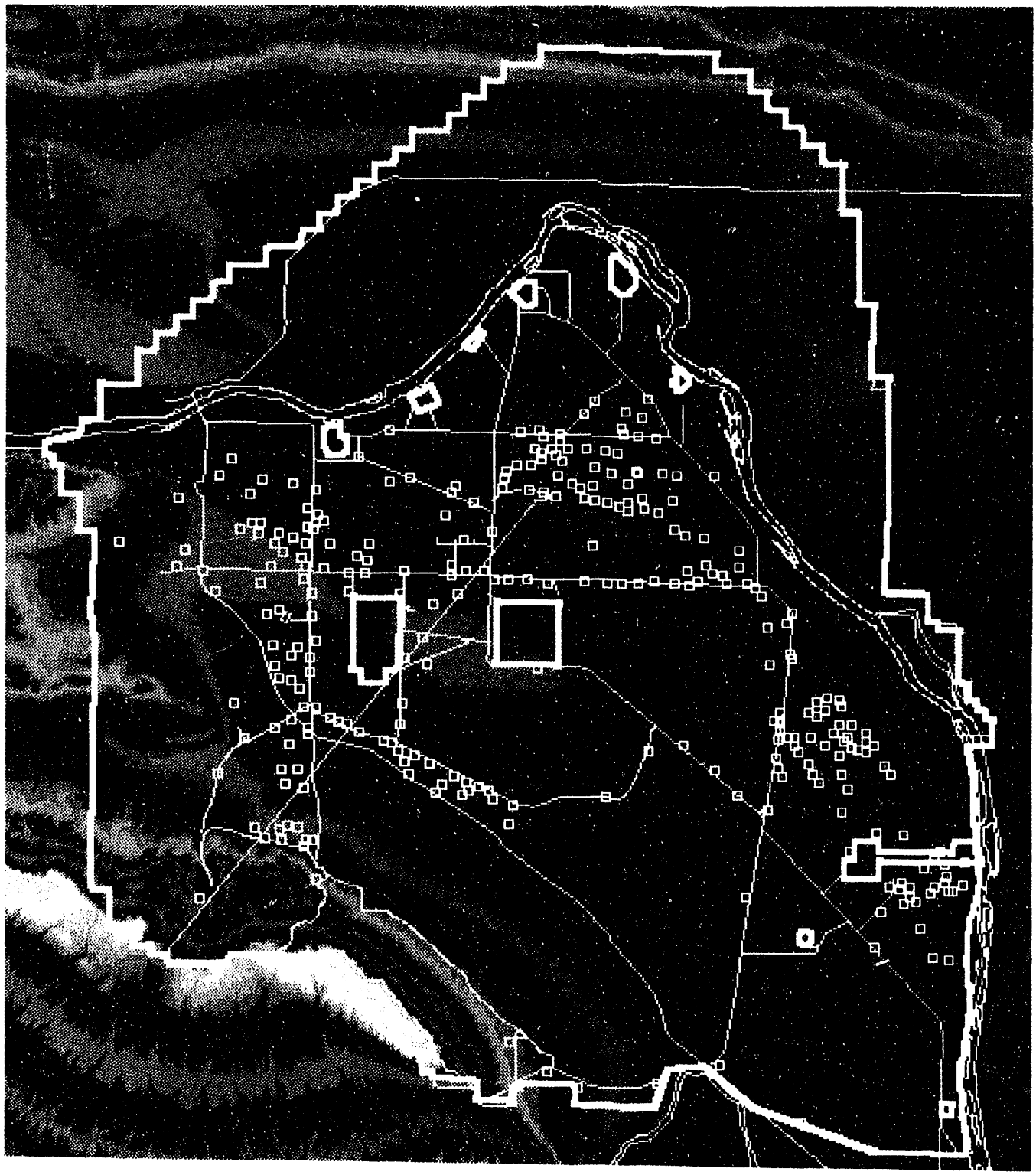

FIGURE 1. GIS Map: Shrike Locational Data. Loggerhead shrikes (*Lanius ludovicianus*) were studied in the spring and summer of 1989 on the Hanford Site. The study was restricted to areas of the Hanford Site south and west of the Columbia River. Surveys were conducted by slowly driving (8-20 km/h) along nearly all of the roads, equivalent to a 154-km vehicular transect. The transect was completed once a month between April and August 1989. The location of each shrike nest was mapped, and the behavior and age (adult or fledgling) of each shrike recorded. Each location was observed three or more times to verify that the nest was in an active breeding territory. The data file and this GIS map contain the locational data for shrike nests (i.e., coordinates for the sitings).

Designs for Environmental Field Studies

J. M. Thomas, L. L. Eberhardt, M. A. Simmons, and V. I. Cullinan

During FY 1992 we continued to conduct research in the areas of observational sampling and sampling for pattern. For observational sampling, our methods were based on and developed from long-term data that describe the dynamics of large mammals. The methods for scaling and sampling for pattern were formulated using plant cover measurements.

Concern over the effects of global change has led to a new emphasis on landscape ecology, because important ecological effects are likely to be expressed at this level. Since ecologists have long recognized the importance of spatial and temporal patterns of heterogeneity in landscapes, and since a change in pattern or loss over large landscapes is encompassed by our research on sampling for pattern, landscape-level research has been a natural extension for this project. Such patterns of heterogeneity are known or hypothesized to affect many ecological phenomena, including population dynamics, life histories, dispersal patterns, species diversity, predation, and patterns of natural selection. However, studies at the landscape level run a larger risk of drawing invalid conclusions than experiments conducted on a single smaller scale that are intended to result in more limited inferences. A reduction of this risk requires that the resolution needed and methods for assessing pattern be carefully considered.

FY 1992 Research Highlights

The current U.S. research agenda for global change neglects the animal components of ecosystems. Reasons for this neglect include the relatively small global biomass of animals, the presumed major role of components of lower stages (e.g., phytoplankton) in trophic diagrams, and severe difficulties in assessing animal populations and their role in ecosystem dynamics. On the other hand, large mammals are perceived by the public and many policy-makers as being of primary importance. In sensitive ecosystems, particularly the Arctic and Antarctic regions, large mammals have a key role in ecosystem dynamics, as evidenced by the short food chains involving large whales and by the emerging understanding of how predation by marine mammals controls some ecosystems.

Research on observational sampling conducted in this project has served to develop technology for assessing populations of large animals and provide new applications and methods for this sampling approach. The effort has had two major components: The first concerns methods of sampling and measuring abundance. The second deals with the analysis of the dynamics of animal populations, which is the area that was stressed during FY 1992. Because these studies require large expenditures for field work and decades of effort that no single research project can provide, the project has concentrated on cooperative efforts with a variety of management agencies. Although these agencies have statutory responsibility for management of species, they often lack the expertise and resources needed for analysis of the data. During this research, advice and analyses have been exchanged for access to long-term data sets. Publications resulting from these efforts include papers on ungulates, feral horses, caribou, and wolves (Eberhardt 1991; Garrott et al. 1991; Eberhardt and Pitcher, in press).

Sampling for Pattern. Combining information from multiple scales of measurement is an essential part of global change and landscape dynamics research. Models and measurements of large-scale phenomena, such as the effects of acid precipitation, global carbon and nitrogen cycles, increased desertification, and climate change, are scale-dependent. Theory suggests that even the interpretation of the role of consumers in influencing spatial-temporal variation in the environment depends on the scale of the data considered. Conclusions appropriate to one scale of environmental heterogeneity may be inappropriate when transferred to another scale. Consequently, the level of resolution and the heterogeneity at all relevant scales must be considered when defining the research goals and sampling design for studies conducted across spatial-temporal scales. Components of ecosystems are interrelated, and an understanding of these relationships will allow scientists to predict community, ecosystem, or

global change due to human disturbance. We have proposed a method for determining the level of resolution needed to study components of ecosystems and their interrelations. The objectives of the research during FY 1992 included further justification of the importance of 1) considering scale in the design and analysis of ecological research and 2) providing a comparison of the methods for examining landscape pattern and scale.

The efficiency of using an array of statistical analyses to detect change in the spatial distribution of vegetation was evaluated with simulation methods. The analyses considered included Hill's patch size analysis, spectral analysis, fractal analysis, and variance ratio and correlation analysis, all methods for describing landscape pattern and scale.

We found that the questions asked most frequently at the landscape level cannot be answered using a single method. However, using a combination of methods does potentially allow scientists to establish agreement in their assessment of ecological pattern and scale. For instance, spectral analysis is more sensitive to small-scale variability, while Hill's analysis is more sensitive to larger-scale variability. Variance ratio and correlation analysis were more reliable than Hill's method in detecting fine-scale variability. Because of the variable sensitivity of each of these methods, the detection of multiple scales and the determination of ecological change must be confirmed by more than one method.

We found that, in general, the patch size analysis of Greig-Smith should confirm peaks in the Hill plots, the troughs in the correlation versus transect segment-length plots, and the sill in the semi-variogram. For periodic data, the troughs in the plots made using Hill's method should correspond to peaks in the spectral analysis, variance ratio, and the point of intersection in the correlation versus transect segment-length plots. For nonperiodic data, peaks in the variance ratio plot should correspond to peaks in the correlation versus transect segment-length plot. Finally, the value of the fractal dimension should be <2 when the correlation versus the intersegment distance plot has a distinct pattern and should be 2 when the plot suggests there is only noise about 0. Likewise when the fractal dimension is 2, there should be no sill in the semi-variogram.

The efficiency of the same statistical analyses for detecting change in the spatial distribution of vegetation through simulation was also compared. The simulation used for this comparison considers removal of vegetation using both random and cluster removal of percent cover data from transects. Extensions planned for the simulation model include random and cluster invasion in conjunction with both removal patterns, using two-dimensional or map data generated from satellite images.

Simulations were run on data collected from a 2050-m-long line-intercept transect across the Arid Lands Ecology (ALE) Reserve on DOE's Hanford Site in southeastern Washington. For both random and cluster removal patterns, the simulation model mimics organisms being dropped onto the transect and allows them each to remove 10% of the vegetative cover in a 1-m cell. If there is less than 10% vegetative cover within an animal's cell, the organism is forced to move randomly into adjacent cells until sufficient vegetation is located within a single cell. More than one organism can be dropped into a cell, but they eat in order of arrival. Any organisms arriving after all the vegetation in a cell is removed must search the adjacent cells. Thus, for example, a cell with 83% cover can accommodate only eight organisms.

Simulations were conducted on an array of the percent cover change (2.5, 5, 7.3, 9.6, 12, and 23%) for 100, 200, 300, 400, 500, and 1000 grazers, respectively. For cluster thinning, Hill's analysis, spectral analysis, and the fractal dimension were less sensitive to change than the variance ratio and correlation analyses. The latter methods detected differences at 5% change and less, depending on which elements were removed, and always detected differences when cover change was greater than 7%. Figure 1 is an example where a 5% change was detected, as noted by the change in the first major peak in the plot from approximately 120 to 60 m. Hill's method, spectral analysis, and fractal dimension detected differences only when the cover change was greater than 9%.

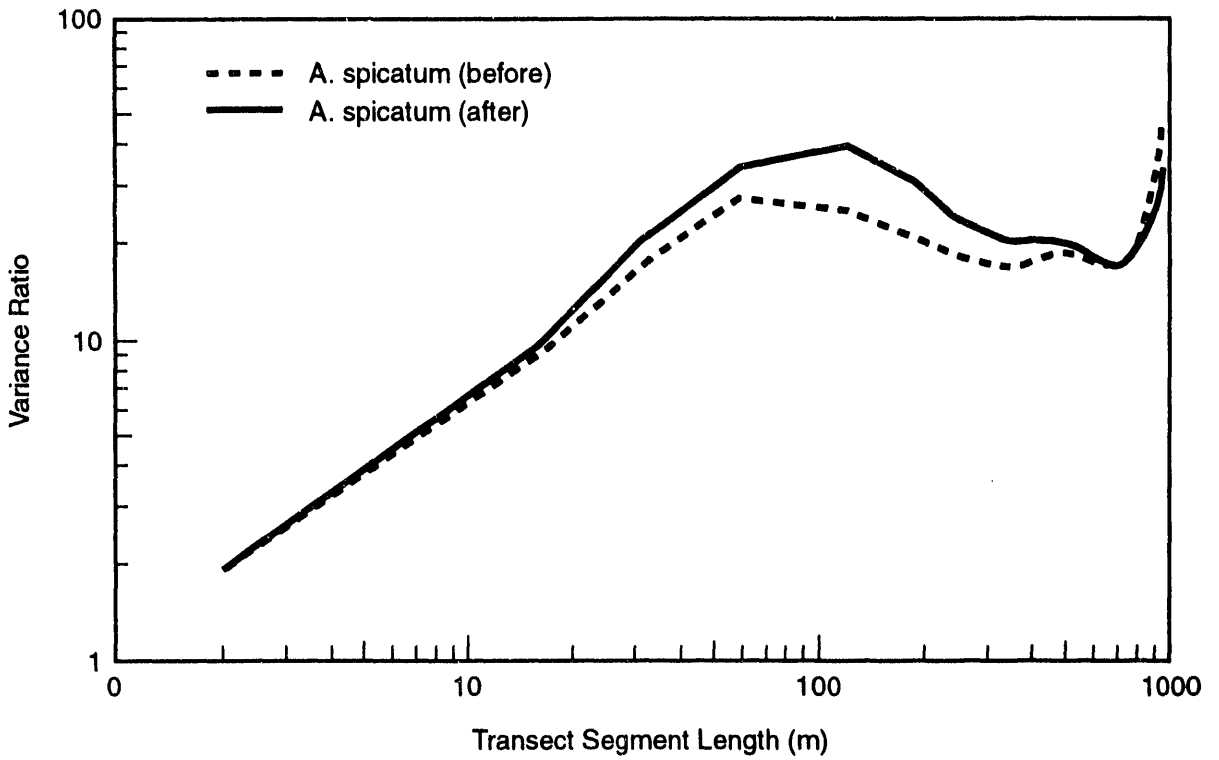

FIGURE 1. Variance Ratio Analysis of *Agropyron spicatum* Both before (solid line) and after (dashed line) Removal of 5% of the Vegetation Through Simulation Using a Cluster Removal Pattern

None of the methods appears to be more efficient in detecting random removal of vegetation. For a simulation using a random placement of organisms, no changes were observed in the estimated patch size or period for each method or for each percentage of cover change from 2.5 to 23%. Figure 2 depicts a 25% change in the percent cover resulting from random thinning; no change is apparent in the resulting peaks and troughs of the variance ratio plot. In fact, as the number of clusters was increased during simulations with cluster placement (i.e, increasing the random component of the cluster removal pattern), the differences in efficiency among the methods were reduced.

Our research on the detection and measurement of scale has found that the scale (defined as the transect or area that provides the most information at the greatest efficiency or smallest error) for transects containing multiple species can be calculated as the weighted average of the scales detected for individual species and for the community. These scales can then be compared to scales calculated from remotely sensed images. Previous work has shown good agreement between field data collected on grasslands in southeastern Washington and Landsat Thematic Mapper (TM) spectral data. We have now extended this work to the juniper woodlands of central Oregon. The dominant vegetation in this area is juniper trees (*Juniperus occidentalis*) and four species of bushes, the sagebrush (*Artemisia tridentata*), green rabbitbrush (*Chrysothamnus viscidiflorus*), gray rabbitbrush (*C. naseousus*), and bitterbrush (*Purshia tridentata*).

The juniper woodland research is part of a large, multidisciplinary study, the Oregon Transect Ecosystem Research Project (OTTER). Part of the study involved using various platforms to collect remotely sensed data, including several high-flying aircraft. We obtained data from a Daedalus Thematic Mapper Simulator (TMS) aboard a high-flying surveillance aircraft. The

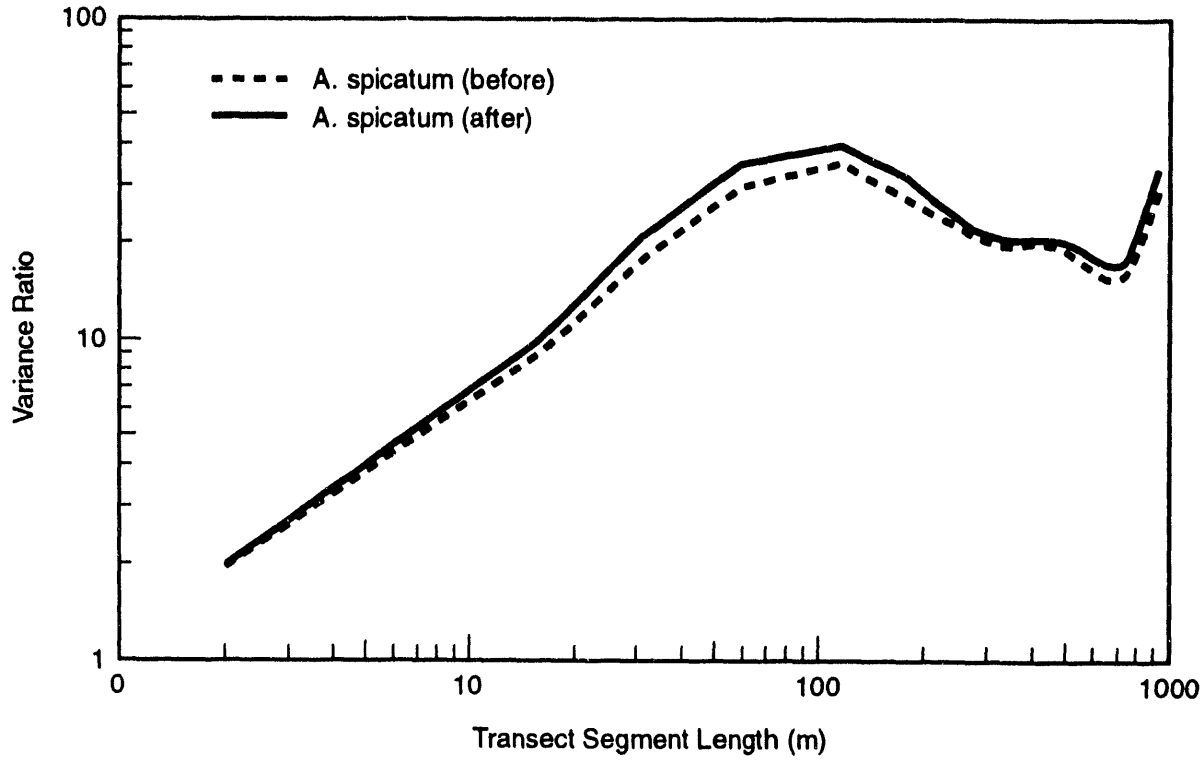

FIGURE 2. Variance Ratio Analysis of *Agropyron spicatum* Both before (solid line) and after (dashed line) Removal of 25% of the Vegetation Through Simulation Using a Random Removal Pattern

Daedalus TMS has a pixel size of 25.8 m and 12 spectral bands; one band, 7, has a wavelength of 0.76-0.90 μm, which corresponds to band 4 for Landsat TM. Scale results for the combined five species measured across the juniper woodland transect agree with the scale calculated from spectral data from the Daedalus TMS remote images (Figure 3). The difference between field data and spectral data for a transect less than 200 m long results from resolution problems at small transect lengths.

Work to date supports the idea that the scale measured remotely corresponds to the scales obtained from field studies. Past research (discussed in last year's annual report) has shown that this measure of scale can be used to detect small levels of change. Thus, this method can perhaps be used to routinely monitor large areas for globally mediated ecological changes.

Observational Studies. Research on developing a quantitative methodology to analyze population dynamics under the category called observational sampling was stressed in FY 1992. Data from a number of species have been utilized, and some of the research results based on these data are presented below.

From an ecological point of view, one of the most important aspects of a study of grizzly bears in Yellowstone National Park (and its environs) is that recovery from the severe stress imposed by closing the major source of artificial food in the 1970s seems to be clearly associated with an increase in early survival. Results so far indicate that adult female survival and reproductive rates remain largely unchanged. Further analysis, in terms of density-regulation models, is planned because of the paucity of actual data for such models describing large mammal populations.

However, an extensive data set is available for the Northern fur seal. General trends for this natural large mammal population are known back

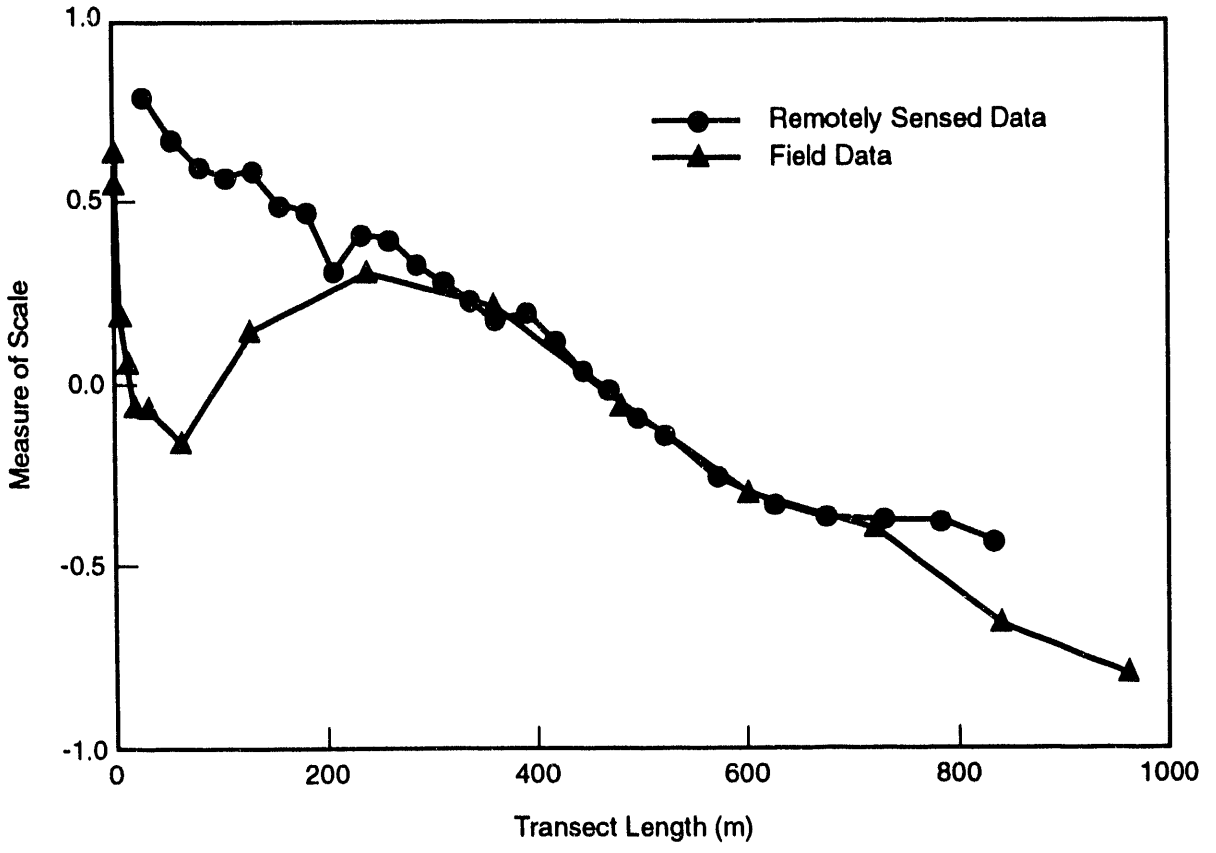

FIGURE 3. Comparison of Scales Measured in the Field and from an Aircraft Using a Daedelus Thematic Mapper Simulator. Scales were calculated from cover data from five species (four bush species and juniper trees) measured over a 5,000-m transect in eastern Oregon.

two centuries, and detailed records are available for the past 40 or 50 years. A substantial decline in numbers began in the mid-1950s and is generally believed to be associated with large-scale commercial fisheries. Several models of the population have been constructed (including two in this project), but none of the models have utilized the full range of population data. Current research is designed to investigate whether a more detailed model might explain several apparent population adjustments over the last 40 years.

Data are also available for the Hawaiian monk seal. A substantial change in conditions occurred in the 1960s, again probably associated with commercial fisheries. Six major population centers are distributed over about 1,000 linear miles. Two of these sites exhibit a severe imbalance in adult sex ratio that likely stems from events occurring in the 1960s. The breeding behavior of the species is such that if the imbalance in adult sex ratio is perpetuated, there will be a loss of these subpopulations. An intriguing research question is why these subpopulations have not adjusted in 30 years, and whether they might only "adjust" through long-term near-extirpation and eventual recolonization. At three other sites, human presence has resulted in the virtual cessation of successful reproduction. Removal of that interference from one site apparently resulted in recovery of the population; another site was restored by "re-stocking" and protection, and similar efforts have begun at the third site. However, over the last three years, the seemingly recovered population has begun to decline through apparent starvation of juveniles and subadults. Inasmuch as this change has been accompanied by small but distinct environmental changes, it offers a

promising prospective experiment in circumstances associated with global climatic changes, as well as information on density regulation and an opportunity to further test the model developed in this project.

The Pacific walrus in the Bering and Chukchi seas may be one of the natural populations least influenced by environmental changes caused by human activities. However, over-harvesting has resulted in the occurrence of three cycles of abundance since commercial harvests began in about 1850. Walrus are probably the keystone species in their ecosystem, due to their pervasive influence on the benthos. Thus, there is a prospect of considering an unusually long cycle of relative abundance forced by human predation on walrus, and its possible role in apparent adjustments exhibited by the walrus population. Development of a population model to describe this situation has been initiated.

The Exxon Valdez oil spill of 1989 resulted in a substantial decline in the number of sea otters in Prince William Sound, Alaska. Extensive population data were obtained and are now being released from confidentiality restrictions imposed by prospective litigation. Continuing studies in connection with restoration efforts are likely and should be of interest in the context of present DOE studies, in view of the energy-related aspect. Inasmuch as sea otters are a keystone species, we have initiated modeling studies to predict ecosystem effects.

Population data on bowhead whales are too limited to offer much information about possible population adjustments, but it is worth considering what is known in about walrus dynamics, inasmuch as the two species occupy roughly the same ecosystem. Bowheads were severely overexploited beginning in about 1848, with diminishing commercial harvests up to 1914. Low reproductive rates resulted in a long recovery time. Research has been initiated to develop a model of this species to describe the slow growth of whale populations.

Because caribou have been a concern in energy development (e.g., on the Alaska pipeline), the predator-prey dimension of this ecosystem must be considered. Our caribou-wolf data represent one of the few instances where actual population data are available for a predator-prey system involving large mammals. This particular population crashed in the late 1960s, from 90,000 to 100,000 down to about 10,000. There is considerable controversy over the role of wolves in the decline. Since wolves are regarded as a keystone species, our models of this event will be very valuable from both practical and theoretical standpoints.

References

Eberhardt, L. L. 1991. "Models of Ungulate Population Dynamics." *Rangifer* 7:24-29.

Eberhardt, L. L., and K. W. Pitcher. "A Further Analysis of the Nelchina Caribou and Wolf Data." *Wildlife Society Bulletin* (in press).

Garrott, R. A., D. B. Siniff, and L. L. Eberhardt. 1991. "Growth Rates of Feral Horse Populations." *Journal of Wildlife Management* 55:641-648.

Laboratory-Directed Research and Development

Laboratory-Directed Research and Development

Laboratory-directed research and development is conducted to develop new and promising scientific concepts that have a high potential for advancing the state of knowledge in environmental sciences. This section describes innovative research on the forefront of science that offers opportunities for future important contributions.

Chemical Desorption/Dissolution

C. C. Ainsworth

The primary purpose of this project is to develop techniques suitable for measuring the kinetic constraints on the desorption/ dissolution processes that govern mobilization of contaminants from solid surfaces and matrices that are common to DOE sites. A second purpose is to develop the capability to combine spectroscopic tools with kinetic reaction techniques to enhance our understanding of important solid/liquid interface geochemical reactions.

Research in FY 1991 focused on developing a stop-flow system for aqueous suspensions that could be combined with electron spin resonance (ESR) spectroscopy to measure reactant species *in situ* on a time scale of microseconds. The oxidation-reduction reaction between Cr^{3+} and a common manganese oxide was followed by observing the increasing ESR signal of Mn^{2+} as Cr^{3+} was oxidized at the manganese oxide surface according to the reaction

$$1.5\ MnO_2 + Cr^{3+} + H_2O =$$

$$HCrO_4^- + 1.5\ Mn^{2+} + H^+$$

Several inorganic metals (e.g., manganese, copper, vanadium) and many organic free radicals and radical cations can be used as ESR probes. With the use of appropriate probes, the reaction kinetics of important geochemical reactions can be discerned at time scales that allow a more complete understanding of mechanisms and pathways.

In FY 1992, research focused on understanding both the kinetic mechanism of adsorption or desorption of divalent metals at the aluminum and iron oxide-water interface and the sorbate's structure and bonding environment. Spectroscopically, emphasis was placed on using extended X-ray absorption fine structure (EXAFS) and X-ray absorption near edge structure (XANES) spectroscopy to delineate the bonding environment of divalent metals (e.g., copper) at the oxide-water interface. This information was used in conjunction with pressure-jump relaxation techniques and other spectroscopic determinations (e.g., ESR) to elucidate a chemical kinetic mechanism that would describe the adsorption/desorption process. Through the development of such information, a basic understanding of contaminant desorption and of the possible universality of kinetic mechanisms of metal adsorption and desorption (e.g., of uranium, cadmium, and cobalt) are being developed.

In FY 1993, research into metal cation adsorption/desorption kinetics will continue and will include studies involving metal oxyanion (chromium and arsenic) interactions at the solid-water interface. Additional studies will investigate the surface speciation and chemical reactions that control the interfacial processes of simple organic acids. The emphasis of these studies will be on determining the effectiveness of kinetic techniques (i.e., relaxation kinetics, continuous flow systems, and stop-flow systems) in discriminating rate-limiting reactions at the solid-water interface, and on linking these findings to spectroscopic measurements in an attempt to isolate important rate parameters. This research will be completed in late FY 1993.

Enzymatic Transformation of Inorganic Chemicals

Y. A. Gorby and H. Bolton, Jr.

In the past, inorganic contaminants, including radionuclides and toxic heavy metals, have been disposed of at U.S. Department of Energy (DOE) sites. In some cases, these inorganic contaminants have migrated and may threaten the quality of domestic groundwater supplies. To predict the fate of such toxic inorganic contaminants, it is vital to understand the factors that influence their solubility and migration. Microbial activity can directly influence the oxidation state, and thus the solubility, of some multivalent metals. Some anaerobic bacteria, known as iron reducers, can couple the complete oxidation of reduced organic matter with the reduction of iron(III) to iron(II). It has recently been demonstrated that these iron-reducing bacteria will also reduce uranium. As a result of uranium respiration, soluble uranium(VI) is converted to the insoluble uranium(IV) precipitate uraninite. This metabolism offers potential for the remediation of water contaminated with uranium. During FY 1991, this project demonstrated that iron-reducing bacteria can also reduce chromium [from chromium(VI) to chromium(III)]. Given that chromium(III) forms insoluble hydroxides at approximately neutral pH and is less toxic than the soluble oxidized chromium(VI), it may be possible to make use of this metabolism as an effective means of removing chromate from contaminated waste waters and of determining its fate in natural anaerobic environments.

FY 1992 Research Highlights

In FY 1992, we focused on the enzymatic transformation of the cobalt-ethylenediaminetetraacetic acid (EDTA) complex, a contaminant mixture that is unique to DOE sites. The synthetic chelator EDTA forms water-soluble complexes with many radionuclides and heavy metal cations. For this reason it is a common decontaminating agent in the nuclear industry and for the processing of nuclear materials. Historically, contaminated wash fluids or solidified wastes were disposed of in shallow trenches and covered with a thin layer of soil. This codisposal of radionuclides, metals, and EDTA profoundly altered the geochemistry of natural systems and, in some cases, resulted in the far-field migration of inorganic contaminants and radionuclides, including radioactive cobalt (^{60}Co). The extent of migration in subsurface environments relates to both the stability of the radionuclide-EDTA complex and the sorptive capacity of subsurface particulates.

The stability constants of metal-chelate complexes and their adsorption behavior are often influenced by the oxidation state of the metal moiety. For instance, cobalt(III)-EDTA is a highly stable complex [log stability constant (K) = 41] and, at neutral pH, adsorbs only weakly to negatively charged particulates, such as aluminum oxides. In comparison, cobalt(II)-EDTA is much less stable (log K = 17) and absorbs to a much greater extent. Theoretically, therefore, reduction reactions involving ^{60}Co-EDTA [changing the cobalt from cobalt(III) to cobalt(II)] should reduce the mobility of this radionuclide in saturated subsurface environments.

The objective of this study was to determine whether bacteria that are known to use heavy metals and radionuclides as electron acceptors for growth have the ability to reduce the cobalt in cobalt(III)-EDTA to the less stable and less mobile cobalt(II)-EDTA. Only with such information is it possible to predict the fate of radioactive ^{60}Co in contaminated subsurface environments that may harbor metal-reducing bacteria.

Three metal-reducing bacteria were tested for their ability to use cobalt(III)-EDTA as an electron acceptor: *Geobacter metallireducens*, *Shewanella putrefaciens*, and a new isolate, bacterial strain BrY. The bacteria were cultured in a chemically defined anaerobic growth medium with iron(III) as the electron acceptor. Cells were washed three times in sodium bicarbonate buffer under a stream of anaerobic gas. The washed cells were then injected into an anaerobic solution that contained cobalt(III)-EDTA as the sole potential terminal electron acceptor, with an appropriate electron donor (acetate for *G. metallireducens* and lactate for *S. putrefaciens* and BrY). The reduction of cobalt(III)-EDTA was detected as a loss in absorbance at 535 nm, a characteristic wavelength for this complex.

The results demonstrate that these bacteria can enzymatically reduce cobalt(III)-EDTA to cobalt(II)-EDTA under anaerobic conditions (Figure 1). The reduction of cobalt(III)-EDTA occurred only in the presence of active cells and an appropriate electron donor. In tubes that either contained heat-killed cells or lacked an electron donor, cobalt(III)-EDTA reduction was not observed.

The bacteria were also tested for their ability to gain energy for growth from cobalt(III)-EDTA reduction. The cells grew in a chemically defined medium with cobalt(III)-EDTA as the sole electron acceptor (Figure 2). Cell growth correlated with cobalt(III)-EDTA reduction and ceased when all of the cobalt(III)-EDTA had been reduced. These results extend the range of electron acceptors known to be suitable for anaerobic growth to include a complex that is known to exist only as a product of human activity, i.e., cobalt(III)-EDTA.

Future Research

This discovery has importance because the metabolism may influence the fate of ^{60}Co in contaminated subsurface environments at DOE sites. We hypothesize that microbial reduction of cobalt(III)-EDTA will retard ^{60}Co migration in environments in which iron-reducing bacteria predominate. In our future research, we will expand our experimental systems to monitor ^{60}Co and heavy metal migration in simulated subsurface environments. Information gained by this approach will increase our understanding of the processes that dictate the fate of radioactive cobalt in a number of contaminated DOE sites.

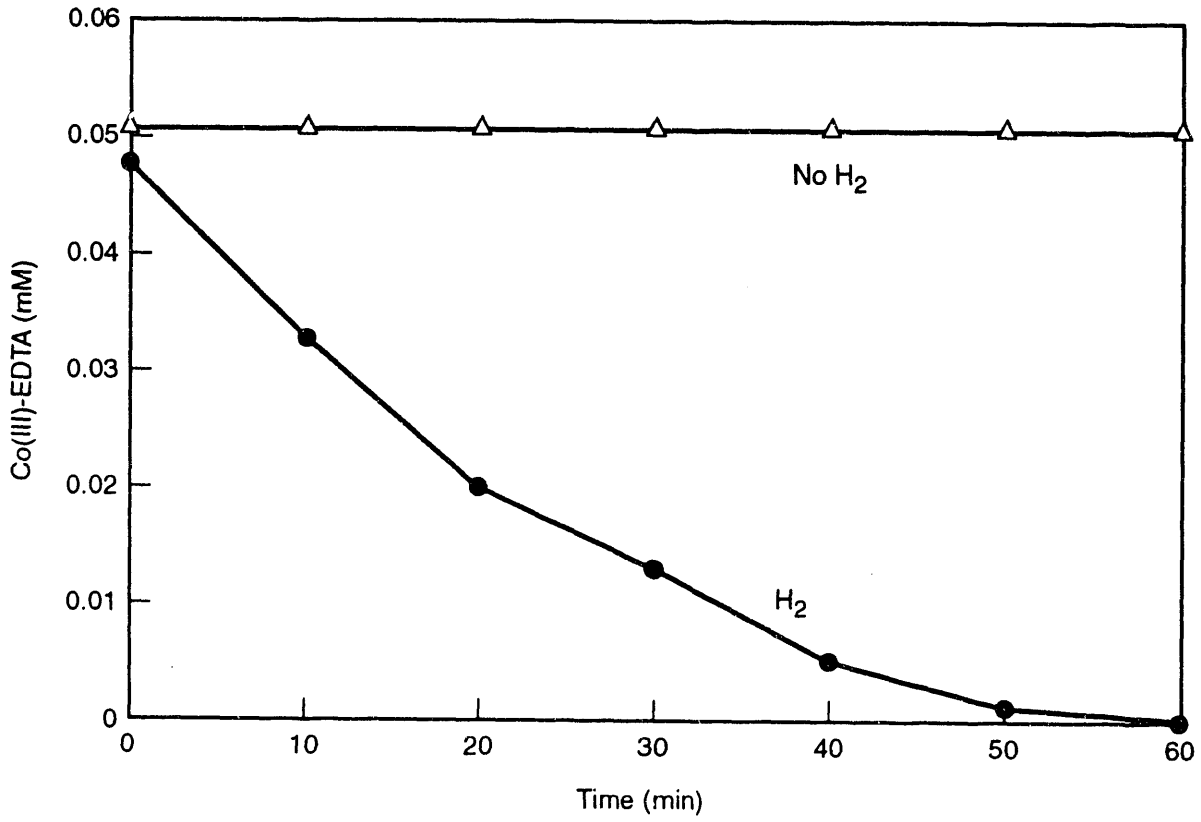

FIGURE 1. Cobalt(III)-EDTA Reduction by a Cell Suspension of Bacterium BrY. The reduction of cobalt(III)-EDTA was detected in the presence of cells and H_2 gas, which served as the electron donor. No reduction of cobalt(III)-EDTA was found when no H_2 gas was added. Similar results were obtained with cell suspensions of *G. metallireducens* and *S. putrefaciens* (data not shown).

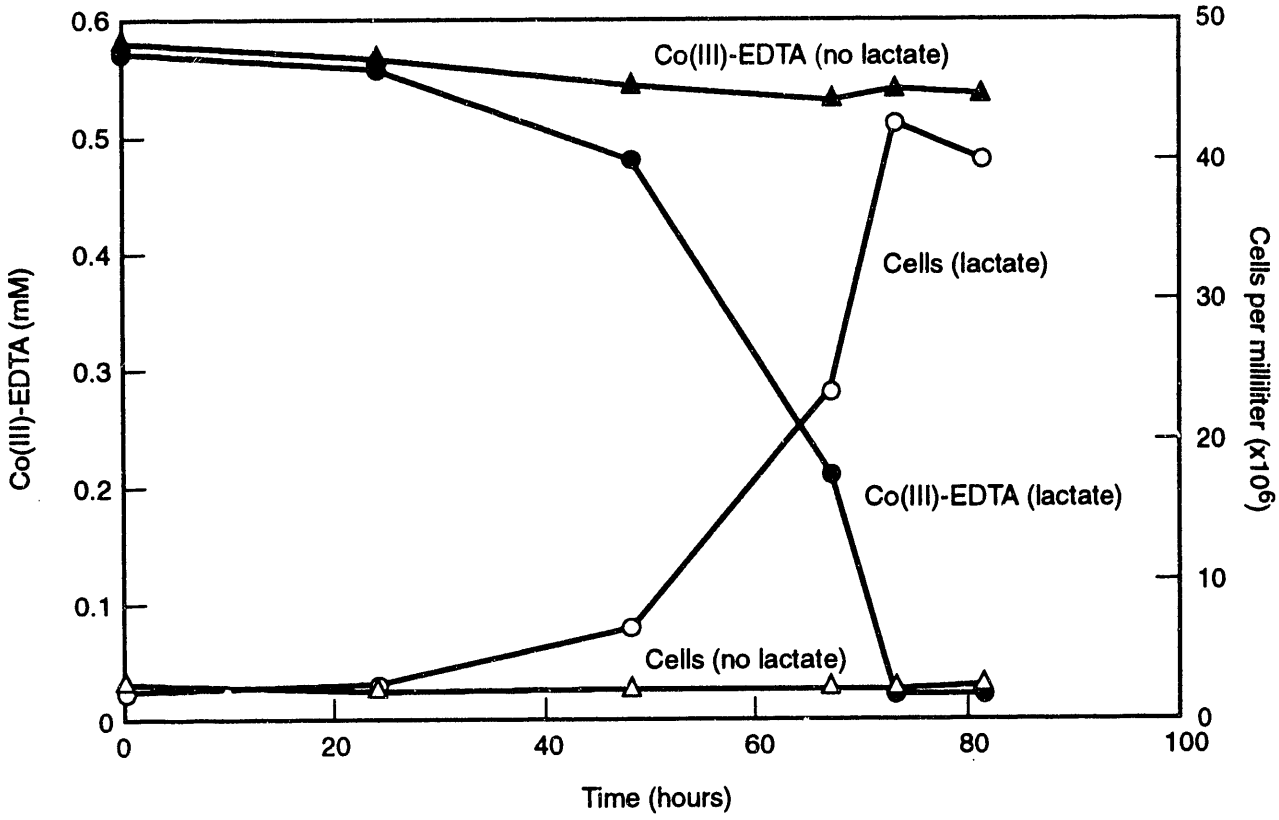

FIGURE 2. Growth of Bacterium BrY with Cobalt(III)-EDTA as the Sole Terminal Electron Acceptor. Cell numbers increased with a corresponding decrease in the concentration of cobalt (III)-EDTA. No change in either cell number or the concentration of cobalt(III)-EDTA was detected in cultures that lacked the electron donor (lactate). Similar results were obtained with cell suspensions of *G. metallireducens* and *S. putrefaciens* (data not shown).

Bioremediation: Biodegradative Enzyme Design

R. L. Ornstein

The objective of this research is to develop both advanced concepts and PNL's capabilities for improving subsurface bioremediation of contaminants at DOE sites through rational redesign and genetic engineering of enzyme-mediated microbial biodegradation. Remediation of subsurface environments is important not only to DOE, but also to the U.S. Department of Defense (DoD), the U.S. Environmental Protection Agency (EPA), and the private sector.

The nature of deep contamination (which is commonly dilute, highly dispersed, and inaccessible) limits or even precludes the application of many of the remediation strategies that are currently being used to remediate surface and near-surface contamination. Cost-effective remediation of synthetic substances in deep subsurface environments is, for the most part, limited to novel bioremediation alternatives (Brockman and Ornstein 1991). The widespread use of synthetic organic compounds, such as halogenated hydrocarbons, has strained the capacity and, in some cases, exceeded the inherent functionality of naturally occurring biodegradative systems. Although microorganisms have tremendous capacity to evolve to meet new selection pressures, the timescale required for them to do so, depending on the complexity of the necessary underlying metabolic modifications, may be unacceptably long when hazardous substances are involved (Ornstein 1991).

Thus rational redesign has the unique advantage of its ability to foster discovery of new enzymic forms that would otherwise have an extremely low probability of evolving biologically under either laboratory-controlled or natural conditions. (Such a low probability is to be expected when evolution of the enzyme requires several simultaneous and specific amino acid changes to efficiently catalyze a significantly different substrate.) To successfully carry out a rational enzyme redesign study for altering an enzyme's specificity or improving its efficiency, certain prerequisites are essential: adequate enzyme structural data, an understanding of the mechanism(s) of action, and a cloned gene.

Such information is available for the P450cam variant of the ubiquitous biodegrading and detoxifying superfamily of enzymes known as cytochromes P450. However, even though high-resolution experimental enzyme structures are invaluable for understanding structure-function relations, the structural image obtained is just an average in time and space. Non-average structures, which are not resolvable by experimental methods, are also important, because activity is not necessarily understandable from a consideration of the average structure only. (By analogy, the average structure of a person over a period several days would essentially be that of a person sleeping in bed. From such an average picture, it would be hard to distinguish an active football quarterback from one who had been sleeping for several days. The functionally important, i.e., distinguishing, motions of the quarterback occur only very briefly over any three-day period and would not be expected to show up in an average picture. Similarly, many enzymes are thought to adopt functionally critical conformations only transiently; these transient conformations are unlikely to be "visible" even by high-resolution experimental methods.) Computer simulations that start from a high-resolution experimental structure are capable of uncovering such structures. In view of the immense computational resources required to adequately simulate an enzyme's dynamic motions, only now are such simulations becoming cost-effective. Based on the simulations, experiments can be designed to refute or confirm the significance of each transient population, to establish its possible role in activity. Given this vantage, one would have a reasonable chance of successfully carrying out rational enzyme redesign.

FY 1992 Research Highlights

Collaborative experiment/theory studies with scientists at several universities are at different stages of maturity. Collaborative studies on cytochrome P450cam have been under way for about two years with Steve Sligar at the University of Illinois/Urbana and more began recently with Larry Wackett at the University of Minnesota. In FY 1992, PNL initiated a collaboration with Dick Janssen and Bauke Dijkstra of the University of Groningen (The Netherlands) on the biodegradative enzyme alkane dehalogenase. Some of our recent studies to better understand structure-function-dynamic relations for cytochrome P450cam and to redesign its specificity and improve its efficiency are described below.

Structure-Function-Dynamic Relations: Understanding Lock-and-Key Specificity. Cytochrome P450cam hydroxylates camphor, forming 5-hydroxycamphor with essentially 100% regiospecificity, and norcamphor is hydroxylated to form three products (45% 5-, 47% 6-, and 8% 3-hydroxynorcamphor) (Atkins and Sligar 1987, 1988). However, our previous simulations of norcamphor-bound P450cam predicted predominantly (from 68% to 88%) 5-hydroxynorcamphor (Bass et al. 1992; Paulsen and Ornstein 1992). One possible explanation for this discrepancy is that the simulations were performed using D-norcamphor, while the experiments were conducted with racemic norcamphor. The suggestion that norcamphor is the D-isomer was based on its similarity with the native substrate D-camphor. Indeed, using the reported crystallographic structure for norcamphor-bound P450cam would model norcamphor as the D-isomer (Raag and Poulos 1989). Unfortunately, the two stereomers have never been separated. In FY 1992, three simulations each of the L- and D-isomers of norcamphor bound to cytochrome P450cam were compared to account for the effects of substrate orientation and the assignment of random velocities. The results show that the L-isomer of norcamphor is predicted to form

predominantly 6-hydroxynorcamphor, while the D-isomer forms mainly 5-hydroxynorcamphor (Bass and Ornstein, in press). From these data, it can be inferred that racemic norcamphor will form non-racemic 5- and 6-hydroxynorcamphors after oxidation by cytochrome P450cam.

Proof-of-Principle: Redesigning Cytochrome P450cam. Before attempting to redesign the activity of P450cam for a substrate significantly different from camphor, we chose to first modify the specificity of P450cam for the analogue substrate norcamphor. Achieving such an intermediate goal will give considerable confidence and guidance toward modifying the specificity of P450cam to initiate the degradation pathway for targeted pollutants. To date, two predictions have been confirmed experimentally. The first involved mutating amino acid 87 based on the molecular dynamics simulation results, which indicated that this amino acid's very unusual dynamic mobility was correlated with the enzyme's catalytic efficiency (Bass et al. 1992; Paulsen et al. 1991). Changing amino acid 87 from phenylalanine to tryptophan resulted in a 100% increase in coupling efficiency, in semi-quantitative agreement with the prediction (Bass et al., in press).

Our second successful prediction involved an alteration of specificity and efficiency of cytochrome P450cam hydroxylation of 1-methyl-norcamphor. The wild enzyme hydroxylates the 3, 5, and 6 positions of norcamphor, but only the 5 and 6 positions of 1-methyl-norcamphor. For camphor, the degree of coupling is 100%, but for both norcamphor and 1-methyl-norcamphor, the efficiency is dramatically lowered, to 12 and 50%, respectively. Based on modeling and simulation results, it appeared that mutating position 185 from threonine to phenylalanine would eliminate hydroxylation at the 3 position and dramatically increase coupling. The mutant was constructed and the product profile and coupling were determined experimentally. Coupling was doubled and hydroxylation at the 3 position was essentially abolished, both in agreement with the prediction (Paulsen et al., in press).

References

Atkins, W. M., and S. G. Sligar. 1987. "Metabolic Switching in Cytochrome P450cam: Deuterium Isotope Effects on Regiospecificity and the Monoxygenase/Oxygenase Ratio." *Journal of the American Chemical Society* 109:3754-3760.

Atkins, W. M., and S. G. Sligar. 1988. "Deuterium Isotope Effects in Norcamphor Metabolism by Cytochrome P450cam: Kinetic Evidence for the Two-Electron Reduction of a High-Valent Iron-Oxo Intermediate." *Biochemistry* 27:1610-1616.

Bass, M. B., and R. L. Ornstein. "Substrate Specificity of Cytochrome P-450cam for L- and D-Norcamphor as Studied by Molecular Dynamics Simulations." *Journal of Computational Chemistry* (in press).

Bass, M. B., M. D. Paulsen, and R. L. Ornstein. 1992. "Substrate Mobility in a Deeply Buried Active Site: Analysis of Norcamphor Bound to Cytochrome P-450$_{cam}$ as Determined by a 201 psec Molecular Dynamics Simulation." *PROTEINS: Structure, Function, and Genetics* 13:26-37.

Bass, M. B., D. Filipovic, S. G. Sligar, and R. L. Ornstein. "The F87W Mutation of Cytochrome P450cam Increases the Coupling between Norcamphor Oxidation and NADH Reduction: Molecular Dynamics Simulation and Site-Directed Mutagenesis." In *Proceedings of the National Academy of Science, U.S.A.* (in press).

Brockman, F. J., and R. L. Ornstein. 1991. "Enhanced Bioremediation of Subsurface Contamination: Enzyme Recruitment and Redesign." In *Hazardous Materials Control/ Superfund '91, Proceedings of the 12th National Conference*, pp. 264-266. Hazardous Materials Control Research Institute, Greenbelt, Maryland.

Ornstein, R. L. 1991. "Why Timely Bioremediation of Synthetics May Require Rational Enzyme Redesign: Preliminary Report on Redesigning Cytochrome P450cam for Trichloroethylene Dehalogenation." In *On Site Bioreclamation: Processes for Xenobiotic and Hydrocarbon Treatment*, eds. R. E. Hinchee and R. F. Olfenbuttel, pp. 509-514. Butterworth-Heinemann, Boston, Massachusetts.

Paulsen, M. D., and R. L. Ornstein. 1992. "Predicting Product Specificity and Coupling of Cytochrome P450cam." *Journal of Computer-Aided Molecular Design* 6:449-460.

Paulsen, M. D., M. B. Bass, and R. L. Ornstein. 1991. "Analysis of Active Site Motions from a 175-picosecond Molecular Dynamics Simulation of Camphor-Bound Cytochrome P450cam." *Journal of Biomolecular Structure & Dynamics* 9:187-203.

Paulsen, M. D., D. Filipovic, S. G. Sligar, and R. L. Ornstein. "Controlling the Regiospecificity and Coupling of Cytochrome P450cam: T185F Mutant Increases Coupling and Abolishes 3-Hydroxy-norcamphor Product." *Protein Science* (in press).

Raag, R., and T. L. Poulos. 1989. "The Structural Basis for Substrate-Induced Changes in Redox Potential and Spin Equilibrium in Cytochrome P450cam." *Biochemistry* 28:917-922.

Genetic Profiling of Subsurface Microorganisms

G. L. Stiegler

Contributors

L. C. Stillwell and J. M. Heineman

Indigenous subsurface microorganisms have great potential for use in bioremediation efforts at DOE sites. However, scientific information characterizing the microorganisms involved in the degradation of important complex organic molecules is limited. A first step in the studies of these microbes is to identify the organism. For instance, it is important to have a means of rapidly identifying and monitoring important microbes used in *in situ* methods that enhance microbial numbers and biodegradative efficiencies. Methods of rapid identification will also be used for *in situ* identification of bioengineered microbes used in remediation.

Microbial identification methods are generally based on morphological characteristics. Direct microscopic examination and application of classical differential staining methods have a long history of use for microbial characterization. More specific methods of microbial identification are based on the high affinity of antibodies to microbial antigenic determinants, and immunological-based assays have been used extensively for clinical diagnostics. In this project, we are adapting a faster and more general approach to microbe identification. The method uses polymerase chain reaction (PCR) analysis (Saiki et al. 1988) of sequence-variable regions of the 16S rRNA gene. Nucleotide sequence analysis of 16S rRNA PCR products provides data for designing specific probes that are used for phylogenetic studies and microorganism identification (Barry et al. 1990; Rogall et al. 1990).

The prokaryotic ribosome, a necessary component of the protein-synthesizing machinery in the bacterial cell, consists of protein components and three unique RNA species termed the 5S, 16S, and 23S rRNA. Each rRNA molecule has an evolutionarily conserved nucleotide sequence, and differences in its molecular structure can provide information about the relatedness of different microbial isolates (Noller 1984). Knowledge of the rRNA gene sequences and the establishment of an accessible sequence database have benefited ongoing microbial taxonomic and phylogenetic studies. Although each of the rRNA (5S, 16S, and 23S) sequences has been used for molecular characterization and microbial identification, the 16S rRNA gene, because of its larger size and greater number of variable regions, provides a more favorable molecule for analysis (Pace et al. 1987). The approximately 1500-base-pair (bp) 16S rRNA gene can be easily analyzed by DNA sequence analysis, and its large size provides ample nucleotide variation to be a sensitive measure of evolutionary

change. Sequence analysis of several 16S rRNA genes has shown that highly conserved gene regions are interspersed with regions of considerable variability. Characterization of these variable regions provides information that can be used to develop molecular probes for identifying microbes (Barry et al. 1990).

FY 1992 Research Highlights

In this project, we are using PCR methods on mixed populations of microbes to define 16S rRNA deoxyoligonucleotide primers. The PCR primer sequences that we are using are based on the *Escherichia coli* 16S rRNA gene sequence. However, it is important that the PCR primers selected do not exhibit a bias by amplifying predominantly *E. coli* gene sequence-variable regions. Initially, to investigate this possible sequence bias, we are examining several of the resulting PCR amplification products for variability.

PCR Amplification and DNA Sequence Analysis. We are adapting a general method based on the PCR reaction that allows us to analyze specific sequence-variable regions in the 16S rRNA gene (Barry et al. 1990, 1991). The sequence information we obtain will be used to design specific probes and assays for microbial identification. The scheme we are using to examine the 16S rRNA sequence-variable regions is shown in Figure 1. Briefly, our approach has been to design and synthesize deoxyoligonucleotide PCR primers based on the conserved sequence of the *E. coli* 16S rRNA gene. The data shown in Figure 2 were generated with *E. coli*-established PCR primers to a variable 100-bp 16S rRNA gene region located at nucleotide positions 1399 through 1499 near the 3′ terminus of the16S rRNA gene. The PCR analysis is initiated in two amplification stages; the first uses primers identical to the *E. coli* 16S rRNA gene sequence at nucleotide positions 1388 and 1511 (Noller 1984). The amplification products are analyzed qualitatively by gel electrophoresis. Often the amplification yields multiple non-16S rRNA gene PCR products, and this complicates further nucleotide sequence analysis. We obtain a pure 16S rRNA PCR gene product in the second stage of analysis, by additional amplification using a nested PCR primer set derived from internal sequences adjacent to the initial amplification primers. The nested primers have an additional 6-bp Bam *H1* restriction endonuclease site synthesized at their 5′ terminus. The endonuclease recognition site is subsequently used to facilitate molecular cloning of the PCR products. The DNA sequence analysis and comparisons were performed on double-stranded recombinant DNA using an automated Applied Biosystems 373 A DNA sequencer and software.

Single-Strand Conformational Polymorphism Assay (SSCP). We are adapting a single-strand conformational polymorphism (SSCP) assay (Ainsworth et al. 1991; Murakami et al. 1991; Hayashi 1991) for identifying bacterial species. The assay gives a genetic fingerprint that is unique for a given species. The SSCP assay is based on initial PCR amplification of a given 16S rRNA gene sequence and the subsequent electrophoretic analysis of the denatured PCR product. The comparative migrational differences of the single-strand DNA molecule provide a profile that is species-specific. The SSCP assay is carried out by [^{32}P] 5′ end-labeling a single PCR primer. The resulting PCR amplification product is double-stranded with a single radiolabeled strand. Strands of the same length but varying in nucleotide composition migrate differentially when electrophoresed on a non-denaturing polyacrylamide gel. The technique used is very sensitive to nucleotide composition and can separate strands that differ by a single nucleotide base. The SSCP method provides a reproducible migrational pattern for each variable 16S rRNA sequence. The migrational pattern is specific for a species and can be used as a fingerprint for identification. The SSCP migrational differences are shown in Figure 3 for a number of unique PCR amplification products corresponding to the 1399 through 1499 variable sequence. The differences in nucleotide sequence for these samples are as indicated in Figure 2.

Future Research

The data that we are gathering from PCR-mediated 16S rRNA gene sequence analysis will be used to design species-specific primers and fluorescently tagged deoxyoligonucleotide probes. The species-specific primers will be used for ligation chain reaction (LCR) amplification

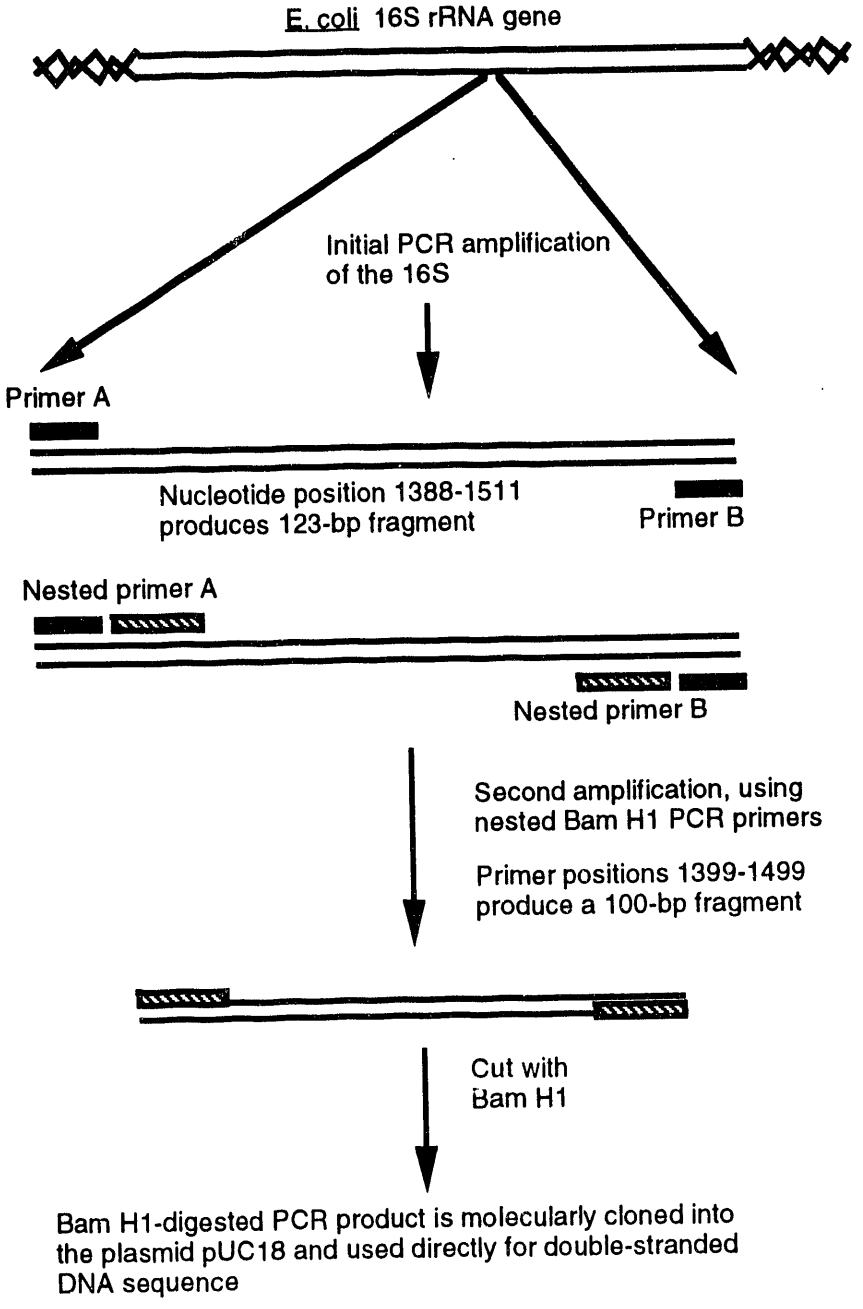

FIGURE 1. Method of PCR Amplification, Cloning, and Nucleotide Sequence Analysis of 16S rRNA Gene Sequence-Variable Regions

reactions, based on the use of a thermostable DNA ligase enzyme (Barany 1991). Deoxyoligonucleotides that match only the 16S rRNA sequence of the bacterial species of interest are synthesized. It is critical to have an exact sequence homology at the junction of two ligation reaction substrate deoxyoligonucleotides. If the match is not homologous, the ligation reaction does not proceed exponentially, resulting in the absence of an identifiable LCR product. Only those bacteria having the correct nucleotide sequence will give a positive result. The ligation-mediated PCR method is easily amenable to automation.

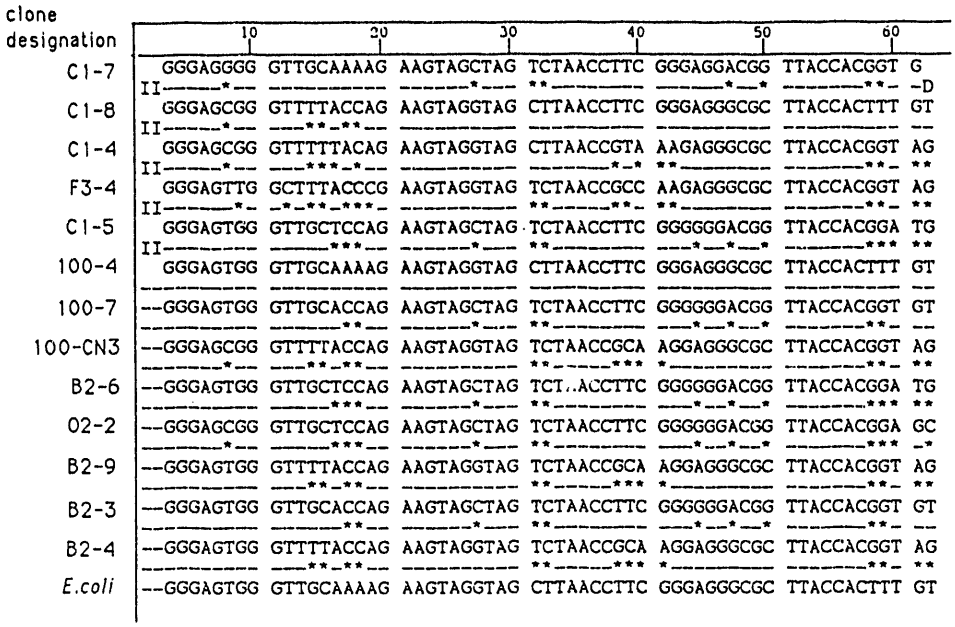

FIGURE 2. The 16S rRNA Gene Sequence Determined for Cloned Gene Nucleotide Positions Amplified Between Nested Primers Beginning at Base 1399 and Ending at Base 1499. The primer sequences are invariant and excluded from the analyzed sequence. The displayed sequence is the region amplified corresponding to bases 1414 to 1474. All variant cloned sequences are compared against the standard *E. coli* 16S rRNA gene sequence. Designations to the left of the figure, C1-7, C1-8, etc., are arbitrary designations we have used to label individual cloned 16S rRNA gene regions. Asterisks (*) indicate bases varying from *E. coli*.

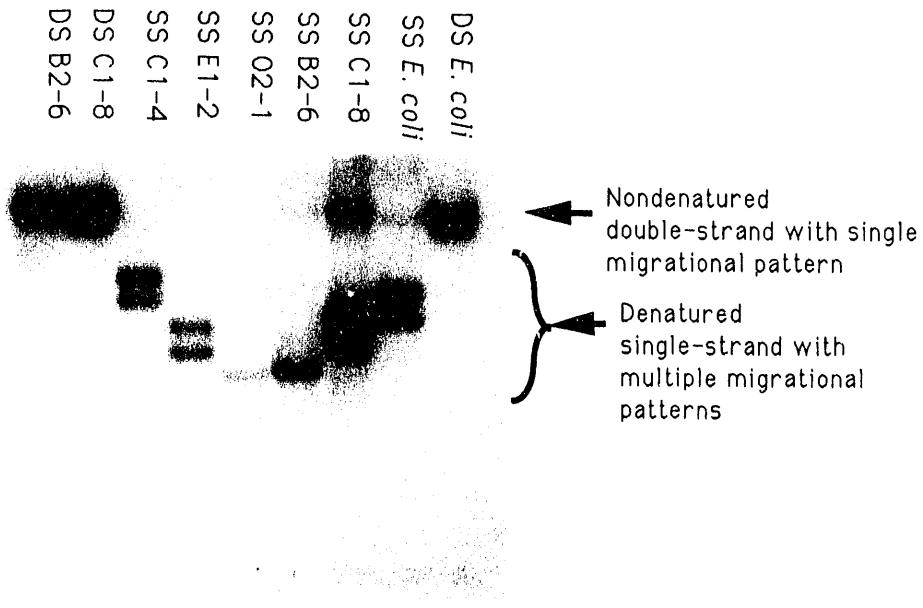

FIGURE 3. SSCP Analysis of PCR Products Amplified from Isolated 16S rRNA Recombinant Clones. The products shown in the autoradiogram were produced by [^{32}P] labeling of the 5'-end of nested primer B shown in Figure 1. The labeled PCR products were analyzed by denaturation and electrophoresis of a 6% nondenaturing polyacrylamide gel. The designation SS is for denatured single-strand product and DS is for nondenatured double-strand product. The labels C1-8, B2-6, 02-1, E1-2, C1-4, and *E. coli* designate individual cloned PCR products.

The knowledge of specific sequence differences in 16S rRNA gene sequence-variable regions can be exploited to design fluorescently labeled deoxyoligonucleotide probes that will identify single microbial cells in a mixed population (Delong et al. 1989; Amann et al. 1990). Methods have been developed to hybridize fluorescently labeled deoxyoligonucleotides with formaldehyde-fixed, intact cells and then view the probe interaction directly by fluorescence microscopy. The method is reliable and proceeds rapidly because of the abundance of rRNA in bacterial cells. It is also possible to simultaneously identify individual cell types by coincidence use of different fluorescently labeled probes. Identification using fluorescently labeled probes is also adaptable to automated analysis.

The goal for this project is to develop specific molecular probes for identifying bacterial species deemed important to understanding subsurface mocrobial processes. Probe development will emphasize specificity, rapidity of use, and potentially patentable methods of automated analysis based on probe specificity.

References

Ainsworth, P. J., L. C. Surh, and M. B. Coulter-Mackie. 1991. "Diagnostic Single-Strand Conformational Polymorphism (SSCP): A Simplified Non-Radioisotopic Method as Applied to a Tay-Sachs B1 Variant." *Nucleic Acids Research* 19:405-406.

Amann, R. I., L. Krumholz, and D. A. Stahl. 1990. "Fluorescent-Oligonucleotide Probing of Whole Cells for Determinative, Phylogenetic, and Environmental Studies in Microbiology." *Journal of Bacteriology* 172:762-770.

Barany, F. 1991. "The Ligase Chain Reaction in a PCR World." *PCR Methods and Applications* 1:5-16.

Barry, T., R. Powell, and F. Gannon. 1990. "A General Method to Generate DNA Probes for Microorganisms." *BioTechnology* 8:233-236.

Barry, T., G. Colleran, M. Glennon, L. K. Dunican, and F. Gannon. 1991. "The 16S/23S Ribosomal Spacer Region as a Target for DNA Probes to Identify Eubacteria." *PCR Methods and Applications* 1:51-56.

Delong, E. F., G. S. Wickham, and N. R. Pace. 1989. "Phylogenetic Strains: Ribosomal RNA-Based Probes for the Identification of Single Cells." *Science* 243:1360-1363.

Hayashi, K. 1991. "PCR-SSCP: A Simple and Sensitive Method for Detection of Mutations in the Genomic DNA." *PCR Methods and Applications* 1:34-38.

Murakami, Y., M. Katahira, R. Makino, K. Hayashi, S. Hirohashi, and T. Sekiya. 1991. "Inactivation of the Retinoblastoma Gene in a Human Lung-Carcinoma Cell-Line Detected by Single-Strand Conformational Polymorphism Analysis of the Polymerase Chain Reaction Product of cDNA." *Oncogene* 6:37-42.

Noller, H. F. 1984. "Structure of Ribosomal RNA." *Annual Review of Biochemistry* 53:119-162.

Pace, N. R., D. A. Stahl, D. J. Lane, and G. J. Olsen. 1987. "The Analysis of Natural Microbial Populations by Ribosomal RNA Sequences." *Advances in Microbial Ecology* 9:1-55.

Rogall T., J. Woters, T. Flohr, and E. C. Bottger. 1990. "Towards a Phylogeny and Definition of Species at the Molecular Level Within the Genus *Mycobacterium*." *International Journal of System Bacteriology* 40:323-330.

Saiki, R. K., D. H. Gelfand, S. Stoffel, S. J. Scharf, R. Higuchi, G. T. Horn, K. B. Mullis, and H. A. Erlich. 1988. "Primer Directed Enzymatic Amplification of DNA with a Thermostable DNA Polymerase." *Science* 239:487-491.

Probing of DNA in Environmental Microbial Populations

R. J. Douthart

The objective of this project has been to develop a new concept for DNA fragment analysis that would allow a number of DNA samples to be analyzed automatically and rapidly. To meet this need, PNL staff have developed a unique drum electrophoresis device on which a DNA sequencing ladder or restriction enzyme fragments can be deposited. This device, coupled with a gel assembly (ribbon channel plate) developed by a related project, is expected to make it possible to characterize very small quantities of DNA as well as to increase the rate of analysis by orders of magnitude. The objective of research in FY 1992 was to apply the device to probing small quantities of DNA rapidly. If the device proves viable, it will be used to rapidly characterize and study the genome of microorganisms that can be used in the transformation of contaminants in the environment.

Studies with a moving drum electrophoresis apparatus prior to FY 1992 indicated that a vertical device was feasible, with current being carried by the liquid interface between the drum and a nylon screen fixed to the drum surface on which DNA fragments are electrophoresed. Its advantages were reduced leakage and ease of loading. However, two major technical difficulties forced abandonment of the more conventional vertical design. These difficulties were the entrapment of bubbles and the occurrence of a substantial temperature difference (30°C or more) at the interface between the plate and the drum. To overcome these difficulties, the device was modified to a less conventional design, so that the attitude at which the electrophoresis plates impinge on the drum is horizontal. The new horizontal device tends to allow bubbles to escape and thermostatic control at the junction is much easier. The new design has not yet been thoroughly tested, although a prototype has been built and assembled. A patent application for the device is being developed contingent on demonstration of performance.

The ability to conduct large-scale DNA sequencing and other characterization will allow definition of the genome of microorganisms capable of carrying out specific environmental functions. Once developed, this methodology should allow probing of DNA from environmental microbial populations, providing information critical to determination of the origin and response of populations to manipulation for restoration. The concept will also be applicable to efforts to distinguish the origins of microorganisms in deep subsurface environments through characterization of microbial DNA. Thus a fully operational device will be an important tool that will be incorporated in and support future research to understand and use important microbial processes in the environment.

Use of Probes in DNA Fingerprinting

F. C. Leung and D. A. Cataldo

The use of low C_0t DNA as a probe for DNA fingerprinting assays has been validated for identification and phylogeny of fungal cultures. The novel aspect of this approach is that it does not require cloning and screening of a genomic library to identify a repetitive sequence clone to use as a probe in a DNA fingerprinting assay. The objective of this project is to determine whether the use of low C_0t DNA as a probe can be extended to prokaryotes.

Three bacterial cultures were obtained from Jim Fredrickson at PNL: *Escherichia coli*, F199, and *Pseudomonas putida*. Genomic DNA was extracted and low C_0t DNA was isolated from all three cultures. The genomic DNA from all three cultures were cut with *Hae* III, *Hinf* I, and *Alu* 1. The DNA fragments were then separated by agroase gel electrophoresis, transferred onto paper, and probed with low C_0t DNA from *E. coli*, F199, or *P. putida* and labeled by random priming. As Figure 1 shows, when we used low C_0t DNA from *E. coli* as a probe, it hybridized almost exclusively to *E. coli*. (There was slight cross-hybridization with *P. putida*.) Figures 2 and 3 show that when we used low C_0t DNA from F199 or *P. putida* as a probe, similar results were obtained. The F199 low C_0t DNA hybridized almost exclusively to F199, and the *P. putida* low C_0t DNA hybridized almost exclusively to *P. putida*. The methodology was

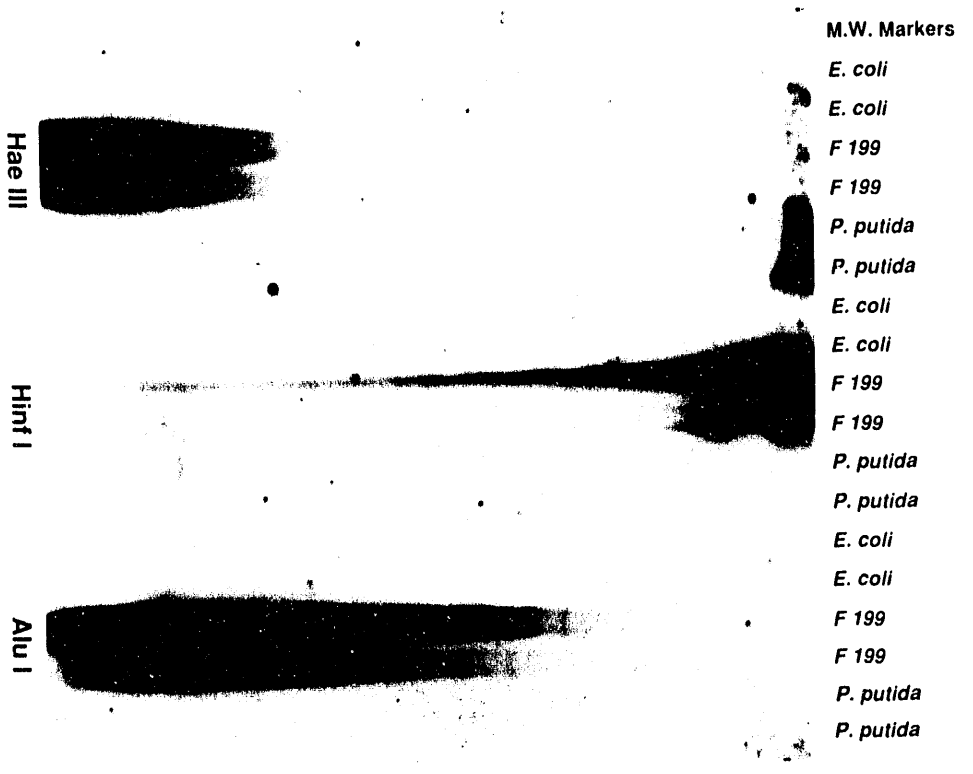

FIGURE 2. Autoradiogram of *Escherichia coli*, F199, and *Pseudomonas putida* Genomic Cut with *Hae* III, *Hinf* I, and *Alu* I and Probed with F199 low C_0t DNA Labeled with ^{32}P.

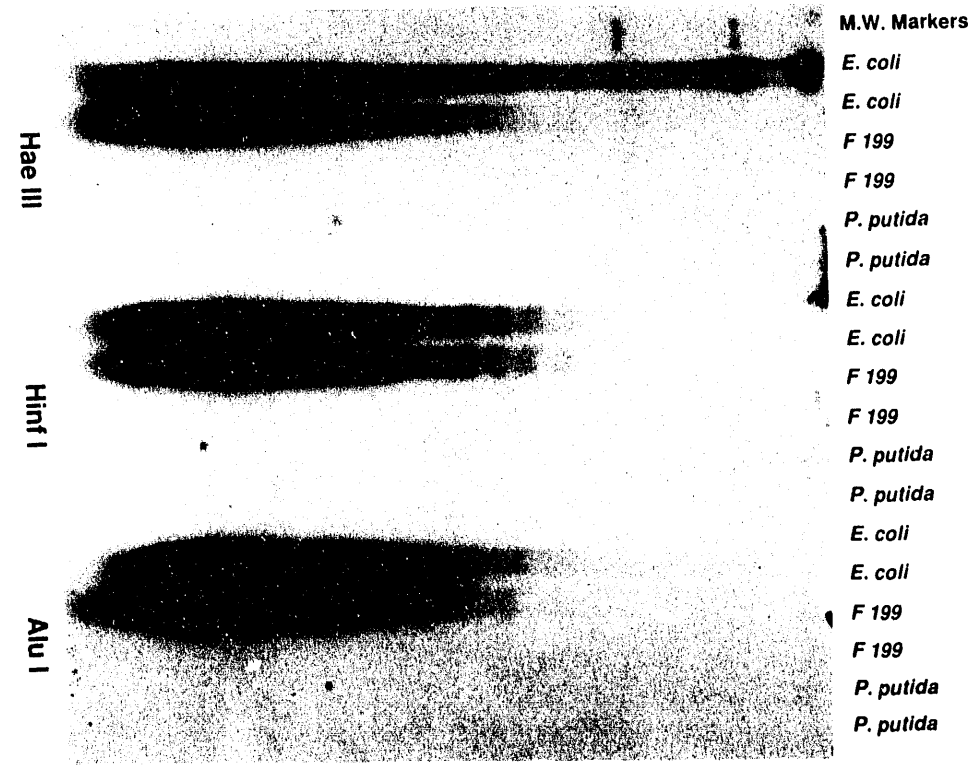

FIGURE 1. Autoradiogram of *Escherichia coli*, F199, and *Pseudomonas putida* Genomic Cut with *Hae* III, *Hinf* I, and Alu I and Probed with *E. coli* low C_0t DNA Labeled with ^{32}P.

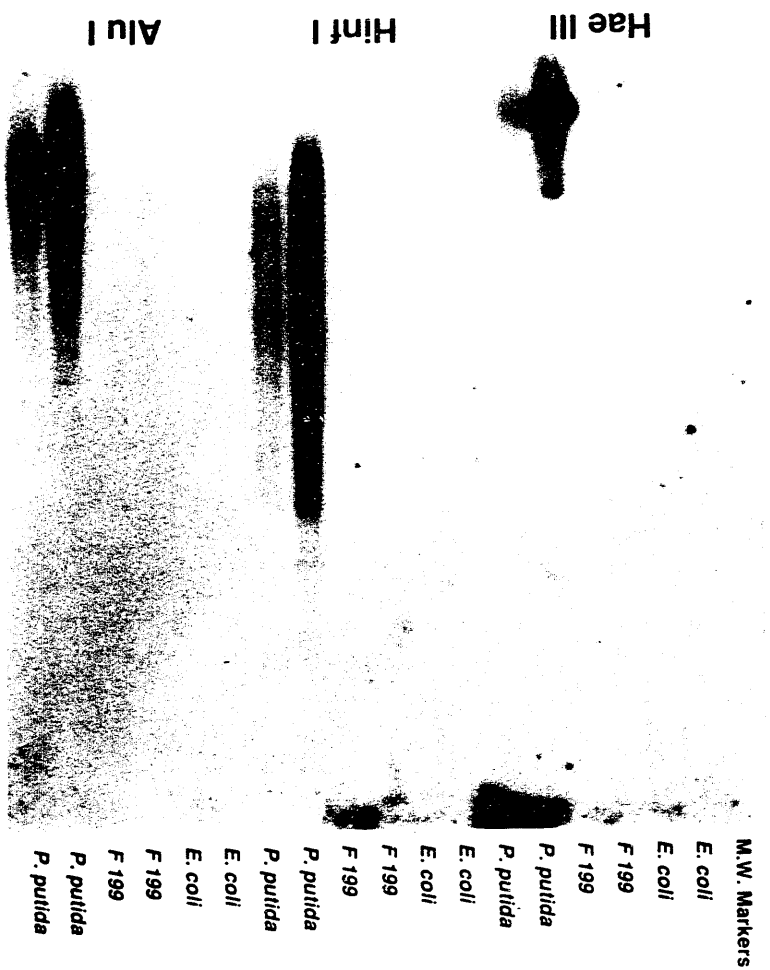

FIGURE 3. Autoradiogram of *Escherichia coli*, F199, and *Pseudomonac putida* Genomic Cut with *Hae* III, *Hinf* I, and *Alu* I and Probed with *P. putida* low C_0t DNA Labeled with ^{32}P.

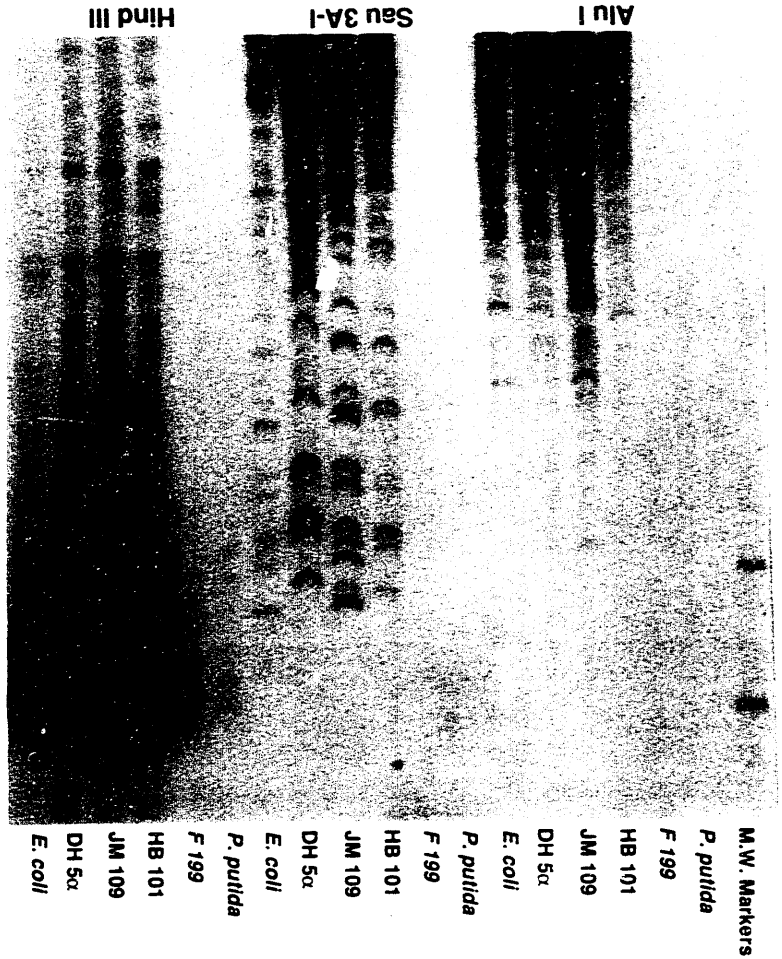

FIGURE 4. Autoradiogram of *Pseudomonas putida*, F199, HB 101, JM 109, DH 5*α*, and *Escherichia coli* Genomic Cut with *Alu* I, *Sau3A* I, and *Hind* III and Probed with *E. coli* low C_0t DNA Labeled with ^{32}P.

validated by these data, which demonstrate that *E. coli*, F199, and *P. putida* are genetically distant from each other. The overexposed lanes in Figures 1, 2, and 3 are due to the use of higher C_0t value DNA (>1.0) as a probe. We have determined that DNA with a C_0t value of about 1.0 is best for use as a probe in DNA fingerprinting (Figure 4).

In addition, when we used low C_0t DNA from *E. coli* as a probe in DNA fingerprinting, we could resolve individual differences among four closely related strains of *E. coli*: HB 101, JM 109, DH 5*α*, and *E. coli* (Figure 4). These results are a demonstration of the use of low C_0t DNA as a probe in DNA fingerprinting for closely related bacteria.

These data support the use of low C_0t DNA as a probe in DNA fingerprinting of closely related bacteria. In FY 1993, we hope to extend the low C_0t DNA technology to study population markers in bacteria. We also hope to use this technology to identify and characterize the genetic origin of subsurface bacteria isolated from sediments at the Hanford Site or other DOE sites.

Scale Averaging of Effective Parameters

T. R. Ginn

The overall goal of this research project is to examine both the theoretical basis for and the practical performance of effective-parameter representations of flow and transport transients in subsurface media characterized by multiple scales or evolving scale heterogeneities.

A principal hindrance to our ability to understand, simulate, and predict groundwater flow and transport dynamics is uncertainty in estimating the parameters for mathematical models of the subsurface physics. In particular, it is typically impossible to measure, either directly or indirectly, the transport property of concern on the field scale. Available data usually include flow and transport properties measured indirectly on scales much smaller than the field scale. Thus hydraulic conductivity is measured not directly as conductivity, but rather as flow through a controlled volume of aquifer (such as a core section from a well). Then a physically based model for this flow, which involves the conductivity of the volume sampled (e.g., the core), is inverted or calibrated for that value of the core-scale conductivity that makes the model flow match the observed data. Such data are often the primary source for values for field-scale parameters. That is, conductivity values from a few cores are averaged to determine the conductivity for a cube or slab of much greater size, perhaps kilometers long on a side.

This sort of averaging provides a rudimentary means of scaling information up to larger scales: the small-scale data are used to provide parameter values for large-scale models. Upscaling methods are generally hard to validate because not only are the large-scale parameter values immeasurable, they may be nonexistent. That is, the derivation of the differential equation on which the flow model is based requires that parameter values exist on a certain scale; this scale may be smaller than that of the large-scale model parameters. Consequently, values of the large-scale parameters that render the model even a crude representation of reality may not exist; for these reasons, the large-scale parameter values that are used are termed "effective values."

The inadequacy of this averaging approach in general and specifically its inability to capture aspects of aquifer heterogeneity that control field-scale transport are well documented (e.g., Journel and Alabert 1990). On the other hand, the accuracy and validity of deterministic flow models (and our confidence in their use in developing remediation strategies) depend very heavily on our ability to upscale small-scale data to the model scale and to incorporate hydrogeological and other data into the geologic depictions by means of inverse analysis. Although an immense amount of recent effort in the field has centered on the effects of field-scale and multi-scale heterogeneity on flow and transport prediction accuracy, little attention has been paid to the core issues: under what conditions do effective-parameter representations accurately capture flow transients, and what is the

relationship between these representations and the small-scale data available?

The objective of this work is to refine a groundwater flow and transport model calibration tool for understanding conditions for valid effective-parameter representations and determining ways to upscale aquifer transport properties.

FY 1992 Research Highlights

Research for FY 1992 focused on the refinement of a specialized inverse technique (developed under FY 1991 support) to determine of the existence of groundwater flow and transport parameters in the heterogeneous subsurface, and on the application of this technique to synthetic geologic structures with heterogeneities on evolving scales.

The inverse method involves the calibration of a system of ordinary differential equations that represent the transient flow dynamics of a stressed heterogeneous aquifer. The method identifies conditions for the existence, identifiability, and uniqueness of effective parameters of a representation of the subsurface flow regime that is spatially discretized but continuous in time (Ginn et al. 1990; Ginn and Cushman 1992). These spatial discretizations result from the application of numerical methods, such as finite differences or finite elements, which are the most common tools for solving field-scale flow and transport models. The inversion method is unique in that it comprises a direct analytical solution to the inverse problem for transient systems. The value of the method is that it treats transient aquifer hydraulic data analytically, without approximation in the time domain.

Work in FY 1992 progressed on the use of the inverse tool in both numerical experimentation and on analytical examination regarding the existence of effective parameters for groundwater flow. For both, the focus was on the following canonical problem: Suppose that the transient hydraulic response of an aquifer (e.g., a pumping test) is perfectly represented by a system of ordinary differential equations (ODEs) written for a very high level of resolution. The hydraulic response, however, can be observed at only a few points distributed throughout the aquifer. These points correspond to nodal locations for a much coarser representation of the aquifer flow system, which also takes the form of a linear system of ODEs. This coarse model corresponds to a field-scale model of an aquifer with heterogeneities on scales below that of the model. Our goal is to find conditions under which the coarse model adequately represents the groundwater flow dynamics in a transient setting. Specifically, we seek conditions for the existence of effective parameters for the coarse model that afford an accurate representation of the flow field.

The design of the numerical experiments required coding of the inverse algorithm for exercises with synthetic geological representations, as well as the coding of a "forward" transient solver for the simulation of aquifer hydraulics. The forward solution scheme that was encoded is based on the matrix exponential formulation of the high-resolution ODE system (Ginn et al. 1990). Figure 1 shows the steady-state solution for piezometric head in a heterogeneous two-dimensional synthetic aquifer with impermeable boundaries. The head field is the long-term response to equivalent pumping injection and withdrawal rates at opposing corners of the aquifer. This figure is an animated sequence of the hydraulic response to pumping, where the head is initially flat.

Although much effort in recent years has been directed to synthetic generation of aquifer realizations, most if not all of the approaches used to date involve statistically homogeneous systems with heterogeneities on at most a single scale. The experimental design for this project focused on devising a way to generate simulated aquifers with heterogeneities over multiple scales. The primary requirement for numerical aquifer synthesis is that multiscale heterogeneity complexity be captured in the models. Techniques from percolation theory were applied to devise an algorithm that generates two-dimensional maps of complex geologic structures. The geologic maps are made up of randomly sized "percolation clusters" in which the probability distribution of cluster size is controlled by a single parameter, the percolation probability (see Figure 2). The concept for this

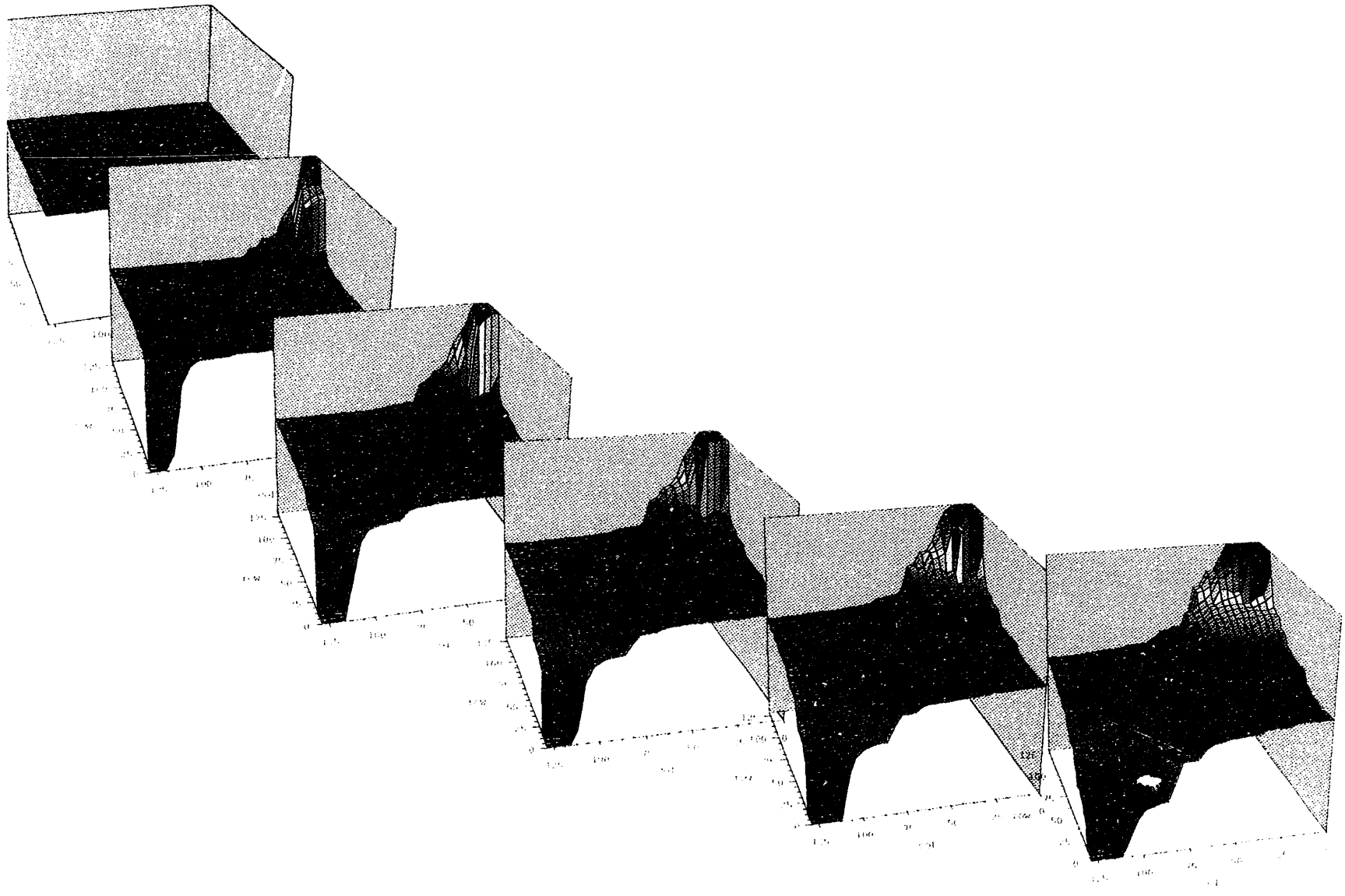

FIGURE 1. Steady-State Response of a Heterogeneous Aquifer to Cyclic Pumping at Opposing Corners

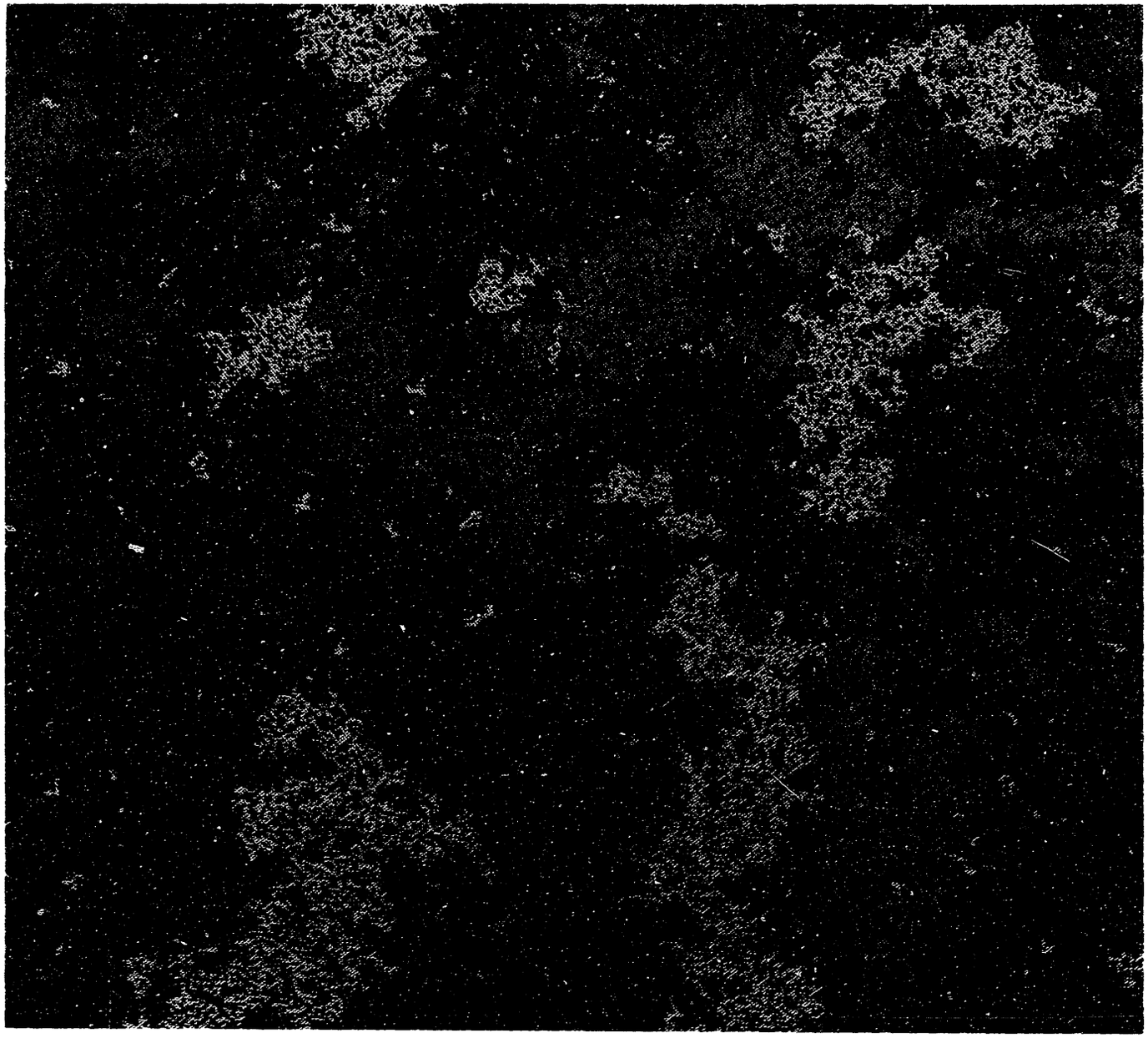

FIGURE 2. Two-Dimensional Percolation Map at the Threshold Probability, Showing Heterogeneous Clusters of All Possible Length Scales

approach originated through discussions with Harlan Foote and Charles Cole of PNL. If the colors of each cluster in Figure 2 correspond to a geologic or petrophysical subunit with its own unique transport property value (e.g., hydraulic conductivity), then control of the percolation probability gives control of the spectrum of heterogeneity scales in the synthetic aquifer. For example, Figure 2 shows a synthetic map of geostructure with heterogeneity on all scales of the representation from the smallest (that of a pixel) to the largest (that of the figure).

Based on both the analytical work and the numerical experiments, it appears that for many cases, no accurate effective-parameter representation exists when heterogeneities are on multiple scales, including scales beneath (i.e., at a higher resolution than) the scale of the effective parameters. This means in general that the differential equation often assumed to hold for field-scale groundwater flow may be inappropriate. These results helped spur a continuing collaborative effort with J. Cushman of Purdue University to derive, from basic statistical mechanical principles, a groundwater flow and transport equation that is valid for geologic media with heterogeneities over multiple scales. The principal characteristic of the new equation is that classical diffusive product terms are replaced by a generalization involving convolutions in space and time between the factors of the diffusion product terms.

Future Research

For FY 1993, extensive numerical experiments will involve application of the transient inverse operator to percolation-based geologic models like that depicted in Figure 2. The potential benefits of this work are significant. By carefully designing synthetic aquifer classes, we may be able to determine for real systems which geologic settings afford effective-parameter treatment and which do not. This determination can lead in turn to qualitative and quantitative measures of confidence in modeling remediation schemes. Furthermore, for cases where effective-parameter representations are accurate, we will obtain data on both the effective-parameter values (from the inverse method) and the high-resolution/small-scale heterogeneities (by synthetic aquifer construction). Analysis of these data will indicate how small-scale data should be averaged to obtain field-scale flow parameters. Current knowledge on how to do this is limited to severely simplified geologic settings, and averaging or upscaling of small-scale data is currently an area of active research in the field. The experimental approach described here is a particular focus (see, for example, Cole et al. 1985; Desbarats 1987; Deutsch 1989; King 1989; and Durlofsky 1992). However, all of this previous work has involved only steady-state flow regimes. Thus, the unique aspects of the present work are that 1) transient phenomena are addressed directly, and 2) a *set* of effective parameters is determined for a field-scale system, rather than a single homogenizing value for the entire aquifer. These aspects of practical field-scale modeling have not been addressed in previous efforts.

Preliminary testing of the experimental setup has already provided independent confirmation of some past findings and conjectures concerning the existence of effective parameters. These results relate to simplified depictions of geology, such as perfectly layered systems with flow along or across the layers. The first experiments planned for FY 1993 will address these cases in detail and then we will proceed to the next level of geologic complexity, as well as focusing on even more complex percolation-based geologic models.

Some valuable directions for new work have already been illuminated through the mathematical analysis and the numerical experiments, and on that basis research has been initiated in two new areas.

One of these areas concerns the need for a stochastic version of the transient inverse operator. Mathematical analysis directed toward this goal has now been initiated. We have already discovered that the existing tools for a stochastic treatment of the transient solute transport operator are not appropriate for the groundwater flow problem. All of the existing tools are methods of spectral decomposition of the stochastic flow-operator equation and require that the matrix operator involved be a rapidly fluctuating random function of time. In solute transport problems, particle dispersion includes

a "random walk" component that does in some cases satisfy this requirement. In groundwater flow problems, however, the matrix operator is, by construction, always independent of time. Thus classical operator decompositions (e.g., Kabala and Sposito 1991) as applied to solute transport models will not suffice for the simpler flow problems, although such approaches have been suggested (Zeitoun and Braester 1991). Work on this issue has been initiated with informal collaboration with Z. Kabala of the University of California at Riverside and J. Cushman of Purdue University.

For FY 1993, we plan experiments involving both very simple and very complex models of heterogeneous geologic structures and will analyze the results for indications of the conditions for existence of effective-parameter representations. Analysis of the results of these experiments, together with continued mathematical analysis, will also be directed to finding proper averaging techniques for determining effective parameters from small-scale data.

Work will also continue on two new branches of the study: the derivation of a stochastic operator expansion for uncertain but non-fluctuating matrix operators appearing in ODEs, and the derivation and testing of non-local balance laws for subsurface transport.

The method for calibration by inversion of a linear system of ordinary differential equations developed under this support may also be used in fields other than groundwater flow and transport, such as population dynamics, physical diffusion, and medical/biological system response, which use the same general mathematical model. Expansion of the review of relevant literature has identified many researchers in surprisingly disparate fields who are seeking solutions to precisely the same mathematical challenges. Therefore, FY 1993 funds will support direct contact with these scientists and the transfer of this new technology to their respective fields.

References

Cole, C. R., H. P. Foote, D. A. Zimmerman, and C. S. Simmons. 1985. "Understanding, Testing and Development of Stochastic Approaches to Hydrologic Flow and Transport Through the Use of the Multigrid Method and Synthetic Data Sets." Paper presented at the International Symposium on the Stochastic Approach to Subsurface Flow, June 3-7, 1985, Fontainebleau, France.

Desbarats, A. J. 1987. "Numerical Estimation of Effective Permeability in Sand-Shale Formations." *Water Resources Research* 23:273-286.

Deutsch, C. 1989. "Calculating Effective Absolute Permeability in Sandstone/Shale Sequences." *SPE Formation Evaluation*, September 1989, pp. 343-348.

Durlofsky, L. J. 1992. "Representation of Grid Block Permeability in Coarse-Scale Models of Randomly Heterogeneous Porous Media." *Water Resources Research* 28:1791-1800.

Ginn, T. R., J. H. Cushman, and M. H. Houck. 1990. "A Continuous-Time Inverse Operator for Groundwater and Contaminant Transport Modeling: Deterministic Case." *Water Resources Research* 26:241-252.

Ginn, T. R., and J. H. Cushman. 1992. "A Continuous-Time Inverse Operator for Groundwater and Contaminant Transport Modeling: Model Identifiability." *Water Resources Research* 28:539-549.

Journel, A. G., and F. G. Alabert. 1990. "New Method for Reservoir Mapping." *Journal of Petroleum Technology* February 1990, pp. 212-218.

Kabala, Z. J., and G. Sposito. 1991. "A Stochastic Model of Reactive Solute Transport with Time-Varying Velocity in a Heterogeneous Aquifer." *Water Resources Research* 27:341-350.

King, P. R. 1989. "The Use of Renormalization for Calculating Effective Permeability." *Transport in Porous Media* 4:37-58.

Sposito, G., D. A. Barry, and Z. J. Kabala. 1991. "Stochastic Differential Equations in the Theory of Solute Transport Through Inhomogeneous Porous Media." In *Advances in Porous Media*, Volume 1, ed. M.Y. Corapcioglu, pp. 295-309, Elsevier, New York.

Zeitoun, D. G., and C. Braester. 1991. "A Neumann Expansion Approach to Flow Through Heterogeneous Formations." *Stochastic Hydrology and Hydraulics* 5:207-226.

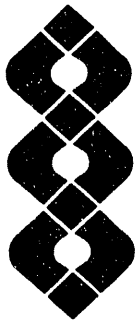

Interactions with Educational Institutions

Interactions with Educational Institutions

As part of its mission, PNL contributes to strengthening and enhancing mathematics, science, and technology education by building partnerships and developing collaborative programs with elementary and secondary schools and with colleges and universities. As part of the education initiative PNL 2000, the Laboratory has been one of the major organizers of a statewide effort to implement systemic change in mathematics, science, and technology education. Also as part of PNL 2000, the number of new Laboratory-university partnerships reached a record level this year. Through its education programs, students and faculty are provided access to some of the Laboratory's unique human and technical resources, such as the Subsurface Environmental Research Facility, Environmental Research Park, and Aerosol Wind Tunnel Research Facility.

Pre-university programs are coordinated by PNL's Science Education Center. The Office of University Programs coordinates minority institution and university programs. The Northwest College and University Association for Science (NORCUS) and the Associated Western Universities (AWU) provide the mechanisms for student and faculty appointments to university programs.

Pre-University Interactions

PNL scientists participate in such pre-university education activities as 1) classroom instruction and demonstrations; 2) student apprenticeships, workshops, and field days in the laboratory; 3) teacher workshops and research participation; and 4) technical support and assistance to local and regional schools. The Arid Lands Ecology facility in particular provides an important part of environmental education activities conducted for pre-university students and teachers.

Each summer, middle and secondary school mathematics, science, and technology teachers are assigned to work on environmental research projects as part of DOE's Teacher Research Associates Program. These eight-week assignments are made based on the educational background and teaching experience of program participants. This year nearly half of the 40 national/regional appointees were assigned to projects in earth and environmental sciences.

Projects in 1992 included such activities as 1) modeling transport of subsurface contaminants; 2) programming a model of heat and moisture flux on the land surface and studying the effects in a mesoscale climate model; 3) assisting in basic and applied research tasks related to plant ecology, revegetation, and plant physiology; and 4) testing waste-form leaching and subsequent interactions of leachate with barrier materials and soils. All of the teachers participating in the program developed instructional strategies to use in their classrooms based on their experiences at the Laboratory.

As part of DOE's national effort to stimulate student interest in science, mathematics, and technology, PNL scientists worked with middle school students in the OPTIONS in Science program to explore career options. They also assisted middle school teachers in teaching science using actual research approaches.

Researchers worked with elementary school teachers participating in Science Alive, a three-week program in environmental sciences for schools in the Yakima Valley and Tri-Cities that serve large numbers of Hispanic, American Indian, and black students. The teachers participated in hands-on problem-solving field and laboratory experiences led by PNL scientists.

Researchers participated in a two-week honors institute in environmental sciences for high school students from around the world. Studies concerned shrub-steppe plant assessment, groundwater modeling, habitat enhancement, and stream water quality.

Researchers made presentations at local, regional, and community schools through the Sharing Science with Schools program. These

presentations covered such subjects as environmental microbiology, plant and wildlife ecology, and environmental transport of pollutants.

University Interactions

Through the NORCUS, AWU, and Science Engineering Research Semester (SERS) programs, PNL gives university undergraduate and graduate students and postdoctoral scientists and faculty an opportunity to work with staff in research activities and to participate in seminars, scientific meetings, and symposia.

During FY 1992, many university faculty, undergraduate, and graduate students participated in environmental sciences programs. A total of 68 NORCUS appointees were assigned to environmental sciences this year, more than double the number who participated in FY 1991. In addition, through AWU, 16 students and faculty worked with PNL researchers in environmental sciences, with four in regular laboratory assignments and seven as part of the Environmental Management Career Opportunities Research Experience (EMCORE). Three undergraduate students also participated in environmental sciences studies under the SERS program. Some of student and faculty involvement is described below, and details are provided in the research progress reports.

During the year, the Environmental Sciences Program also hosted many visiting scientists representing universities nationally and internationally, for workshops, seminars, and DOE program reviews. Many new joint PNL-university partnerships are expected to be established in the next year in the environmental sciences, as a result of new Laboratory-university partnerships with major U.S. universities.

Subsurface Science

The Subsurface Chemistry of Organic-Ligand-Radionuclide Mixtures project has maintained active relationships with several universities through both subcontracts and collaborative research. Funds were provided to Dr. Mark Brusseau of the University of Arizona, who was a visiting scientist at PNL from June through September 1992. He assisted in the conceptualization of the intermediate-scale, co-contaminant experiments with cobalt-EDTA and performed several column experiments with cobalt-EDTA to evaluate hypotheses regarding the influences of mineralogic heterogeneity on reactive species transport.

A SERS undergraduate student, Heather Lumppio, spent a semester and the summer working on the Microbial Sequestration and Bioaccumulation of Radionuclides and Metals Project at PNL in FY 1992. Nicole Flint, a SERS undergraduate student, spent her fall semester working on the project.

The Subsurface Microbial Processes Project provided educational experience for a number of undergraduate and graduate students over the past year. The students and aspects of their work are listed below:

Christy Kelley (University of Washington) and Siegrid Lui (Stanford University), NORCUS, microbiological analysis of Hanford confined aquifer GEMHEX samples.

Heath D. Watts and Jennifer J. Walker, NORCUS, optimization of solid growth medium for isolation and culture of microorganisms from the terrestrial subsurface.

Barry Holbert, SERS, lipid profile analysis of subsurface bacteria and an independent experiment on heterogeneity of subsurface bacteria.

Ken Wagnon (Eastern Washington University), molecular probe analysis of confined aquifer anaerobic bacteria and culturing of anaerobic bacteria in unconfined aquifer GEMHEX sediments.

Michael Truex (Washington State University), role of starvation in induction of quinoline catabolic genes in a subsurface bacterium.

The Subsurface Microbial Processes Project also collaborated with faculty at a variety of academic institutions, including

Dr. David Balkwill (Florida State University), characterization of deep subsurface bacteria.

Interactions with Educational Institutions

As part of its mission, PNL contributes to strengthening and enhancing mathematics, science, and technology education by building partnerships and developing collaborative programs with elementary and secondary schools and with colleges and universities. As part of the education initiative PNL 2000, the Laboratory has been one of the major organizers of a statewide effort to implement systemic change in mathematics, science, and technology education. Also as part of PNL 2000, the number of new Laboratory-university partnerships reached a record level this year. Through its education programs, students and faculty are provided access to some of the Laboratory's unique human and technical resources, such as the Subsurface Environmental Research Facility, Environmental Research Park, and Aerosol Wind Tunnel Research Facility.

Pre-university programs are coordinated by PNL's Science Education Center. The Office of University Programs coordinates minority institution and university programs. The Northwest College and University Association for Science (NORCUS) and the Associated Western Universities (AWU) provide the mechanisms for student and faculty appointments to university programs.

Pre-University Interactions

PNL scientists participate in such pre-university education activities as 1) classroom instruction and demonstrations; 2) student apprenticeships, workshops, and field days in the laboratory; 3) teacher workshops and research participation; and 4) technical support and assistance to local and regional schools. The Arid Lands Ecology facility in particular provides an important part of environmental education activities conducted for pre-university students and teachers.

Each summer, middle and secondary school mathematics, science, and technology teachers are assigned to work on environmental research projects as part of DOE's Teacher Research Associates Program. These eight-week assignments are made based on the educational background and teaching experience of program participants. This year nearly half of the 40 national/regional appointees were assigned to projects in earth and environmental sciences.

Projects in 1992 included such activities as 1) modeling transport of subsurface contaminants; 2) programming a model of heat and moisture flux on the land surface and studying the effects in a mesoscale climate model; 3) assisting in basic and applied research tasks related to plant ecology, revegetation, and plant physiology; and 4) testing waste-form leaching and subsequent interactions of leachate with barrier materials and soils. All of the teachers participating in the program developed instructional strategies to use in their classrooms based on their experiences at the Laboratory.

As part of DOE's national effort to stimulate student interest in science, mathematics, and technology, PNL scientists worked with middle school students in the OPTIONS in Science program to explore career options. They also assisted middle school teachers in teaching science using actual research approaches.

Researchers worked with elementary school teachers participating in Science Alive, a three-week program in environmental sciences for schools in the Yakima Valley and Tri-Cities that serve large numbers of Hispanic, American Indian, and black students. The teachers participated in hands-on problem-solving field and laboratory experiences led by PNL scientists.

Researchers participated in a two-week honors institute in environmental sciences for high school students from around the world. Studies concerned shrub-steppe plant assessment, groundwater modeling, habitat enhancement, and stream water quality.

Researchers made presentations at local, regional, and community schools through the Sharing Science with Schools program. These

presentations covered such subjects as environmental microbiology, plant and wildlife ecology, and environmental transport of pollutants.

University Interactions

Through the NORCUS, AWU, and Science Engineering Research Semester (SERS) programs, PNL gives university undergraduate and graduate students and postdoctoral scientists and faculty an opportunity to work with staff in research activities and to participate in seminars, scientific meetings, and symposia.

During FY 1992, many university faculty, undergraduate, and graduate students participated in environmental sciences programs. A total of 68 NORCUS appointees were assigned to environmental sciences this year, more than double the number who participated in FY 1991. In addition, through AWU, 16 students and faculty worked with PNL researchers in environmental sciences, with four in regular laboratory assignments and seven as part of the Environmental Management Career Opportunities Research Experience (EMCORE). Three undergraduate students also participated in environmental sciences studies under the SERS program. Some of student and faculty involvement is described below, and details are provided in the research progress reports.

During the year, the Environmental Sciences Program also hosted many visiting scientists representing universities nationally and internationally, for workshops, seminars, and DOE program reviews. Many new joint PNL-university partnerships are expected to be established in the next year in the environmental sciences, as a result of new Laboratory-university partnerships with major U.S. universities.

Subsurface Science

The Subsurface Chemistry of Organic-Ligand-Radionuclide Mixtures project has maintained active relationships with several universities through both subcontracts and collaborative research. Funds were provided to Dr. Mark Brusseau of the University of Arizona, who was a visiting scientist at PNL from June through September 1992. He assisted in the conceptualization of the intermediate-scale, co-contaminant experiments with cobalt-EDTA and performed several column experiments with cobalt-EDTA to evaluate hypotheses regarding the influences of mineralogic heterogeneity on reactive species transport.

A SERS undergraduate student, Heather Lumppio, spent a semester and the summer working on the Microbial Sequestration and Bioaccumulation of Radionuclides and Metals Project at PNL in FY 1992. Nicole Flint, a SERS undergraduate student, spent her fall semester working on the project.

The Subsurface Microbial Processes Project provided educational experience for a number of undergraduate and graduate students over the past year. The students and aspects of their work are listed below:

Christy Kelley (University of Washington) and Siegrid Lui (Stanford University), NORCUS, microbiological analysis of Hanford confined aquifer GEMHEX samples.

Heath D. Watts and Jennifer J. Walker, NORCUS, optimization of solid growth medium for isolation and culture of microorganisms from the terrestrial subsurface.

Barry Holbert, SERS, lipid profile analysis of subsurface bacteria and an independent experiment on heterogeneity of subsurface bacteria.

Ken Wagnon (Eastern Washington University), molecular probe analysis of confined aquifer anaerobic bacteria and culturing of anaerobic bacteria in unconfined aquifer GEMHEX sediments.

Michael Truex (Washington State University), role of starvation in induction of quinoline catabolic genes in a subsurface bacterium.

The Subsurface Microbial Processes Project also collaborated with faculty at a variety of academic institutions, including

Dr. David Balkwill (Florida State University), characterization of deep subsurface bacteria.

Dr. David Boone (Oregon Graduate Institute), analysis of samples from the DOE/Texaco exploratory origins project. Dr. Boone assisted in defining the community structure of the samples, which resulted in detection and isolation of several strains of unique thermophilic Mn(IV)-reducing bacteria.

Dr. Thomas Kieft (New Mexico Institute of Mining and Technology; NORCUS student support), microscopic analysis of GEMHEX samples from Hanford's confined aquifer.

Dr. Raina Miller (University of Arizona; NORCUS student support), investigation of biosurfactant-aided biodegradation of organic chemicals

Dr. Andy Ogram (Washington State University), extraction and analysis of bacterial DNA in GEMHEX samples from the unconfined aquifer.

There was also collaborative interaction between the Pore-Water Chemistry Project and universities participating in the Deep Microbiology Subprogram. In particular, this included collaboration with T. Phelps (University of Tennessee) and T. Kieft (New Mexico Institute of Mining and Technology).

Under the Numerical Model of Transient Radon Flux project, Tom Borak and Milan Gadd of Colorado State University (CSU) continue to use the Rn3D code to simulate transient radon flux measurements from the CSU experimental facility. They have also made use of PNL's recent study of the effects of winds on radon concentration profiles beneath a slab-on-grade house with dry gravel of various thicknesses surrounding the outer surfaces of the slab.

Terrestrial Science

The Defining Resource Islands Using Multiple-Variable Statistics project interacts extensively with Jeffrey L. Smith, a U.S. Department of Agriculture – Agricultural Research Service soil scientist at Pullman, Washington, who is concerned with nitrogen dynamics of arid ecosystems. At Smith's laboratory, both a post-doctoral fellow (Dr. Jay Halvorson) and a graduate student (Dan Mummey) were funded by this project to aid in conducting the research reported for this fiscal year.

On the Effects of Nitrogen and Water on the Efficiency of Water and Nitrogen Use project, S. O. Link interacted with several graduate students who either were funded from this program in FY 1992 or had been in the past. Doug Jeffries, who worked under J. M. Klopatek at Arizona State University, has now taken a faculty position in the University of the Ozarks in Arkansas. Project staff are cooperating on publications based on his work at the Arid Lands Ecology (ALE) Reserve. Lenny Schwarz is currently working under J. M. Klopatek and staff are also cooperating on publications based on his work at the ALE Reserve. Joseph Healy, a new graduate student working under R. A. Black at Washington State University, is pursuing a master's degree on the water relations of *Artemisia tridentata*. S. O. Link has also interacted with Rob Kremer, a student under Steve Running of the University of Montana, in his studies of landscape predictions of soil water dynamics on the ALE Reserve.

Laboratory-Directed Research and Development

The Enzymatic Transformation of Inorganic Chemicals project funds a post-doctoral research associate, Yuri A. Gorby, who has developed a new technical area at PNL. A SERS undergraduate student, Daniel Drecktrah, and a SERS graduate student, Frank Cacovva, spent a semester and the summer, respectively, working on this project at PNL. Drecktrah was from the University of Wisconsin and is now pursuing a Ph.D. in Biochemistry at Cornell University. Cacovva is a Ph.D. candidate in Microbiology at the University of Oklahoma.

In FY 1992, the Biodegradative Enzyme Design project continued a coupled theory-experimental collaboration with Dr. Steven G. Sligar (Departments of Biochemistry and Chemistry of the University of Illinois at Urbana), who is a leading expert in the area of site-directed mutagenesis and biochemical mechanistic experiments for P450cam mutants. A joint theoretical effort was continued with Professor Robert Rein's group (State University of New York at Buffalo and Roswell Park Memorial Institute) to develop major extensions and improvements to

the capabilities of molecular dynamics simulation programs for enzyme studies. In FY 1992, the project also hosted and supported several SERS/NORCUS pre- and post-doctoral students.

The Genetic Profiling project supported an undergraduate, Jill Heineman, and a graduate student, Lisa Stillwell, through the NORCUS program. Both have worked with the project for several years and become valuable collaborators in the field of molecular biology.

Continued collaboration with John Cushman of Purdue University has been instrumental in advancing research in the Scale Averaging of Effective Parameters project, especially in the areas of non-local transport and stochastic transient inverse methods. New university interactions in FY 1992 included informal work with Zbigniew Kabala of the University of California at Riverside. The work with Dr. Kabala is focused on the stochastic inverse operator.

Technology
Transfer

Technology Transfer

The transfer of information and technology is important to DOE, and especially to the Subsurface Science Program, which emphasizes fundamental research on subsurface environments in support of the need to address the problems associated with more than 40 years of waste generation and disposal at DOE sites. Basic research within the Subsurface Science Program is aimed at developing an understanding of subsurface systems and has led to the discovery of new research tools, methods, and remediation concepts and principles that have immediate or long-term applications. A program of technology and information transfer ensures that the findings of these investigations are effectively communicated to other DOE offices, other federal agencies, academia, and industry (which together form the user community). The result is that important advances in the understanding of subsurface environments are contributing to the solution of DOE's long-term problems in environmental restoration and waste management. The fundamental nature of this research has also led to discoveries that may support industrial developments, such as uses of natural microbiological products and processes.

Identification of new opportunities for technology and information transfer from the Subsurface Science Program is an integral function of the Environmental Science Research Center (ESRC) at PNL. The ESRC was formed as part of the Subsurface Science Program to support its basic scientific mission, to facilitate the use of fundamental knowledge for developing innovative *in situ* remediation concepts, and to aid in the transfer of information and technology between the Subsurface Science Program and the user community. In support of the Subsurface Science Program's mission as a fundamental science program, publication in the open scientific literature is the principal mechanism for communicating research results. However, the Subsurface Science Program also sponsors technical meetings and round-table discussions that act as forums for technology transfer. The ESRC coordinates several of these efforts and continues to identify new ways to facilitate information and technology transfer.

The objective of the ESRC's technology transfer program is to better integrate information and technology transfer into Subsurface Science Program programmatic activities, both to identify new opportunities sooner and to ensure that they are acted on in a timely manner. To accomplish this, the ESRC facilitates regular communication and interactions among Subsurface Science Program investigators and, when appropriate, incorporates consideration of technology and information transfer at Subsurface Science Program meetings throughout the year.

Information transfer to the user community proceeds along a number of paths, including scientific publication and public meetings to describe basic research results. However, to facilitate transfer of concepts to the user community, an experimental program of more structured interactions has been undertaken in FY 1992-93. This program involves projects both at PNL and elsewhere.

Under this program, the Subsurface Science Program has successfully transferred research protocols for aseptic drilling and sample handling to DOE's Office of Technology Development (OTD) in the Office of Environmental Restoration and Waste Management (EM). These protocols are currently being employed by OTD's Integrated Demonstrations at Hanford and the Savannah River Site. To extend the availability of these capabilities, a series of workshops is planned at other DOE sites where knowledge of subsurface microbial systems is needed and where *in situ* remediation alternatives are being considered.

Fundamental research in the Subsurface Science Program has been directed toward the development of an experimental approach to investigate the feasibility of manipulating coupled microbiological and chemical processes, as a means of altering oxidation-reduction conditions in an aquifer. This research has resulted in new concepts, experimental designs, and research tools for investigating the interactive effects of subsurface physical, chemical, and microbial processes on redox conditions in the field. The

field manipulation experimental design and related information have now been transferred to EM for implementation. Close coordination between the Subsurface Science Program and EM is being maintained to facilitate a field test of the new concepts within the OTD, either through one of the integrated demonstrations or through the *In Situ* Remediation Integrated Program. A continuing liaison with EM will be maintained to assist in the incorporation of the experiment into applied research programs.

Deep microbiology research sponsored by the Subsurface Science Program at the Hanford Site and other DOE sites has provided a variety of microorganisms for inclusion in the Subsurface Microbial Culture Collection (SMCC) at Florida State University. Supported by the Subsurface Science Program, the SMCC includes of 7,000 strains of microorganisms from the Savannah River Site, the Idaho National Engineering Laboratory, the Hanford Site, and elsewhere that may be a unique genetic resource. The potential value of the SMCC is that the microbial strains were isolated from previously unexplored subsurface environments. Two strains have already been shown to possess novel properties. One of these has been shown to be capable of degrading a broad array of hydrocarbons under conditions of low oxygen, a property that may be unique to this organism. A second isolate from the subsurface produces a pigment that is sensitive to pH (deep blue in alkaline conditions and red in acid) and also to oxidation/reduction conditions (redox). Potential biomedical applications of the pigment include its use as a pH or redox indicator in diagnostic procedures. The possible value of the SMCC as a source of novel bioactive compounds is recognized by industry. For example, one pharmaceutical company has purchased a subset of the strains, and the Subsurface Science Program is working simultaneously with several biotechnology companies and with the National Cancer Institute, Natural Products Branch, to develop a collaborative research and screening program centered on the collection.

For the past several years, PNL researchers C. S. Simmons, J. W. Cary, and J. F. McBride have conducted fundamental research on how organic fluids behave in subsurface environments. Because nonaqueous phase liquids may travel separately from either water or organic vapors in the subsurface environment, the scientists needed a tool to detect organic liquids specifically. Furthermore, because subsurface environments are heterogeneous and the behavior of organic liquid is complicated, it was important to be able to monitor different phases at many individual locations. To meet their needs, they developed a new sensor that works on the principle that transmission of light through a translucent porous material corresponds to the amount of liquid that is present in its immediate vicinity. Testing showed that as soon as an organic liquid reaches the sensor, the output signal changes, meaning that it is extremely sensitive and quick to respond. This new sensor has the additional advantage of being composed of inexpensive and durable materials, the choice of which makes the sensor specific to particular kinds of fluids. The sensor technology received an R&D 100 award in 1991 and a Federal Laboratory Consortium award in 1992, and was recently licensed to an electronics and industrial control company that specializes in the detection of contaminants in soil. This company will use the sensor for detecting leaks in underground pipelines and storage tanks. The company also plans to continue development of the sensor to enable detection of a wider range of organic liquids. For example, the sensor is being employed at Air Force bases where soils and groundwater are contaminated with solvents and fuel hydrocarbons.

Other transferred technology includes a PNL-developed air permeameter that permits the *in situ* measurement of air permeability properties of sediments. When calibrated against laboratory estimates of hydraulic conductivity, this tool allows the determination of variability in the field. The air permeameter is currently being field tested by the EM in the VOC Arid Site Integrated Demonstration Program at the Hanford Site.

In addition to these efforts to transfer information, the ESRC has a scientific outreach program. Information and technology are transferred by conducting national workshops, participating in scientific meetings, publication in the open scientific literature, and involvement of universities and industry in the Cooperative

Research and Development Agreement (CRADA) process. Through this program, the scientific community nationwide has participated in refining research directions for the Subsurface Science Program and in opportunities for multi-institutional involvement in studies of complex processes, and multidisciplinary field research programs, such as the Geological, Microbiological, and Hydrological EXperiment (GEMHEX).

Publications and Presentations

Publications

Subsurface Science

Ainsworth, C. C., J. K. Fredrickson, and S. C. Smith. 1992. "The Effect of Sorption on the Degradation of Aromatic Acids and Bases." In *Sorption and Degradation of Agrichemicals*. Soil Science Society of America, Madison, Wisconsin.

Bolton, H., Jr., and R. E. Wildung. "Bioaccumulation of Radionuclides and Metals by Microorganisms: Potential Role in the Separation of Inorganic Contaminants and for the *in situ* Treatment of the Subsurface." In *First Hanford Separations Science Workshop Proceedings* (in press).

Bolton, H., Jr., S. W. Li, and A. E. Plymale. 1992. "Radionuclide Bioaccumulation by Subsurface Microorganisms." *Abstracts of the 203rd American Chemical Society Meeting*, p. GEOC 170.

Bolton, H., Jr., S. W. Li, D. J. Workman, and D. C. Girvin. "Biodegradation of Synthetic Chelates in Subsurface Sediments from the Southeast Coastal Plain." *Journal of Environmental Quality* (in press).

Bolton, H., Jr., D. J. Workman, D. C. Girvin, S. W. Li, and S. D. Harvey. 1992. "Mineralization of Metal-NTA Complexes by *Pseudomonas* Strain ATCC 29600." *Agronomy Abstracts*, p. 250.

Brockman, F. J., T. L. Kieft, J. K. Fredrickson, B. N. Bjornstad, S. W. Li, W. Spangenburg, and P. E. Long. 1992. "Microbiology of Vadose Zone Paleosols in South-Central Washington State." *Microbial Ecology* 23:279-301.

Cary, J. W., J. F. McBride, and C. S. Simmons. 1991. "Assay of Organic Liquid Contents in Predominantly Water-Wet Unconsolidated Porous Media." *Journal of Contaminant Hydrology* 8:135-142.

Cary, J. W., G. W. Gee, and C. S. Simmons. 1991. "Using an Electro-Optical Switch to Measure Soil Water Suction." *Soil Science Society of America Journal* 55:1798-1800.

Gassman, P. L., D. C. Girvin, and H. Bolton, Jr. 1992. "Adsorption of Co^{2+}, Nitrilotriacetic Acid (NTA) and Co-NTA Chelate on Gibbsite." *Agronomy Abstracts*, p. 237.

Gee, G. W., C. T. Kincaid, R. J. Lenhard, and C. S. Simmons. 1991. "Recent Studies of Flow and Transport in the Vadose Zone." In *U.S. National Report to International Union of Geodesy and Geophysics 1987-1990, Reviews of Geophysics, Supplement*, pp. 227-239, American Geophysical Union, Washington, D.C.

Girvin, D. C., P. L. Gassman, and H. Bolton, Jr. "Adsorption of Aqueous Cobalt Ethylenediaminetetraacetate by δ-Al_2O_3: Effects of Oxidation State, Ionic Strength, and Sorbent Concentration." *Soil Science Society of America Journal* (in press).

Girvin, D.C., P.L. Gassman, and H. Bolton, Jr. 1992. "EDTA, Co(II)EDTA and Co(III)EDTA Adsorption by δ-Al_2O_3: Triple Layer Modeling." *Agronomy Abstracts*, p. 237.

Holford, D. J., S. D. Schery, J. L. Wilson, and F. M. Phillips. "Modeling Radon Transport in Dry, Cracked Soil." *Journal of Geophysical Research* (in press).

Jayasinghe, D. S., B. J. Brownawell, H. Chen, and J. C. Westall. "The Determination of Henry's Constants of Organic Compounds of Low Volatility: Methyl Anilines in Methanol-Water." *Environmental Science and Technology* (in press).

Lenhard, R. J. 1992. "Measurement and Modeling of Three-Phase Saturation-Pressure Hysteresis." *Journal of Contaminant Hydrology* 9:243-269.

McBride, J. F., C. S. Simmons, and J. W. Cary. 1992. "Interfacial Spreading Effects on One-Dimensional Organic Liquid Infiltration in Water-Wetted Porous Media." *Journal of Contaminant Hydrology* 11:1-25.

Murphy, E. M., J. A. Schramke, J. K. Fredrickson, H. W. Bledsoe, A. J. Francis, D. S. Sklarew, and J. C. Linehan. 1992. "The Influence of Microbial Activity and Sedimentary Organic Carbon on the Isotope Geochemistry of the Middendorf Aquifer." *Water Resources Research* 28(3):723-740.

Prunty, L. 1992. "Thermally Driven Water and Octane Redistribution in Unsaturated, Closed Soil Cells." *Soil Science Society of America Journal* 56:707-714.

Smith, S. C., C. C. Ainsworth, S. J. Traina, and R. J. Hicks. 1992. "Effect of Sorption on the Biodegradation of Quinoline." *Soil Science Society of America Journal* 56:737-746.

Stevens, T. O., J. P. McKinley, and J. K. Fredrickson. "Bacteria Associated with Deep, Alkaline, Anaerobic Groundwaters in SE Washington." *Microbial Ecology* (in press).

Thomas, D. M., J. M. Cotter, and D. J. Holford. "Experimental Design for Soil Gas Radon Monitoring." *Journal of Radioanalytical and Nuclear Chemistry* (submitted).

Truex, M. J., F. J. Brockman, D. L. Johnstone, and J. K. Fredrickson. 1992. "Effect of Starvation on Induction of Quinoline Degradation for a Subsurface Bacterium in a Continuous-Flow Column." *Applied Environmental Microbiology* 58:2386-2392.

Zachara, J. M., C. T. Resch, and S. C. Smith. 1992. "Influences of Humic Substances on Co^{2+} by a Subsurface Mineral Separate and Its Mineralogic Components." *Geochimica et Cosmochimica Acta* (in press).

Terrestrial Science

Bolton, Jr., H., J. K. Fredrickson, and L. F. Elliott. 1992. "Microbial Ecology of the Rhizosphere." In *Soil Microbial Ecology, Applications in Agricultural and Environmental Management*, ed. F. B. Metting, Jr., pp. 27-63 Marcel Dekker, New York.

Bolton, Jr., H., J. L. Smith, and S. O. Link. "Soil Microbial Biomass and Activity of a Disturbed and Undisturbed Shrub-Steppe Ecosystem." *Soil Biology & Biochemistry* (in press).

Bromenshenk, J. J., J. L. Gudatis, S. R. Carlson, J. M. Thomas, and M. A. Simmons. 1991. "Population Dynamics of Honey Bee Nucleus Colonies Exposed to Industrial Pollutants." *Apidolgie* 22:359-369.

Bromenshenk, J. J., S. R. Carlson, J. M. Thomas, J. L. Gudatis, M. A. Simmons, and J. C. Simpson. 1992. "Field Validation of Pollution Monitoring Around Puget Sound with Honey Bees." *Apidolgie* (submitted).

Cullinan, V. I. and J. M. Thomas. "An Intercomparison of Quantitative Methods for Examining Landscape Pattern and Scale." *Landscape Ecology* (in press).

Downs, J. L., and S. O. Link. 1992. "Changes in Hydraulic Resistance of *Bromus tectorum* under Enhanced Nitrogen and Water Conditions." *Supplement to the Bulletin of the Ecological Society of America* 73:160.

Eberhardt, L. L. 1991. "Experimental Ecology. Review of: Ecological Experiments: Purpose, Design and Execution, by N. G. Hairston." *Ecology* 72:1904-1905.

Eberhardt, L. L. 1991. "Models of Ungulate Population Dynamics." *Rangifer* 7:24-29.

Eberhardt, L. L. 1992. "An Analysis of Procedures for Implementing the Dynamic Response Method." *Marine Mammal Science* 8(3):201-212.

Eberhardt, L. L., and J. M. Breiwick. 1992. "Impact of Recent Population Data on Historical Population Levels of Bowhead Whales Inferred from Simulation Studies." *Report of the International Whale Commission* 42:485-489.

Eberhardt, L. L., and M. A. Simmons. 1992. "Assessing Rates of Increase from Trend Data." *Journal of Wildlife Management* 56:603-610.

Eberhardt, L. L., and J. M. Thomas. 1991. "Designing Environmental Field Studies." *Ecological Monographs* 72(2):53-73.

Eberhardt, L. L., and K. W. Pitcher. "A Further Analysis of the Nelchina Caribou and Wolf Data." *Wildlife Society Bulletin* (in press).

Evans, R. D., R. A. Black, and S. O. Link. 1991. "Reproductive Growth During Drought in *Artemisia tridentata* Nutt." *Functional Ecology* 5:676-683.

Garrott, R. A., D. B. Siniff, and L. L. Eberhardt. 1991. "Growth Rates of Feral Horse Populations." *Journal of Wildlife Management* 55:641-648.

Gee, G. W., M. D. Campbell, and S. O. Link. 1991. "Arid Site Water Balance Using Monolith Lysimeters." In *Lysimeters for Evapotranspiration and Environmental Measurement*, eds. R. G. Allen, T. A. Howell, W. O. Pruitt, I. A. Walter, and M. E. Jensen, pp. 219-227. American Society of Civil Engineers, New York.

Jeffries, D. L., S. O. Link, and J. M. Klopatek. "CO_2 Fluxes of Cryptogamic Crusts. I. Response to Resaturation." *New Phytologist* (in press).

Jeffries, D. L., S. O. Link, and J. M. Klopatek. "CO_2 Fluxes of Cryptogamic Crusts. II. Response to Dehydration." *New Phytologist* (in press).

Jeffries, D. L., J. M. Klopatek, S. O. Link, and H. Bolton, Jr. 1992. "Acetylene Reduction of Cryptogamic Crusts from a Blackbrush Community as Related to Resaturation/Dehydration." *Soil Biology and Biochemistry* (in press).

Link, S. O., D. E. Gibbons, G. M. Petrie, R. R. Kirkham, L. E. Rogers, and P. A. Beedlow. 1991. "Estimation of Latent Heat Flux Using Quantitative Landsat Thematic Mapper Satellite Data in a Shrub-Steppe Ecosystem." *Supplement to the Bulletin of the Ecological Society of America* 72:177.

Link, S. O., J. L. Downs, M. E. Thiede, T. B. Chadwell, and H. Bolton, Jr. 1992. "The Effect of Water and Nitrogen on *Bromus tectorum* in the Field." *Supplement to the Bulletin of the Ecological Society of America* 73:250-251.

Link, S. O., W. J. Waugh, J. L. Downs, M. E. Thiede, J. C. Chatters, and G. W. Gee. "Effects of Coppice Dune Topography and Vegetation on Soil Water Dynamics in a Cold-Desert Ecosystem." *Journal of Arid Environments* (submitted).

Simmons, M. A., V. I. Cullinan, and J. M. Thomas. 1992. "Satellite Imagery as a Tool to Evaluate Ecological Scale." *Landscape Ecology* 7:77-85.

Smith, J. L., J. J. Halvorson, and H. Bolton, Jr. 1992. "Spatial Relationships of Soil Microbial Biomass Processes in an Arid Shrub-Steppe Ecosystem." In *Abstracts of the Sixth International Symposium on Microbial Ecology*, p. 285.

Thiede, M. E., S. O. Link, R. J. Fellows, and P. A. Beedlow. "Analysis of an Acute Dose of Gamma Radiation on Stem Diameter Growth, Carbon Gain, and Biomass Partitioning in *Helianthus annuus*." *Experimental and Environmental Botany* (in press).

Laboratory-Directed Research and Development

Arnold, G. E., and R. L. Ornstein. "A Molecular Dynamics Simulation of Bacteriophage T4 Lysozyme." *Protein Engineering* (in press).

Bass, M. B., D. F. Hopkins, W. A. Jaquish, and R. L. Ornstein. 1992. "A Method for Determining the Positions of Polar Hydrogens Added to a Protein Structure That Maximizes Protein Hydrogen Bonding." *PROTEINS: Structure, Function, and Genetics* 12:266-277.

Bass, M. B., M. D. Paulsen, and R. L. Ornstein. 1992. "Molecular Dynamics Simulations of Norcamphor-Cytochrome P-450cam and Mutations of P-450cam Designed to Alter the Product Specificity." In *Cytochrome P-450: Biochemistry and Biophysics*, eds. A. I. Archakov and G. I. Bachmanova, pp. 680-685. INCO-TNC, Moscow, Russia.

Bass, M. B., M. D. Paulsen, and R. L. Ornstein. 1992. "Substrate Mobility in a Deeply Buried Active Site: Analysis of Norcamphor Bound to Cytochrome P-450cam as Determined by a 201 psec Molecular Dynamics Simulation." *PROTEINS: Structure, Function, and Genetics* 13:26-37.

Bass, M. B., and R. L. Ornstein. "Substrate Specificity of Cytochrome P-450cam for L- and D-Norcamphor as Studied by Molecular Dynamics Simulations." *Journal of Computational Chemistry* (submitted).

Bass, M. B., D. Filipovic, S. G. Sligar, and R. L. Ornstein. "Increasing the Coupling between Norcamphor Oxidation and NADH Reduction in the P450cam Reaction by Molecular Dynamics Simulation and Site-Directed Mutagenesis." *Protein Engineering* (in press).

Braatz, J. A., M. D. Paulsen, and R. L. Ornstein. 1992. "3 nsec Molecular Dynamics Simulation of the Protein Ubiquitin and Comparison with X-ray Crystal and Solution NMR Structure." *Journal of Biomolecular Structure & Dynamics* 9:935-949.

Braatz, J. A., M. B. Bass, and R. L. Ornstein. "Predicted Structures of the Cytochrome P450 *Streptomyces griseolus* Enzymes P450su1 and P450su2." *Protein Science* (submitted).

Brockman, F. J., and R. L. Ornstein. 1991. "Enhanced Bioremediation of Subsurface Contamination: Enzyme Recruitment and Redesign." In *Hazardous Materials Control/Superfund '91, Proceedings of the 12th National Conference*, pp. 264-266. Hazardous Materials Control Research Institute, Greenbelt, Maryland.

Cushman, J. H., and T. R. Ginn. "A Statistical Mechanical Derivation of Non-Local Transport in Porous Media with Evolving Heterogeneities." *Water Resources Research* (submitted).

Filipovic, D., M. D. Paulsen, P. J. Loida, R. L. Ornstein, and S. G. Sligar. "Ethylbenzene Hydroxylation by Cytochrome P450cam." *Biochemical and Biophysical Research Communications* (submitted).

Filipovic, D., M. D. Paulsen, J. D. Ropp, I. C. Gunsalus, R. L. Ornstein, and S. G. Sligar. "Prediction of the Three-Dimensional Structure of Cytochrome P450lin Using Homology Modelling and Molecular Dynamics." In *Proceedings of the National Academy of Science USA* (in press).

Gorby, Y. A., H. Bolton, Jr., and D. R. Lovley. 1992. "Microbial Chromium Reduction and Immobilization." *Abstracts of the 203rd American Chemical Society Meeting*, p. GEOC 130.

Gorby, Y. A., D. B. Drecktrah, D. C. Girvin, J. M. Zachara, and H. Bolton, Jr. 1992. "Enzymatic Co(III)-EDTA Reduction." In *Abstracts of the 6th International Symposium on Microbial Ecology*, p. 98.

Paulsen, M. D., and R. L. Ornstein. 1991. "A 175 psec Molecular Dynamics Simulation of Camphor-Bound Cytochrome P450cam." *PROTEINS: Structure, Function, and Genetics* 11:184-204.

Paulsen, M. D., and R. L. Ornstein. "Predicting Product Specificity and Coupling for Catalysis by Cytochrome P450cam." *Journal of Computer-Aided Molecular Design* 6 (in press).

Paulsen, M. D., and R. L. Ornstein. "Substrate Mobility in Thiocamphor-Bound Cytochrome P450cam: An Explanation of the Conflict Between the Observed Product Profile and the X-ray Structure." *Protein Engineering* (submitted).

Paulsen, M. D., M. B. Bass, and R. L. Ornstein. 1991. "Analysis of Active Site Motions from a 175 psec Molecular Dynamics Simulation of Camphor-Bound Cytochrome P450cam." *Journal of Biomolecular Structure & Dynamics* 9:187-203.

Paulsen, M. D., D. Filipovic, S. G. Sligar, and R. L. Ornstein. "Controlling the Regiospecificity and Coupling of Cytochrome P450cam: T185F Mutant Increases Coupling and Abolishes 3-Hydroxy-norcamphor Product." *Protein Science* (submitted).

Sokalski, A., J. Lai, N. Luo, S. Sun, M. Shibata, R. L. Ornstein, and R. Rein. 1991. "Ab Initio Study of the Electrostatic Multipole Nature of Torsional Potentials: Hydrogen Peroxide and Methyl Disulfide (CH_3SSCH_3)." *International Journal of Quantum Chemistry: Quantitative Biology Symposium* 18:61-71.

Sokalski, W. A., M. Shibata, R. L. Ornstein, and R. Rein. 1992. "Cumulative Atomic Multipole Moments Complement Any Atomic Charge Model to Obtain More Accurate Electrostatic Properties." *Journal of Computational Chemistry* 13:883-887.

Sokalski, W. A., M. Shibata, R. L. Ornstein, and R. Rein. "Point Charge Representation of Multicenter Multipole Moments in Calculation of Electrostatic Properties." *Theoretica Chimica Acta* (in press).

Sokalski, W. A., D. A. Keller, R. L. Ornstein, and R. Rein. "Effects of the Multipole Correction on Charge Distribution: I. Peptides." *Journal of Computational Chemistry* (submitted).

Sun, S., N. Luo, R. L. Ornstein, and R. Rein. 1992. "Protein Structure Prediction Based on Statistical Potential." *Biophysical Journal* 62:104-106.

Presentations

Subsurface Science

Bolton, H., Jr. 1991. "Chemical/Microbiological Factors Controlling the Subsurface Transport of Chelated Radionuclides." Paper presented at the Biodegradation/Microbial Physiology Subprogram Meeting of the Subsurface Science Program, Gaithersburg, Maryland, December 4, 1991.

Bolton, H., Jr. 1992. "Coupled Microbial-Geochemical Experiments." Paper presented at the DOE Coupled Processes Subprogram Meeting, Richland, Washington, February 28, 1992.

Bolton, H., Jr., S. W. Li, and A. E. Plymale. 1992. "Radionuclide Bioaccumulation by Subsurface Microorganisms." Paper presented at Symposium on Microbial Catalysts in Metal Biogeochemistry, American Chemical Society, San Francisco, California, April 10, 1992.

Brockman, F. J., T. L. Kieft, J. K. Fredrickson, B. N. Bjornstad, and P. E. Long. 1991. "Moisture Recharge and Organic Carbon as Factors Controlling Vadose Zone Microbial Communities at the Hanford Site." Paper presented at the 38th Pacific Northwest American Geophysical Union, Richland, Washington, October 1991.

Fredrickson, J. K., F. J. Brockman, S. W. Li, J. P. McKinley, T. L. Kieft, D. B. Ringelberg, and D. C. White. 1992. "Microbial Activity and Community Structure in an Unsaturated Subsurface Paleosol as Influenced by O_2 and Mixing." Paper presented at the 6th International Symposium on Microbial Ecology, Barcelona, Spain, September 6-11, 1992.

Lenhard, R. J., T. G. Johnson, and J. C. Parker. 1991. "Experimental Observations of Non-aqueous Phase Liquid Behavior: Implications for Modeling." Paper presented at the American Geophysical Union Fall Meetings, San Francisco, California, December 9-12, 1991.

Lenhard, R. J. 1991. "Measurement and Modeling of Air-Water Saturation-Pressure Relations." Paper presented at the Annual Soils Science Society of America Meetings, Denver, Colorado, October 27-November 1, 1991.

Long, P. E., J. K. Fredrickson, E. M. Murphy, S. A. Rawson, J. P. McKinley, F. J. Brockman, and B. N. Bjornstad. 1991. "Geohydrologic and Geochemical Controls on Subsurface Microorganisms in Late Cenozoic Sediments, Southcentral Washington." Paper presented at the Geological Society of America Meetings (Abstracts with Programs 23(5):A377), San Diego, California, October 21-24, 1991.

Long, P. E., E. M. Murphy, S. A. Rawson, J. K. Fredrickson, B. N. Bjornstad, F. J. Brockman, and J. P. McKinley. 1991. "Subsurface Microorganisms in Late Cenozoic Sediments of the Hanford Site, Southcentral Washington." Paper presented at the American Geophysical Union Fall Meeting, San Francisco, California, December 9-12, 1991.

Murphy, E. M. 1991. "Microbial Origins in Groundwater." Paper presented at the DOE Microbial Origins Workshop, Lewes, Delaware, October 15-16, 1991.

Murphy, E. M. 1992. "A Trip Along a Flow Path· Results From the Savannah River Site Study." Paper presented at the DOE Deep Microbiology Investigators Meeting, Las Vegas, Nevada, January 14-16, 1992.

Murphy, E. M., and B. D. Wood. 1992. "Intermediate-Scale Experiments in Support of Deep Microbiology." Paper presented at DOE Deep Microbiology Investigators Meeting, Las Vegas, Nevada, January 14-16, 1992.

Murphy, E. M. 1992. "Carbon Isotopes and Microbial Processes in Groundwater." Paper presented at the American Geophysical Union Spring Meeting, Montreal, Quebec, May 12-13, 1992.

Murphy, E. M. 1992. "An Evaluation of Microbial Origins in Groundwater Using Geochemical and Isotopic Analyses." Paper presented at the Informational Meeting on Basic Research in Geomicrobiology and Subsurface Heterogeneity, DOE Subsurface Science Program, Germantown, Maryland, August 11, 1992.

Murphy, E. M., and B. D. Wood. 1992. "Potential Field Sites in Support of Microbial Origins." Paper presented at the Informational Meeting on Basic Research in Geomicrobiology and Subsurface Heterogeneity, DOE Subsurface Science Program, Germantown, Maryland, August 11, 1992.

Murphy, E. M. 1992. "Factors Controlling Microbial Transport in the Subsurface." Paper presented at the DOE Evolutionary Clocks Workshop, Annapolis, Maryland, September 30 - October 2, 1992.

Murphy, E. M. 1992. "Geochemical Dating Techniques." Paper presented at the DOE Evolutionary Clocks Workshop, Annapolis, Maryland, September 30 - October 2, 1992.

Schramke, J. A., and E. M. Murphy. 1991. "Reaction-Path Modelling and ^{14}C Age-Dating of Groundwater from the Middendorf Formation near the Savannah River Site," Paper presented at the American Geophysical Union Fall Meeting, San Francisco, California, December 9-12, 1991.

Simmons, C. S., R. J. Lenhard, and A. H. Demond. 1991. "A General Analytical Model of Three-Phase Immiscible Fluid Relative Permeability." Paper presented at the American Geophysical Union Fall Meeting, San Francisco, California, December 9-12, 1991.

Stevens, T. O. 1992. "Properties of Dissimilatory Fe(III)-Reducing Bacteria from Different Ecological Niches." Paper presented at the Annual Meeting of the American Chemical Society, San Francisco, California, April 5-10, 1992.

Stevens, T. O., S. W. Li, and J. K. Fredrickson. 1992. "Microbiology of Deep Terrestrial Subsurface Formations in the Northwest United States." Paper presented at the Sixth International Symposium on Microbial Ecology, Barcelona, Spain, September 6-11, 1992.

Stevens, T. O., H. D. Watts, J. J. Walker, and J. K. Fredrickson. 1992. "Optimization of Solid Growth Medium for Isolation and Culture of Microorganisms from the Terrestrial Subsurface." Paper presented at the 92nd General Meeting of the American Society for Microbiology, New Orleans, Louisiana, May 26-30, 1992.

Terrestrial Science

Bolton, H., Jr., J. J. Halvorson, and J. L. Smith. 1992. "Nitrogen Distribution and Mineralization Under *Artemisia tridentata*." Paper presented at Ecological Society of America National Meeting, Honolulu, Hawaii, August 11-13, 1992.

Cullinan, V. I., and J. M. Thomas. 1992. "Detecting Ecological Change." Paper presented at Ecological Society of America National Meeting, Honolulu, Hawaii, August 11-13, 1992.

Cullinan V. I., J. M. Thomas, and M. A. Simmons. 1992. "Detecting Ecological Change." Paper presented at Seventh Annual Landscape Ecology Symposium, Corvallis, Oregon, April 8-10, 1992.

Downs, J. L., L. G. McWethy, S. O. Link, D. E. Gibbons, and G. M. Petrie. 1992. "Land Cover/Vegetation Classification of an Eastern Washington Shrub-Steppe Environment." Paper presented at the Seventh Annual U. S. Landscape Ecology Symposium, Corvallis, Oregon, April 8-11, 1992.

Halvorson, J. J., J. L. Smith, H. Bolton, Jr., and R. E. Rossi. 1992. "Mapping Resource Islands under Plants Using Geostatistics." Paper presented at Ecological Society of America National Meeting, Honolulu, Hawaii, August 11-13, 1992.

Halvorson, J. J., J. L. Smith, and H. Bolton, Jr. 1992. "Spatial Relationships of Soil Microbial Biomass Processes in an Arid Shrub-Steppe Ecosystem." Paper presented at the Sixth International Symposium on Microbial Ecology, Barcelona, Spain, September 6-11, 1992.

Inouye, R. S., D. Frank, T. Reynolds, and J. M. Thomas. 1992. "Temporal Variability in Ecosystems: Variation among Trophic Levels." Paper presented to Ecological Society of America, Honolulu, Hawaii, August 11-13, 1992.

Link, S. O. 1991. "The Ecology and Physiology of a Successful Invasive Winter-Annual Grass, *Bromus tectorum*." Invited seminar, Botany Department, University of Washington, Seattle, Washington, November 23, 1991.

Link, S. O., D. E. Gibbons, G. M. Petrie, R. R. Kirkham, L. E. Rogers, L. G. McWethy, and P. A. Beedlow. 1992. "Estimation of Latent Heat Flux Using Quantitative Landsat Thematic Mapper Satellite Data in a Shrub-Steppe Ecosystem." Presented at the Seventh Annual U. S. Landscape Ecology Symposium, Corvallis, Oregon, April 8-11, 1992.

Simmons, M. A., V. I. Cullinan, and J. M. Thomas. 1992. "Interpretation of Scale at the Community Level." Paper presented to Ecological Society of America, Honolulu, Hawaii, August 11-13, 1992.

Smith, J. L., J. J. Halvorson, and H. Bolton, Jr. 1992. "Measurement and Use of Soil Microbial Biomass Values in Ecological Studies." Paper presented at Ecological Society of America National Meeting, Honolulu, Hawaii, August 11-13, 1992.

Thomas, J. M. 1991. "Designs for Environmental Field Studies." Invited Seminar, Savannah River Ecology Laboratory, Aiken, South Carolina, December 12, 1991.

Thomas, J. M. 1992. "Aspects of Designing Impact Studies." Invited paper, presented to the Workshop on Field Study Design held at the Institute of Ocean Sciences, Sidney, British Columbia, May 11-12, 1992.

Thomas, J. M., M. A. Simmons, and V. I. Cullinan. 1991. "Methods of Measuring Landscape Level Effects on Plant Cover." Paper presented to Society for Risk Assessment, Baltimore Maryland, December 8-11, 1991.

Watts, H. D., T. O. Stevens, and J. M. Thomas. 1992. "Optimization of Media for Subsurface Microorganisms." Paper presented to Montana Academy of Sciences, Bozeman, Montana, March 27-28, 1992.

Waugh, W. J., B. H. Werle, and S. O. Link. 1991. "Plant Water Relations in Small Monolith Lysimeters." Paper presented to the Soil Science Society, Denver, Colorado, October 27 - November 1, 1991.

Laboratory-Directed Research and Development

Arnold, G. E., and R. L. Ornstein. 1992. "A Molecular Dynamics Analysis of Haloalkane Dehalogenase." Poster presented at the Sixth Annual Symposium of the Protein Society, Abstract M40, San Diego, California, July 1992.

Bolton, H., Jr. 1992. "Coupled Microbial-Geochemical Experiments." Paper presented at the DOE Coupled Processes Subprogram Meeting, Richland, Washington, February 28, 1992.

Gorby, Y. A. 1992. "Enzymatic Co(III)EDTA Reduction." Paper presented at the Sixth International Symposium on Microbial Ecology, Barcelona, Spain, September 6-11, 1992.

Gorby, Y. A. 1992. "Microbial Chromium Reduction and Immobilization." Paper presented at the 203rd American Chemical Society Meeting, San Francisco, California, April 9, 1992.

Hughes, M. P., M. D. Paulsen, and R. L. Ornstein. 1992. "Fluctuations in the Proposed Access Channel of Cytochrome P-450cam from a Molecular Dynamics Simulation." Poster presented at the American Association for the Advancement of Science Annual Meeting, Chicago, Illinois, February 1992.

Ornstein, R. L. 1992. "Coupling of Molecular Modeling and Experimental Studies for Rational Redesign of Substrate Specificity of Biodegradative Enzymes." Paper presented at the Ninth Annual Meeting of the Pacific Northwest Association of Toxicology, Richland, Washington, September 1992.

Ornstein, R. L. 1992. "Protein Molecular Dynamics Simulations: (1) Comparison of a 3-nsec Run with X-ray & NMR Structures and (2) Cytochrome P450cam Structure-Function Relationships." Talk presented to the U.S. Army, Chemical Research, Development and Engineering Center, Edgewood, Maryland, June 1992.

Ornstein, R. L. 1992. "Protein Molecular Dynamics Simulations: Structure & Function." Talk presented to Department of Biochemistry and Chemistry, University of Illinois, Urbana, Illinois, February 1992.

Ornstein, R. L. 1992. "Protein Molecular Dynamics Simulations: Structure & Function." Talk presented to Department of Physics, University of Washington, Seattle, Washington, March 1992.

Ornstein, R. L. 1992. "Rational Redesign of Biodegradative Enzymes for Environmental Cleanup." Talk presented to Department of Environmental Sciences, Washington State University—Tri-Cities, Richland, Washington, September 1992.

Ornstein, R. L. 1992. "Redesign of Cytochrome P-450cam for Enhanced Biodegradation." Paper presented at the Conference on Bioinorganic and Biotechnological Aspects of Environmental Chemistry, Florence, Italy, August 1992.

Ornstein, R. L. 1992. "Redesign of Cytochrome P-450cam for Enhanced Biodegradation." Talk presented at SANDOZ, Basel, Switzerland, September 1992.

Ornstein, R. L. 1992. "Redesign of Cytochrome P-450cam for Enhanced Biodegradation." Talk presented at the University of Groningen, Groningen, the Netherlands, September 1992.

Ornstein, R. L. 1992. "Structure-Function-Dynamics of Cytochrome P450cam and Rational Redesign." Talk presented at Battelle Columbus, Columbus, Ohio, March 1992.

Ornstein, R. L. 1992. "Structure-Function-Dynamics of Cytochrome P450cam and Rational Redesign." Talk presented at the Oregon Graduate Institute, Beaverton, Oregon, April 1992.

Ornstein, R. L., and F. J. Brockman. 1991. "Enhanced Bioremediation of Subsurface Contamination: Enzyme Recruitment and Redesign." Paper presented at the Hazardous Materials Control Research Institute Twelfth Annual National Conference: Hazardous Materials Control/Superfund '91, Washington, D.C., December 1991.

Paulsen, M. D., and R. L. Ornstein. 1992. "Controlling the Regiospecificity and Coupling of Cytochrome P450cam." Poster presented at the Sixth Annual Symposium of the Protein Society, Abstract M49, San Diego, California, July 1992.

Sun, S., N. Luo, R. L. Ornstein, and R. Rein. 1992. "Protein Structure Prediction: Reduced Representation Approach." Poster presented at Sixth Biophysical Discussion of the Biophysical Society, Airlier, Virginia, January 1992.

Author Index

Author Index

Distribution

Distribution

OFFSITE

D. Anderson
ENVIROTEST
1108 NE 200th Street
Seattle, WA 98155-1136

Assistant Secretary
Environment, Safety
& Health
EH-1, FORS
U.S. Department of Energy
Washington, DC 20585

S. I. Auerbach
Oak Ridge National Laboratory
Building 1505, MS-6036
P.O. Box 2008
Oak Ridge, TN 37831-6036

J. A. Auxier
Auxier and Associates
111 Mabry Hood Road
Knoxville, TN 37771

F. Badgley
13749 NE 41st Street
Seattle, WA 98125

D. L. Balkwill
Department of Biological
Sciences
309 Nuclear Research Bldg.
Florida State University
Tallahassee, FL 32306

R. M. Baltzo
Radiological Safety Division
University of Washington
Seattle, WA 98105

A. D. Barker
Battelle Columbus
Laboratories
505 King Avenue
Columbus, OH 43201

W. W. Barker, Chairman
Department of Biology
Central Washington University
Ellensburg, WA 98926

N. F. Barr
ER-72, GTN
U.S. Department of Energy
Washington, DC 20585

J. E. Baublitz
EM-40, TREV
U.S. Department of Energy
Germantown, MD 20874

J. R. Beall
ER-72, GTN
U.S. Department of Energy
Washington, DC 20585

P. A. Beedlow
U. S. Environmental
Protection Agency
200 SW 35th Street
Corvallis, OR 97333

M. H. Bhattacharyya
BIM Division, Bldg. 202
Argonne National Laboratory
9700 South Cass Avenue
Argonne, IL 60439

R. A. Black
Department of Botany
Washington State University
Pullman, WA 99164

L. Bliss
Department of Botany
University of Washington
Seattle, WA 98105

H. S. Bolton
National Oceanic &
Atmospheric Administration
HG Hoover Building,
Room 5222
Department of Commerce
LAX 1
Washington, DC 20230

T. Borak
Colorado State University
Dept. of Radiation &
Radiation Biology
Fort Collins, CO 80523

C. M. Borgstrom
EH-25, FORS
U.S. Department of Energy
Washington, DC 20585

A. Brodsky
16412 Kipling Road
Derwood, MD 20855

W. Broecher
Lamont Geological
Observatory
Columbia University
Palisades, NY 10964

D. R. Buhler, Chairman
Toxicology Program
Oregon State University
Corvallis, OR 97331

G. Burley
Office of Radiation Programs,
ANR-458
U.S. Environmental Protection
Agency
Washington, DC 20460

L. K. Bustad
College of Veterinary Medicine
Washington State University
Pullman, WA 99164-7010

S. Calcese
Water Resources Center
University of Wisconsin
1975 Willow Drive
Madison, WI 53706

M. Caldwell
Department of Range Science
Utah State University
Logan, UT 84322

J. T. Callahan
Associate Program Director
Ecosystems Studies Program
National Science Foundation
Washington, DC 20585

H. H. Cheng, Head
Department of Soil Science
University of Minnesota
1991 Upper Buford Circle
St. Paul, MN 55108

G. Chesters, Director
Water Resources Center
University of Wisconsin
1975 Willow Drive
Madison, WI 53706

Chief
Game Management Division
Department of Game
600 North Capitol Way
Olympia, WA 98501

J. S. Coleman
ER-15, GTN
U.S. Department of Energy
Washington, DC 20585

J. Corey
Environmental Sciences
Savannah River Laboratory
Drawer E
Aiken, SC 29801

Council on Environmental Quality
722 Jackson Place, NW
Washington, DC 20503

R. Crawford, Director
IMAGE
University of Idaho
Moscow, ID 83843

T. V. Crawford
Atomic Energy Division
Savannah River Laboratory
Aiken, SC 29808

J. H. Cushman
Water Resources Research Center
Purdue University
Lilly Hall
West Lafayette, IN 47907

R. C. Dahlman
ER-74, GTN
U.S. Department of Energy
Washington, DC 20585

G. Davis, Chairman
Medical & Health Sciences Division
Oak Ridge Associated Universities
P.O. Box 117
Oak Ridge, TN 37831-0117

J. T. Davis
San Francisco Field Office
U.S. Department of Energy
1333 Broadway
Oakland, CA 94612

J. F. Decker
ER-3, FORS
U.S. Department of Energy
Washington, DC 20585

R. S. Denning
Battelle Columbus Laboratories
505 King Avenue
Columbus, OH 43201

U.S. Department of Energy
Environment & Health Division
P.O. Box 5400
Albuquerque, NM 87115

G. DePlanque, Director
U.S. Department of Energy-EMEL
375 Hudson Street
New York, NY 10014

Director
New England Marine Laboratories
Washington Street
P.O. Box 1637
Duxbury, MA 02332

Director
Washington State Department of Ecology
Olympia, WA 98501

T. J. Dobry, Jr.
DP-641, GTN
U.S. Department of Energy
Washington, DC 20585

DOE/Office of Scientific & Technical Information (12)

H. Drucker
Argonne National Laboratory
9700 South Cass Avenue
Argonne, IL 60439

R. Dyer
ANR-461
Office of Radiation Programs
U.S. Environmental Protection Agency
401 M Street SW
Washington, DC 20460

J. Eby
Washington Department of Wildlife
600 Capital Way N
Olympia, WA 98501-1091

S. Echols
U.S. Environmental Protection Agency
Pacific Ecosystems Branch, ERL-N
Hatfield Marine Science Center
2111 SE Marine Science Drive
Newport, OR 97365-5260

D. N. Edgington
University of Wisconsin
Center for Great Lakes Studies
P.O. Box 413
Milwaukee, WI 53201

C. W. Edington, Director
National Research Council
2101 Constitution Avenue, NW
Washington, DC 20418

W. H. Ellett
BRER--National Research Council, MH-370
2101 Constitution Avenue, NW
Washington, DC 20418

L. F. Elliott
USDA - ARS
Oregon State University
3450 SW Campus Way
Corvallis, OR 97331-7102

R. D. Evans
Department of Botany
Washington State University
Pullman, WA 99164

S. J. Farmer
17217 77th Avenue W.
Edmonds, WA 98020

C. W. Frank
EM-53, FORS
U.S. Department of Energy
Washington, DC 20585

D. J. Galas
ER-70, GTN
U.S. Department of Energy
Washington, DC 20585

T. F. Gesell
Idaho Field Office
U.S. Department of Energy
785 DOE Place
Idaho Falls, ID 83402-4149

W. C. Ghiorse
Microbiology Department
415 Stocking Hall
Cornell University
Ithaca, NY 14853

R. D. Gilmore, President
Environmental Health Sciences, Inc.
Nine Lake Bellevue Building
Suite 220
Bellevue, WA 98005

W. G. Gold
Department of Botany, KB-15
University of Washington
Seattle, WA 98195

E. D. Goldberg
Scripps Institute of Oceanography
La Jolla, CA 92039

M. Goldman
Department of Radiological Sciences (VM)
University of California
Davis, CA 95616

G. Goldstein
ER-73, GTN
U.S. Department of Energy
Washington, DC 20585

F. B. Golley
Institute of Ecology
University of Georgia
Athens, GA 30601

D. J. Grimes
ER-74, GTN
U.S. Department of Energy
Washington, DC 20585

K. Grossman
P.O. Box 1680
Sag Harbor, NY 11963

J. D. Hair
National Wildlife Federation
1400 16th Street, NW
Washington, DC 20036

J. J. Halvorson
U.S.D.A.-Agricultural Research Service
215 Johnson Hall
Washington State University
Pullman, WA 99164

W. R. Hansen
MS-F643
Los Alamos National Laboratory
P.O. Box 1663
Los Alamos, NM 87545

W. Happer
ER-1, FORS
U.S. Department of Energy
Washington, DC 20585

F. Harrison
Biomedical & Environmental Research Program
Lawrence Livermore National Laboratory, C-523
P.O. Box 808
Livermore, CA 94550

D. W. Hayne
Department of Statistics
North Carolina State University
Box 8203
Raleigh, NC 27695-8203

R. Horton
Department of Agronomy
Iowa State University
Ames, IA 50011

F. Hutchinson
Department of Molecular Biophysics & Biochemistry
Yale University
260 Whitney Avenue
P.O. Box 6666
New Haven, CT 06511

H. Ishikawa, General Manager
Nuclear Safety Research Association
P.O. Box 1307
Falls Church, VA 22041

K. L. Jackson, Chairman
Radiological Sciences Group SB-75
University of Washington
Seattle, WA 98195

D. Janecky
Group INC-7, MS J514
Los Alamos National Laboratory
P.O. Box 1663
Los Alamos, NM 87545

A. Janetos
U.S. Environmental Protection Agency
401 M Street, SW
Washington, DC 20460

A. W. Johnson
Vice President for Academic Affairs
San Diego State University
San Diego, CA 92182

L. J. Johnson
Idaho National Engineering Laboratory
IRC MS 2203
P.O. Box 1625
Idaho Falls, ID 83415

D. Johnstone
Department of Civil and Environmental Engineering
Washington State University
Pullman, WA 99164

G. Y. Jordy
ST-11, GTN
U.S. Department of Energy
Washington, DC 20585

C. Keller
Los Alamos National Laboratory
KS K305
P. O. Box 1663
Los Alamos, NM 87545

C. K. Keller
Department of Geology
Washington State University
Pullman, WA 99164-2812

B. J. Kelman
Failure Analysis Associates, Inc.
P.O. Box 3015
Menlo Park, CA 94025

R. F. Kendall
National Institute for Petroleum & Energy Research
P.O. Box 2128
Bartlesville, OK 74005

H. Kibby
U.S. Environmental Protection Agency
200 SW 35th Street
Corvallis, OR 97333

J. Klopatek
Department of Botany
Arizona State University
Tempe, AZ 85287

M. Kosorok
Department of Statistics
Brigham Young University
Provo, UT 84602

R. T. Kratzke
NP-40, FORS
U.S. Department of Energy
Washington, DC 20585

D. Krenz
Albuquerque Field Office
U.S. Department of Energy
P.O. Box 5400
Albuquerque, NM 87115

S. V. Krupa
Dept. of Plant Pathology
495 Borlaug Hall
1991 Upper Buford
University of Minnesota
St. Paul, MN 55108

R. T. Lackey
U.S. Environmental Protection Agency
200 SW 35th Street
Corvallis, OR 97333

D. A. Laird
Soil Tilth Laboratory
USDA-ARS
Ames, IA 50011

Librarian
Colorado State University
Documents Department--The Libraries
Ft. Collins, CO 80523

Librarian
Environmental Research Laboratory
U.S. Environmental Protection Agency
Sabine Island
Gulf Breeze, FL 32561

Librarian
Environmental Research Laboratory
U.S. Environmental Protection Agency, ORD
Narrangansett, RI 02882

Librarian
Environmental Research Laboratory-Duluth
N. A. Jaworski, Director
6201 Congdon Blvd.
Duluth, MN 55804

Librarian
Frances Penrose Owen Science & Engineering Library
Washington State University
Pullman, WA 99164-3200

Librarian
Health Sciences Library, SB-55
University of Washington
Seattle, WA 98195

Librarian
Report Library, MS P364
Los Alamos National Laboratory
P.O. Box 1663
Los Alamos, NM 87545

Librarian
Northwest and Alaska Fisheries Center
National Marine Fisheries Service, NOAA
2725 Montlake Blvd., East
Seattle, WA 98112

Librarian
Robert S. Kerr Environmental Research Laboratory
U.S. Environmental Protection Agency, ORD
Ada, OK 74320

Librarian (Serials Section)
University of Washington
Seattle, WA 98195

Librarian
Washington State University
Pullman, WA 99164-6510

Library
Holcomb Research Institute
Butler University
Indianapolis, IN 46208

Library
Serials Department (#80-170187)
University of Chicago
1100 East 57th Street
Chicago, IL 60637

O. R. Lunt
Laboratory of Biomedical & Environmental Sciences
University of California
900 Veteran Avenue
Los Angeles, CA 90024-1786

M. MacCracken
Atmospheric and Geophysical Sciences Division
Lawrence Livermore National Laboratory
P.O. Box 5507
Livermore, CA 94550

J. R. Maher
ER-8, GTN
U.S. Department of Energy
Washington, DC 20585

C. R. Mandelbaum
EP-60, FORS
U.S. Department of Energy
Washington, DC 20585

J. Mangeno
Department of the Navy
Nuclear Propulsion Directorate
0808 National Center ND2, 3rd Floor Mail Room
Washington, DC 20362-5101

B. Manowitz
Energy and Environment Division
Brookhaven National Laboratory
Upton, NY 11973

R. S. Marianelli
ER-14, GTN
U.S. Department of Energy
Washington, DC 20585

O. D. Markham
Radiological and Environmental Sciences Laboratory
U.S. Department of Energy
785 DOE Place
Idaho Falls, ID 83402

S. Marks
8024 47th Place West
Mukilteo, WA 98275

K. Marsh
Lawrence Livermore National Laboratory
P.O. Box 808
Livermore, CA 94550

W. H. Matchett
Graduate School
New Mexico State University
Box 3G
Las Cruces, NM 88003-0001

H. M. McCammon
ER-74, GTN
U.S. Department of Energy
Washington, DC 20585

R. O. McClellan, President
Chemical Industry Institute of Toxicology
P.O. Box 12137
Research Triangle Park, NC 27709

C. B. Meinhold
Radiological Sciences Division
Bldg. 703M
Brookhaven National Laboratory
Upton, NY 11973

F. M. Molz
Department of Civil Engineering
Auburn University
238 Harbert Engineering Center
Auburn, AL 36849

D. B. Moore-Shedrow
Westinghouse Savannah River Company
773-A, A-229
Aiken, SC 29803

J. J. Morgan
California Institute of Technology
Mail Code 138-78
Pasadena, CA 91125

W. F. Mueller
New Mexico State University
Box 4500
Las Cruces, NM 88003-4500

I. Murarka
Electric Power Research Institute
3412 Hillview Avenue
Palo Alto, CA 94304

T. Murphy, Director
Environmental Research Laboratory
U.S. Environmental Protection Agency
200 SW 35th Street
Corvallis, OR 97333

J. R. Naidu
129B Safety and Environmental Protection Division
Brookhaven National Laboratory
Upton, NY 11973

T. Nash III
Department of Botany
Arizona State University
Tempe, AZ 85287

N. S. Nelson
Office of Radiation Programs (ANR-461)
U.S. Environmental Protection Agency
401 M Street, SW
Washington, DC 20460

J. M. Nenhold
Department of Wildlife Resources
Utah State University
Logan, UT 84322-5200

W. R. Ney, Executive Director
National Council on Radiation Protection and Measurements
7910 Woodmont Avenue
Suite 1016
Washington, DC 20014

C. R. Nichols
Idaho Field Office
U.S. Department of Energy
785 DOE Place
Idaho Falls, ID 83402

Nuclear Regulatory Commission
Advisory Committee on Reactor Safeguards
Washington, DC 20555

E. O'Donnell
Mail Stop NLS-260
Nuclear Regulatory Commission
Washington, DC 20555

C. Olsen
ER-74, GTN
U.S. Department of Energy
Washington, DC 20585

P. C. Owczarski
Science Applications
International Corp.
1845 Terminal Drive
Richland, WA 99352

R. E. Pacha
Department of Biological
Sciences
Central Washington University
Ellensburg, WA 98926

A. Patrinos
ER-74, GTN
U.S. Department of Energy
Washington, DC 20585

G. Petersen
Department of Agriculture
Pennsylvania State University
University Park, PA 16802

L. Petrakis
Department of Applied
Science
Brookhaven National
Laboratory
Upton, NY 11973

G. F. Pinder
University of Vermont
College of Engineering
and Mathematics
Office of the Dean
101 Votey Building
Burlington, VT 05405-0156

W. Piver
National Institutes of Environ-
mental Health Sciences
P.O. Box 12233
Research Triangle
Park, NC 27709

R. Rabson
ER-17, GTN
U.S. Department of Energy
Washington, DC 20585

D. P. Rall, Director
National Institutes of
Environmental Health
Sciences
P.O. Box 12233
Research Triangle
Park, NC 27709

Regional Director
EPA Regional Office
1200 6th Avenue
Seattle, WA 98101

D. E. Reichle
Environmental Sciences
Division
Oak Ridge National
Laboratory
P.O. Box 2008
Oak Ridge, TN 37831-6037

C. A. Reilly
Bldg. 203, Room 1101
Argonne National Laboratory
9700 South Cass Avenue
Argonne, IL 60439

J. F. Reynolds
Phytotron, Department of
Botany
Duke Unversity
Durham NC 27706

C. R. Richmond
Oak Ridge National
Laboratory
4500N, MS-62523
P.O. Box 2008
Oak Ridge, TN 37831-6253

C. Riordan
Office of Research &
Development
U.S. Environmental Protection
Agency
Washington, DC 20460

B. E. Rittmann
Department of Civil
Engineering
University of Illinois
Urbana, IL 61801

S. L. Rose
ER-72, GTN
U.S. Department of Energy
Washington, DC 20585

R. D. Rosen, Tech. Librarian
Environmental Measurements
Laboratory
U.S. Department of Energy
376 Hudson Street
New York, NY 10014

R. E. Rossi
FSS International, Inc.
654 Bair Island Rd.
Suite 205
Redwood, CA 94063

E. J. Rykiel, Jr.
Center for BioSystems
Modeling
Dept. of Industrial Engineering
Texas A&M University
College Station, TX
77843-3131

L. Sagan
Electric Power Research
Institute
3412 Hillview Avenue
Palo Alto, CA 94304

M. Schulman
ER-70, GTN
U.S. Department of Energy
Washington, DC 20585

R. S. Scott
EM-20, FORS
U.S. Department of Energy
Washington, DC 20585

G. H. Setlock
Rockwell International
North American Space Operations
Rocky Flats Plant, MS-250
P.O. Box 464
Golden, CO 80402

R. B. Setlow
Brookhaven National Laboratory
Upton, NY 11973

P. H. Silverman
Lawrence Berkeley Laboratory
Bldg. 50A/5104
Berkeley, CA 94720

J. Simmons
Bioaffects Analysis Branch
U.S. Environmental Protection Agency
401 M Street, SW
Washington, DC 20460

R. M. Simon
ER-3, FORS
U.S. Department of Energy
Washington, DC 20585

W. K. Sinclair, President
National Council on Radiation Protection
7910 Woodmont Avenue
Suite 1016
Bethesda, MD 20814

J. Skalski
Center for Quantitative Science
HR-20
3737 15th Avenue, N
Seattle, WA 98195

S. Sligar
Department of Biochemistry
415 Roger Adams Laboratory
1209 W. California Street
Urbana, IL 61801

D. A. Smith
ER-72, GTN
U.S. Department of Energy
Washington, DC 20585

G. S. Smith
New Mexico State University
Box 3-I
Las Cruces, NM 88003-0001

J. L. Smith
USDA-ARS
215 Johnson Hall
Washington State University
Pullman, WA 99164

M. Smith
Department of Ecology
NUC-MIX-WASTE Library
PV-II, Bldg. 99-So. Sound
Olympia, WA 98504

M. Smith, Director
Savannah River Ecology Laboratory
University of Georgia
Savannah River Plant
P.O. Box A
Aiken, SC 29801

L. E. Sommers
Department of Agronomy
Colorado State University
Ft. Collins, CO 80523

J. N. Stannard
University of California
17441 Plaza Animado #132
San Diego, CA 92128

R. W. Starostecki
NS-1, FORS
U.S. Department of Energy
Washington, DC 20585

L. F. Stickel
Patuxent Wildlife Research Center
Laurel, MD 20810

E. T. Still
Kerr-McGee Corporation
P.O. Box 25861
Oklahoma City, OK 73125

P. M. Stone
ST-20, FORS
U.S. Department of Energy
Washington, DC 20585

J. M. Suflita
Department of Botany & Microbiology
University of Oklahoma
Norman, OK 73019

A. Swartzman
Center for Quantitative Studies
University of Washington
3737 15th Avenue
Seattle, WA 98115

Technical Information Service
Room 773A
Savannah River Laboratory
Aiken, SC 29801

D. Thomas
Hawaii Institute of Geophysics
University of Hawaii
2525 Correa Road
Honolulu, HI 96822

M. L. Thompson
Department of Agronomy
Iowa State University
Ames, IA 50011

L. O. Tiffin
Swan Valley Route
Seeley Lake, MT 59868

University of Washington
Department of Biostatistics
School of Public Health and
Com. Med.
SC-32
Seattle, WA 98195

P. J. Unkefer
Mail Stop C346
Los Alamos National
Laboratory
Los Alamos, NM 87545

A. J. Valocchi
Department of Civil
Engineering
University of Illinois
Urbana, IL 61801

P.K.M. van der Heijde
Colorado School of Mines
Institute for GW Res. & Ed.
Golden, CO 80401

R. I. Van Hook
Environmental Sciences
Division
Oak Ridge National Laboratory
Oak Ridge, TN 37831

G. L. Voelz
MS-K404
Los Alamos National
Laboratory
P.O. Box 1663
Los Alamos, NM 87545

B. W. Wachholz
Radiation Effects Branch
National Cancer Institute
EPN, Room 530
8000 Rockville Pike
Bethesda, MD 20892

R. A. Walters
Assistant to the Associate
Director
MS-A114
Los Alamos National
Laboratory
P.O. Box 1663
Los Alamos, NM 87545

J. C. Westall
Department of Chemistry
Oregon State University
153 Gilbert Hall
Corvallis, OR 97331

W. W. Weyzen
Electric Power Research
Institute
3412 Hillview Avenue
Palo Alto, CA 94303

R. W. Whicker
Department of Radiology &
Radiation Biology
Colorado State University
Ft. Collins, CO 80521

R. P. Whitfield
EM-40, FORS
U.S. Department of Energy
Washington, DC 20585

F. J. Wobber
ER-74, GTN
U.S. Department of Energy
Washington, DC 20585

R. W. Wood
ER-71, GTN
U.S. Department of Energy
Washington, DC 20585

R. G. Woodmansee
Department of Range Science
Colorado State University
Fort Collins, CO 80523

S. R. Wright
Savannah River Field Office
U.S. Department of Energy
P.O. Box A
Aiken, SC 29801

FOREIGN

M. Anderson
Library
Department of National Health
& Welfare
Ottawa, Ontario
CANADA

D. C. Aumann
Institut für Physikalische
Chemie
Universität Bonn
Abt. Nuklearchemi
Wegelerstrabe 12
5300 Bonn 1
GERMANY

M. R. Balakrishnan, Head
Library & Information Services
Bhabha Atomic Research
Centre
Bombay-400 085
INDIA

A. M. Beau, Librarian
Département de Protection Sanitaire
Commissariat à l'Énergie Atomique
BP No. 6
F-92265 Fontenay-aux-Roses
FRANCE

G. Bengtsson,
Director-General
Statens Stralskyddsinstitut
Box 60204
S-104 01 Stockholm
SWEDEN

D. J. Beninson
Gerencía de Protección Radiológica y Seguridad
Comisión Nacional de Energia Atómica
Avendida del Libertador 8250
2 o Piso Of. 2330
1429 Buenos Aires
ARGENTINA

A. Bianco
ENEA, Dipart. Protezione
Via le Regina Margherita 125
I-00198 Roma
ITALY

Cao Shu-Yuan, Deputy Head
Laboratory of Radiation Medicine
North China Institute of Radiation Protection
P.O. Box 120
Tai-yuan, Shan-Xi
PEOPLE'S REPUBLIC OF CHINA

M. Carpentier
Commission of the European Communities
200 rue de la Loi
B-1049 Brussels
BELGIUM

M. A. Carregado
Gerencía de Protección Radiológica y Seguridad
Comisión Nacional de Energía Atómica
Casilla de Carreo 40
1802 Aeropuerto Int.
Ezeiza
ARGENTINA

Chen Xing-An
Laboratory of Industrial Hygiene
Ministry of Public Health
2 Xinkang Street
Deshengmenwai, Beijing 100088
PEOPLE'S REPUBLIC OF CHINA

R. Clarke
National Radiological Protection Board
Chilton, Didcot
Oxon OX11 ORQ
ENGLAND

Commission of the European Communities
DG XII - Library SDM8 R1
200 rue de la Loi
B-1049 Brussels
BELGIUM

H.A.M. De Gruyf
Head Laboratory of Ecotoxicology
National Institute of Public Health & Environmental Hygiene
P.O. Box 1
3720 BA Bilthoven
THE NETHERLANDS

Deng Zhicheng
North China Institute of Radiation Protection
P.O. Box 120
Tai-yuan, Shan-Xi
PEOPLE'S REPUBLIC OF CHINA

G. M. Desmet
Commission of the European Communities
DG XII
200 rue de la Loi
B-1049 Brussels
BELGIUM

Director
Centre d'Etudes Nucléaires
Commissariat à l'Énergie Atomique
Fontenay-aux-Roses (Seine)
FRANCE

Director
Laboratorio di Radiobiologia Animale
Centro di Studi Nucleari Della Casaccia
Comitate Nazionale per l'Energia Nucleare
Casella Postale 2400
I-00100 Roma
ITALY

D. Djuric
Institute of Occupational and Radiological Health
11000 Beograd
Deligradoka 29
YUGOSLAVIA

Estacao Agronómica Nacional
Biblioteca
2780 Oeiras
PORTUGAL

L. Feinendegen, Director
Institut für Medezin
Kernsforschungsanlage Jülich
Postfach 1913
D-5170 Jülich
GERMANY

R. M. Fry, Head
Office of the Supervising Scientist for the Alligator Rivers Region
P.O. Box 387
Bondi Junction NSW 2022
AUSTRALIA

A. Geertsema
Saso Technology (Pty), Ltd.
P.O. Box 1
Sasolburg 9570
REPUBLIC OF SOUTH AFRICA

A. R. Gopal-Ayengar
73-Mysore Colony
Mahul Road, Chembur
Bombay-400 074
INDIA

A. Grauby
Service d'Etudes at de Recherches sur l'Environment
Commissariat à l'Énergie Atomique
Caderache, No. 1
BAT 153 13115
St. Paul Les Durance
FRANCE

J. L. Head, Director
Department of Nuclear Science & Technology
Royal Naval College, Greenwich
London SE10 9NN
ENGLAND

M. D. Hill
Assessments Department
National Radiological Protection Board
Chilton, Didcot
Oxon OX11 ORQ
ENGLAND

International Atomic Energy Agency
Documents Library
Attn: Mrs. Javor
Kaerntnerring 11
A-1010 Vienna 1
AUSTRIA

K. E. Lennart Johansson
Radiofysiska Inst.
Regionsjukhuset
S-901 85 Umeå
SWEDEN

H.-J. Klimisch
BASF Aktiengesellschaft
Abteilung Toxikologie, Z470
D-6700 Ludwigshafen
GERMANY

G. H. Kraft
c/o GSI Postbox 110541
Planck Str.
D-6100 Darmstadt
GERMANY

T. Kumatori
National Institute of Radiological Sciences
4-9-1, Anagawa-4-chome, Inage-ku
Chiba-shi 263
JAPAN

Li De-Ping, Director
North China Institute of Radiation Protection
P.O. Box 120
Tai-yuan, Shan-Xi
PEOPLE'S REPUBLIC OF CHINA

Librarian
Australian Nuclear Science & Technology Organization
Private Mail Bag 1
Menai NSW 2234
AUSTRALIA

Librarian
Centre d'Etudes Nucléaires de Saclay
P.O. Box 2, Saclay
Fig-sur-Yvette (S&O)
FRANCE

Librarian
CSIRO
314 Albert Street
P.O. Box 89
East Melbourne, Victoria
AUSTRALIA

Librarian
CSIRO
Division of Atmospheric Research
Station Street
Aspendal, Victoria 3195
AUSTRALIA

Librarian
CSIRO
Division of Wildlife and Ecology
P.O. Box 84
Lyneham, ACT 2602
AUSTRALIA

Librarian
Department of Fisheries
and Oceans
Freshwater Institute
501 University Crescent
Winnipeg, Manitoba R3T 2N6
CANADA

Librarian
Department of Fisheries
and Oceans
Pacific Biological Station
P.O. Drawer 100
Nanaimo, British Columbia
V9R 5K6
CANADA

Librarian
HCS/EHE
World Health Organization
CH-1211 Geneva 27
SWITZERLAND

Librarian
Kernforschungzentrum
Karlsruhe
Institut für Strahlenbiologie
Postfach 3640
D-7[illegible] Karlsruhe 1
GERMANY

Librarian
Max-Planck-Institut
für Biophysics
Forstkasstrabe
D-6000 Frankfurt/Main
GERMANY

Librarian
Ministry of Agriculture,
Fisheries & Food
Fisheries Laboratory
Lowestoft, Suffolk NR33 OHT
ENGLAND

Librarian
National Institute of
Radiological Sciences
4-9-1, Anagawa-4-chome,
Inage-ku
Chiba-shi 263
JAPAN

Librarian
Supervising Scientist for the
Alligator Rivers Region
P.O. Box 387
Bondi Junction NSW 2022
AUSTRALIA

Library
Atomic Energy of Canada,
Ltd.
Whiteshell Nuclear Research
Establishment
Pinawa, Manitoba ROE 1LO
CANADA

Library (Serials Section)
British Geological Survey
Nicker Hill, Keyworth
Nottingham NG12 5GG
ENGLAND

Library
Department of Fisheries
and Oceans
West Vancouver Laboratory
4160 Marine Drive
West Vancouver, BC V7V
1N6
CANADA

Library
Department of Meteorology
University of Stockholm
Arrhenius Laboratory
S-106 91 Stockholm
SWEDEN

B. Lindell
National Institute of
Radiation Protection
Fack S-104 01
Stockholm 60
SWEDEN

A. M. Marko
9 Huron Street
Deep River, Ontario
KOJ 1PO
CANADA

H. Matsudaira,
Director-General
National Institute of
Radiological Sciences
4-9-1, Anagawa-4-chome,
Inage-ku
Chiba-shi 263
JAPAN

H. J. Metivier
Institut de Protection
et de Sûreté Nucléaire
Centre d'Études de Service
de Fontenay-aux-Roses
BP No. 6
F-92265 Fontenay-aux-Roses
FRANCE

S. F. Mobbs
National Radiological
Protection Board
Chilton, Didcot
Oxon OX11 ORQ
ENGLAND

C. Myttenaere
Laboratoire de Physiologie
Végétale (VYVE)
Place Crois du Sud, 4
B-1348 Louvain-La-Neuve
BELGIUM

J. C. Nénot, Deputy Director
Centre d' Etudes Nucléaires
BP No. 6
F-92260 Fontenay-aux-Roses
FRANCE

R. Osborne
Atomic Energy Commission
of Canada, Ltd.
Chalk River Nuclear
Laboratories
Chalk River, Ontario KOJ 1JO
CANADA

O. Pavlovski
Institute of Biophysics
Ministry of Public Health
Givopisnaya 46
Moscow D-182
RUSSIA

V. Prodi
Department of Physics
University of Bologna
Via Irnerio 46
I-40126 Bologna
ITALY

Reports Librarian
Harwell Laboratory, Bldg. 465
UKAEA
Harwell, Didcot
Oxon OX11 ORB
ENGLAND

P.J.A. Rombout
Inhalation Toxicology
Department
National Institute of Public
Health and Environmental
Protection
P.O. Box 1
NL-3720 BA Bilthoven
THE NETHERLANDS

M. Rzekiecki
Commissariat à l'Énergie
Atomique
Centre d'Etudes
Nucleaires de Cadarache
BP No. 13-St. Paul
Les Durance
FRANCE

H. Smith
International Commission on
Radiological Protection
P.O. Box 35
Didcot
Oxon OX11 ORJ
ENGLAND

J. W. Stather
National Radiological
Protection Board
Building 383
Chilton, Didcot
Oxon OX11 ORQ
ENGLAND

Sun Shi-Quan, Head
Radiation-Medicine
Department
North China Institute of
Radiation Protection
P.O. Box 120
Tai-yuan, Shan-Xi
PEOPLE'S REPUBLIC OF
CHINA

G. Tarroni
ENEA-PAS-FIBI-AEROSOL
Laboratorio Fisica Sanitaria
Via Ercolani 8
I-40138 Bologna
ITALY

J. W. Theissen
Radiation Effects Research
Foundation
5-2 Hijiyama Park
Minami-Ku
Hiroshima 732
JAPAN

K. W. Timmis, Director
Division of Microbiology
National Centre for
Biotechnology
Mascheroder Weg
D-3300, Braunschweig
GERMANY

D. Van As
Atomic Energy Corporation
P.O. Box 582
Pretoria 0001
REPUBLIC OF SOUTH AFRICA

Vienna International Centre
Library
Gifts and Exchange
P.O. Box 100
A-1400 Vienna
AUSTRIA

Wang Hengde
North China Institute of
Radiation Protection
P.O. Box 120
Tai-yuan, Shan-Xi
PEOPLE'S REPUBLIC OF
CHINA

Wang Renzhi
Institute of Radiation Medicine
11# Tai Ping Road
Beijing
PEOPLE'S REPUBLIC OF
CHINA

Wang Ruifa,
Associate Director
Laboratory of Industrial Hygiene
Ministry of Public Health
2 Xinkang Street
Deshengmenwai, Beijing 100088
PEOPLE'S REPUBLIC OF CHINA

Wang Yibing
North China Institute of Radiation Protection
P.O. Box 120
Tai-yuan, Shan-Xi
PEOPLE'S REPUBLIC OF CHINA

Wei Lü-Xin
Laboratory of Industrial Hygiene
Ministry of Public Health
2 Xinkang Street
Deshengmenwai, Beijing 100088
PEOPLE'S REPUBLIC OF CHINA

B. C. Winkler, Director
Licensing
Raad Op Atomic
Atoomkrag Energy Board
Privaatsk X 256
Pretoria 0001
REPUBLIC OF SOUTH AFRICA

Wu De-Chang
Institute of Radiation Medicine
27# Tai Ping Road
Beijing
PEOPLE'S REPUBLIC OF CHINA

ONSITE

DOE Richland Field Office (3)

R. D. Freeberg A5-19
D. R. Segna A5-90
M. W. Tiernan A5-55

Hanford Environmental Health Foundation

T. Henn H1-02

Westinghouse Hanford Company (4)

M. R. Adams H6-01
L. C. Brown H6-20
R. M. Mitchell H6-04
D. E. Simpson B3-55

Pacific Northwest Laboratory (174)

C. C. Ainsworth K3-61
J. E. Amonette K6-81
R. W. Baalman K1-50
J. F. Bagley K1-64
W. J. Bair K1-50 (2)
C. A. Baldwin P7-58
R. M. Bean P8-08
M. P. Bergeron K6-77
B. N. Bjornstad K6-96
G. D. Black K7-28
H. Bolton K4-06
C. J. Brandt K6-04
F. J. Brockman K4-06
T. M. Brouns P7-41
L. L. Cadwell P7-54
J. W. Cary K6-77
D. A. Cataldo K4-12
T. D. Chikalla P7-75
C. R. Cole K6-77
S. D. Colson K2-14
J. L. Cox P8-38
E. A. Crecelius SEQUIM
V. I. Cullinan SEQUIM
R. J. Douthart K4-13
J. L. Downs P7-54
D. W. Dragnich K1-46
T. H. Dunning K2-18
L. E. Eary K6-81
L. L. Eberhardt P7-54
R. M. Ecker SEQUIM
C. E. Elderkin K6-03
R. A. Elston SEQUIM
R. J. Fellows K4-12
B. J. Fimiani BWO
J. K. Fredrickson K4-06
H. D. Freeman P8-38
J. S. Fruchter K6-81
T. R. Garland K3-61
G. W. Gee K6-77
E. S. Gilbert P7-82
T. R. Ginn K6-77
D. C. Girvin K3-61
W. A. Glass K4-13
Y. A. Gorby K4-06
M. J. Graham K6-80
R. H. Gray K1-33
L. K. Grove K6-86
P. C. Hays K6-86
D. J. Holford K6-77
L. A. Holmes K1-29
C. J. Hostetler K6-81
P. M. Irving K6-98
E. A. Jenne K6-81
J. R. Johnson K3-53
R. N. Kickert P7-54
M. L. Knotek K1-48
W. W. Laity K2-50
R. J. Lenhard K6-77
F. C. Leung K4-13
M. W. Ligotke P7-54
S. O. Link P7-54
P. E. Long K6-84
J. A. Mahaffey P7-82
J. L. McElroy P7-46
J. P. McKinley K3-61
G. L. McVay K2-45
B. D. McVeety K4-12
F. B. Metting P7-54
E. M. Murphy K3-61
G. P. O'Connor P7-54
R. L. Ornstein K2-18
T. L. Page B1-40
J. F. Park P7-52
W. T. Pennell K6-04

R. W. Perkins P7-35
S. A. Rawson K6-84
W. H. Rickard P7-54
R. G. Riley K6-81 (5)
K. R. Roberson K6-77
L. E. Rogers P7-54 (5)
M. F. Romine K4-06
J. L. Ryan P7-25
G. F. Schiefelbein P8-38
R. P. Schneider P7-56
J. A. Schramke K6-81
R. Shikiar HARC
D. B. Shipler K6-89
B. D. Shipp K1-73
C. S. Simmons K6-77
M. A. Simmons P7-54
R. L. Skaggs K6-77
F. A. Spane K6-96
T. O. Stevens K4-06
T. L. Stewart K1-25
G. L. Stiegler P7-56
G. M. Stokes K1-74
J. A. Stottlemyre K6-75
G. P. Streile K6-77
B. R. Stults K2-20
J. E. Szecsody K6-77
J. C. Templeton K6-81
W. L. Templeton K1-30
T. S. Tenforde K1-50 (15)
M. E. Thiede P7-54
J. M. Thomas P7-54
R. C. Thompson P7-58
S. L. Thorsten P7-54
P. Van Voris K4-12
B. E. Vaughan K1-66
V. R. Vermeul K6-77
C. R. Vest BWO
W. C. Weimer P7-22
M. D. Wessel P7-54
R. E. Wildung P7-54 (20)
W. R. Wiley K1-46
L. D. Williams K1-41
B. D. Wood K6-77
G. L. Work K7-02
J. V. Wright K6-84
G. E. Wukelic K6-84
J. S. Young K6-81
J. M. Zachara K3-61
J. D. Zimbrick P7-58
Health Physics Department Library
Life Sciences Library (2)
Publishing Coordination
Technical Report Files (5)

END

DATE
FILMED
7/22/93